Optimising Novel Dental Composites for Paediatric Patients

Thesis submitted by

Nabih Alkhouri

For the degree of

Doctor of Philosophy

Eastman Dental Institute

UCL

2019

Candidate declaration

I, Nabih Alkhouri confirm that the work presented in this thesis is my own. Where information has been derived from other sources, I confirm that this has been indicated in the thesis.

X
_____
Nabih Alkhouri

Acknowledgement

Abstract

Since amalgam use to restore children`s teeth is no longer an option due to Minamata agreement and with the absence of a viable strong and easy to apply material, a need for a novel restoration has become essential.

The aim of this research was therefore to develop a novel children's composite that would enable a simpler and pain-free restorative method and be a feasible alternative for the difficult to place resin restorations and the weak glass ionomers.

The initial eight formulations studied incorporated an adhesion promoting monomer, 4META (3wt%) within a base monomer, UDMA (72wt%) combined with low shrinkage diluent monomer PPGDMA (24wt%) and the photoinitiator camphorquinone (1wt%). This was mixed with a glass powder phase at two Powder/ Liquid ratios (PLR, 5:1 or 3:1). The glass filler contained different levels of two new novel additives to enable placement on caries affected dentine following minimal tooth excavation; antibacterial PolyLysine (PLS, 5 or 2wt%) and a remineralising agent Monocalcium Phosphate monohydrate, (MCP, 8 or 4wt%).

Tests were performed to determine maximum levels of active agents that could be added whilst maintaining properties that would enable compliance with composite ISO and safety requirements. Studies included light curing kinetics, interaction of cured material with water (sorption and solubility, mass and volume changes, and release of agents) and mechanical properties (Flexural strength and modulus). These studies lead to a predicted optimal formulation with PLS of 4wt%, MCPM of 8wt% and PLR 3:1.

The optimal formulation was large scale manufactured and the above studies repeated. Furthermore, testing of adhesion to tooth structure by means of microleakage, adaptation to cavity walls, shear bond strength and formation of resin tags within carious dentine was assessed. Finally, the ability to precipitate minerals and inhibit enzymatic activity at the adhesion interface was tested.

Results showed that the proposed formulations were stable when aged at 60ºC for 6 months and had high monomer conversion (~>65%) when light-cured for 40s even with samples of 3mm thickness. Formulations of higher PLS and MCP content also exhibited higher water sorption and solubility values due to the hydrophilicity and release of these components. This was expected and observed to reduce the early mechanical properties, but the results showed that flexural strength and modulus levelled off after 3 months of soaking cured discs in water. The flowability of the paste and the PLS and MCP content were all positive factors in achieving better penetration and resin tags

formation within the collagen mesh. This collagen mesh was a standardised caries-like model which was created during this study.

The final optimised formulation results showed the material to be radio-opaque. It achieved >75% monomer conversion and was mechanically strong (120MPa biaxial flexural strength and 3.5GPa modulus). The water sorption and solubility values were just higher than the ISO recommended maximum values that were set for composites of non-releasing ability. The material also outperformed commercial comparators in terms of self-etching the enamel and adapting to the sound cavity walls. Furthermore, it also formed long and extensive tags (more than 200µm long) within collagen mesh (formic acid demineralised coronal tooth slices) and naturally carious dentine. Finally, the optimised material exhibited precipitation of minerals at the adhesion interface. Tags and mineral precipitation helped explain observation of matrix metalloproteinase (MMP) inhibition at the tooth / carious dentine interface. The results were used to support applications to MHRA for clinical trials and a notified body for CE mark.

In conclusion, the research presented has achieved its aim to develop a marketable material that has the potential to address problems arising with amalgam ban.

Impact statement

Over the past 7 years, the numbers of children referred to the Eastman Dental Hospital due to caries has increased from ~2000 to over 5000 per year. For many, by the time they are seen, restoration is no longer feasible and tooth extraction is the only option. With the ban on amalgam fillings in paediatric patients in 2018, current complexity of composite placement and poor performance of glass ionomer cements, this issue is likely to get worse.

The cost of dentistry to the NHS is more than £3.4 billion per year. Despite being preventable, the cost of children and young adolescents' teeth extractions under GA in 2015-2016 was more than £50 million (£836 per extraction). Furthermore, increasing sugar consumption in low- and middle-income countries is leading to worse conditions and making dental treatment unaffordable. Untreated dental caries remains the tenth most prevalent disease amongst children, affecting 9% of the global child population. It is however, the most prevalent condition amongst adults, affecting 34% of them globally. Although the disease is linked to the socioeconomic level amongst many other factors, high-income countries still suffer high prevalence of the disease (Peres et al., 2019). It affects 12% of 3-year olds and 1 in 4 of 5-year olds in the UK. These numbers surge to 60-90% of school age children.

The work described in this thesis was sufficient to convince a German company to full scale manufacture and package an optimised formulation. It also supported a successful application to MHRA and ethics committees for a first in man clinical trial that started in January 2019. Furthermore, data has been supplied to a UK company to enable CE mark and distribution. Preliminary clinical indications have shown the optimised material enables composite restoration of children's teeth using a simpler, pain-free and minimally invasive approach. This approach will be better accepted by children and could help resolve the growing crisis of not being able to treat children's teeth in general dental practice. Thereby, potentially reduce the escalating numbers referred to NHS hospitals.

The enzyme inhibition effect that the optimised material exhibited could also be the cornerstone for future developments. This effect would reduce the failure rate that normal resin composites usually suffer from due to adhesion interface degradation.

Table of Contents

N.B. The sleeve attached to the thesis cover contains a CD-ROM of the visual videos and 3D results.

List of Symbols

<u>**Greek letters**</u>

β_c	Centre of deflection
β	Deflection
ρ	Density
φ	Polymerisation shrinkage
υ	Poisson ratio

<u>**English letters**</u>

μg	Microgram
μL	Microliter
μm	Microns
A_b	Bonding area
a.u	Absorbance unit
b	Width of beam shape sample at the centre
Ba	Barium
$C_{(\%)}$	Monomer conversion
Ca	Calcium
cm	Centimetre
d	Day
D_a	Density of air at a given temperature
D_w	Density of water at a given temperature
E	Modulus of elasticity
F	Force
g	Gram
H	Hydrogen
h	Height of beam shape sample at the centre
H^+	Hydrogen ions
h_0	Peak height (absorbance) at initial time
h_t	Peak height (absorbance) at final time
II	Roman number 2

IX	Roman number 9
J	Joule
kV	Kilovolt
l	Length of beam shape sample
L	Litre
m	Mass
M	Molarity
m (preceded by number)	Month
m_0	Initial dry mass
m_{dt}	Dry mass at a given time point
mg	Milligram
min	Minute
mL	Millilitre
mm	Millimetre
mM	Millimolar
ms	Milliseconds
m_w	Molecular weight
m_{wt}	Mass under water (wet weight)
N	Newton
n	Sample number
n_i	Number of C=C bonds per molecule
nm	Nanometre
O	Oxygen
P	Phosphorus
R	PLS release
R_g	Gas constant
r	Radius
R_{PL}	PLR ratio
R_b	Number of reacted C=C in a unit of volume
R_t	Release into water at a given time point
S	Flexural strength
s	Seconds
Si	Silica
T	Temperature
t	Time
T_a	Aluminium equivalent thickness
t_{AA}	Time of accelerated ageing

t_{RT}	Time at room temperature
T_s	Sample thickness
V	Volume
V_0	Initial volume
V_{dt}	Volume at a given time point
w	Week
W_i	Monomer molecular weight
W_{sl}	Water solubility
W_{sp}	Water sorption
x_i	Monomer mass fraction in the liquid phase
y	Year

List of Abbreviations

10-MDP	10-Methacryloyloxydecyl dihydrogen phosphate
4META	4-methacryloyloxyethyl trimellitate anhydrous
ACP	Amorphous calcium phosphate
ART	Atraumatic restorative technique
AS	Artificial saliva
ATR	Attenuated total reflectance
AU	Absorbance unit
BFM	Biaxial flexural modulus
BFS	Biaxial flexural strength
Bis-EMA	Bisphenol A ethoxy dimethacrylate
Bis-GMA	Bisphenol A glycidyl methacrylate
BSI	British standards institute
CaP	Calcium phosphate
CHX	Chlorhexidine
CI	Confidence interval
CLSM	Confocal laser scanning microscope
CQ	Camphorquinone
DCPA	Dicalcium phosphate anhydrous
DIN	Deutsches Institut für Normung (German Institute for Standardization)
DMA	N,N-Dimethylacrylamide
DMP1	Dentine matrix protein-1
DMPT	N, N-dimethyl-p-toluidine
ECOHIS	Early childhood oral health impact scale
EDI	Eastman dental institute
EDX	Energy dispersive X-ray
FDA	US food and drug administration
FDI	Fédération Dentaire Internationale (World Dental Federation)

FHA	nanofluorohydroxyapatite
FTIR	Fourier transform spectroscopy
GAG	Glycosaminoglycan
GI	Glass ionomer
GIC	Glass ionomer cement
GPa	Giga Pascal
GPDM	Glycerolphosphate dimethacrylate
HA	Hydroxyapatite
HEMA	Hydroxyethyl methacrylate
HPLC	High performance liquid chromatography
ISO	International standards organisation
LC	Light cured
MCP	Monocalcium phosphate monohydrate
MHRA	Medicines and Healthcare products Regulatory Agency
MMP	Matrix metalloproteinase
MPa	Mega Pascal
MPTS	3-methacryloxypropyl trimethoxysilane
N.B	Note well
N/A	Not available
NaOCl	Sodium Hypochlorite
NTGGMA	Na-N-tolyglycine glycidyl methacrylate
PAMAM	Poly-amide amine
PLR	Powder/ liquid ratio
PLS	PolyLysine
PMDM	Pyromellitic Dimethacrylate
PP	Phosphophoryn
PPGDMA	Polypropylene glycol dimethacrylate
ppm	Particle per million
QAM	Quaternary ammonium methacrylates
RMGIC	Resin modified glass ionomer cement
rpm	Revolutions per minute

RT	Room Temperature
SBF	Simulated body fluid
SDF	Silver diamine fluoride
SEM	Scanning electron microscope
SQRT	Square root
TCP	Tricalcium phosphate
TEGDMA	Triethylene glycol dimethacrylate
TTCP	Tetracalcium phosphate
UDMA	Urethanedimethacrylate
UV	Ultraviolet
WHO	World health organisation
XCT	X-ray computed tomography

List of Tables

List of Figures

1   Literature Review

1.1   Tooth hard tissues structure

1.1.1   Enamel

Enamel is the milky-white outer layer covering the crowns of teeth (see Figure 1-1) (Hsieh et al., 2013). It is composed of minerals, mainly hydroxyapatite ($Ca_{10}(PO_4)_6.2OH$), which form 97% of its weight. This high mineral content makes it the hardest tissue in the human body. Enamel is transparent and becomes more opaque when demineralised during a carious attack (white spots or incipient caries). Its thickness varies and is thickest at the incisal or occlusal surfaces (about 2.5mm in permanent teeth). Enamel is of ectodermal origin and is formed by ameloblasts which disappear after completion of formation. This tissue cannot regenerate because it is acellular but does undergo continuous remineralisation/ demineralisation under balanced conditions (Curzon and Duggal, 2003; Chen and Liu, 2014; Peres et al., 2019).
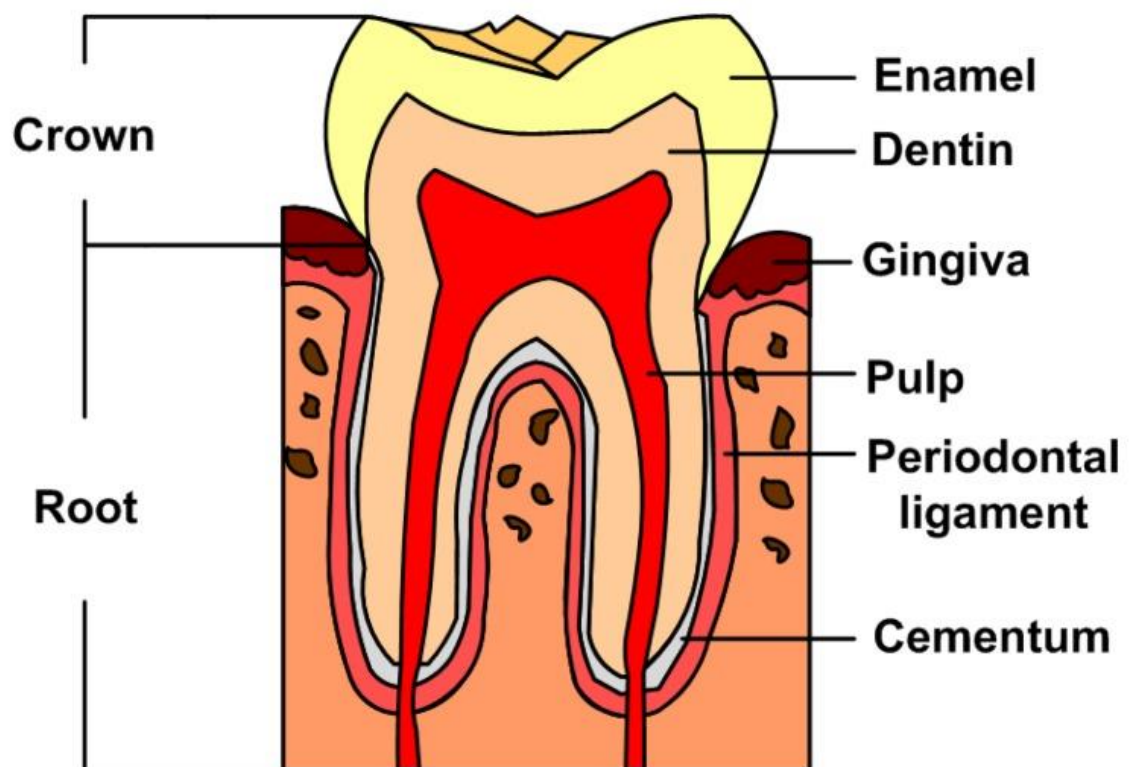
Figure 1-1 Diagram of tooth structure. Adapted from "Hsieh, Yao-Sheng et al. 2013". Copyright certificates are attached at the end of the thesis.

1.1.2 Dentine

Dentine supports the enamel and also forms the main hard tissue of teeth roots where it is covered by cementum. It is softer, more yellowish, opaque and less mineralised when compared to enamel. Dentine consists of an inorganic phase (70% hydroxyapatite by weight) and 20% organics (mainly type I collagen) in addition to 10% of water. Dentine surrounds and protects the dental pulp (in the centre of the tooth). It is formed by the odontoblasts, which form later on the outer layer of the dental pulp. Dentine formation continues as long as the pulp is healthy. Until the tooth is functional, the dentine formed is called primary dentine. Subsequently, secondary dentine formation takes place near the pulp and continues for the rest of life. Under a stimulus (such as caries, thermal or chemical), formation of a different type of dentine; reparative dentine, happens at a faster rate to protect the pulp. The innermost layer of dentine is not fully mineralised and is called pre-dentine (it is the matrix secreted by odontoblasts).

When odontoblasts form dentine, they leave processes in the matrix which lengthen and occupy a tubular structure called the dentinal tubules. These tubules are higher in number and wider nearer to the pulp in comparison to the area next to the dentine-enamel junction (mantle dentine, the first formed layer of dentine). The tubules are surrounded by the mineralised dentine which can be differentiated into the peritubular and intertubular dentine. Peritubular dentine, unlike intertubular, is not formed by pre-dentine and does not contain collagen fibrils but mainly minerals and non-collagenous proteins. Hydroxyapatite crystals in dentine are usually smaller and of irregular shape in comparison to enamel. These crystals deposit on the collagen framework to mineralise the matrix and form dentine.

Other non-collagenous proteins that contributes to the organic phase of dentine include proteins, proteoglycans and enzymes (such as matrix metalloproteinases MMPs). The most abundant non-collagenous protein is phosphophoryn (PP). This protein plays a major role in mineralisation of dentine. It is very acidic (contains aspartic acid) and acts as a mineral nucleator. Dentine matrix protein 1 (DMP-1) is also one of the common proteins in dentine. Glycosaminoglycans (GAGs), which form part of the proteoglycans, play a role in linking the collagen fibrils together and are negatively charged. Proteoglycans and glycosaminoglycans are highly concentrated around the tubules. The core of proteoglycan ensures the matrix stability while the GAG affects tissue mechanics. Research also showed chondroitin sulphate to be highly detectable at peritubular dentine as well as calcium, phosphorus and sulphate ions. (Pashley, 1989; Marshall et al., 1997; Marshall Jr et al., 1997; Kinney et al., 2003; Goldberg et al., 2011; Retrouvey et al., 2012;

Chen and Liu, 2014; Bleicher et al., 2015; Sloan, 2015; Bertassoni, 2017; de Mattos Pimenta Vidal et al., 2017)

1.2 Dental caries

1.2.1 Epidemiology and effect on quality of life

Dental decay is one of the most common human diseases and affects almost 100% of adults and 60-90% of school children across the world (WHO, 2012) (Jurgensen and Petersen, 2013). Dental caries and related treatment are the main contributors to the healthcare cost of dental disease, which is estimated at US$442 billion (Listl et al., 2015) globally and £3.4 billion per year in the UK (HSCIC 2015). In England, dental decay was the most common reason for a young child (aged 5 to 9 years old) to be admitted to hospital in order for the infected teeth to be surgically removed under general anaesthesia in 2012/2013. The number of admissions increased by 14% between 2010/11 and 2013/14 (Faculty of Dental Surgery) (Surgery, 2015) . More than 63,000 children (younger than 19 years old) were admitted to hospitals in 2014/2015 to have their affected teeth extracted. More updated figures from Public Health England show that 1 in 4 of 5-year-old children have dental caries affecting 3-4 of their teeth on average, mostly untreated. Amongst 3-year olds, 12% suffered from dental caries with an average of 3-4 teeth being affected. In North West England, 26% of children missed about 3 days of school due to pain and infections caused by dental caries. There was little or no change in the severity and prevalence of the disease in the latest report by Public Health England (2018).

The cost of the 40,970 extractions of multiple teeth in under 18 year olds carried out in the 2014/15 period was £35 million according to Local Government Association (2016) with the average cost of £836 per extraction in hospital. This increased to a total cost of £50.5 million in 2015/2016, £7.8 millions of these were spent on extractions for under 5-year-old children.

Teeth are not only important for eating, they are also part of speech development and help to maintain self-esteem. As a result, caries can affect the child`s quality of life on many levels. If treatment is delayed, caries can cause severe pain and might lead to abscesses, difficulty eating, sleeping problems and missing school days (Anil and Anand, 2017). Early childhood oral health impact scale (ECOHIS) is shown in Figure 1-2 and research showed moderate to large effect of oral health on quality of life in preschool children (M. C. Ferreira et al., 2017). These findings are confirmed by many studies that proved the effect of the negative caries experience on quality of life of both children and

their families (Brignardello-Petersen, 2017; Chaffee et al., 2017; Martins et al., 2017) and that receiving treatment improved their quality of life drastically (Wong et al., 2017).

Child impact domain

How often has your child, because of dental problems or the need for dental treatment:

1…had pain in the teeth, mouth or jaws?
2…had difficulty drinking hot or cold beverages?
3…had difficulty to chew food?
4…had difficulty for pronouncing any words?
5…Missed pre-school or day-care?
6…had difficulty sleeping?
7…been annoyed or bad-tempered?
8…avoided laughing or smiling when around other children?
9…avoided talking?

Family impact domain

How often have you or another family member, due to dental problems or dental treatment of your child:

10…felt uspet?
11…felt guilty?
12…had to take hours or days off work?
13…had the family's economic situation affected?

Figure 1-2 Early childhood oral health impact scale (ECOHIS)

1.2.2 Aetiology

Dental decay is a multifactorial disease with the main risk factors being the bacteria, the diet or the environment (Anil and Anand, 2017). From a microbiological point of view, it is caused by multiple species of bacteria; mainly the gram-positive carbohydrate-fermenting *Streptococcus mutans* and *lactobacillus* (Larsen and Fiehn, 2017). Non-effective brushing and bad oral hygiene habits lead to food accumulation and biofilm formation and thus dental decay (Kaminska et al., 2016). This ecological hypothesis means that the demineralisation will overweigh the remineralisation process. These biofilms are made up of different bacteria and poly-saccharides matrix (Reese and Guggenheim, 2007). Bacterial secretion of acid causes a drop in pH and tooth minerals to start dissolving (Wolff and Larson, 2009).

Once bacteria reach dentine, they start dissolving it as well (Fusayama et al., 1966). Caries can develop faster through dentine than enamel as it is less mineralised (70% versus 96% mineral content by weight, respectively), has increased surface area of the apatite and higher carbonate content (Baldassarri et al., 2008; Goldberg et al., 2011). All these factors increase dentinal dissolution susceptibility according to Craig`s Restorative Dental Materials (2012).

Different layers of carious dentine can be identified in a carious lesion (see Figure 1-3) (Mazzoni et al., 2015b). There are two main layers determined by bacterial count and

degree of demineralisation. Infected dentine is the outer layer with high bacterial count and total demineralisation. Deeper layer is known as affected dentine; it contains less bacteria and is only partly demineralised. A third translucent layer may form at the base of the carious lesion. This is highly mineralised due to pulp reaction to defend itself (Fusayama et al., 1966; Fusayama and Terachima, 1972; Anderson et al., 1985; Angker et al., 2004). Restorative materials currently used require removal of both infected and affected dentine layers to place the filling in a caries free cavity.
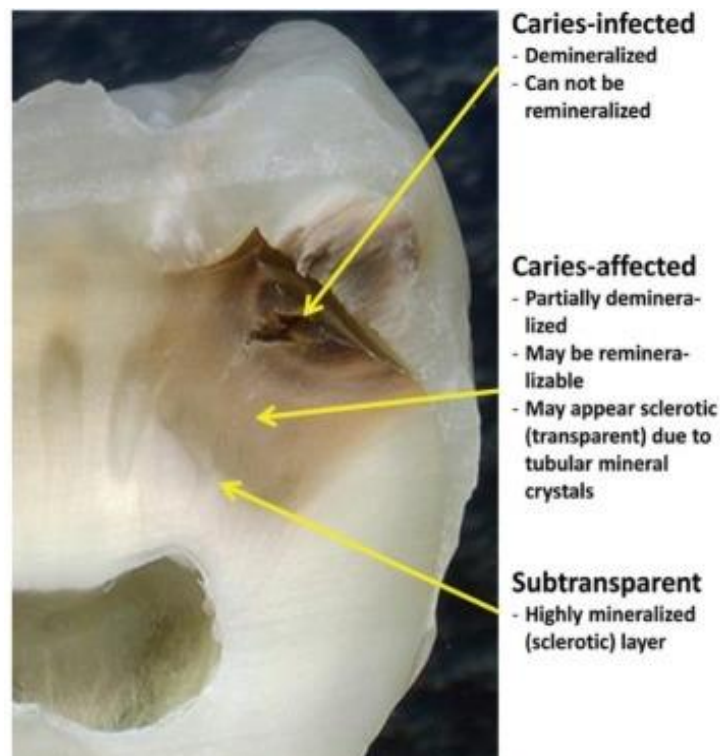
Figure 1-3 Carious dentine layers. Adapted from "Mazzoni, A et al. 2015b". Copyright certificates are attached at the end of the thesis.

Dentine consists of a considerable number of organics, as mentioned before. Therefore, the demineralisation process cannot be the only process involved in developing caries. There is a major role played by the deproteinisation of this organic phase (Takahashi and Nyvad, 2016).

One group of enzymes responsible for the deproteinisation of the organic matrix of dentine are the matrix metalloproteinases (MMPs). These enzymes get activated during a carious attack. They are naturally available in dentine and saliva. They are calcium and zinc dependant enzymes. 23 members of MMPs have been identified and they can be divided into 6 families based on their specificity. Activation of these enzymes requires an acidic environment created by bacterial acids during caries progress. Additionally, acid etching can cause the enzymes to be activated and lead to the degradation at the adhesion interface and the following failure of the restoration.

The presence of MMP-2, MMP-9 (gelatinase), MMP-8 (collagenase), MMP-3 (stromelysin) and MMP-20 in dentine has been reported. The most abundant are MMP-8 of the collagenase and MMP-9 of the gelatinase family. Their role in caries is confirmed but not yet well understood. It was thought that upon demineralising dentine, bacterial protease will degrade collagen. Studies, however, showed the inability of cariogenic bacteria to degrade collagen *in vitro*. Also, although MMPs get activated by an acidic environment, they work better in neutral pH. This is achieved by the buffering effect of the saliva. Research has proven the presence of active MMP-2, -9, -8 and -3 in carious dentine.

Cysteine cathepsin and proteoglycan are other non-collagenous proteins in the dentine that are involved in caries progression. Cysteine cathepsin is more abundant and active in deeper lesions, which may mean that the pulp and the odontoblasts are also involved. Unlike MMPs, cysteine cathepsin works better in an acidic environment (pH=5) (Visse and Nagase, 2003; Chaussain-Miller et al., 2006; Boushell et al., 2011; Mazzoni et al., 2011; Mazzoni et al., 2015a; Tjaderhane et al., 2015; Femiano et al., 2016).

1.3 Treatment options

When children`s teeth get carious, treatment options include:

- Trying to arrest the caries (stop their progress) without restoring cavities. This entails using remineralising agents such as fluorides.
- Restore the teeth without total removal of caries using the atraumatic restorative technique (ART). This requires removal of the very soft caries (infected dentine) using hand instruments, saving the affected dentine then application of a glass ionomer restoration.
- Restore the teeth upon total removal of caries with one of the commercially available restorative materials.

1.3.1 Fluoride

Fluoride has been widely used in dentistry to produce a surface less susceptible to caries by replacing the hydroxyl in the hydroxyapatite crystals. The result is the less soluble Fluor-apatite. Fluoride has been either incorporated in dental restorations (such as the glass ionomers) or as varnish, gel and most recently, silver diamine fluoride (SDF 38%), which was proved to be effective in arresting primary dentition caries (Contreras et al., 2017; Milgrom et al., 2018). SDF was also suggested to be used for dentine hypersensitivity and root caries (Hendre et al., 2017). When caries are confined to enamel, sodium fluoride varnish 5% showed also efficacy in arresting those caries (Gao

et al., 2016). Fluoride application, up to four times yearly, can help prevent caries in primary and permanent dentition as well, especially when used in conjunction with fluoride toothpaste (Marinho et al., 2004; Marinho et al., 2013; Marinho et al., 2015). However, SDF shows faster effect and can be used even in carious dentine (Duangthip et al., 2016; Duangthip et al., 2018; Ruff and Niederman, 2018).

1.3.2 Atraumatic restorative technique (ART)

The atraumatic restorative technique is a minimally invasive approach to restore carious teeth without the total removal of caries. It is beneficial in areas where there is limited access to dental settings. It is also important in managing caries in anxious or uncooperative patients, especially children. It entails restoring carious lesions upon manual removal of the very soft caries using hand instruments only. Therefore, there is no need for delivering local anaesthesia or use of high-speed drilling handpiece. An adhesive restoration is applied to seal these cavities. The most commonly used material is the self-cure glass ionomer (GIC) although resin-modified glass ionomers (RMGIC) or composite resins can be used when resources are more readily available. These materials can be equally used since the evidence of higher failure rate with GIC in comparison to RMGIC and resin composites remains low (Dorri et al., 2017b). This technique, alongside fluoride varnish and fissure sealants, form an important method in prevention programmes (Frencken et al., 1996; Frencken et al., 2014; Byrd, 2016; Hesse et al., 2016; de Medeiros Serpa et al., 2017; Dorri et al., 2017a). The evidence supporting partial excavation to avoid pulp exposure is strong, especially in cases where the pulp is healthy and vital (Ricketts et al., 2013).

Another concept that has been developed in the last 10 years and requires no removal of caries in primary dentition is the Hall technique. It simply applies preformed stainless-steel crown to carious teeth (unless it requires pulp treatment). It depends on the concept of sealing these cavities to arrest caries. Many randomised clinical trials have been performed to test this method and the evidence shows a very high success rate of more than 90%, clinically and radiographically, without recurrent pain or infection of the treated teeth. The method is becoming more accepted by children and parents but has the disadvantages of the metal colour of the stainless steel crown and the need for two visits (Innes et al., 2007; N. Innes et al., 2015; Clark et al., 2017; Innes et al., 2017; Santamaria and Innes, 2018). Systematic reviews showed that stainless steel crowns applied using Hall technique outperformed other direct restorations and suffered less failure (N. P. T. Innes et al., 2015).

1.3.3 Total caries removal and restoration

Total caries removal requires delivering local anaesthesia and the use of a drilling handpiece. The cavity should be totally caries free prior to restoration application. Commercially available restorative materials are variable and have different indications, but clinician opinion and ease of use might play a role in treatment decision making. Restorative options include many materials, such as mercury amalgam, dental resin composites, glass ionomer (GI) and compomers. Each of these materials has its own advantages and disadvantages.

Amalgam fillings are considered relatively strong and have antibacterial effect (Wallman-Bjorklund et al., 1987; Wang and Liu, 2000; Ertugrul et al., 2003). However, due to the Minamata agreement (Minamata convention on mercury, UN, 2013) (Federation, 2014), all mercury containing products are phased out from use for children. Additionally, glass ionomer restoration longevity and clinical performance can be poor (Folwaczny et al., 2001; van Dijken and Pallesen, 2010). Henceforth, dental composites and compomers will be the only viable alternative for larger cavities.

The lack of antibacterial effect in dental composites requires a total removal of carious tissues before placing a restoration (Hickel et al., 2007). To do so, multiple complicated steps must be followed by clinicians to ensure proper adhesion to tooth structure. These steps include etching enamel and dentine, applying primer / bonding agent and finally placing the material in less than 2 mm thickness layers (to achieve high degree of conversion) (Romero et al., 2017; Rothmund et al., 2017). Thus, giving local anaesthesia and using the high-speed drilling handpiece are required. Furthermore, these fillings can suffer high failure rate because of fracture and recurrent disease (secondary caries) as a result of the complicated adhesion process (Baratieri and Ritter, 2001; Loguercio et al., 2003; Namgung et al., 2013; Kim et al., 2017).

All previously mentioned problems make placing such a material to restore children`s teeth both difficult and traumatic. With lack of skills among general dental practitioners to manage children's behaviour in a dental office, most of these children will end up being referred to specialists. The long painful waiting period will lead to deeper lesions and greater need for extraction instead of simple treatment.

1.4 Resin composites and their composition

Composite resin materials are prepared by mixing two phases; the liquid phase (monomers, usually a dimethacrylate) and the powder phase (reinforcing glass fillers). Additionally, a silane coupling agent is needed to bind the filler to the monomers, and

initiators / activators to promote the polymerisation and cross-linking setting reaction (Ferracane, 2011).

Figure 1-4 summarises the evolution of dental composites. Changes basically focused on incorporating smaller filler particles to improve polishability and wear resistance when these materials are used for anterior or posterior restorations, respectively. Other changes are related to the liquid phase (the organic matrix) and they focused on reducing the stress generated by polymerisation shrinkage. Recent developments aim to produce bulk fill, self-adhesive, antibacterial or remineralising materials (Ferracane, 2011; Meereis et al., 2018).
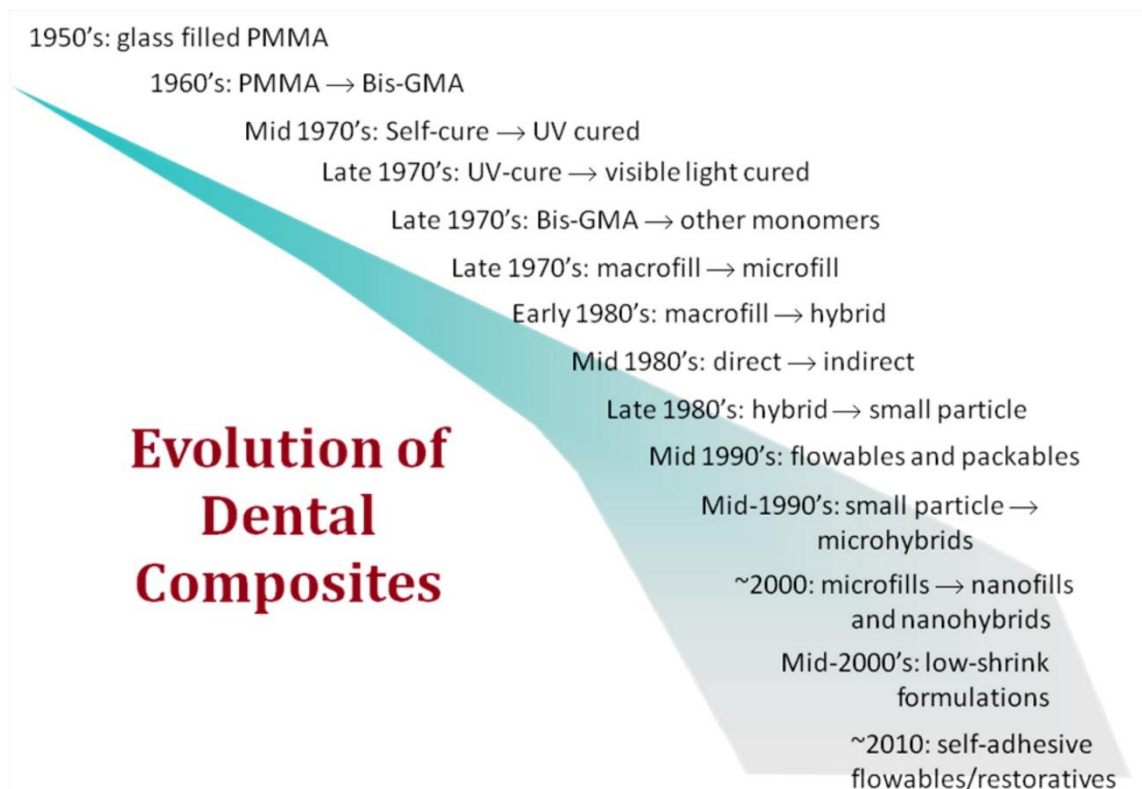
Figure 1-4 Evolution of dental composites. Adapted from Ferracane J. L. 2011. Copyright certificates are attached at the end of the thesis.

1.4.1 Liquid phase (the organic matrix):

Bis-GMA (bisphenol A glycidyl dimethacrylate) is the most commonly used base monomer in commercial dental composites. Bis-GMA is highly viscous due to the hydrogen bonding interactions that occur between the hydroxyl groups and the methacrylate group. Therefore, it must be mixed with other diluent monomers to adjust viscosity such as TEGDMA (triethylene glycol dimethacrylate), Bis-EMA (ethoxylated bisphenol-A dimethacrylate), UDMA (urethane dimethacrylate) or other monomers (Ferracane, 1995; Peutzfeldt, 1997; Fugolin and Pfeifer, 2017).

When these monomers are polymerised, they suffer shrinkage according to the number of polymerisable units which they contain. This shrinkage will lead to stress and is strongly related to the final degree of conversion. Insufficient bond strength will result in gap formation and failure of the restoration. Therefore, new developments have produced new monomers to reduce polymerisation shrinkage and stress (Feng et al., 2010). These new monomers were based on ring-opening polymerisable moieties (such as Filtek LS which incorporated silorane) or on molecules of higher molecular weight. Researchers also aimed to reduce the clinical steps needed to bond a restoration to the tooth structure or to eliminate the layering method needed to ensure sufficient polymerisation by developing self-adhesive or bulk-fill composites (Fugolin and Pfeifer, 2017). Figure 1-5 shows the molecular structure of the most commonly used monomers and their alternatives. The modified urethane dimethacrylate (modified UDMA, Dupont, GC) has higher molecular weight in comparison to the traditional UDMA and bis-GMA and thus reduces shrinkage.
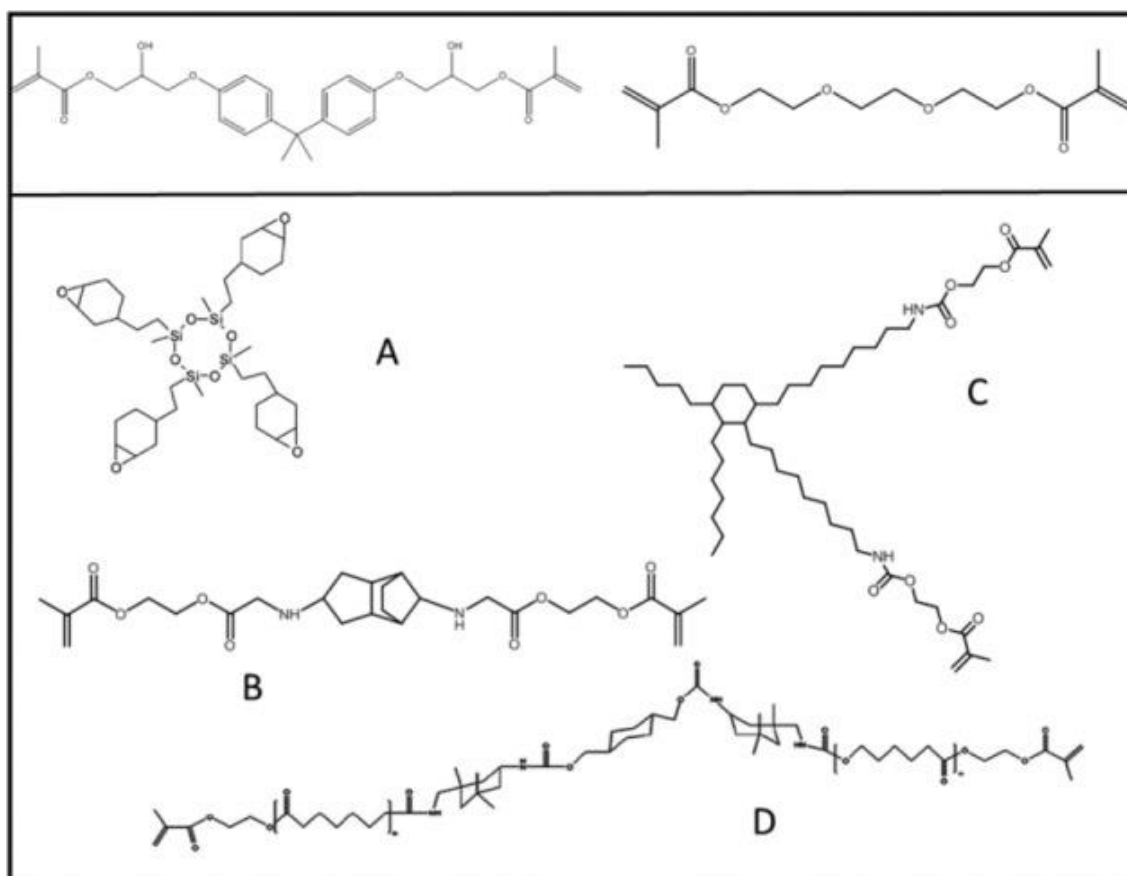
Figure 1-5 Top: Molecular structures of BisGMA (bisphenol A glycidyl dimethacrylate) (left) and TEGDMA (triethylene glycol dimethacrylate) (right). Bottom: Molecular structure of alternative monomers currently used in commercial products. (A) Oxirane (Filtek LS; 3M-ESPE), (B) TCD-urethane (Venus Diamond; Heraeus Kulzer), (C) dimeracid dimethacrylate (N'Durance; ConfiDental-Septodont), and (D) DuPont DX-511 (Kalore; GC America). Adapted from Fugolin A. P. P. & Pfeifer C. S. 2017. Copyright certificates are attached at the end of the thesis.

As mentioned before, TEGDMA, which is a more flowable diluent monomer, can be added to UDMA and Bis-GMA to produce less viscous resin. This resin can be better filled with glass. TEGDMA also enhances conversion by providing a less viscous reaction medium (Reed, 1997). Number of double bonds per unit of volume decides shrinkage values; the higher the number the higher the shrinkage. TEGDMA has lower molecular weight and more double bonds per unit of weight and hence shows higher shrinkage in comparison to UDMA and Bis-EMA. Consequently, UDMA and Bis-EMA are favourable to reduce shrinkage (Yap et al., 2000).

Hydroxyethyl methacrylate (HEMA) is a hydrophilic monomer of low molecular weight. It can be used as a monomer that promotes adhesion to tooth structure and it is soluble in water, ethanol and acetone. Therefore, it is widely used in adhesive systems. However, HEMA shows high values of water sorption whether cured or not (Van Landuyt et al., 2007).

1.4.2 Filler phase

Various fillers have been incorporated in composites. Quartz, colloidal silica, and silica glass containing barium, strontium, and zirconium are examples of the fillers used. These fillers can lead to higher strength and modulus of elasticity and lower polymerisation shrinkage, thermal expansion and water sorption (Chen, 2010). The amount, size, distribution and type (such as fibres) of filler particles are all important in controlling packable composite consistency (Choi et al., 2000).

Macrofill traditional dental composites had filler particles that measured about 50µm. These composites showed high strength but were difficult to polish and more plaque retentive. Therefore, the microfill composites were developed for aesthetics reasons with an average size of silica filler particles of about 40nm. Thus, these composites were actually original nanofill composites. They were more aesthetic and polishable but due to low level of fillers, they were weak and only suitable for non-load bearing areas. The filler level could be increased by incorporating pre-polymerized resin fillers (PPRF) within the structure of microfill.

Subsequently, the macrofill particles size was reduced by grinding to produce small particle hybrid composites, called midifills. These had an average filler particle size of slightly greater than 1µm in addition to 40nm fumed silica. Further developments led to microhybrid composites with smaller particles of 0.4–1.0µm in addition to nanofillers. The so-called universal composites can be used for anterior and posterior restorations since they show improved aesthetic and mechanical properties combined. More recently, nanofill composites were introduced. These have the highest aesthetic and polishability

properties due to containing only nanoscale fillers (Klapdohr and Moszner, 2005; Ferracane, 2011).

1.4.3 Silane coupling agents

Coupling agents are important to form covalent bonds between the organic matrix and the fillers to enhance mechanical properties of dental composites. These agents are used to coat the fillers. They have a functional group which links from one side to the filler via hydroxyl groups and the other can copolymerise into the polymers when cured. A commonly employed example is 3-methacryloxypropyl trimethoxysilane (MPTS) (Chen, 2010).

1.4.4 Visible-light initiator

Polymerisation of light-cured composites is initiated by irradiation using a blue light-curing gun with a wavelength range of 410-500nm. This light is absorbed by an α-diketone photoinitiator. One of the commonly used initiators is camphorquinone (CQ), accelerated by a tertiary amine. When CQ is excited, it reacts with a co-initiator to produce free radicals. These radicals will trigger the polymerisation process by crosslinking monomers (Lee et al., 1993).

It is worth mentioning that some commercial products have used different photoinitiators to produce materials that are more colour stable since the CQ is yellow. For example, PPD (1-phenyl-1,2-propanedione), Lucirin TPO (monoacylphosphine oxide) or Irgacure 819 (bisacylphosphine oxide) have been used (Stansbury, 2000).

1.5 Developments in resin composites

1.5.1 Bulk-Fill composites

Bulk-fill resin composites were introduced in the early 2000`s to avoid the layering technique and simplify restoration method. They are available as both flowable and packable consistencies. Bulk-fill composites must have sufficient depth of cure which is achieved by increasing the amount of photoinitiators, incorporating novel photoinitiators or using larger or more translucent fillers in the composition (Miletic et al., 2017; Son et al., 2017). However, higher photoinitiators content might cause less polymerisation in deeper composite layers due to paste discolouration. Flowable bulk-fill composites generally have lower filler content and hence lower mechanical properties unlike the packable version. Therefore, they can only be used in low load-bearing areas (Fugolin and Pfeifer, 2017). Modified UDMA was used in some of these composites to reduce

shrinkage-related stress and cusp deformation. Prepolymerised resin filler particles were also used to avoid excessive shrinkage (Fugolin and Pfeifer, 2017).

In vitro studies have confirmed that bulk-fill materials (such as Filtek Z350XT, Venus Charisma Diamond, SDR/Esthet-X and Tetric EvoCeram), when used for posterior restorations, did not suffer high cusp deformation or polymerisation stress, and that the fracture resistance was improved (Leprince et al., 2014; Fronza et al., 2015; Rosatto et al., 2015; Van Ende et al., 2017).

1.5.2   Self-Adhesive composites

During the last 10 years, flowable self-adhesive composites were introduced. Commercial examples include Vertise flow (Kerr) and Fusio Liquid Dentin (Pentron Clinical). These materials contain the conventional methacrylate system, but also incorporate acidic monomers (glycerolphosphate dimethacrylate- GPDM for example). Adhesive monomers are widely used in bonding systems and can adhere to tooth structure mechanically and maybe chemically (Ferracane, 2011). Glycerol phosphate dimethacrylate is also a self-etching monomer and links to other methacrylates (Yuan et al., 2015). Self-etch and bond composites would simplify restorative procedures, potentially eliminating the need for multiple bonding steps.

4-META (4-methacryloyloxyethyl trimellitate anhydride) is another adhesion-promoting monomer. It works by demineralising tooth structure mimicking the etching effect. Adhesion to tooth structure has been reported to be improved when 4-META is incorporated in the formulation (Van Landuyt et al., 2007).

1.5.3   Remineralising materials

Remineralising composites can replace the minerals loss from tooth structure to prevent progress of dental caries (L. Zhang et al., 2016). Many calcium and phosphate ion-releasing components have been introduced. These include calcium fluoride ($nCaF_2$), amorphous calcium phosphate (nACP), nanohydroxyapatite (nHA), nanofluorohydroxyapatite (nFHA), dicalcium phosphate anhydrous (DCPA) (Xu et al., 2006; Xu et al., 2007) and tetracalcium phosphate (TTCP) (Xu et al., 2009). The focus was on repairing small carious lesions (Li et al., 2014). Adding acidic monomers positively enhanced minerals release from a material to arrest caries. This could be due to the carboxylate group that chelated calcium and phosphate ions from surrounding environment and recharged the material with minerals (L. Zhang et al., 2016). Poly-amide amine (PAMAM) also enhanced remineralisation by serving as mineral nucleation

template, and when combined with calcium phosphate, it inhibited caries by neutralising bacterial acids (Liang et al., 2016).

Calcium and phosphate nanoparticles can remineralise early lesions and research showed promising results and various applications of such products due to their affinity towards collagen fibrils (Melo et al., 2013; Cheng et al., 2015). Non-collagenous proteins can regulate the nucleation and growth of minerals as part of the dentine biomineralisation process. These proteins include dentine matrix protein (DMP1) and dentine phosphophoryn (PP) (He and George, 2004). Non-collagenous protein analogues were reported to enhance biomimetic mineralisation on different levels (intrafibrillar and interfibrillar of dentine collagen fibrils) when used in combination with bioactive materials. However, this research was done *in vitro* without bacterial challenge (Cao et al., 2015).

Fluoride-releasing composites have been developed by either incorporating water soluble fluoride salts (NaF or SnF_2) or binding the fluoride to the organic matrix or the filler (Arends et al., 1995). Fluoride release levels are lowest with composites and increase with polyacid-modified composites then resin-modified glass ionomers and the highest with conventional glass ionomers (Asmussen and Peutzfeldt, 2002; Attar and Önen, 2002). This is strongly related to fluoride amount and the material matrix. However, research showed some conflict in terms of how effective fluoride-releasing materials are in inhibiting recurrent caries (Wiegand et al., 2007).

Fluoride can also have an antibacterial effect by inhibiting bacterial colonization and interfering with bacterial metabolism and dental plaque acidogenicity. Furthermore, fluoride can affect bacterial enzymes such as acid phosphatase, pyrophosphatase, peroxidase and catalase (Hamilton, 1990).

1.5.4 Antibacterial materials

Recurrent caries are one of the most common reasons for composite resin restorations future failure due to gaps and bacterial penetration at the adhesion interface (Lempel et al., 2015). As a result, efforts focused on incorporating antibacterial agents in composite materials. Some examples of these agents include:

- Quaternary ammonium methacrylates (QAMs) (Cheng et al., 2015; K. Zhang et al., 2016),
- Dimethylaminododecyl methacrylate (DMAHDM),
- bis(2-methacryloyloxyethyl) dimethylammonium bromide (QADM),
- 12-methacryloyloxydodec-ylpyridinium bromide (MDPB),
- methacryloxylethylcetylammonium chloride (DMAE-CB),

- quaternary ammonium polyethylenimine (QPEI),
- chlorhexidine (CHX),
- and PolyLysine (PLS).

1.5.4.1 Silver, amorphous calcium phosphate and quaternary ammonium methacrylates (QAMs)

Silver has antibacterial effects. It is also antifungal and antiviral. Silver ions can deactivate bacterial enzymes, causing a halt in DNA replication processes and consequently cell apoptosis (Rai et al., 2009). When silver was combined with amorphous calcium phosphate (nACP) in a resin composite, there was a dual benefit of antibacterial and remineralising effects. This was especially under acidic conditions where calcium and phosphate ion release increased drastically (Xu et al., 2011; Cheng et al., 2012).

When silver was combined with quaternary ammonium methacrylates (QAMs), stronger, more potent and durable antibacterial activity was observed. The positively charged QAMs can attach to the negatively charged bacterial membranes causing membrane disruption and cytoplasmic leakage which lead to their explosion and death due to osmotic pressure (Namba et al., 2009). Many QAM formulations have been produced and these include:

- methacryloxylethyl cetyl dimethyl ammonium chloride (DMAE-CB),
- quaternary ammonium polyethylenimine (PEI),
- quaternary ammonium dimethacrylate (QADM)
- and dimethylaminododecyl methacrylate (DMADDM).

Figure 1-6 shows a variety of antibacterial monomers that have been used in dental adhesives (Cocco et al., 2015). However, in all discussed attempts to incorporate these antibacterial agents in adhesives or restorations, release was a key factor to get the maximum benefit. If these components are not released into the surrounding environment, the antibacterial effect will be limited or might even vanish.

Figure 1-6 Structural formula of antibacterial monomers incorporated into dental adhesives. Adapted from Cocco et al. 2015. Copyright certificates are attached at the end of the thesis.

1.5.4.2 Chlorhexidine (CHX)

Attempts to include chlorhexidine in composite materials have also been addressed in the literature. Chlorhexidine can cause rapid damage to the outer cell membrane when in contact, but that damage is not enough to induce cytolysis or apoptosis. Then, by passive diffusion, CHX can cross the bacterial cell membrane and attack the bacterial cytoplasmic or inner cell membrane. This leads to leakage of the cytoplasm and thereby apoptosis (Cheng et al., 2017).

1.5.4.3 PolyLysine (PLS)

The use of PLS in dental composites was developed at UCL and is patent protected (WO2015015212A1). The technology has been licensed to Schottlander Dental Company.

ε-Poly-L-lysine (εPLS) is a homo-poly-amino acid characterized by the peptide bond between the carboxyl and epsilon-amino groups of L-lysine. It has a broad antibacterial spectrum (Gram-positive and -negative bacteria) and is stable at different temperatures and acidity conditions. It is produced by bacteria (Streptomyces albulus) by a fermentation process and used in Far East Asia as a food preservative, which is approved by the US food and drug administration (FDA) (Hiraki et al., 2003; FDA, 2004). The mechanism of its antibacterial effect is based on adsorption to the bacterial cell. The producing bacteria have a membrane aminopeptidase that degrades εPLS for self-protection purposes (Shima et al., 1984; Yoshida and Nagasawa, 2003).

εPLS, which is positively charged, interacts with the negatively charged phospholipid head groups, consequently causing a curvature folding on these membranes and leading to formation of vesicles and disturbance of membrane integrity (Hyldgaard et al., 2014). Other mechanisms include inducing oxidative stress by reactive oxygen species (ROS), and the response in which the cell cycle stops and DNA repair / mutagenesis is triggered (Ye et al., 2013). Figure 1-7 summarises the mechanism of PLS antibacterial action.
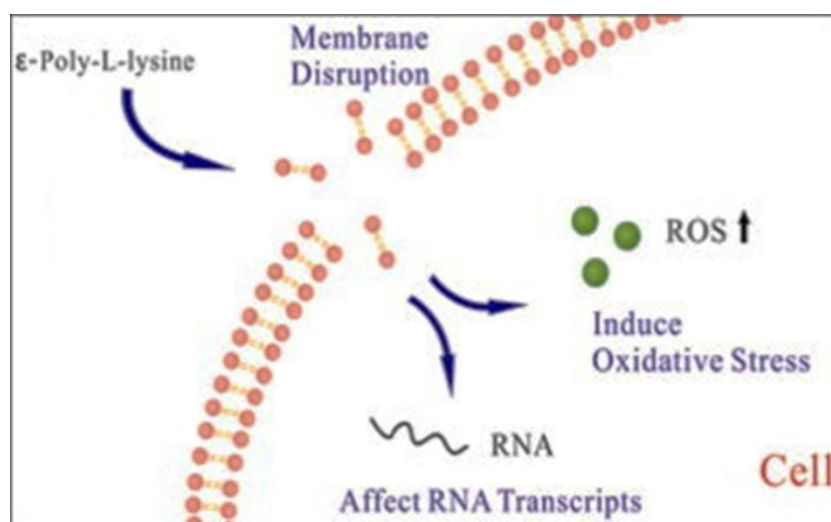
Figure 1-7 PLS mechanism of antibacterial action. Adapted from Ye et al. 2013. Copyright certificates are attached at the end of the thesis.

1.6 Developing the experimental formulations in this study

In the new experimental formulations described in this thesis, two novel agents were added to a conventional composite filler (PolyLysine PLS and Monocalcium phosphate

monohydrate MCP). This was mixed with an adhesion and etching promoting monomer (4META) dissolved in a low shrinkage liquid dimethacrylate phase. The monomers used in the liquid phase were UDMA (bulk monomer) and a novel low shrinkage diluent monomer (Polypropylene glycol dimethacrylate, PPGDMA) with CQ as an initiator. The formulations are detailed in the next chapter in 2.1.4.

If PLS is proved to be released into carious dentine, it can help kill any residual bacteria in the cavity upon placing the restoration. The release of MCP (remineralising agent) may encourage minerals precipitation (Hydroxyapatite formation) within the tooth structure (Aljabo et al., 2016b; L. Zhang et al., 2016; Xie et al., 2017). Such a property would help close any gap between the restoration and the cavity walls allowing better adhesion to tooth structure and less chance of recurrent disease. Another benefit would be remineralising of demineralised dentine. Thus, complete removal of carious tissues would not be required, and a minimally invasive technique may be applied by removing infected dentine only and saving the affected layer for self-repair. This could also limit the usage of injection and drilling. The adhesive monomer (4META) may encourage deep penetration and effective bonding with disease affected dentine. Achieving high degree of conversion would enable bulk filling the cavity following one step rather than the layering technique.

Previous results that led to development of these formulations have used many different compositions. The formulations were, however, always prepared by mixing two phases; liquid and powder. The powder phase contained glass fillers (powder and fibres), antibacterial agent (either Chlorhexidine or PolyLysine up to 10%wt) and remineralising agent (MCP or TCP or both). The liquid phase previously contained different combinations of:

- UDMA,
- TEGDMA or PPGDMA (diluent),
- 4META, HEMA or Pyromellitic Dimethacrylate (PMDM) (adhesion promoting monomer),
- CQ (initiator),
- and N, N-dimethyl-p-toluidine (DMPT) or Na-N-tolyglycine glycidyl methacrylate (NTGGMA) (activator) (Leung et al., 2005; Mehdawi et al., 2013; Aljabo et al., 2015; Aljabo et al., 2016a; Panpisut et al., 2016; Walters et al., 2016; Kangwankai et al., 2017; Panpisut et al., 2019).

This database was used to optimise a new formulation with varying amounts of MCP and PLS and two different powder / liquid ratios (PLR). The factorial analysis has helped weigh the relative effects of these variables on different tested properties.

1.7   How to regulate and CE mark

Medical devices are regulated by the Medicines and Healthcare products Regulatory Agency (MHRA). Medical devices can be divided into three main categories based on their potential for hazardous effects. According to the guidance document by the "European commission DG health and consumer" for classification of medical devices, rule 8 (see Figure 1-8) states that dental fillings fall within class IIa unless a remineralising or an antibacterial effect are to be claimed.
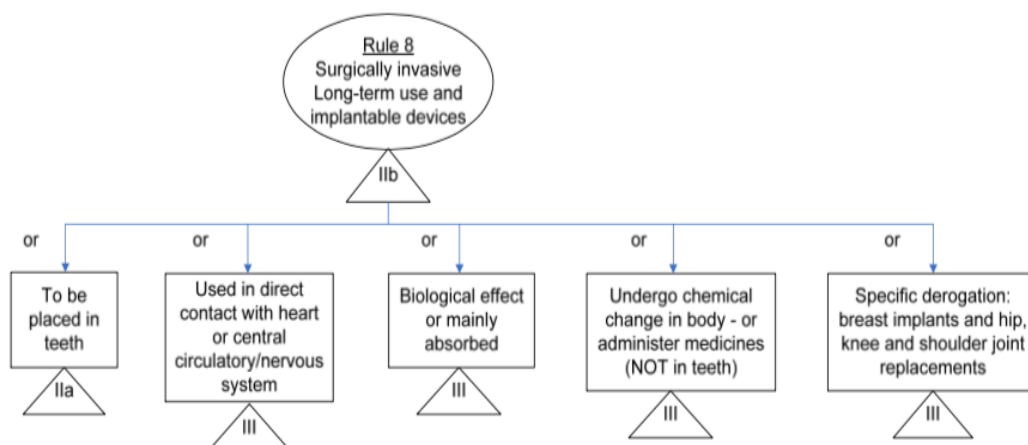
Figure 1-8 Rule 8 of the guidance document by the European commission DG health and consumer, for classification of medical devices. Copyright certificates for re-use of figures are attached at the end of the thesis.

Dental fillings fall within the category of surgically invasive implantable devices for long-term use (> 30 days). If these materials are bioactive and the manufacturer claims and shows hydroxyapatite formation, this will render the device has a biological effect which falls within class III. An antibacterial effect, however, will complicate things even more and make the device a class III medical device.

The aim of our research group was to CE mark an optimised formulation in collaboration with industry. The CE mark shows that the released product is considered fit for its purpose and meets the safety requirements in the directives. It will also help commercialise the product anywhere in the European Union.   As supporting dental companies were unwilling to market a class III device, this thesis focus was on the basic properties of a class IIa device that could be marketable without antibacterial or remineralising claims.

The steps to assure compliance of a class IIa medical devices are as follows:

- Classification: class IIa according to rule 8
- Choose conformity assessment route.

- Technical file: all data related to testing the final product.
- Get certification from a notified body.
- Declaration of conformity.
- Post market surveillance and handling complaint and safety issues.

Once certification from the notified body is received, the manufacturer can CE mark the products and start commercialising.

The technical file must contain the following (French-Mowat and Burnett, 2012):

- General description of the product.
- Design, how to manufacture and components.
- Risk analysis.
- The test results; how the product was tested and all relevant data.
- The measurements adopted to ensure safety of the product.
- The pre-clinical investigations.
- The clinical evaluation.
- The label and instructions for use.

1.7.1 Tests needed to comply with regulations

Standards published by the international standards organisation (ISO) were scanned to get relevant test protocols to apply to the proposed formulations and acquire data. Additionally, test protocols developed previously within the group or within this thesis were used. The main features tested were:

- chemistry and light curing kinetics,
- interactions with water (such as water sorption and solubility and mass and volume change),
- mechanical properties,
- biocompatibility
- radio-opacity,
- and adhesion to tooth structure

The project presented in this thesis starts with comparing eight different proposed formulations to choose an optimal one. After that, a proposed optimal final formulation was predicted and then manufactured and tested to ensure compliance with requirements.

1.8 Statement of problem

In order to overcome the previously addressed issues with current restorative materials and to comply with the Minamata Convention recommendation of mercury-amalgam restorations phase-down (FDI, 2014), a novel material is needed. This material should have some specific properties to enable its use to restore carious teeth of paediatric patients in an atraumatic way.

A bulk fill material is more feasible as a viable alternative when treating paediatric patients rather than the layering technique followed with resin composites. Therefore, higher depth of cure is favourable for such a material. Additionally, the proposed material should have an adequate strength to avoid future failure due to fracture. Resin modified glass ionomer restorations showed poor clinical performance which may be related to their lower strength compared to resin composites (Folwaczny et al., 2001; van Dijken and Pallesen, 2010). Resin composites have good strength but require more steps to apply (layering technique and bonding steps) (Baratieri and Ritter, 2001; Loguercio et al., 2003; Hickel et al., 2007; Namgung et al., 2013; Kim et al., 2017; Romero et al., 2017; Rothmund et al., 2017)

To be able to release the unique additives (PLS and MCP), it is expected that the formulation will show higher mass and volume change and higher water sorption and solubility. Early PLS release could beneficially kill any residual bacteria in the cavity. This is especially useful if the proposed formulation is meant to be applied in an ART (Atraumatic Restorative Technique) manner which does not require removal of all carious layers. MCP release will also help remineralise remnant caries.

In addition, however, these new components need to provide other key benefits and unique selling points so that antibacterial and remineralising claims are not required. Discoveries in this thesis show these include more effective cavity sealing through volume expansion, tubule penetration / tag formation and restoration interface or fracture site apatite precipitation. The studies will further demonstrate how effective sealing may help prevent the enzyme activated collagen degradation that can be observed with other material restorations.

1.9 Aims

The general aim of the following *in vitro* studies was to optimise a novel composite formulation suitable for children's teeth. The research stages were:

Stage 1. Assessment of whether the proposed eight formulations (F1- F8) conformed to ISO requirements of composites and how they compared with commonly used commercial materials (Glass ionomers and resin composite). The tested properties described in this thesis (Chapter 3) include:

- o Light-curing kinetics:
    - ▪ Delay time
    - ▪ Subsequent rate of reaction
    - ▪ Final monomer conversion
    - ▪ Calculated shrinkage
- o Interaction of cured discs with water
    - ▪ Water sorption and solubility
    - ▪ Mass and volume change and acidity
    - ▪ PolyLysine release
- o Mechanical properties using two different methods:
    - ▪ Three-point bending method
    - ▪ Biaxial flexural method

Stage 2. Creation of a caries-like model (collagen mesh) by demineralising sound dentine discs. This mesh was used to test the ability of the experimental formulations to penetrate and form tags (Chapter 4). The effect of varying PLS and MCP content on the studied properties were shown through the use of factorial analysis.

Stage 3. Based upon work in the first two stages, a final optimised formulation was predicted and prepared in house (F9) or by a manufacturer (F10) (DMG, Schottlander). The tests performed on these formulations (described in chapters 5, 6 and 7) were as follows:

- o Light-curing kinetics
- o Mechanical properties; biaxial flexural strength and modulus
- o Water sorption and solubility
- o Radio-opacity

Stage 4. The fourth stage included evaluating the ability of the optimised formulation F10 to adhere to tooth structure by checking its ability to:

- o self-etch enamel prior to light-curing,

- o adapt to cavity walls,
- o form tags within carious dentine or the collagen mesh model,
- o limit microleakage at the material/tooth interface
- o bond to enamel and dentine.

Stage 5. The final stage included testing the ability of F10 to remineralise caries-affected dentine and inhibit MMP activity at the adhesion interface.

The final optimised formulation F10, as of Jan 2019, has been going through clinical trials to support CE marking.

Content of the following chapters are as follows:

- In Chapter 2, a general description of the materials and methods used in different tests is explained.
- In Chapters 3 and 4, the focus is on the first eight proposed experimental formulations to gather as much data as possible to enable selecting an optimal formulation and understand how the components affect the studied properties.
- Chapter 5 summarises the results of chapters 3 and 4 and explains the chosen composition of the final formulations, F9 and F10, through a comparison of their main properties.
- Chapter 6 addresses the tests related to adhesion to tooth structure and whether using the final formulation without pre-etch and bond will be feasible.
- Chapter 7 demonstrates the ability of F10 to remineralise carious dentine and inhibit MMP activity.

The thesis structure is summarised in the following flowchart.

```
Thesis structure
│
├── Chapter 1:
│   literature review
│
├── Chapter 2:
│   Materials and methods
│
├── Chapters related to the
│   first eight formulations
│   │
│   ├── Chapter 3:                          ├── Chapter 4:
│   │   Basic properties of the first       │   Resin tags formation
│   │   eight experimental                  │
│   │   formulations                        │
│   │   │                                   │
│   │   └── light curing kinetics,          └── Creating caries-like
│   │       intercations of the discs           collagen discs to check
│   │       with water and                      ability to penetrate
│   │       mechanical properties
│
├── Chapters related to the final
│   formulations
│   F9 and F10
│   │
│   ├── Chapter 5:              ├── Chapter 6:              ├── Chapter 7:
│   │   Summary of chapters 3, 4│   Adhesion to tooth      │   The effect of the novel
│   │   and the basic properties│   structure              │   additives, MCP and PLS
│   │   of F9, F10              │   (F9, F10)               │
│   │                          │   │                       │
│   │                          │   └── Self-etch, cavity    └── Remineralising effect
│   │                          │       adaptation, tags         and MMP inhibition
│   │                          │       formation,
│   │                          │       microleakage and
│   │                          │       shear bond strength
│
├── Chapter 8:
│   General conclusion
│
└── Chapter 9:
    Future work
```

2   Materials and Methods

Thesis structure

Chapter 1:
literature review

Chapter 2:
Materials and methods

Chapters related to the first eight formulations

Chapter 3:
Basic properties of the first eight experimental formulations

Chapter 4:
Resin tags formation

light curing kinetics, intercations of the discs with water and mechanical properties

Creating caries-like collagen discs to check ability to penetrate

Chapters related to the final formulations
F9 and F10

Chapter 5:
Summary of chapters 3, 4 and the basic properties of F9, F10

Chapter 6:
Adhesion to tooth structure (F9, F10)

Chapter 7:
The effect of the novel additives, MCP and PLS

Self-etch, cavity adaptation, tags formation, microleakage and shear bond strength

Remineralising effect and MMP inhibition

Chapter 8:
General conclusion

Chapter 9:
Future work

This chapter summarises the materials and methods used in this research. For the materials section, the following was included:

- preparing storage solutions,
- commercial comparators used,
- chemicals used in the experimental formulations and their Raman and Fourier transform (FTIR) spectra,
- protocol for preparing the experimental formulation pastes,
- and preparing composite discs to be used in experiments.

The methods detailed in this section included those that were used frequently in more than one chapter or the ones recommended by ISO. Any variation in these tests is detailed in the methods section of relevant chapters. These tests include:

- Light-curing kinetics (delay time, rate of reaction, monomer conversion and calculated shrinkage)
- Interaction of light-cure discs with water:
    - Water sorption and solubility (ISO 4049-2009)
    - Mass and volume change and acidity (H^+ release)
    - PolyLysine release
- Mechanical properties
    - Three-point bending flexural strength and modulus (ISO 4049-2009)
    - Biaxial flexural strength and modulus
- Radio-opacity ISO 13116:2014
- Adhesion to tooth structure
    - Microleakage with enamel and dentine (ISO/TS 11405:2015)
    - Cavity adaptation
    - Shear bond strength (ISO 29022:2013)

2.1 Materials

2.1.1 Preparing solutions

2.1.1.1 Simulated body fluid (SBF) preparation

The simulated body fluid was prepared in accordance with ISO 23317:2014 (BSI, 2014a). To prepare 1L, The amounts of the chemicals used, and their weights are stated in Table 2-1.

Table 2-1 Chemicals used to prepare Simulated Body Fluid

Component		Quantity for 1L
Deionised water	H_2O	700 mL
Sodium Chloride	NaCl	8.035 g
Sodium Hydrogen Carbonate	$NaHCO_3$	0.355 g
Potassium Chloride	KCl	0.225 g
Di-potassium hydrogen phosphate trihydrate	$K_2HPO_4.3H_2O$	0.231 g
Magnesium Chloride Hexahydrate	$MgCl_2.6H_2O$	0.311 g
1M Hydrochloric acid solution	HCl	39 mL
Calcium Chloride Dihydrate	$CaCl_2.2H_2O$	0.371 g
Sodium Sulphate	Na_2SO_4	0.072 g
Tris-hydroxymethyl Aminomethane (TRIS)	$((HOCH_2)_3CNH_2)$	6.118 g

Plastic containers were used to prepare and store SBF to avoid apatite nucleation. Hygroscopic components were measured quickly. The apparatus was set by placing a plastic beaker filled with 700mL deionised water in a water bath with the temperature set at 36.5±1.5°C. Components were then gradually added following the same sequence in the table above (except for the last component; TRIS). Calcium Chloride was added very carefully to avoid precipitation. By the end of adding these components, the temperature was checked again (36.5±1.5°C). At this point, the pH should be around 2±1.

Subsequently, TRIS was added gradually (with enough time to allow the pH to settle after each addition) until pH reached 7.3. Temperature was set again at 36.5±0.5°C and TRIS added until pH reached 7.45. At this stage, hydrochloric acid solution was used to bring down the pH to 7.42. TRIS and hydrochloric acid were added alternately to keep the pH between 7.42 and 7.45 and the temperature at 36.5±0.2°C until all TRIS was added. Final pH was then brought back to 7.4 by using hydrochloric acid. The prepared solution was moved to a 1L flask and topped up with deionised water to reach a volume of 1L. It was then stored in a plastic bottle in the fridge and used within 1 month as long as the pH was stable, and the solution is clear.

2.1.1.2 Artificial saliva (AS) preparation

The artificial saliva was prepared following DIN 53160-1:2010 instruction (DIN, 2010):

The chemicals and their amounts are detailed in Table 2-2. To prepare a litre of artificial saliva (AS), the sodium and potassium salts were dissolved in 900mL of deionised water in a glass flask with magnetic stirrer plate. Calcium and Magnesium chlorides were then added gradually until a clear solution was achieved. The acid solution (hydrochloric acid 1M) was then added carefully with the pH meter (calibrated with buffer solutions) immersed in the mixing flask until a final pH of 6.8±0.1 was achieved. Solution was then moved to a volumetric flask and topped up with deionised water to a final volume of 1000mL.

The solution was stored at room temperature and pH checked before every use. If it had turned acidic, a base (potassium hydroxide KOH 1M) was used to adjust the pH.

Table 2-2 Chemicals used to prepare Artificial Saliva

Component		Quantity for 1L
Magnesium Chloride Hexahydrate	$MgCl_2.6H_2O$	0.17g
Calcium Chloride Dihydrate	$CaCl_2.2H_2O$	0.15g
Di-potassium hydrogen phosphate trihydrate	$K_2HPO_4.3H_2O$	0.76g
Potassium Carbonate	K_2CO_3	0.53g
Sodium chloride	NaCl	0.33g
Potassium Chloride	KCl	0.75g
1M Hydrochloric acid solution	HCl	To adjust pH value to 6.8

2.1.1.3 Buoyancy medium preparation

The buoyancy medium was used along with the density kit (Mettler Toledo, AG204) for composite disc mass and volume change measurements. It was prepared in accordance with ISO 17304:2013 (BSI, 2013b) by topping up 5g of Sodium Lauryl sulphate with deionised water in a glass bottle until a final weight of 500g. The bottle was then sealed and shaken until the solution was clear then stored at room temperature. The solution can be used for up to one month but was always prepared one day before using it.

2.1.2 Commercial restorative materials

The restorative materials that were used as a comparator in this research are mentioned in Table 2-3 with their composition (according to leaflets published on the manufacturers` websites). Fuji IX and Fuji II LC were chosen for their relatively easy clinical application method (also used in ART technique). Activa is gaining more popularity and is commercialised based on its bioactivity (remineralising effect). Filtek z250 is a standard composite resin material that has been used extensively in previous group work as a comparator.

Table 2-3 The commercial restorative materials and their composition

Material	Description	Manufacture	Composition
Fuji II LC	Resin modified glass ionomer	GC America	- Powder: liquid ratio 3.2/1 - Powder: Alumino-fluoro-silicate glass - Liquid: HEMA 25-50%, Polycarboxylic acid, UDMA 1-5%, DMA 1-5%, Camphorqunone <1%
Fuji IX GP	fluoride releasing glass ionomer	GC America	- Powder: liquid ratio 3.6/1 - Liquid: Distilled water 50%, Polyacrylic acid 40%, Polycarboxylic acid - Powder: Alumino-fluoro-silicate glass, Polyacrylic acid powder
Activa Kids	Bioactive restorative material (RMGI)	Pulpdent	Blend of diurethane and other methacrylates with modified polyacrylic acid, Silica and Sodium fluoride
Filtek Z250 (shade B3)	Aesthetic, light-cured, radiopaque composite	3M ESPE	BIS-GMA and a blend of UDMA and Bis-EMA(6) The particle size distribution is 0.01µm to 3.5µm with an average particle size of 0.6µm a combination of silica filler, zirconia filler, and zirconia/silica cluster filler
Scotchbond Universal Adhesive	Adhesive agent	3M ESPE	MDP Phosphate Monomer, Dimethacrylate resins, HEMA, Vitrebond™ Copolymer Filler, Ethanol, Water, Initiators, Silane

2.1.3 Chemicals used in experimental formulations

The chemical agents used and their purpose in the experimental composites are mentioned in Table 2-4. The rationale behind selecting these components was thoroughly discussed in the first chapter. Raman and Fourier transform (FTIR) spectrometers were used to acquire the spectra of these chemicals and assign detected peaks to related chemical structure.

Table 2-4 Chemicals used to prepare the experimental formulations

Agent: Its role in the composition	Company and Lot number
Urethane dimethacrylate UDMA: Basic monomer	DMG 100112/97406
Poly(propylene glycol) dimethacrylate PPGDMA 400: Diluent monomer	Polysciences 626208
4-methacryloyloxyethy trimellitate anhydride (4META): Adhesive monomer	Polysciences 697058
Camphorquinone (CQ): Initiator	DMG 100134/90339
Glass particles 7micron: Filler	DMG 020684/680326
Glass particles 0.7micron: Filler	DMG 02110/688344
Fumed silica: Filler	Aerosil OX50, Evonik industries, Germany 153022145
Monocalcium phosphate monohydrate (MCP): Remineralising agent	Himed, NY, USA. MCP-369925
PolyLysine (PLS): Antibacterial agent	Handary, Belgium. Epolyly, 020120160203,

The Raman and FTIR spectra of these chemicals are shown in Figure 2-1 and Figure 2-2. The mean peaks of these chemical spectra are explained in Table 2-5.
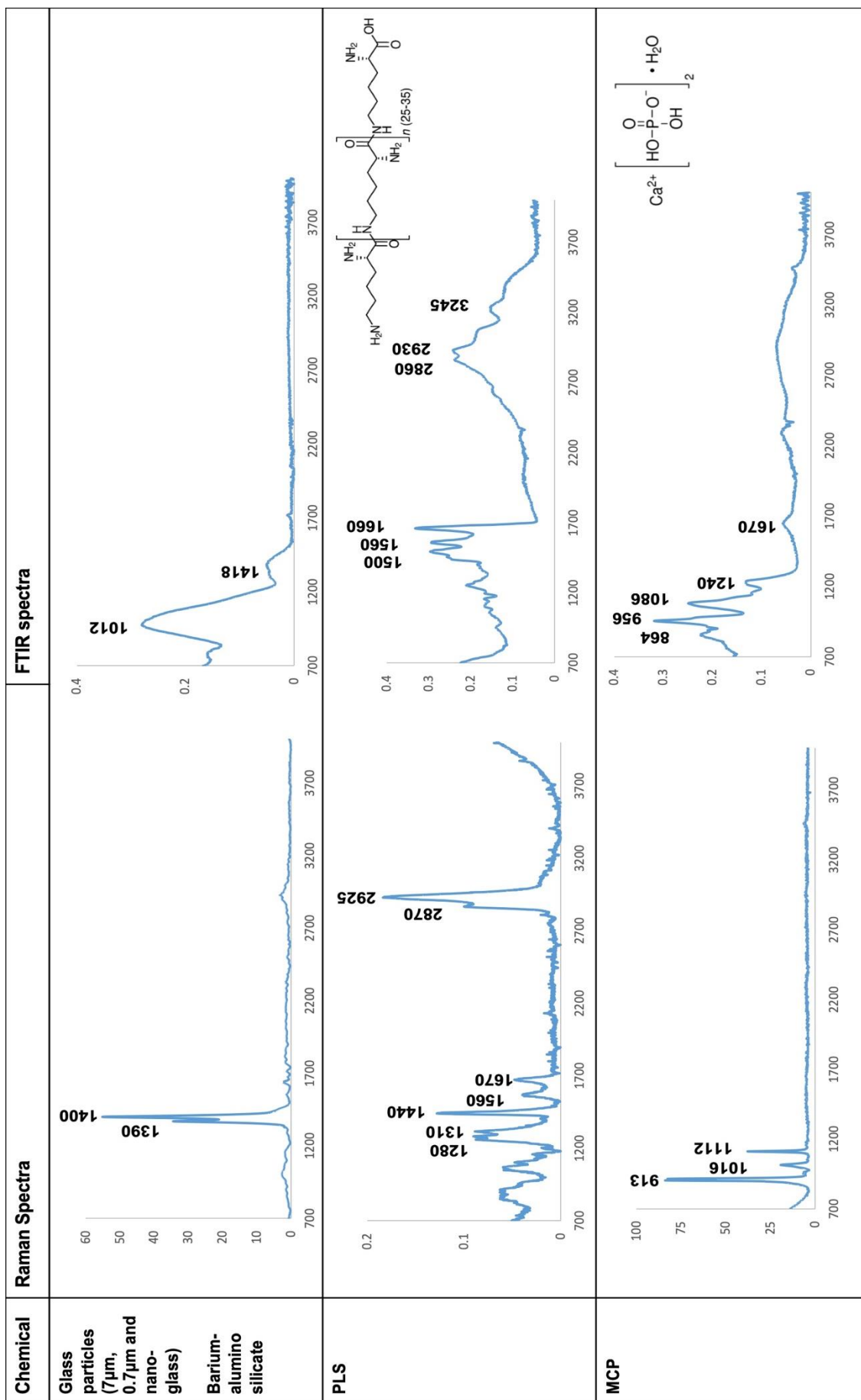
Figure 2-1 Raman and FTIR spectra of chemicals used in the powder phase of the experimental composites
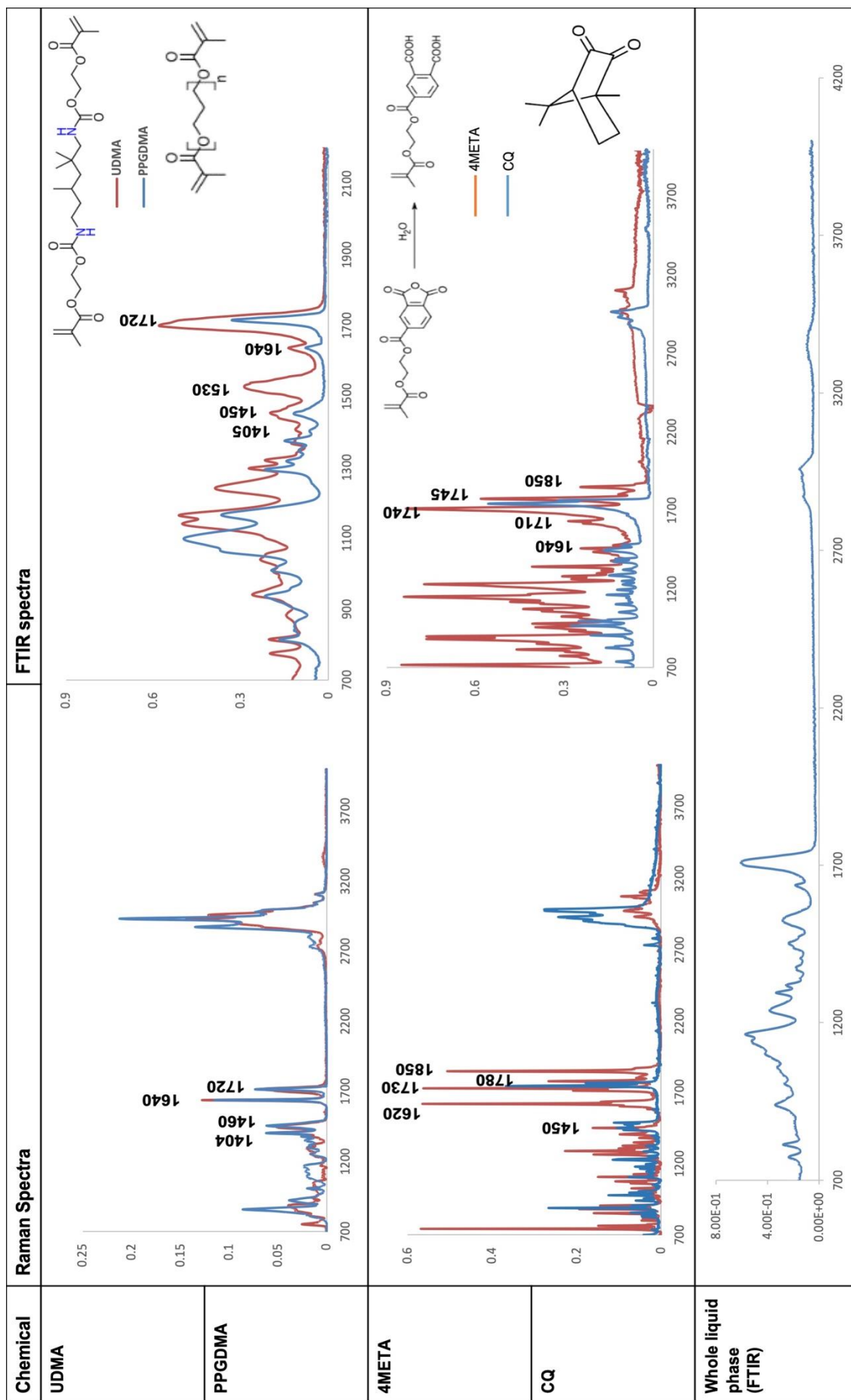
Figure 2-2 Raman and FTIR spectra of chemicals used in the liquid phase of the experimental composites

Table 2-5 Peaks assignment of chemicals Raman and FTIR spectra

Chemical agent	Raman spectra		FTIR spectra	
	Peak (cm^{-1})	Assignment	Peak (cm^{-1})	Assignment
Glass	1390	Glass peak	1012	SiO stretch
	1400	Glass peak	1418	Glass peak
PLS	1280	Amide III	1500	NH$_3^+$
	1310	Amide III	1560	Amide II N-H
	1440	CH$_2$	1660	Amide I C=O
	1560	NH$_2$	2860	CH$_2$ stretch
	1670	Amide I C=O	2930	CH$_2$ stretch
	2870	CH$_2$ stretch	3245	N-H
	2925	CH$_2$ stretch		
MCP	913	PO4	956	PO symmetric
	1016	PO4	1086	PO asymmetric
	1112	PO4	1670	OH
UDMA/PPGDMA	1404	C-H with C=C	1405	C-H with C=C
	1460	C-H scissor	1450	C-H scissor
	1640	C=C stretch	1630	C=C stretch
	1720	C=O stretch	1640	C=C stretch
			1720	C=O stretch
4META	1450	C-H	1640	C=C
	1620	C=C methacrylate	1710	C=O
	1730	C=O	1745	C=O
	1780	C=O	1850	C=O
	1850	C=O		
CQ	1450	C-H	1740	C=O
	1730	C=O		

2.1.4 Experimental materials paste preparation

In the current study, the liquid phase was mixed by adding 4META 3%wt (acidic monomer) and CQ 1%wt (initiator) to PPGDMA 24%wt (diluent monomer) and stirring for two hours at room temperature on a magnetic stirrer hot plate (Jeo Tech) until a clear liquid was obtained. UDMA 72%wt was then added as a base monomer and stirred for 24 hours until the liquid was again clear. The powder phase consisted of PLS (5% or 2%wt), MCP (8% or 4%wt) and 3 different sizes of glass particles (7µm, 0.7µm and Nano glass particles at 60%wt, 30%wt and 10%wt of total glass weight, respectively). Powder and liquid were combined in 25mL plastic pots at two different powder/liquid ratios (PLR: 3 or 5) and mixed for 40s in a speed mixer (Synergy speed mixer) at 3500rpm. Pastes

were stored in black pots (light-proof) at room temperature until used (usually small amounts were prepared to be used up within one month).

The 8 formulation variables were based upon a 2 level, 3 variables factorial design. The variables for different formulations are summarised in Table 2-6.

Table 2-6 Composite variables (PLR and percentage of PLS or MCP) in different formulations

	PLR	PLS (%)	MCP (%)
F1	5	5	8
F2	5	5	4
F3	5	2	8
F4	5	2	4
F5	3	5	8
F6	3	5	4
F7	3	2	8
F8	3	2	4

2.1.5 Samples preparation (cured composite discs)

Discs were prepared using a metal circlip as a mould (10mm inner diameter and 1mm thickness) pressed between two acetate sheets (Figure 2-3). These were pressed between two glass blocks to make sure that any excess was squeezed out, thickness was consistent, and any oxygen inhibition layer was avoided. Light-curing time was for 40s on each side with a rotational movement of the LED curing gun (wavelength range: 450-470nm, intensity from 1100-1330mW/cm^2, Demi Plus, Kerr, USA). Discs were then detached carefully from circlips and edges were finished to remove any sharp edges by means of fine grit-paper (size 1200). Compressed air was used to blow away any dust created while polishing.
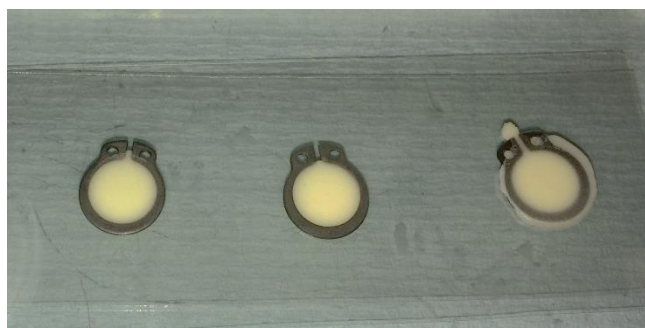
Figure 2-3 Example of disc-shape samples preparation

This method was always followed to prepare composite discs unless stated differently (water sorption and solubility test for example).

2.2 Methods

2.2.1 Light-curing kinetics of the pastes

Light-curing kinetics at the bottom of the sample was measured using FTIR (Perkin Elmer, UK) along with an Attenuated Total Reflectance attachment (ATR, Specac Ltd., UK). ATR-FTIR detects conversion of monomers into polymers in the lower surface of the material (in contact with the diamond). The spectral wavenumber range acquired was from 700 to 4000cm^{-1} at resolution of 4cm^{-1} for 15 minutes at 24°C (Young et al., 2004). Three repetitions were tested for each formulation and the curing started 30s after beginning of scanning. Example of the FTIR spectra before and after light-curing is shown in Figure 2-4.
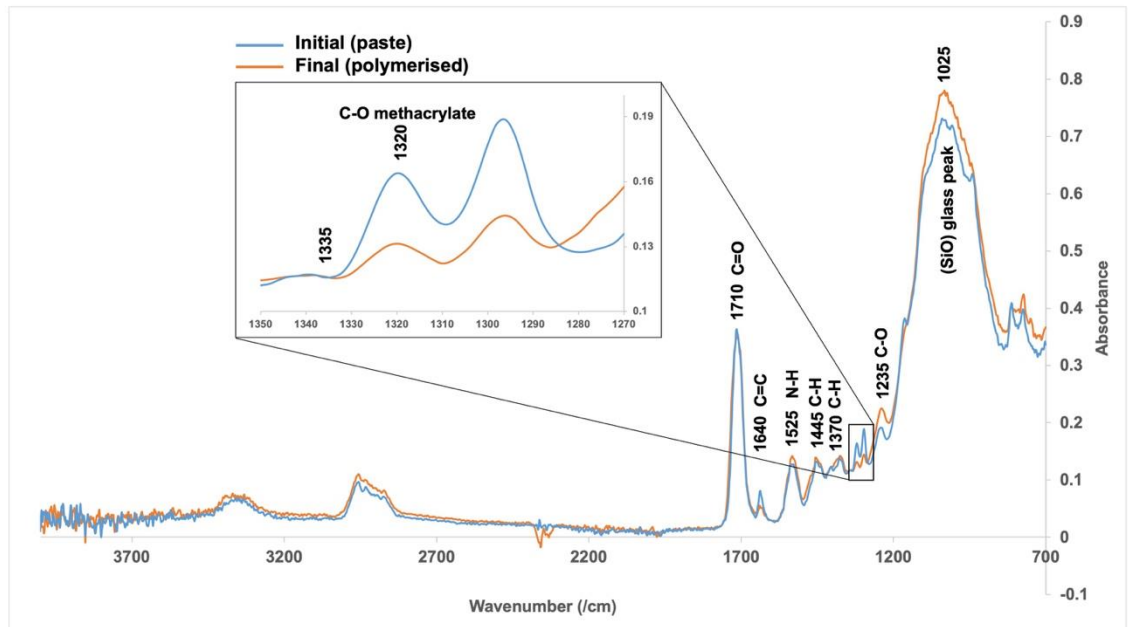
Figure 2-4 Representative FTIR spectra of the experimental composite (before and after light-curing), showing the peak used to plot profile

Monomer conversion converts the composite paste into a solid material. It results in bonding of the monomers in the liquid phase together to form first linear chains (up to 50% conversion) and then a crosslinked network of polymer chains. Beer-Lambert law states that absorbance of light is proportional to the component concentration, thickness and absorption coefficient. Hence, the following equation was used to calculate monomer conversion (Dewaele et al., 2006; Young et al., 2008):

$$C(\%) = \frac{100(h_0 - h_t)}{h_0}$$

Equation 2-1

Where h_0 and h_t represent methacrylate C-O peak absorbance at 1320cm^{-1} initially and at time t, using absorbance at 1335cm^{-1} as background (Aljabo et al., 2015). Changes in the height of this peak (most prominent change) reflects changes in the polymerising methacrylate. An example of monomer conversion versus time is given in Figure 2-5. The final conversion was obtained through linear extrapolation of data versus inverse time to zero.
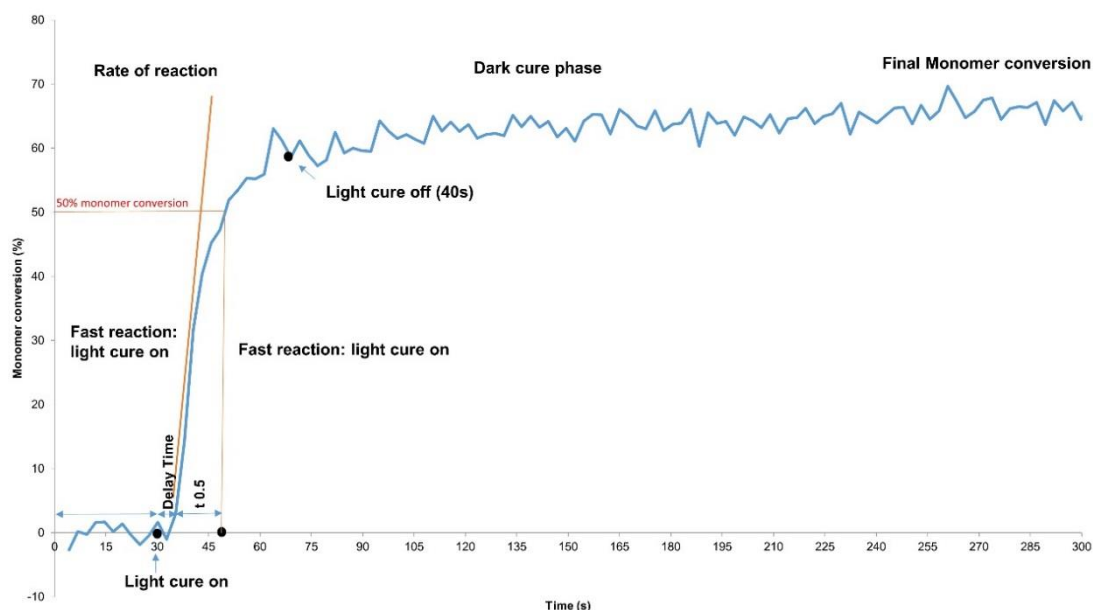
Figure 2-5 Representative FTIR spectrum profile plot of an experimental composite, showing the data points used to calculate delay time, rate of reaction and monomer conversion

Delay time is defined as the time between the start of light-curing and the actual start of monomers converting into polymers. It was calculated from the intercept on the x axis of the line through data in the fast-ascending part of the reaction profile.

The rate of reaction was calculated from the gradient of monomer conversion versus time. Typically, monomer conversion was obtained every 2.5s and 4 points were used to obtain the gradient. The maximum rate of change is provided in this thesis.

Volumetric shrinkage is the result of polymerising C=C groups, where one mole of polymerising C=C bond gives 23cm^3 volumetric change. Therefore, polymerisation shrinkage was calculated using the following equations (Rueggeberg and Tamareselvy, 1995):

$$\varphi = 23R_b \times 100 \qquad\qquad \text{Equation 2-2}$$

$$R_b = \left(M_f\right)C\rho \sum \frac{n_i x_i}{W_i} \qquad\qquad \text{Equation 2-3}$$

Where R_b is number of reacted C=C in a unit of volume, M_f is total mass fraction of monomer in the composite, C is final monomer conversion, ρ is the composite density (2.1 or 1.9 for 5:1 or 3:1 formulations, respectively), n_i is number of C=C per molecule (2 for UDMA, 2 for PPGDMA and 1 for 4META), x_i is monomer mass fraction in the liquid, W_i is the relative monomer molecular weight and Σ indicates summation of all the monomers in the liquid.

2.2.2 Interaction of the cured discs with water

2.2.2.1 Water sorption and solubility

Water sorption and solubility were determined following the instructions in ISO 4049-2009 (BSI, 2009). Disc shaped samples of 16mm diameter by 1mm deep were used. Light-curing method is detailed in relevant chapters.

Discs were dried (conditioned) using a desiccator and drying agent in a 37°C incubator and were weighed daily at room temperature until mass change was less than 0.1mg in a 24 hours period. This mass was recorded as m_1. After that, average thickness (4 readings) and diameter (2 readings) were measured and discs were immersed in 10mL deionised water and incubated at 37°C for 7 days. Discs were weighed again (m_2) then reconditioned (dried again) following the same initial protocol and reweighed (m_3).

The equation used to calculate water sorption (in µg/mm^3) was:

$$W_{sp} = \frac{m_2 - m_3}{V}$$

Equation 2-4

Where m_2 is the mass of sample after immersion in water for 7 days (µg), m_3 is the mass of sample after immersion and reconditioning (µg) and V is the volume of the sample (mm^3). The water sorption value recommended by ISO 4049-2009 for composites should be ≤40µg/mm^3.

The equation used to calculate water solubility (µg/mm^3) was:

$$W_{sl} = \frac{m_1 - m_3}{V}$$

Equation 2-5

Where m_1 is the mass of sample after drying but before immersing in water (µg). The water solubility value recommended by ISO 4049-2009 for composites should be ≤7.5µg/mm^3.

For a better understanding of water sorption and solubility, results in µg/mm^3 were converted into percentage of the initial mass of discs (mass change) using the following equations:

$$Sorption_\% = \frac{m_2 - m_1}{m_1} \times 100$$
Equation 2-6

$$Solubility_\% = \frac{m_3 - m_1}{m_1} \times 100$$
Equation 2-7

2.2.2.2 Mass and volume change, acidity (H$^+$ release)

Percentage change in mass and volume of cured composite discs upon immersion in water was tested using the density determination apparatus with buoyancy medium (2.1.1.3).

Mass of the sample, dry and upon immersion in deionised water (10mL), were used to calculate mass and volume change with the following equations:

$$Mass\ change\ (\%) = \frac{m_{dt} - m_0}{m_0} \times 100$$
Equation 2-8

$$Volume\ change\ (\%) = \frac{V_{dt} - V_0}{V_0} \times 100$$
Equation 2-9

where m_{dt} is the dry mass at a given time point (g), m_0 is the initial dry mass (calculated by linear extrapolation of first 5 data points versus square root of time to zero time), V_{dt} is the volume at a given time point and V_0 is the initial volume (calculated same as m$_0$).

Volume was calculated using the following equation:

$$Volume = F_c \times \frac{m_{dt} - m_{wt}}{D_w - D_a}$$
Equation 2-10

where F$_c$ is the weight correction factor (0.99958), m_{wt} is the mass of the sample under water, D_w is the density of water at a given temperature and D_a is the density of air (0.0012).

To assess the acidity of solutions and determine acid release at different time periods, samples were weighed then placed in 10ml of water and a pH meter (Orion star A111, Thermo Scientific) employed. The concentration of protons ([H$^+$]) in a liquid can be calculated from pH using the following equations:

$$pH = -\log_{10}[H^+]$$ Equation 2-11

$$[H^+] = 10^{-pH}$$ Equation 2-12

The cumulative concentration of acid released from a specimen was therefore estimated using

$$[H^+]\ release = \Sigma([H^+]_s - [H^+]_{dw})$$ Equation 2-13

where $[H^+]_s$ is the concentration of acid in the water in which the sample was stored, $[H^+]_{dw}$ is acid level found in deionised water and Σ indicates the sum over all solutions in which the sample was stored up to time t.

The chemical formula of MCP is $Ca(H_2PO_4)_2.H_2O$. When dissolved in water it can react as shown in the following equation:

$$Ca(H_2PO_4)_2.H_2O \rightarrow CaHPO_4 + H_3PO_4 + H_2O$$ Equation 2-14
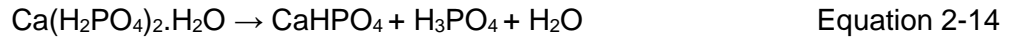
Assuming each phosphoric acid molecule generates only 1 proton the maximum concentration of H^+ expected to be released from a sample can be calculated using:

$$[H^+]_{max} = \frac{R_{PL}}{R_{PL}+1} \times \frac{m_{MCP}}{100} \times m/m_w$$ Equation 2-15

where R_{PL} is the PLR ratio, $\frac{R_{PL}}{R_{PL}+1}$ is the filler fraction by weight, $\frac{m_{MCP}}{100}$ is the MCP mass fraction in the formulation, m is the mass of the sample and m_w is the MCP molecular weight (252). By dividing the [H+] release by this maximum acid level an estimate of the fraction of the MCP that may have dissolved and reacted at a given time can be calculated.

2.2.2.3 PolyLysine release

High performance liquid chromatography (HPLC, Shimadzu) was used to quantify PLS released from discs into deionised water storage solutions. A mobile phase acted as the carrier of the collected solution through the instrument column (stationary phase). This mobile phase consisted of two solvents (solvent A: acetonitrile with 0.1vol% phosphoric acid and solvent B: deionised water with 0.1vol% phosphoric acid). The mixture was automatically pumped through a column (250 x 4.6mm, Phenomenax, Torrance, CA, USA), where different components travelled at different rates based on their interactions with the solvent. Therefore, the tested solution components eject from the column after

different retention times (the higher the interaction with the solvent, the lower the retention time). The resultant solution passed through UV detector and a chromatogram was acquired through the software.

Initially, PLS solutions of different concentrations (10 to 2000ppm) were prepared. High Performance Liquid Chromatograms (using HPLC instrument, Shimadzu) of these solutions were acquired. The HPLC column used 200μL of the solution volume and the test conditions were: 34 minutes total test time, 20 minutes retention time, wavelength was 210nm, bandwidth was set at 4nm and the temperature at 40°C. The instrument acquired 3200 points with 640ms interval using UV and visible light detector. The PLS peak was identified and area under the curve versus concentration was used to obtain a calibration curve. This was then used to calculate the amount of PLS released from composite discs upon immersion in water at different times. The calibration curve and a representative chromatogram are shown in Figure 2-6 and Figure 2-7.
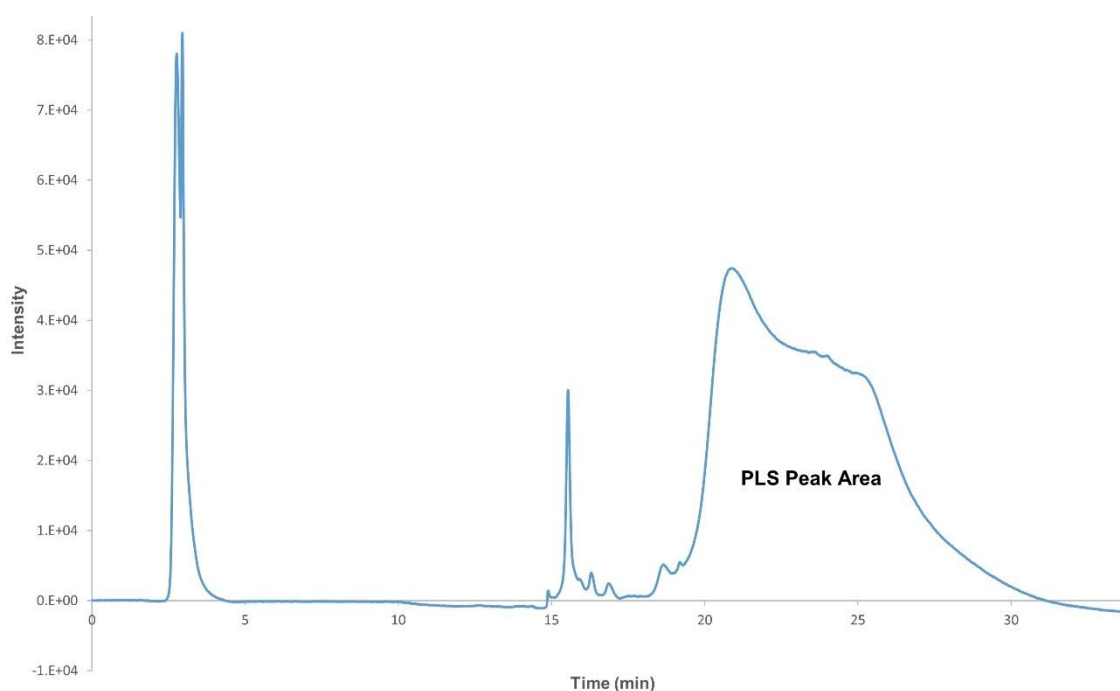
Figure 2-6 Representative PLS chromatogram with the area used to calculate PLS concentration in the tested water based on the calibration curve
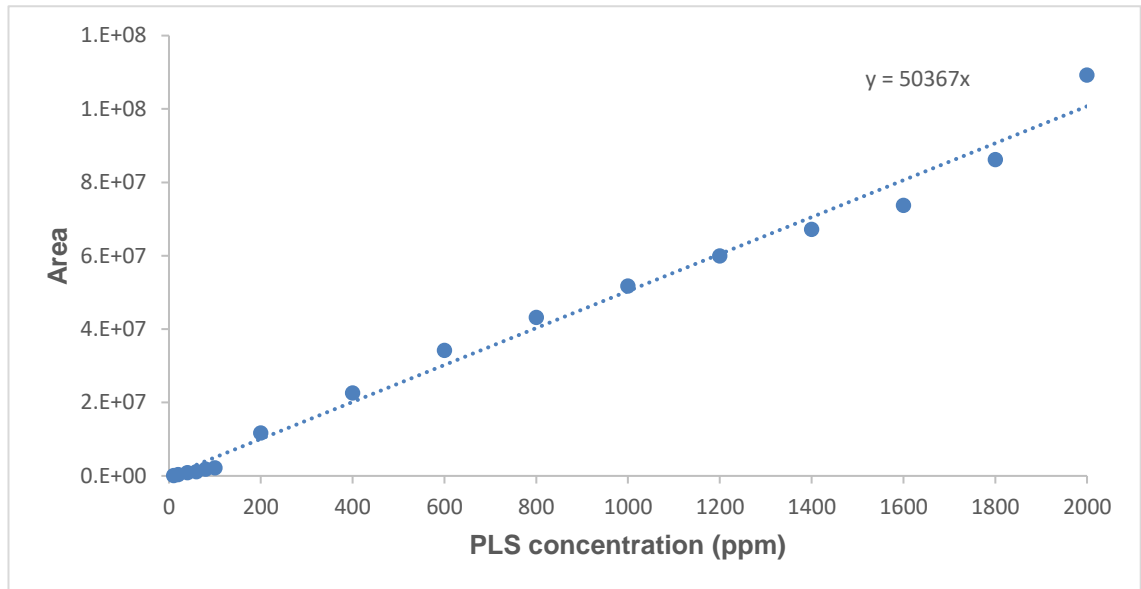
Figure 2-7 PLS calibration curve acquired from different concentrations of PLS solutions (10 to 2000ppm)

The equation used to calculate the cumulative release of PLS was:

$$R(\%) = \frac{100[\sum_0^t R_t]}{m}$$

Equation 2-16

where m is the weight of PLS powder in the sample (g), and R_t is the amount leached into water at each time point t.

2.2.3   Mechanical tests (flexural strength and modulus)

2.2.3.1   *Three-point bending flexural strength and modulus*

Three-point bending flexural strength and modulus were tested following the instructions of ISO 4049-2009 (BSI, 2009). Samples used where beam-shaped and the test instrument used was Shimadzu Autograph (AGS-X, Kyoto, Japan). After applying force at 0.75mm/min until sample fracture, a force versus displacement curve was obtained from the instrument as in Figure 2-8. The figure shows the maximum force point at fracture (used to calculate strength), slope of the curve (used to calculate modulus) and the area under the curve (used to calculate toughness).
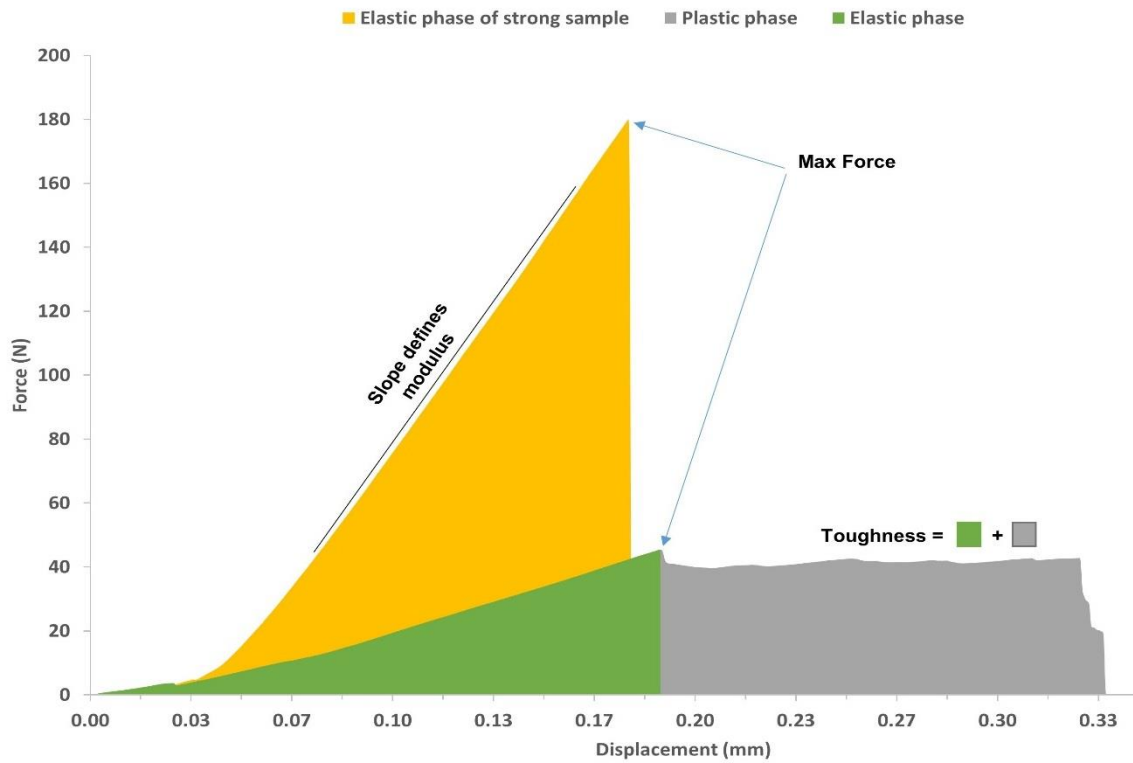
Figure 2-8 Representative graph of force versus displacement showing Max force point selection (F), slope used to calculate modulus and area under the whole curve (toughness) of two samples.

The equations used to calculate 3-point bending flexural strength and modulus of elasticity were:

$$S = \frac{3Fl}{2bh^2}$$
Equation 2-17

$$E = \frac{Fl^3}{4bh^3\beta}$$
Equation 2-18

Where β is deflection of the material (mm) before failure, F is the maximum force (N) reached as the specimen broke and (b,h,l) are the beam dimensions (mm) as shown in Figure 2-9.

Toughness was calculated by measuring the total energy area under the curve (Force versus displacement) which represents the sum of the elastic and plastic phases.

2.2.3.2 Biaxial flexural strength and modulus

The method used to determine biaxial flexural strength and modulus was similar to the three-point bending test. The differences between the two methods were:

- Sample shape (discs)
- The jig used (ball on ring) as in Figure 2-9
- The crosshead speed (1mm/min)
- Followed up till 6 months (until the results levelled off)
- The equations to calculate flexural strength and modulus
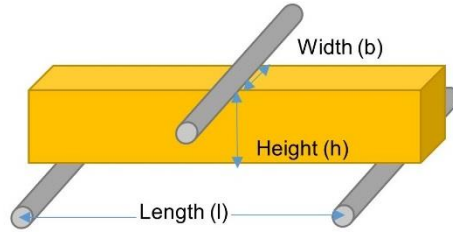
Three-point bending   ## Biaxial flexural strength
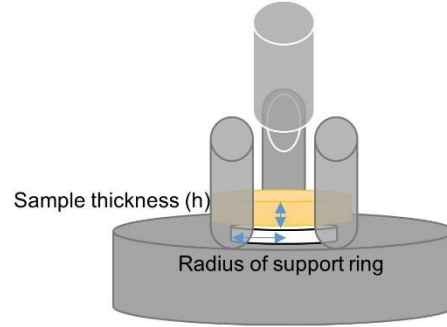
Figure 2-9 Schematic of different jigs, sample shape and sample mounting in mechanical tests

The following equations were used to calculate biaxial flexural strength and modulus assuming that the radius of the loading contact b=t/3 based on the Hertzian theory (Higg et al., 2001):

$$S = \frac{3(1+v)F}{4\pi h^2}\left\{1 + 2ln\left(\frac{a}{b}\right) + \frac{(1-v)}{(1+v)}[1 - \frac{b^2}{2a^2}]\frac{a^2}{r^2}\right\}$$ Equation 2-19

where F is the force (N), h is the sample thickness (mm) v is Poison`s ratio (0.3), a is the radius of the support ring, b is the radius of the loading contact, r is the radius of the sample.

$$E = \left(\frac{\Delta J}{\Delta W_c}\right) * \left(\frac{\beta_c h^2}{q^3}\right)$$ Equation 2-20

where $\left(\frac{\Delta J}{\Delta W_c}\right)$ is the slope gradient of load versus central deflection and β_c is the centre deflection function (β_c=-0.2584+0.8361(1- v ^{2})=0.5024) (Higg et al., 2001), h is the sample thickness and q is the ratio of the radius of the support ring to the radius of the sample (a/r).

2.2.4 Radio-opacity

Radio-opacity of materials was determined following the instructions of ISO 13116:2014 (BSI, 2014b). Any variation in the method is mentioned specifically in the relevant chapter. X-ray photons interactions with the material depends on their wavelength, frequency and energy. The main interactions include:

- Coherent scattering: it occurs with photons of energy less than 10keV,
- Compton effect (scattering): this effect is not related to the atomic number of the scanned material and is less apparent with higher X-ray energy
- Photoelectric effect (absorption): it increases with higher atomic number and decreases with higher X-ray energy (most important in dental X-ray)

Based on the above, the absorption of X-ray photons by the imaged discs might also be explained by Beer-Lambert law.

Composite discs were prepared as in (2.1.5) and X-ray taken using an occlusal X-ray film (Ultra speed D). Specimens were placed on the film beside an aluminium step-wedge (thickness range from 3.14 to 15.84mm with equal incremental increase from step1 to step5). X-ray source was aimed perpendicular to the film with a total of 30cm distance between the X-ray source and the film. The samples were irradiated for 0.2s at 60kV. This procedure was repeated three times using three separate X-ray films. Sample thickness was 1 or 2mm (specified in relevant chapters) although ISO recommends 1mm only.

Films were then developed, fixed, placed on an X-ray reader and imaged for further analysis through image analysis software (ImageJ, Fiji). The sample thickness (T_s) was measured using a digital calliper to an accuracy of 0.01mm. The software was used to evaluate the greyscale of the aluminium steps to create a plot of optical density versus thickness of aluminium (Figure 2-10, Figure 2-11) to which the greyscale of the samples irradiated were compared. Therefore, aluminium thickness equivalent of each sample was established (T_a). The average value of the three repetitions was reported.

Theoretically, the greyscale values span from 0 to 255 (0 is black, 255 is white) and the plot of the aluminium step-wedge should go up to 255 when none of the X-ray photons manage to transmit through the material and down to 0 when no barrier is used (X-ray directly aimed at the film). This will create a linear plot from 0 to 255. However, the x-ray film itself is not white and therefore will not reach a value of 255 and the plot will start to level off at some thickness based on the energy of the X-ray used.

Radio-opacity was calculated by dividing T_a/T_s. An average result was taken out of the three repetitions.

A material is considered radio-opaque if its radio-opacity is equal to or greater than 1mm of aluminium. Radio-opacity of human dentine and enamel are 1.5-2.5mm, respectively.
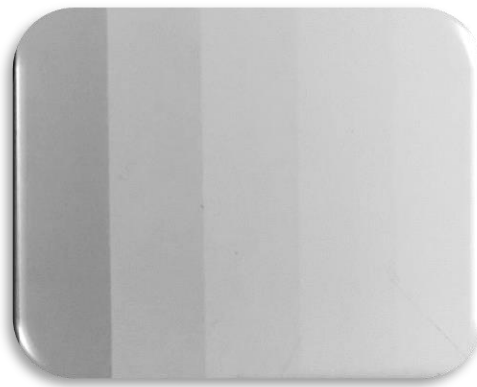
Figure 2-10 X-ray of the aluminium step-wedge used in determining the materials radio-opacity (thicker step on the right)
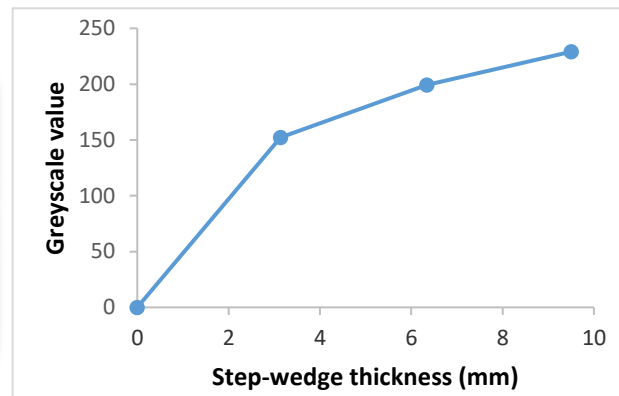
Figure 2-11 Greyscale plot of the aluminium step-wedge which was used to figure out the aluminium equivalent (T_a) of different samples

2.2.5 Adhesion to tooth structure

Adhesion to tooth structure was tested using three different methods; penetration of a blue dye into the bonding interface (microleakage), bond strength to bovine enamel and dentine (shear bond strength) and the restoration adaptation to cavity walls (X-ray Computed Tomography scan XCT). All human teeth used in this research were collected from the Eastman hospital biobank under a generic project ethical approval #1304.

2.2.5.1 Microleakage

The microleakage at the interface between the restoration and tooth structure was tested following the instructions of ISO/TS 11405:2015 (BSI, 2015) but using primary teeth instead of third molars.

Primary molars were used within 6 months of their extraction date (after extraction, teeth were cleaned and disinfected by storing in Chloramine T 1% for 2 days then stored in deionised water in the fridge until used).

Cavity preparation and restoration:

To test microleakage with enamel, round cavities (about 2mm diameter 2mm depth) were drilled into the distal, mesial, buccal and lingual walls of the tooth (n varied between groups, 11 to 31, due to limitations in getting human teeth for research purposes) using a high-speed handpiece with cooling water and cylindrical diamond burs (1.6mm diameter, 4mm length). Each of the cavities was then restored using different materials.

A fine diamond bur was used to polish the fillings and ensure removal of any excess covering the interface between the material and the tooth.

When testing microleakage with dentine, the same methods were followed but with the following adjustments:

- The depth of the cavity was 3mm to compensate for the enamel thickness that will be removed
- Filling surface was polished, and the enamel layer was totally removed (final depth of cavity was about 2mm).

Testing method:

Teeth were incubated in water at 37°C for 24 hours then taken out. To limit dye penetration to the interface only, apices were sealed with adhesive wax and the rest of tooth surface was covered with 2 layers of nail varnish (except for the fillings and 1mm around them). Specimens were immersed in staining solution (aqueous methylene blue 1%) for 4 hours. Subsequently, samples were rinsed, dried and cross-sectioned through the fillings (parallel to the tooth long axis) using a diamond disc to check penetration of the dye into the interface. The cross-sectioned teeth were examined under a magnifier and scored as follows:

- Enamel:
  - o 0: no microleakage
  - o 1: microleakage within enamel only (did not exceed the amelodentinal junction)
  - o 2: microleakage passed the amelodentinal junction (reached dentine) but did not reached the pulpal wall
  - o 3: microleakage reached the pulpal wall
- Dentine:
  - o 0: no microleakage
  - o 1: microleakage did not reach the pulpal wall
  - o 2: microleakage reached the pulpal wall

The deeper the penetration of the dye, the bigger the gap between the restoration and the cavity wall.

2.2.5.2 Cavity adaptation

One of the methods of testing adhesion to tooth structure detailed in ISO/TS 11405:2015 (BSI, 2015) is measuring the gap at the cavity wall/ restoration interface formed upon curing the material. If the bond strength is high enough to resist shrinkage of the material, the gap will be smaller. The method is similar to microleakage test except that at the end, instead of staining the cavities, the surface is grinded down to expose a deeper interface

and the maximum gap formed is measured under x5 magnification. However, this method only takes into consideration one cross-section of the whole volume of the interface and does not evaluate the ability of the material to adapt to cavity walls in general.

Therefore, a novel method was used to evaluate the gap formed as well as adaptation to cavity walls in an attempt to visualise that interface in a 3D model. This method involves the use of X-ray computed tomography (XCT) following the same restoration method as in enamel microleakage test using a primary tooth. The restorative materials used to fill the drilled class V cavities were the optimised formulation, Activa, Fuji IX, Fuji II LC or z250. Each material was applied and light-cured according to the manufacturer instructions (detailed in relevant chapter). Additionally, the experimental composite was used to fill a carious primary molar upon manual excavation of the very soft caries (infected dentine).

Tooth was then scanned by means of XCT to check adaptation of different materials to cavity walls. This method is non-destructive; it enables evaluating the inner structure without having to section the samples. Additionally, it gives high quality X-ray images, which allow evaluating the whole interface in 3D angles rather than the 2D images acquired from a normal X-ray. The XCT scan was performed at the school of engineering, University of Portsmouth, by Dr Alexander Kao and Dr Gianluca Tozzi. Raw data was sent back to Eastman for further analysis.

X-ray computed tomography (XCT) was conducted using an x-ray microscope (Xradia 510 Versa, Carl Zeiss Microscopy, USA) operating at a voltage of 90 kV with a power of 8W and a target current of 89mA. A ZEISS LE5 filter was positioned directly after the x-ray source to filter the x-ray spectrum. A high-resolution tomography was captured for each filling sample using an optical magnification of 4x to achieve an isotropic voxel size of $1.91\mu m$. 2001 projections were collected over 360 degrees at an interval of 0.179 degrees with for each tomography reconstruction. An exposure time of 5s was used for each projection.

2.2.5.3 Shear bond strength

Shear bond strength testing was undertaken following ISO 29022:2013 (BSI, 2013a).

Tooth preparation:

Bovine incisors (Rocholl GmbH, Germany) were stored in deionised water in the fridge and used within 6 months of extraction. Teeth were potted in epoxy resin horizontally with the labial surface facing upwards. Samples were ground using P200 grit paper then

polished using P500 grit paper to expose an adequate flat surface of labial dentine for bonding. The exposed surface allowed testing of bond strength to enamel and dentine as in Figure 2-12.
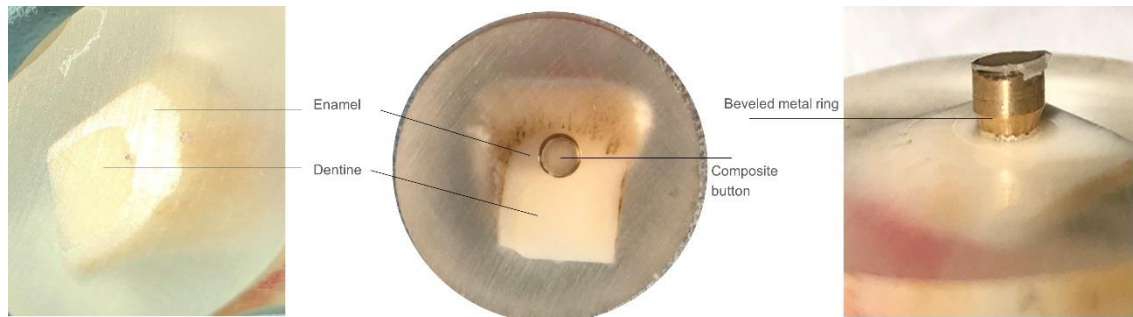
Figure 2-12 Exposed enamel/dentine labial surface (bovine tooth) and the composite button application to the surface

Bonding procedures:

Potted teeth were kept in water at room temperature for 4 hours before applying restorations. A metal button was used to apply the restoration material to the exposed surface (Figure 2-12).

To test bond strength, the method used to apply different materials was according to its manufacturer`s instructions in terms of whether to apply acid etch and/or bond (based on the restored surface; enamel or dentine). Additionally, one group was assigned to test the bond strength of the experimental formulation to acid etched enamel and dentine (30s or 15s, respectively).

Bonding surface was blot dried using filter paper. The following two steps were followed only if recommended by the manufacturer:

- Bonding surface was etched then washed thoroughly and air dried for 5s (using the oil-free air syringe of the dental unit).
- Universal bonding agent (Scotchbond universal, 3M ESPE) was applied on etched surface and rubbed for 20s, air-spread then light-cured for 20s.

Restoration was then applied on top (using a metal button of approximately 3mm diameter and 2mm height). Samples were stored in water and incubated at 37°C for 1 day before testing shear bond strength.

Testing shear bond strength:

A Shimadzu Autograph testing machine (AGS-X, Kyoto, Japan) was used with crosshead speed 1mm/min. The adhesion surface was loaded with a parallel force using

a sharp blade in contact with that surface until failure (Figure 2-13). The following equation was used to calculate shear bond strength:

$$\sigma = \frac{F}{A_b}$$

Equation 2-21

where σ is stress (MPa); F is force (N); A_b is bonding area (mm²).
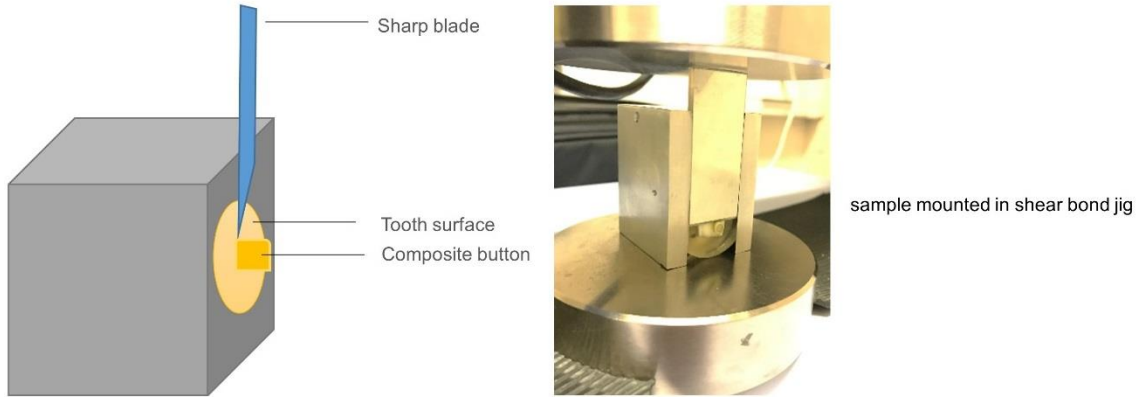
Figure 2-13 Shear bond strength test sample mounting and a schematic of the jig used

2.2.6 Statistical analysis

All values and error bars reported were the mean with 95% confidence intervals (95% CI) unless stated differently in the figure caption.

Factorial analysis for two and three variables (each at high and low levels) was used to measure the effect of variables (a_1, a_2, a_3) and their interactions ($a_{1,2}$, $a_{1,3}$, $a_{2,3}$, $a_{1,2,3}$) on properties of composites (P).The following two equations demonstrate the factorial expression of data in a three variables, two levels factorial analysis (Mehdawi et al., 2013):

$$lnP = <lnP> \pm a_1 \pm a_2 \pm a_{1,2}$$

Equation 2-22

$$lnP = <lnP> \pm a_1 \pm a_2 \pm a_3 \pm a_{1.2} \pm a_{1,3} \pm a_{2,3} \pm a_{1,2,3}$$

Equation 2-23

where $<lnP>$ is the average value of lnP. The average effect of changing each variable (a_i) from low to high was calculated using the following equations:

$$a_i = 0.5 ln\frac{g_h}{g_0}$$

Equation 2-24

where g_h and g_0 are the geometric means of the property of samples sharing the same level of the variable (high versus low, respectively).

The following equations were used to calculate the percentage increase or decrease in property (P) caused by a variable (a_i):

$$Increase\% = 100(exp_{2a_i} - 1)$$

Equation 2-25

$$Decrease\% = 100(\frac{1}{exp_{2a_i}} - 1)$$

Equation 2-26

Figure 2-14 explains the relation between a_i and the corresponding percentage change in the studied property.
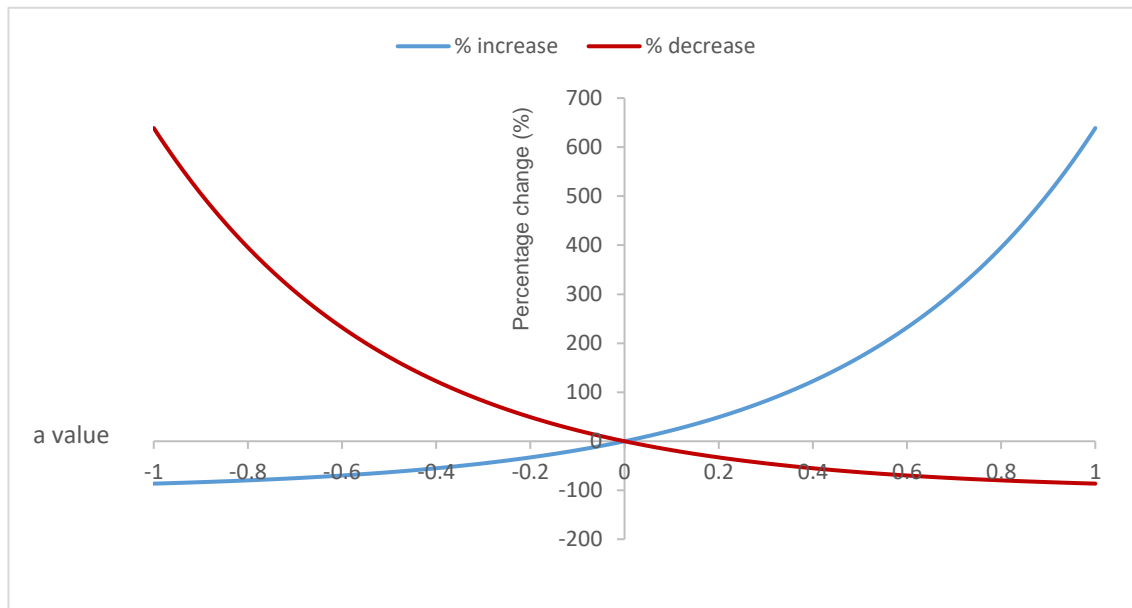
Figure 2-14 a values and the corresponding percentage change in the studied property

If the 95% confidence interval of a variable is less than the magnitude of a_i with minor interaction effect, the effect of that variable is considered significant. Therefore, if the error bar of the variable passes zero, the effect of that variable on the analysed property is not significant.

 SPSS Statistics version 24 for Windows (IBM, USA) was used for statistical analysis. Levene's test was used to assess homogeneity of variance. When variances were equal, data were analysed using one-way analysis of variance (ANOVA) followed by post-hoc Tukey's test for multiple comparisons when needed. Kruskal-Wallis test was used if their variances were not equal followed by pairwise comparisons if needed (Yan et al., 2017). The significance value was p=0.05. Line fitting for regression analysis was undertaken using the Linest function in Microsoft Office Excel 2016 for Windows.

3 Basic Properties of Composite Formulations with Different Levels of Additives

Thesis structure

Chapter 1:
literature review

Chapter 2:
Materials and methods

Chapters related to the first eight formulations

Chapter 3:
Basic properties of the first eight experimental formulations

Chapter 4:
Resin tags formation

light curing kinetics, intercations of the discs with water and mechanical properties

Creating caries-like collagen discs to check ability to penetrate

Chapters related to the final formulations
F9 and F10

Chapter 5:
Summary of chapters 3, 4 and the basic properties of F9, F10

Chapter 6:
Adhesion to tooth structure (F9, F10)

Chapter 7:
The effect of the novel additives, MCP and PLS

Self-etch, cavity adaptation, tags formation, microleakage and shear bond strength

Remineralising effect and MMP inhibition

Chapter 8:
General conclusion

Chapter 9:
Future work

3.1 Abstract

Aims:

The purpose of the work presented in this chapter was to test the light curing kinetics (delay time, rate of reaction, monomer conversion and calculated shrinkage) and stability of the experimental formulations (with varying PLR, PLS and MCP content). The interaction of cured discs with water (water sorption and solubility, mass and volume change and PLS release) and the mechanical properties (three-point bending and biaxial flexural strength and modulus) were also tested.

Materials and methods:

FTIR spectroscopy was used to look at the light-curing kinetics of different thicknesses (1, 2, or 3mm) of F7 at different curing times (10, 20 or 40s). Subsequently, light-curing kinetics of all formulations fresh or aged pastes in comparison to the commercial material Filtek z250 were tested at 24°C using 1 or 4mm thick samples, light-cured for 40s. ISO 4049-2009 methods were followed to test water sorption and solubility and three-point bending flexural strength and modulus. Mass and volume changes were recorded up to 3 months. HPLC was employed to quantify the cumulative amount of PLS released over a course of 2 months. Finally, biaxial flexural strength and modulus of disc-shape specimens were recorded until 6 months and their ability to heal fractures was observed.

Results:

The experimental formulations FTIR spectra showed only minor changes upon ageing and showed high monomer conversion (~>60%) even with aged 4mm samples. This went up to >70% with thinner fresh samples.

The water sorption values ranged from 22 to 56µg/mm^3 while the values of water solubility ranged from 4 to 19.4µg/mm^3. The final mass change ranged from 1.3-3.6% while the final volume change ranged from 1% to 2.7%. The percentage of H$^+$ release ranged from 4.5% to 34.2% of the maximum [H$^+$] that might be released from a sample assuming one molecule of H$^+$ release per molecule of MCP. The final cumulative PLS release after 2 months ranged between 7% and 25.9%.

All formulations passed the ISO minimum requirements of three-point bending flexural strength (≥80MPa) with an average value of 90MPa. They also exhibited a modulus of elasticity of greater than 5GPa. The biaxial flexural strength and modulus results showed as well that mechanical properties levelled off after 3 months of soaking in water. SEM observations confirmed the ability to heal fractures and reprecipitate minerals at crack zones.

Conclusion:

Twenty seconds was sufficient light-curing time to achieve >50% monomer conversion in samples of 2 or 3mm thick. Higher PLR caused an increase in delay time and a decrease in rate of reaction. All formulations appeared to be stable upon ageing.

The additives (PLS and MCP) caused an increase in water sorption and solubility, mass and volume change and H^+ release. All formulations were able to release the novel additive PLS.

Flexural strength of all experimental formulations after one day of soaking in water was higher than 80MPa and the decrease in mechanical properties (caused by the higher content of PLS and MCP) levelled off after 3 months.

3.2 Introduction

Following the Minamata Convention recommendation of mercury-amalgam restorations phase-down (FDI, 2014), novel materials that overcome problems with the other current restorative materials would be timely. Ideally these should have the following properties:

1) Good paste stability with a high level and depth of cure following a short period of light exposure and low associated polymerisation shrinkage. This would enable "bulk fill". This feature is particularly beneficial when treating paediatric patients as it allows a quick single step placement unlike with conventional resin composites.

2) Controlled water sorption to enable expansion to compensate polymerisation shrinkage and release of ions for remineralisation and antibacterial PLS. These features should help reduce bacterial microleakage and increase the feasibility of using the composite with the Atraumatic Restorative Technique (ART) which advocates reduced removal of all caries affected layers.

3) Sufficient long-term mechanical properties and self-healing features that help avoid fracture.

3.3 Hypothesis

The null hypothesis is: There is no significant difference between the proposed experimental formulations and a commercial material (Filtek z250) in terms of light-curing kinetics, water sorption and solubility, mass and volume change, acidity, PLS release and mechanical properties.

3.4 Aims and objectives

By varying the formulations PLR, PLS and MCP content, it will be possible to detect and quantify the effect of each variable and variable interactions on material properties by means of factorial analysis.

The aim of this chapter is to test the basic properties of the proposed experimental composites, which include:

- Light-curing kinetics:
    o Delay time
    o Subsequent rate of reaction
    o Final monomer conversion
    o Calculated shrinkage

- Interaction of cured discs with water
    - Water sorption and solubility
    - Mass and volume change and acidity
    - PolyLysine release
- Mechanical properties using two different methods:
    - Three-point bending method
    - Biaxial flexural method

3.5 Materials and methods

3.5.1 Light-curing kinetics of the pastes

Light-curing kinetics were assessed at 24°C by measuring delay time, rate of reaction, final monomer conversion and calculated shrinkage properties as in (2.2.1).

Initial studies were performed using F7 only. Delay time and rate of reaction were investigated (see Table 2-6) with samples of 1, 2, 3 and 4 mm thickness, the aim being to determine trend lines and minimum exposure times required for more than 50% conversion. Final monomer conversion of F7 was then found for three different thicknesses (1, 2 and 3mm) and three light-curing times (10, 20 or 40s).

Polymerisation kinetics of all eight experimental formulations along with the commercial z250 were then investigated at room temperature (24°C). Two different thicknesses were used (1 and 4mm) to check depth of cure with 40s light-curing exposure time (n=3). The experimental composites were also aged (at 60°C for 6 months) and polymerisation kinetics reassessed (1 and 4mm, 40s exposure time) to test stability of the pastes.

3.5.2 Interaction of the cured discs of all experimental formulations with water

3.5.2.1 Water sorption and solubility

Composite discs (n=6) were prepared as in (2.1.5) but they were larger in diameter (about 16mm) as instructed by ISO 4049-2009 (BSI, 2009). Therefore, to light-cure the samples, 13mm diameter light gun tip was used instead of the regular 6mm one. The exposure time was 40s on each side with rotating motion of the light gun to cover the whole surface of the disc. The sides of the discs were checked for any irregularities, polished accordingly with fine grit abrasive paper (1000) and the dust blown away with compressed air.

Discs were then stored in a desiccator with silica drying agent in a 37°C incubator. Discs were considered totally dry by checking the weight daily (2 hours after moving the samples out of the incubator) until a constant mass (no more than 0.1mg mass loss) was achieved (m_1). The drying process took about 2-3 weeks. Mean diameter (at two perpendicular points) and mean thickness at 4 points were recorded.

Each specimen was then immersed in 10mL deionised water and stored at 37°C for seven days. Samples were blot dried with filter paper to remove visible moisture, waved in the air for 15s and weighed again (m_2). Reconditioning (drying) of the samples was accomplished again in a similar manner (using a desiccator and 37°C incubator) until

constant mass was achieved (m_3). The calculations used to measure water solubility are mentioned in (2.2.2.1)

3.5.2.2   Mass and volume change and acidity (H⁺ release)

Composite discs were prepared as in (2.1.5) (n=3). Each disc was weighed dry and in soapy water (prepared as in 2.1.1.3) (mean of three readings) then immersed in 10mL deionised water and incubated at 37°C. Dry and in-water weight of the discs was recorded (mean of three readings) at 1hr, 3hr, 6hr, 1d, 3d, 1w and then every week till 12 weeks. At each time point the discs were moved into a fresh 10mL of deionised water and the pH of the previous time was measured using pH probe (Orion star A111, Thermo Scientific). Cumulative mass and volume change were calculated as in the equations mentioned in (2.2.2.2). The method of calculating H⁺ release based on pH of the water and the percentage of MCP content is mentioned in (2.2.2.2).

3.5.2.3   PolyLysine release

Composite discs (n=3) were prepared as in (2.1.5). The weight of each disc was recorded. Each sample was immersed in 1mL of deionised water and incubated at 37°C. At each time point (1h, 3h, 6h, 1d, 2d, 3d, 1w, 2w, 1m and 2 months), discs were moved into a fresh 1mL of deionised water. Only 200µL of the collected water were analysed through HPLC machine (Shimadzu) to measure the percentage of the PLS released from discs based on a calibration curve obtained using solutions of known concentration of PLS (between 10 and 100ppm). The percentage of PLS release was calculated through measuring the area under the PLS peak in the chromatograph and comparing it to the calibration curve. The equation used to calculate PLS release is mentioned in (2.2.2.3)

3.5.1 Mechanical tests (flexural strength and modulus)

3.5.1.1   Three-point bending flexural strength and modulus

Composite beams of 3x3x25mm were prepared in a metal mould (n=5) and light-cured for 40s at 5 different points starting in the centre as instructed in ISO 4049-2009. The assembly was then placed in a water bath of 37°C for 15 minutes. The light-cured surface was marked, and the beams were polished manually using a 500 grit abrasive paper. Each sample was then immersed in 10mL of deionised water at 37°C for 24 hours. A Shimadzu Autograph (AGS-X, Kyoto, Japan) was used and the samples were placed in three-point bending jig (as in Figure 2-9) with the cured surface facing upwards. Force was applied with a crosshead speed of 0.75mm/min. Four out of five samples of each

formulation are required to have a flexural strength ≥80MPa to pass the ISO requirements. The equations and method used to calculate 3-point bending flexural strength and modulus of elasticity are mentioned in (2.2.3.1)

3.5.1.2 Biaxial flexural strength and modulus

Composite discs (n=8) were prepared as in (2.1.5). Biaxial flexural strength and modulus of all experimental composites and the commercial (z250) were tested dry and after 1 day, 1 week, 1 month, 3 months and 6 months of immersion in 10mL deionised water at 37°C. A Shimadzu Autograph (AGS-X, Kyoto, Japan) was used with crosshead speed 1 mm/min and the jig used was ball on ring (as in Figure 2-9). The equations and method used to calculate biaxial flexural strength and modulus are mentioned in (2.2.3.2)

Toughness was also calculated as in (2.2.3.2) by measuring the total area under the force versus displacement curve

3.5.1.3 Fracture healing observations

Eight of the discs that did not totally collapse upon biaxial flexural testing were placed in SBF for 2-3 months. Scanning electron microscope (SEM) and Energy dispersive X-ray (EDX) were used to image discs as a qualitative method to assess material ability to self-repair or promote precipitation of minerals. These discs were from different formulations (F1, F3, F4, F6).

3.6 Results

3.6.1 Light –curing kinetics of the pastes

3.6.1.1 Light-curing kinetics of F7 samples

With F7, delay time increased linearly from 2s to 17s, while the rate of reaction decreased linearly from 4.5 to 2%.s^{-1} with increasing sample thickness from 1 to 4mm (Figure 3-1). Monomer conversion (Figure 3-2) with 10s light exposure was sufficient time to achieve more than 50% conversion in 1 or 2mm thickness of the material. No conversion was achieved by curing the 3mm thickness sample of F7 for 10s although 20s was sufficient for more than 50%.
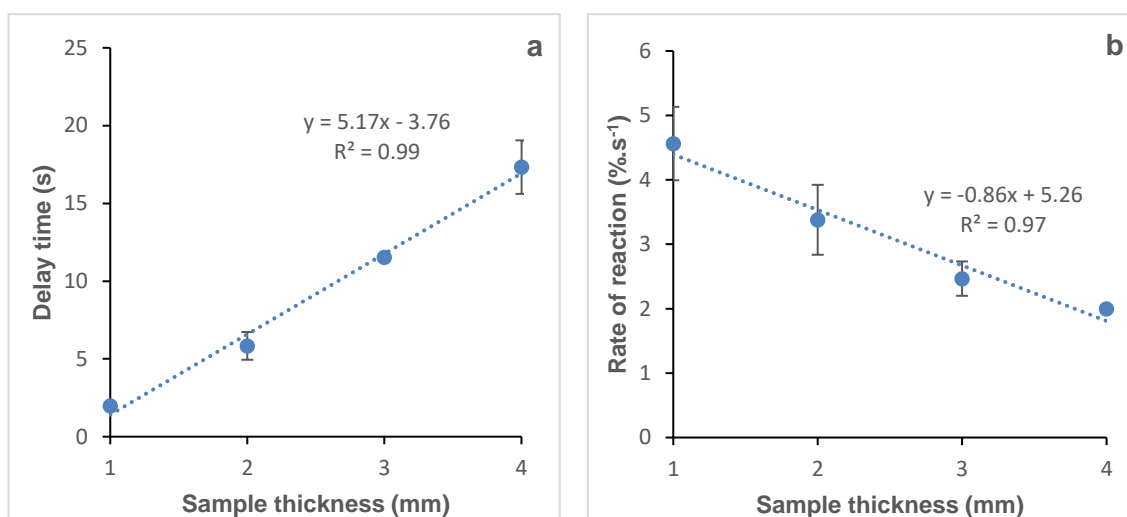
Figure 3-1 Effect of sample thickness on delay time (a) and subsequent rate of reaction (b) at room temperature (24°C) determined by FTIR. Error bars are 95% CI (n=3)
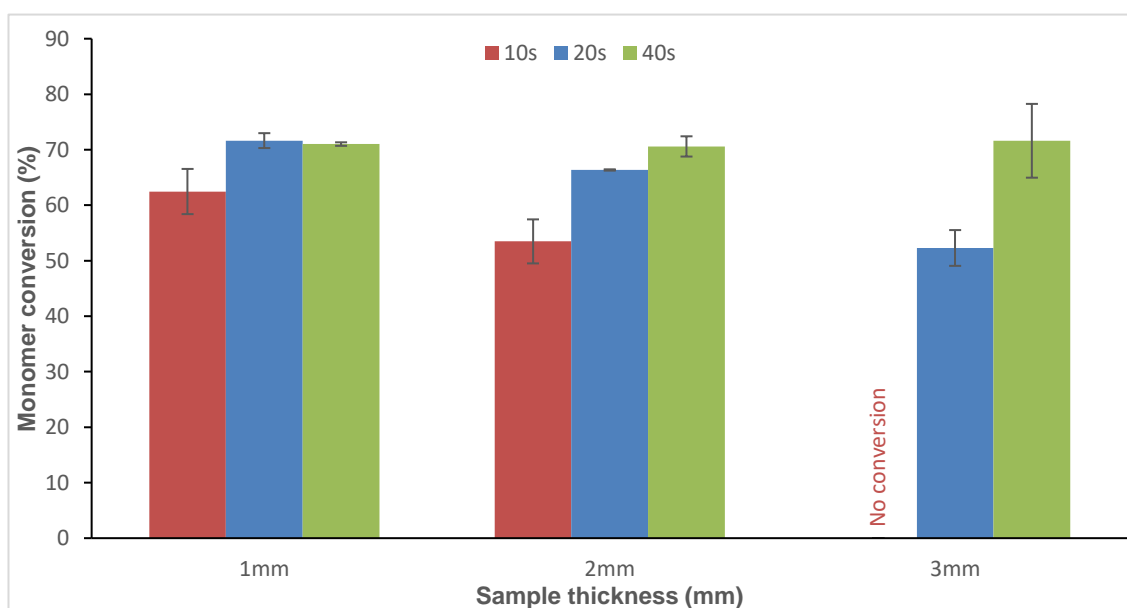
Figure 3-2 Monomer conversion of F7 using three different thicknesses (1, 2 or 3 mm) and three different light-curing times (10, 20, 40s) at room temperature (24°C) determined by FTIR. Error bars are 95% CI (n=3)

3.6.1.2 Average reaction kinetics parameters for all experimental formulations

The delay time, rate of reaction, monomer conversion and calculated shrinkage for all experimental formulations are provided in full in Appendix A. Major differences were seen between the commercial and experimental materials. Furthermore, large effects were caused by thickness and aging, whilst composite PLR, PLS and MCP caused lesser and complex effects. Average results of the 8 formulations, with or without ageing at 1mm or 4mm, are therefore compared with those of z250 in Table 3-1. These are discussed with factorial analysis, to demonstrate smaller effects of experimental composite composition, in the next sections.

Table 3-1 Average values of delay time, rate of reaction, monomer conversion and calculated shrinkage of all 8 experimental formulations upon light-curing the samples for 40s at room temperature (24°C) compared with that of z250. The results are for groups of different thicknesses (1 or 4 mm) and fresh pastes versus aged for 6 months at 60°C. Each group has n=24 and 95% confidence intervals are provided.

	Delay time* (s)	Rate of reaction* (%.s^{-1})	Monomer conversion* (%)	Calculated shrinkage (%)
1mm	2.7 ± 0.0	3.1 ± 0.4	71.7 ± 0.9	2.7 ± 0.3
4mm	16.6 ± 1.8	1.5 ± 0.1	65.8 ± 1	2.5 ± 0.3
1mm aged	4.0 ± 0.8	3.4 ± 0.5	68.6 ± 0.9	2.6 ± 0.3
4mm aged	12.6 ± 1.7	1.8 ± 0.2	62.2 ± 3	2.4 ± 0.3
z250 (1mm)	2.6 ± 0.1	4.9 ± 1	55.1 ± 1.7	N/A
z250 (4mm)	6.1 ± 1.7	1.5 ± 0.2	54.2 ± 2	N/A
*Full results are available in **Appendix A**				

3.6.1.3 Delay time for all experimental formulations

The average delay time for unaged experimental samples was 2.7s for 1mm and 16.6s for 4mm depth. When the samples were aged, delay time went slightly up to 4s with 1mm samples and went down to 12.6s with 4mm samples (Table 3-1). Full results are shown in Figure 10-1, Appendix A.

Factorial analysis of delay times is shown in Figure 3-3. Results for different thickness and aging are analysed separately in order to observe more readily the smaller effects of composition. For 1mm results and 4mm unaged data, variable "a" terms, interaction effects and average error bars were comparable demonstrating no material composition variable had a dominant effect. The major factor to affect delay time when 4mm aged samples were tested was the PLR. Using Equation 2-25, the percentage increase in delay time due to higher PLR was 32% (from 10.8s to 14.2s). In comparison with the >600% increase upon changing thickness this was a small effect. However, there were

strong interaction effects. Furthermore, there was also a PLR / PLS interaction (a_{12} term) complicating the effect.
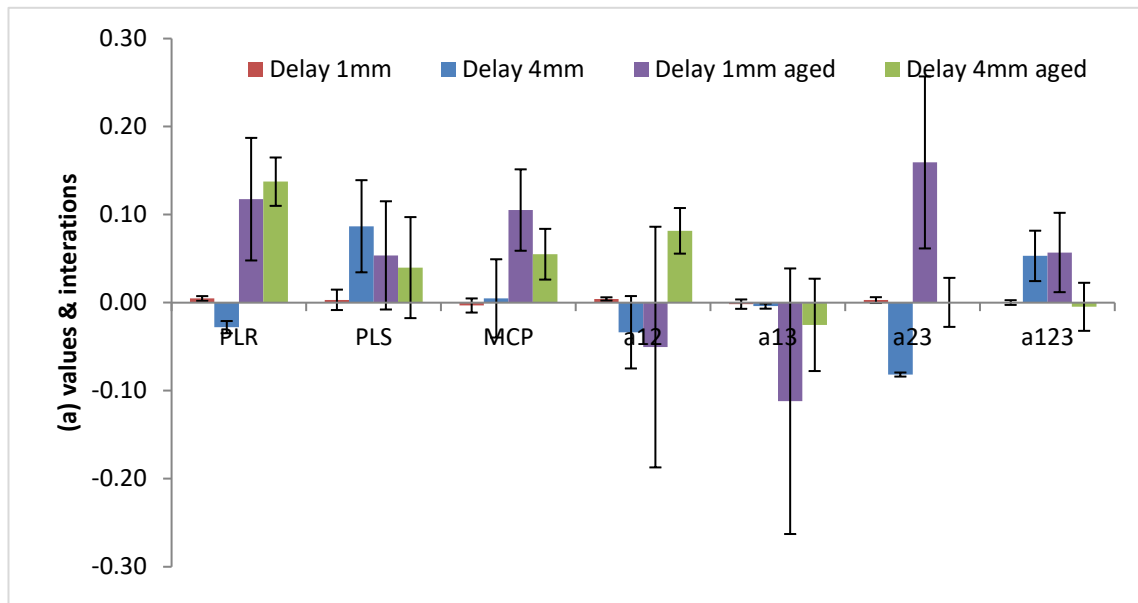
Figure 3-3 Factorial Analysis (a values and interactions) of delay time. a1 is PLR, a2 is PLS and a3 is MCP

3.6.1.4 *Rate of reaction for all experimental formulations*

Average rate of reaction on lower surfaces was halved with thicker samples. On average, it was $3\%.s^{-1}$ and $1.5\%.s^{-1}$ for samples of 1mm and 4mm thickness, respectively. Full results are shown in Figure 10-2, Appendix A. Ageing had a slight effect on the rate of reaction, with the aged formulations showing average values that were $0.3\%.s^{-1}$ higher at both 1 and 4 mm (Table 3-1).

Factorial analysis showed no single variable or interaction had a dominant effect on the rate of reaction (Figure 3-4). Largest magnitude of "a" was ~0.1 which corresponds with ~20% change or $0.5\%.s^{-1}$ change in the value of reaction rate. This was small in comparison with the $1.5\%.s^{-1}$ change observed with thickness variation.
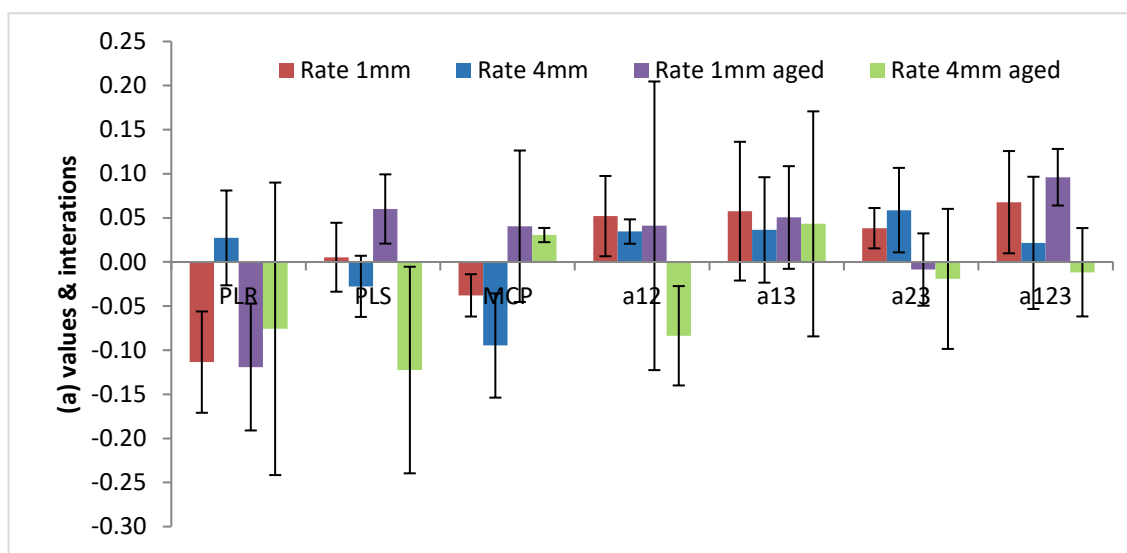
Figure 3-4 Factorial Analysis (a values and interactions) of rate of reaction. a1 is PLR, a2 is PLS and a3 is MCP

3.6.1.5 *Monomer conversion for all experimental formulations*

The average monomer conversion achieved with 1mm thick samples of the experimental formulations was 72%. This went down to 66% when the samples thickness was increased to 4mm. These results were significantly higher than the 55% and 54% conversion achieved by 1mm and 4mm thickness samples of the commercial material z250, respectively ($p = 9.6*10^{-12}$ to $4.5*10^{-3}$) (Figure 3-5). The full results of monomer conversions are in Figure 10-3, Appendix A.
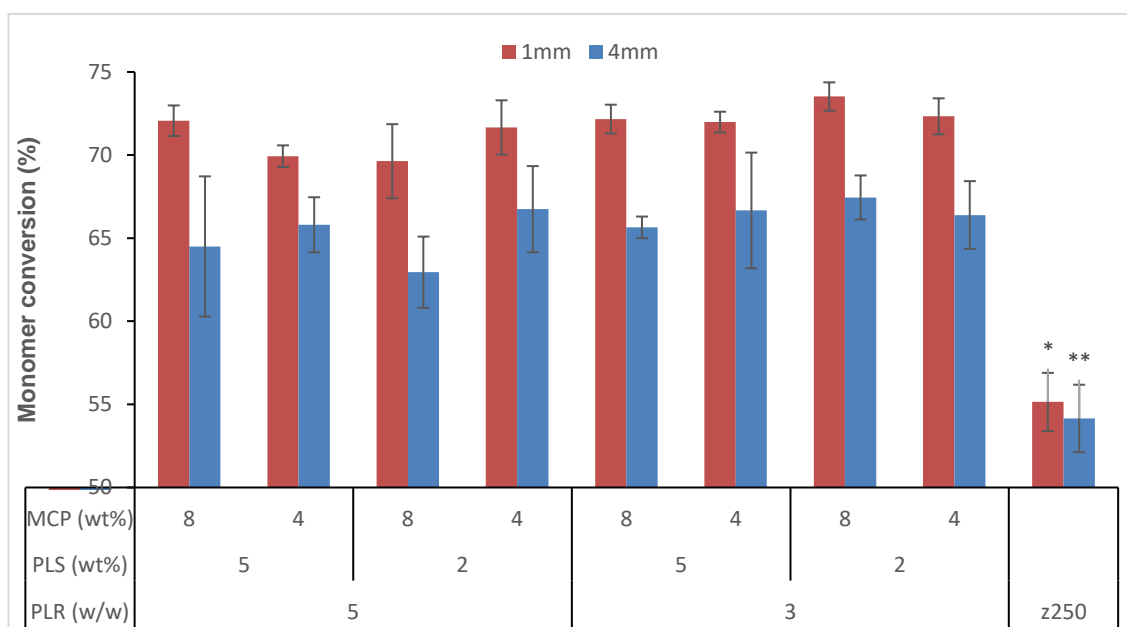
*Figure 3-5 Monomer conversion of all experimental formulations compared to z250 as a control. Samples were light-cured for 40s at room temperature (24°C). * or ** indicates significance from all other groups. Error bars are 95% CI (n=3)*

Factorial analysis of monomer conversion showed that the variables (PLR, PLS, MCP) and their interactions (Figure 3-6) had only minor effect on monomer conversion with unaged samples. However, when formulations were aged, the analysis showed that 4mm thick samples with higher content of PLS caused 11% lower monomer conversion (calculated using Equation 2-26).
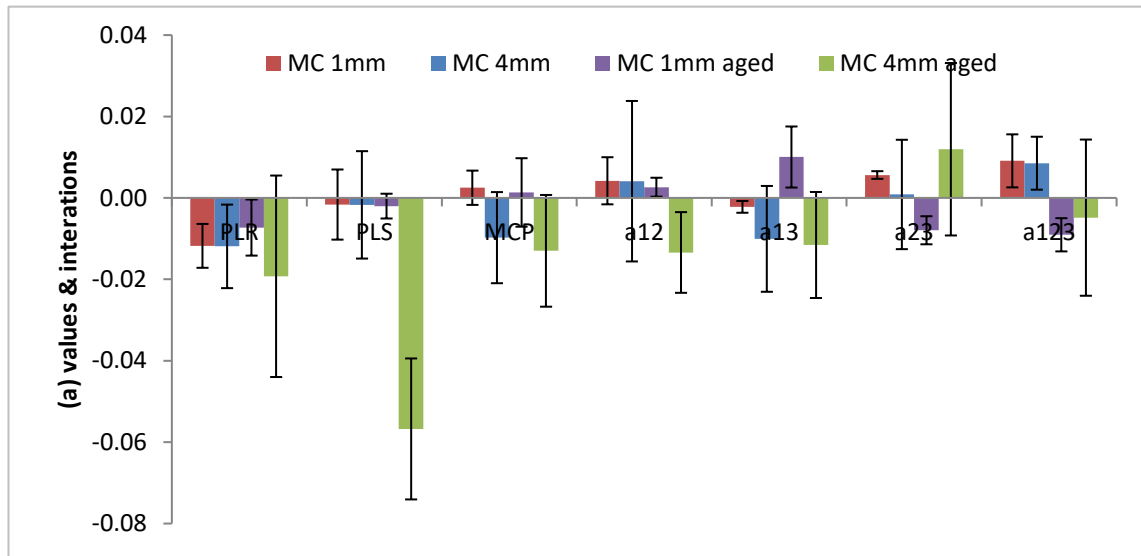
Figure 3-6 Factorial Analysis (a values and interactions) of monomer conversion. a1 is PLR, a2 is PLS and a3 is MCP

3.6.1.6 *Calculated shrinkage for all experimental formulations*

Calculated shrinkage was affected majorly by PLR (Figure 3-7). Using Equation 2-25, the percentage increase in property was calculated. Samples of lower PLR showed 40% increase in calculated shrinkage on average regardless of the thickness or the ageing conditions.
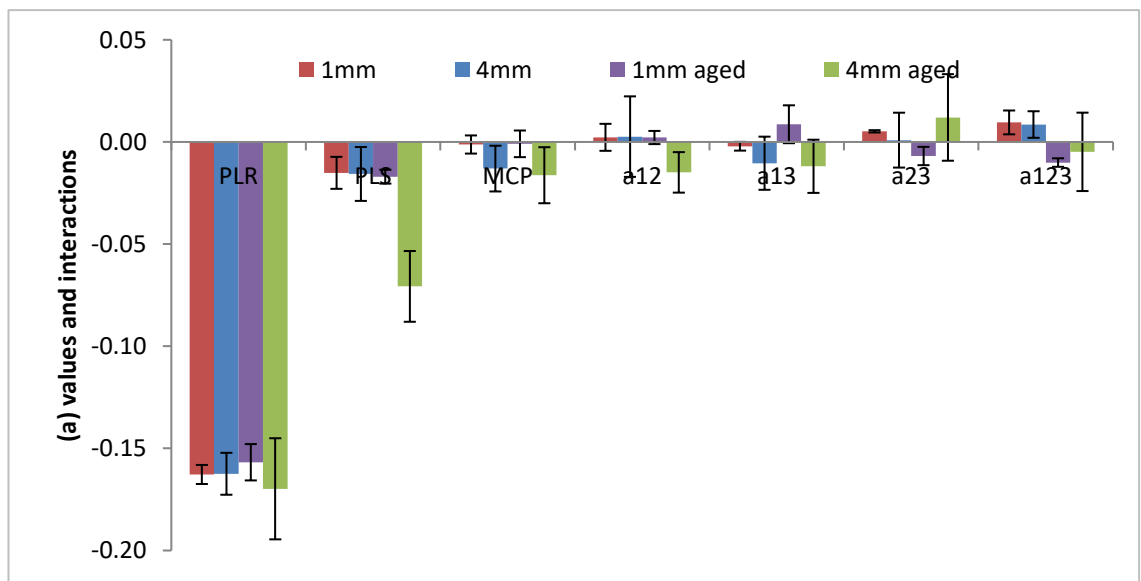
Figure 3-7 Factorial Analysis (a values and interactions) of calculated shrinkage. a1 is PLR, a2 is PLS and a3 is MCP

3.6.1.7 Effect of thickness on light-curing kinetics

To look at the effect of the sample thickness on light-curing kinetics, the PLS and MCP content of the formulations were disregarded and samples were grouped based on two new variables (PLR and thickness). Two variables factorial analysis (Figure 3-8) showed that PLR did not play a major role except with calculated shrinkage while increasing the thickness led to longer delay time but lowered rate of reaction.

Using Equation 2-25 and Equation 2-26, it was concluded that higher PLR caused a 26% decrease in calculated shrinkage. However, increasing the thickness (from 1mm to 4mm) resulted in a surge in delay time from 3s to 17s (by 515%) (see Table 3-1). Thicker samples also showed 51% decrease in rate of reaction, from 3% to 1.5%.
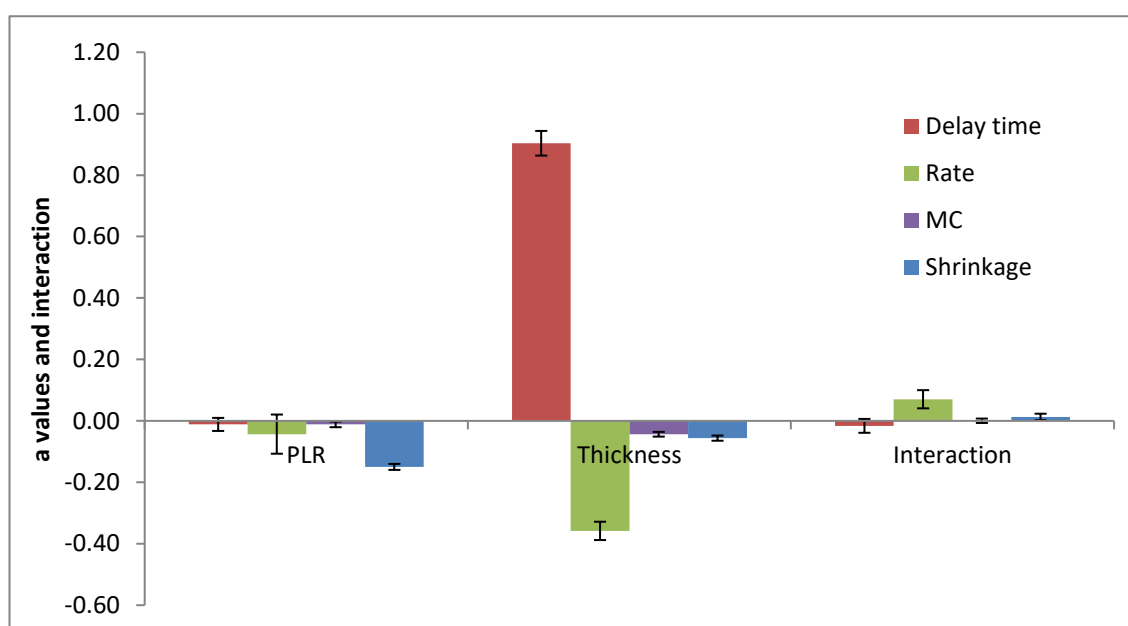
Figure 3-8 Factorial Analysis (a values and interactions) of Delay time, rate of reaction, monomer conversion and calculated shrinkage (PLR versus thickness)

Furthermore, PLR, PLS and MCP content were disregarded as factors and samples were grouped based on thickness and whether they were aged or not. Two variables factorial analysis (thickness versus ageing) (Figure 3-9) showed that ageing did not have a significant effect on delay time or rate of reaction (as error bars are larger or comparable to size of effect) and only caused a decrease in monomer conversion and calculated shrinkage. This decrease was calculated using Equation 2-26 and it was 5% decrease in both properties when samples were aged.
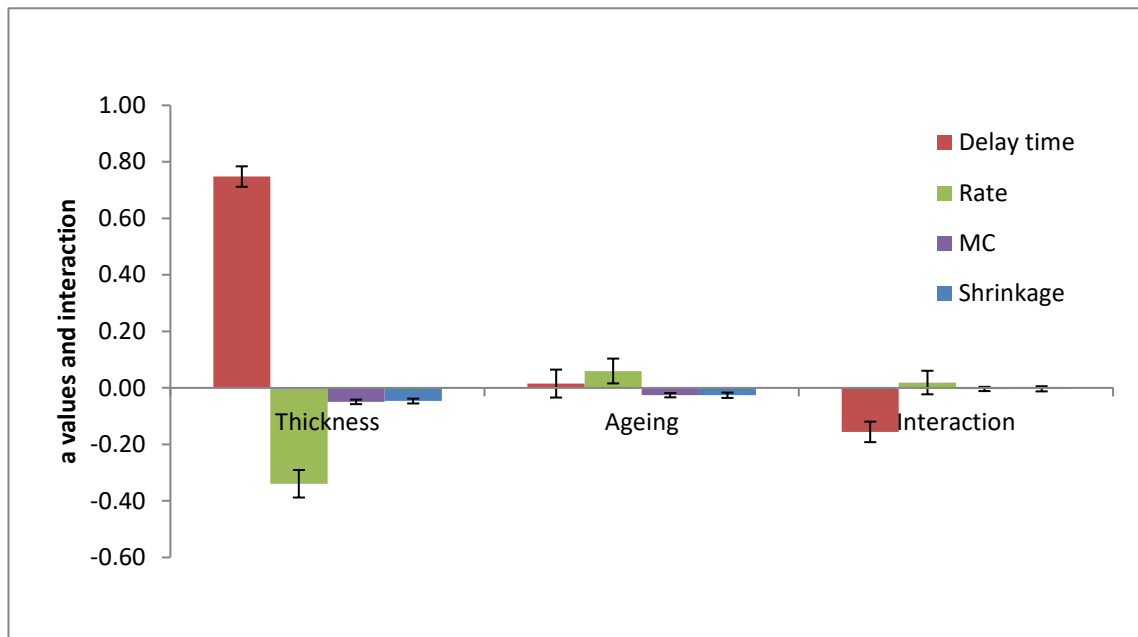
Figure 3-9 Factorial Analysis (a values and interactions) of Delay time, rate of reaction, monomer conversion and calculated shrinkage (Thickness versus ageing)

3.6.1.8   Effect of ageing on FTIR spectra (stability of the pastes)

To further test the stability of the pastes and the effect of ageing on light-curing kinetics, the FTIR spectra of aged versus non-aged samples (before and after light-curing) was investigated using F1 (see Table 2-6) of 4mm thickness as this showed the highest change in monomer conversion when aged (see Figure 3-10). Comparing the non-aged (green) and aged (yellow) paste spectra showed the following:

- Glass peak at ~1100: higher in aged pastes
- The peak at 1240 (polymers peak): aged paste peak is slightly lower
- The peak at 1320 (C-O): no change
- Baseline at 1330: aged paste baseline is higher
- The peak at 1530 (N-H): aged paste peak is lower
- The peak at 1714 (C=O): aged paste peak is lower

After light-curing (blue versus red spectra), the main differences were:

- The peak at 1240 (polymers peak): aged peak is lower
- The peak at 1320 (monomer C-O): aged peak is higher
- The peak at 1530 (N-H): aged peak is lower
- The peak at 1714 (C=O): aged peak is lower
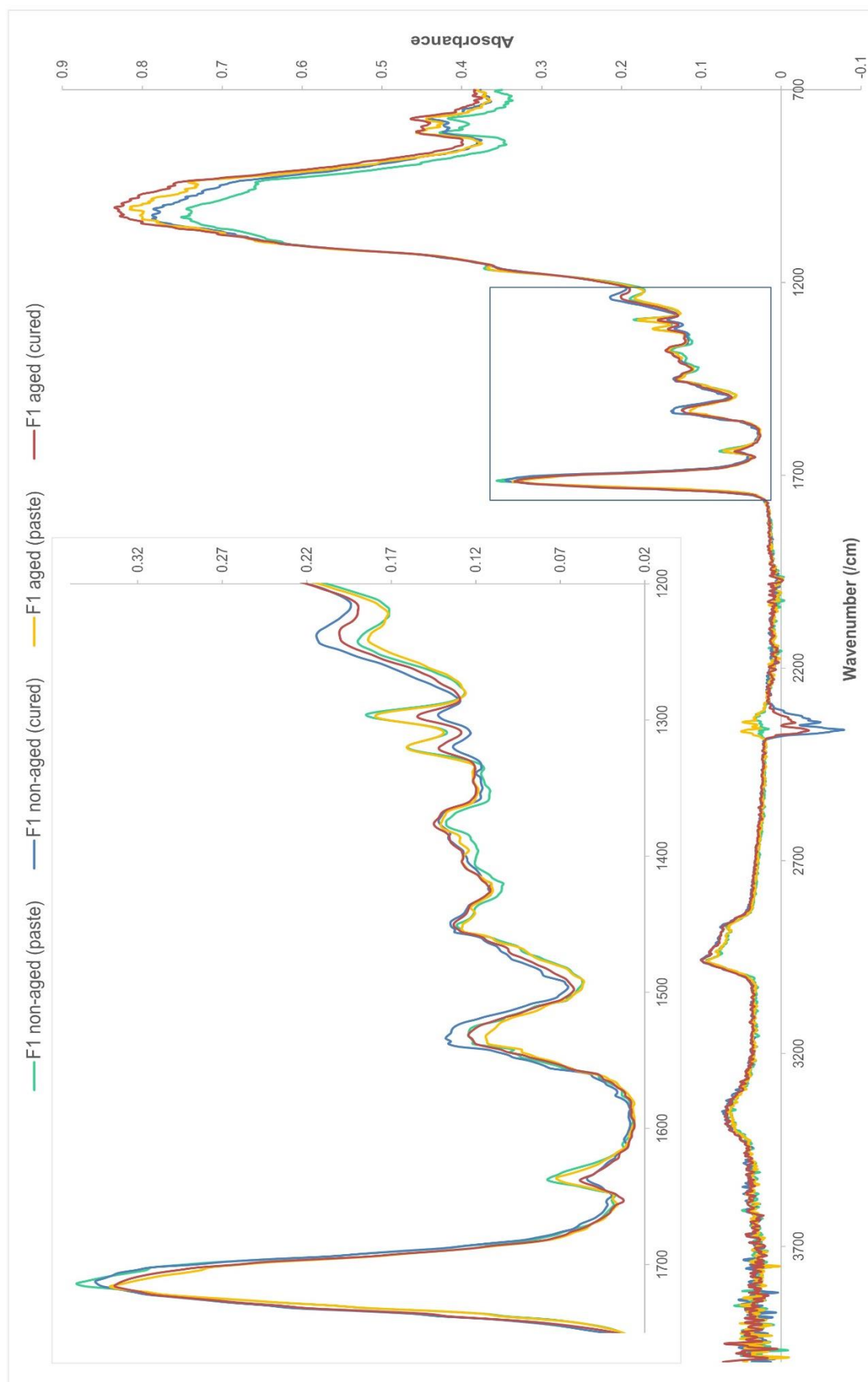
Figure 3-10 FTIR spectra of F1 at 4mm thickness (aged versus non-aged) before and after light-curing

3.6.2 Interaction of the cured discs of all experimental formulations with water

3.6.2.1 *Water sorption and solubility*

The water sorption at 7 days is shown in Figure 3-11. The commercial formulation (z250) showed a significantly lower water sorption (16.4µg/mm^3) than all experimental formulations (P = 4*10^{-6} to 3*10^{-2}). The water sorption results for experimental composites ranged from 22 to 56µg/mm^3. There was an upward trend within each PLR upon increasing MCP and PLS. Whilst average results were higher with PLR 3:1 the MCP and PLS effects were greater with PLR 5:1.
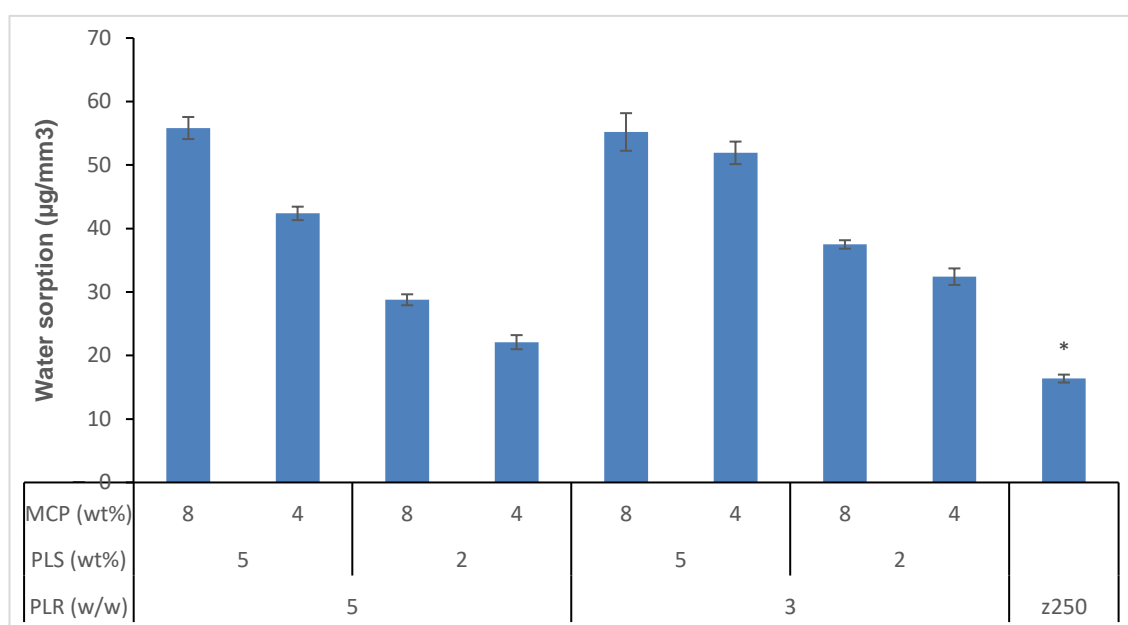
*Figure 3-11 Water sorption of 16 mm diameter discs. * indicates commercial is significantly different from all groups. Error bars are 95% CI (n=6)*

The water solubility results are shown in Figure 3-12. The water solubility for z250 was nearly zero and was significantly lower than all experimental composites (p = 7.2*10^{-13} to 5.2*10^{-9}). The values of water solubility for experimental composites ranged from 4 to 19.4µg/mm^3. As with water sorption there was an upward trend within the same PLR upon increasing MCP and PLS with again high PLR causing a greater change. Average results with PLR 3:1 however, were lower than with PLR 5:1.
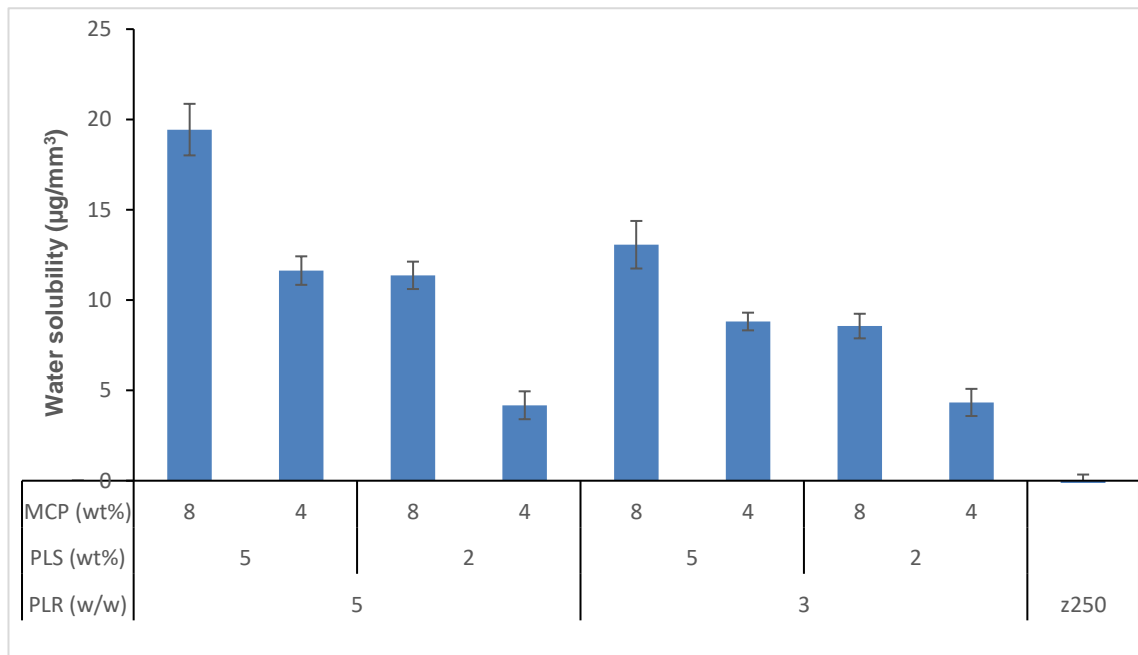
Figure 3-12 Water solubility of 16 mm diameter discs. All groups were significantly different from the control. Error bars are 95% CI (n=6)

Converting the water sorption and solubility results from wt/V ($\mu g/mm^3$) to wt% using Equation 2-6 and Equation 2-7 showed that discs mass increased by up to 2.3% upon immersion in water for 1 week (water sorption) and decreased by up to 1.0% when dried again (water solubility) (see Table 3-2).

Table 3-2 Water sorption and solubility as percentage of initial mass of the discs

	Water sorption (%)	Water solubility (%)
F1	1.9 ±0.08	-1.0 ±0.07
F2	1.6 ±0.05	-0.6 ±0.03
F3	0.8 ±0.06	-0.6 ±0.04
F4	0.9 ±0.06	-0.2 ±0.04
F5	2.3 ±0.13	-0.7 ±0.07
F6	2.3 ±0.08	-0.5 ±0.03
F7	1.5 ±0.03	-0.4 ±0.04
F8	1.4 ±0.06	-0.2 ±0.04

Factorial analysis of water sorption and solubility (Figure 3-13) showed that higher PLS or MCP content caused a considerable increase in water sorption and solubility, while the PLR caused an increase in solubility and a decrease in water sorption. Using Equation 2-25 and Equation 2-26 lower PLR increased the water sorption by 23% whilst it decreased the solubility by 20%. Higher concentrations of PLS increased the water

sorption and solubility by 72% and 99%, respectively. Similarly, higher concentrations of MCP increased the water sorption and solubility by 21% and 93%, respectively.
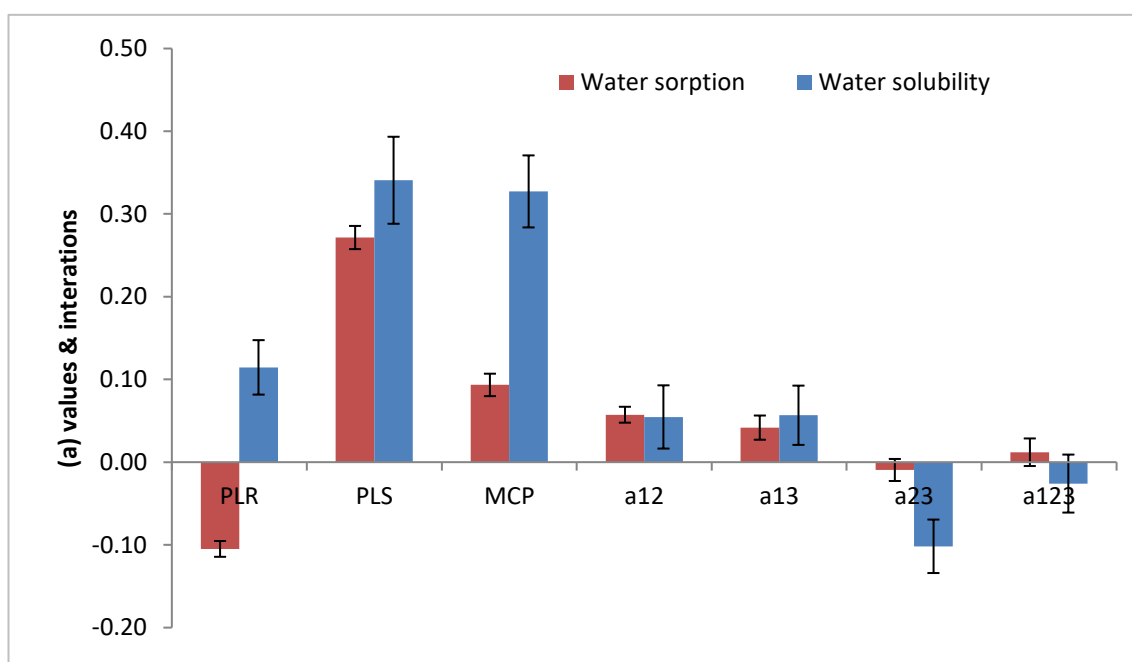
Figure 3-13 Factorial Analysis (a values and interactions) of water sorption and solubility. a1 is PLR, a2 is PLS and a3 is MCP

3.6.2.2 *Mass and Volume change and acidity (H⁺ release)*

3.6.2.2.1   Mass change percentage

The mass change percentage versus square root of time results are shown in Figure 3-14. The commercial z250 showed significantly lower change from 2 weeks onwards. All formulations showed a linear increase in mass change until 2 weeks then started to level off. However, it was noticed that F1 and F5 showed a decrease in mass change starting at 4 weeks onwards. The final mass change ranged from 1.3-3.6%, and the mass change gradient from 6.3-16.8 (100xwt%.hr$^{-0.5}$) (Table 3-3). Therefore, factorial analysis of the final values along with the gradient of the first 2 weeks was applied.
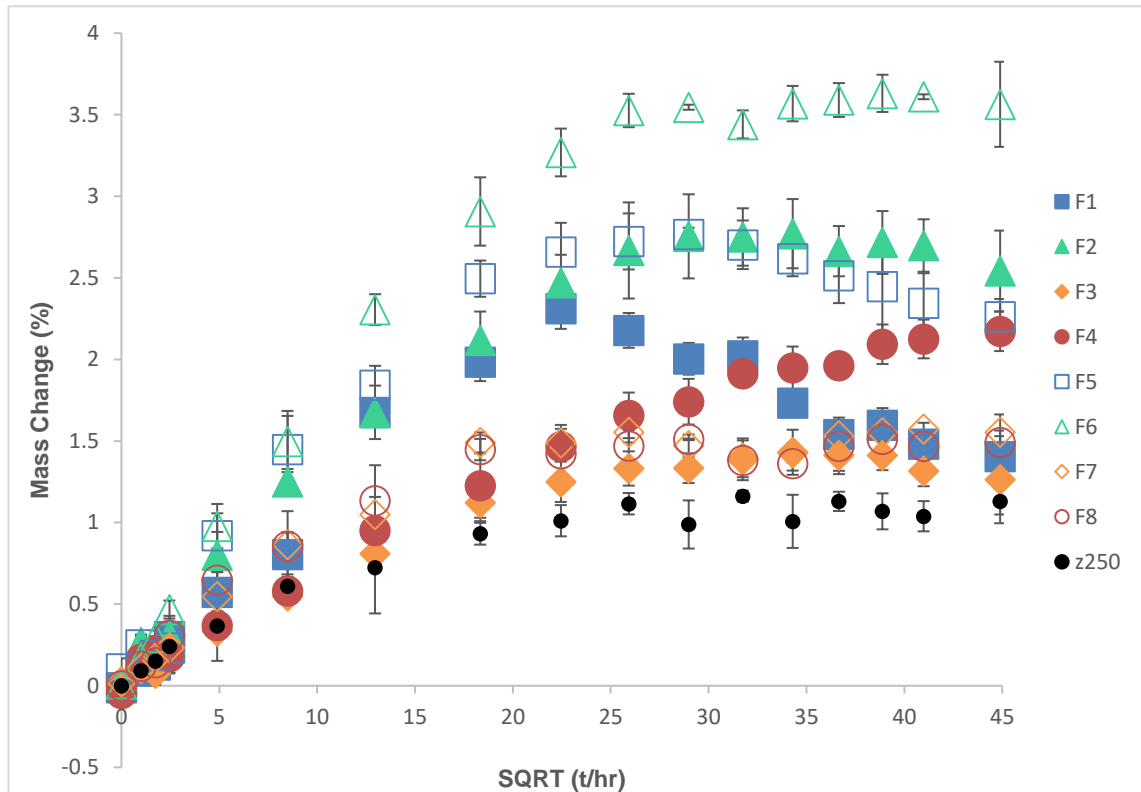
Figure 3-14 Mass change (%) versus SQRT of time for all experimental composites compared to z250. Solid fill marker is high PLR, Blue/Green is high PLS, Square/Diamond high MCP. Error bars are 95% CI (n=3)

Table 3-3 Final mass and volume change (%) and their gradients among all tested formulations

	Mass change gradient (2 weeks) $(100 \times wt\%.hr^{-0.5})$	Final mass change (%)	Volume change gradient (3 months) $(100 \times vol\%.hr^{-0.5})$	Final volume change (%)
F1	11.3 ± 0.8	1.4 ± 0.1	5.6 ± 0.5	2.2 ± 0.2
F2	12.5 ± 0.6	2.5 ± 0.3	5.2 ± 1.0	2.1 ± 0.3
F3	6.3 ± 0.3	1.3 ± 0.3	3.7 ± 0.2	1.6 ± 0.3
F4	7.0 ± 0.8	2.2 ± 0.1	2.5 ± 0.3	1.0 ± 0
F5	14.4 ± 0.7	2.3 ± 0.1	7.5 ± 0.6	2.7 ± 0.3
F6	16.8 ± 0.7	3.6 ± 0.3	5.4 ± 0.4	2.3 ± 0.3
F7	8.5 ± 0.8	1.6 ± 0.1	5.2 ± 0.1	2.0 ± 0.1
F8	8.7 ± 0.9	1.5 ± 0.1	3.2 ± 0.6	1.1 ± 0.5
z250	5.6 ± 0.8	1.1 ± 0.1	3.1 ± 0.7	1.1 ± 0.3
Full results are in Appendix B				

3.6.2.2.2   Volume change percentage

The full results of volume change percentage versus square root of time are shown in Figure 11-2, Appendix B. The commercial z250 showed lower results in comparison to all formulations except F4 and F8. All formulations showed a linear increase in volume change versus SQRT of time throughout the test. For all experimental formulations, volume change gradients ranged from 2.5%/s to 7.5%/s whilst the final volume change

ranged from 1% to 2.7% for the experimental formulations (Table 3-3). The gradient of the whole 3 months data points was used in factorial analysis.

When the results of mass and volume change were compared to each other, it was noticed that the commercial material had an equal mass and volume change of about 1% after 2 months. However, the experimental composites showed mass change higher than volume change with lower MCP and vice versa with higher MCP.

3.6.2.2.3   Gradients of mass and volume change in comparison to final values

Final mass and volume change results along with their gradient versus square root of time over 2 weeks and 3 months, respectively, are summarised in Table 3-3.

The factorial analysis of the final mass and volume change and their gradients is shown in Figure 3-15 . Higher PLR caused a decrease in all these properties while increasing the PLS resulted in an increase in all of them. However, MCP caused a decrease in mass change and its gradient while it increased volume change and its gradient.

Using Equation 2-25 and Equation 2-26, the results in percentage were as follows. Higher MCP levels decreased the gradient of mass change by 9.1% only (in comparison to 32.2% in the final results). Effect of interaction between PLR and PLS on gradient of mass change was insignificant (while it caused a 21.3% decrease in the final results). Lower PLR increased the mass and volume change by 18% and 17%, respectively. It also showed that the higher the PLS content, the higher the mass and volume change (46.7% and 69.4%, respectively). Higher MCP decreased the final mass change by 32.2%, while it increased the final volume change by 38.2%.
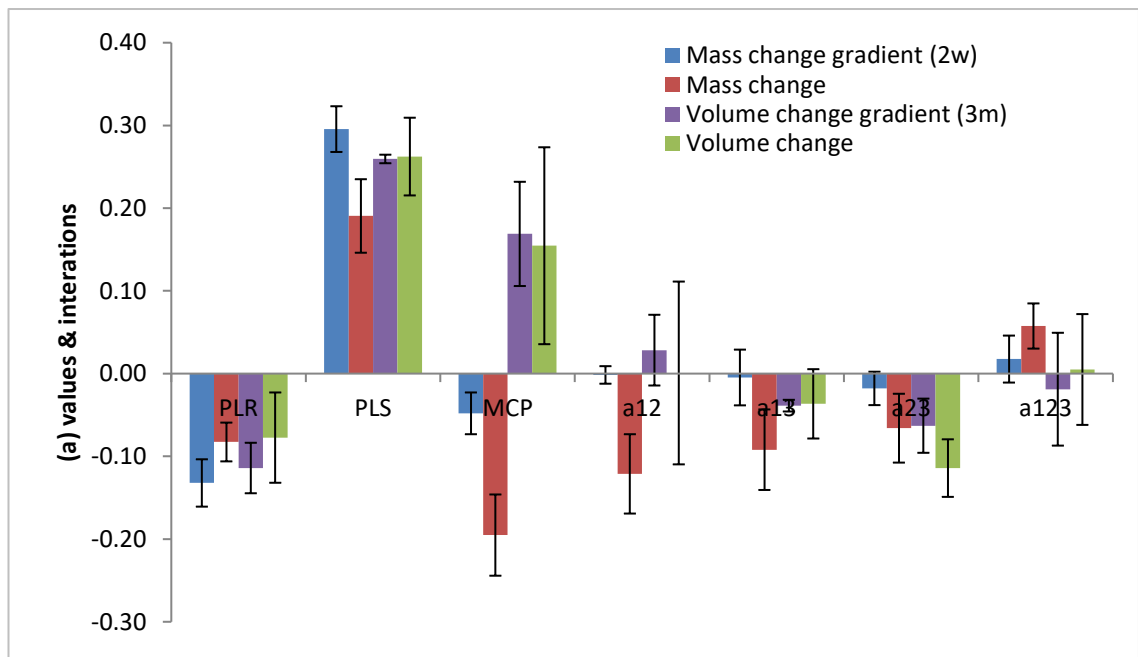
Figure 3-15 Factorial Analysis (a values and interactions) of final mass and volume change and their gradient. a1 is PLR, a2 is PLS and a3 is MCP

3.6.2.2.4 Acidity (H$^+$ release)

The results of number of H$^+$ moles released from discs into water at different time points are shown in Figure 3-16. The percentage of this release ranged from 4.5% to 34.2% of the maximum [H$^+$] that might be released from a sample assuming one molecule of H$^+$ release per molecule of MCP (Figure 3-17).
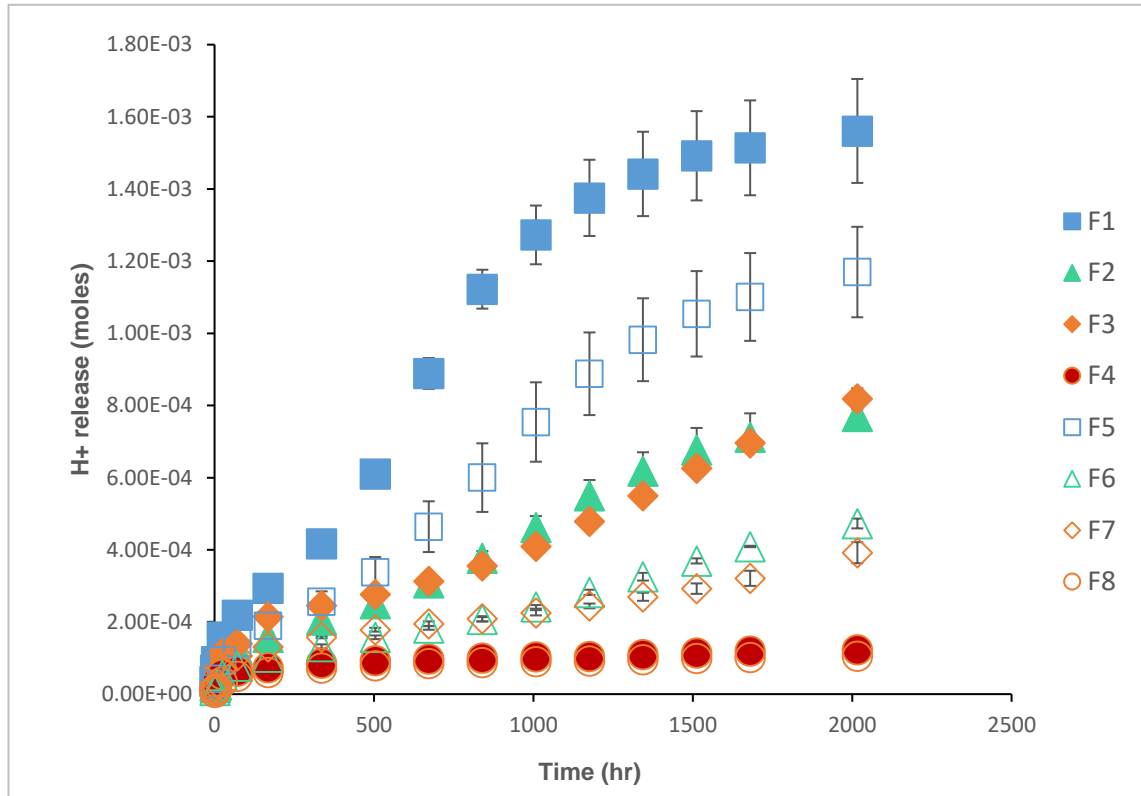
Figure 3-16 Cumulative H$^+$ release (moles) upon immersion in water of all experimental composites. Solid fill marker is high PLR, Blue/Green is high PLS, Square/Diamond high MCP. Error bars are 95% CI (n=3)
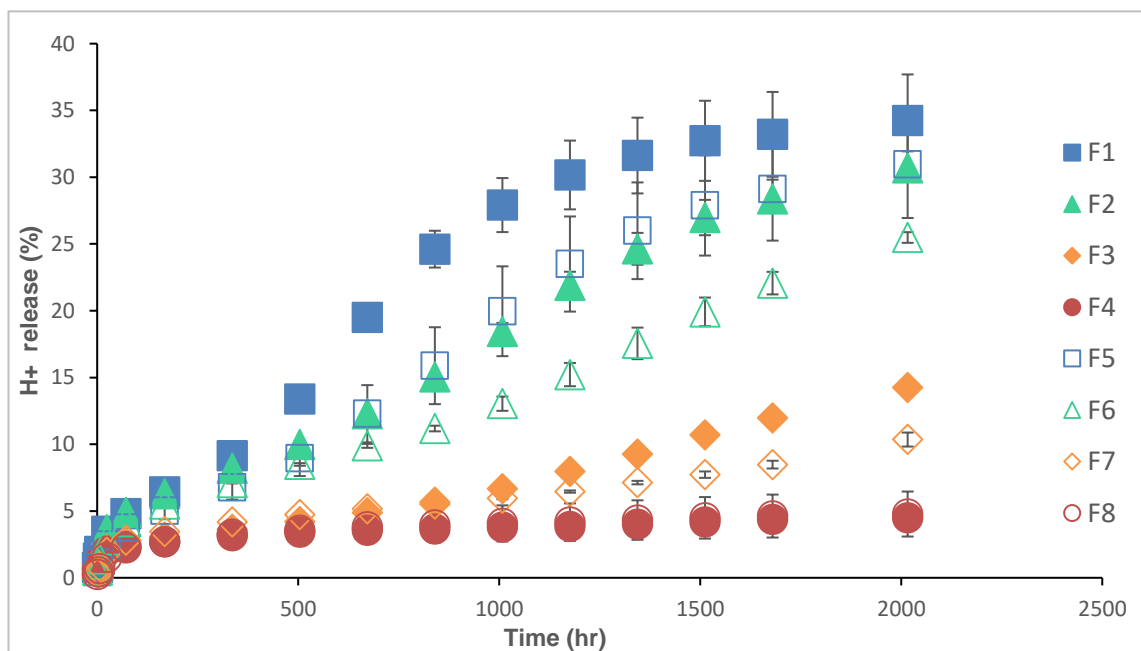
Figure 3-17 Cumulative acidity (H$^+$ percentage release) upon immersion in water of all experimental composites. Solid fill marker is high PLR, Blue/Green is high PLS, Square/Diamond high MCP. Error bars are 95% CI (n=3)

Factorial analysis of the number of H^+ moles released, and the percentage of this release is shown in Figure 3-18. It showed that increasing any variable caused an increase in H^+ release. However, the major factor was PLS content followed by MCP content and the PLR. Using Equation 2-25, formulations with higher PLS, MCP or PLR caused 255%, 233% or 51% increase in number of moles of H^+ released, respectively. The effects of increasing MCP and PLR were lower when the percentage release was considered but both variables still had a positive effect.
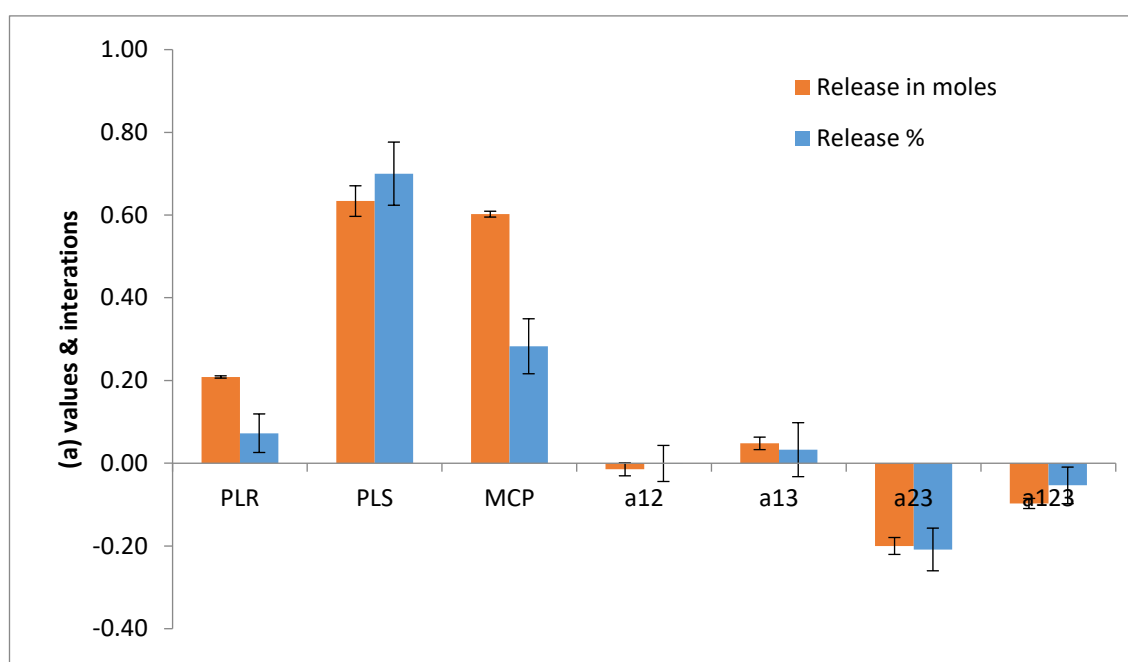
Figure 3-18 Factorial Analysis (a values and interactions) of H^+ release (in moles and as percentage). a1 is PLR, a2 is PLS and a3 is MCP

3.6.2.3 PolyLysine release

Figure 3-19 and Figure 3-20 show the PolyLysine release results (in grams and as a percentage of PLS content) versus SQRT of time. Formulations of lower PLR did not show a burst release of PolyLysine. However, F1 and F2 (higher PLR and PLS formulations) showed initial burst release of 4.6% and 5% PolyLysine within one hour, respectively (Figure 3-20). This was followed by a linear increase in percentage PLS release versus SQRT of time which then levelled off between 1 and 3 weeks. The final cumulative release after 2 months ranged between 7% and 25.9%.
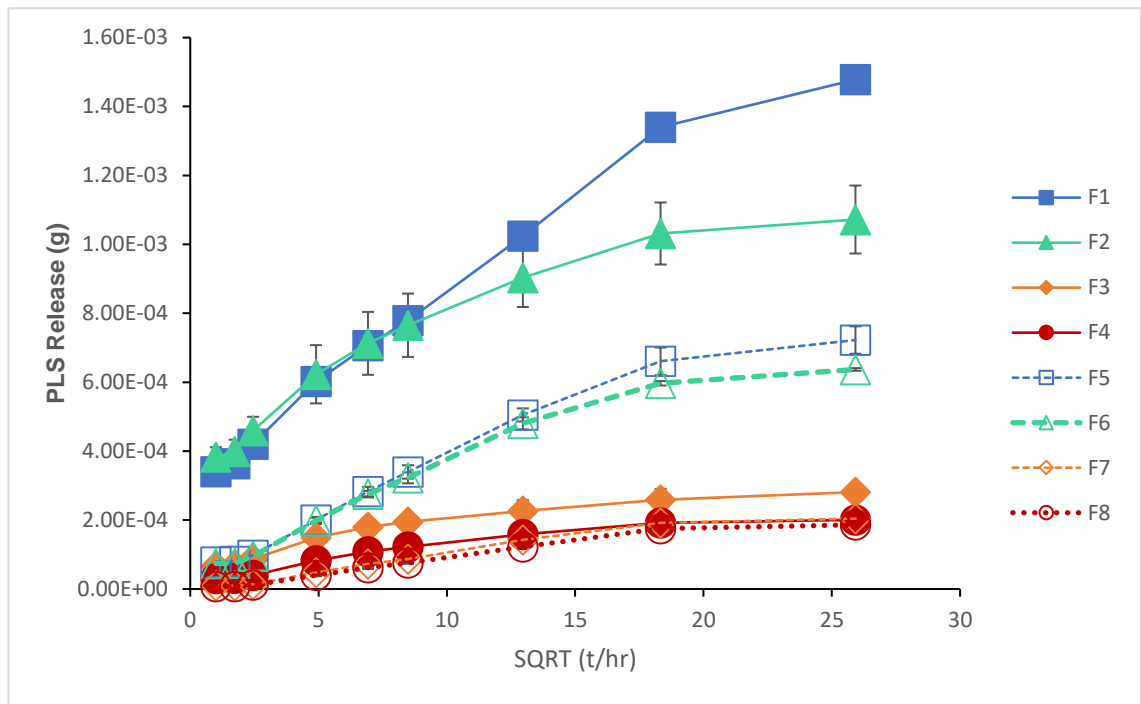
Figure 3-19 Cumulative PolyLysine release (in grams) versus SQRT of time at 37°C. Solid fill marker is high PLR, Blue/Green is high PLS, Square/Diamond high MCP. Error bars are 95% CI (n=3)
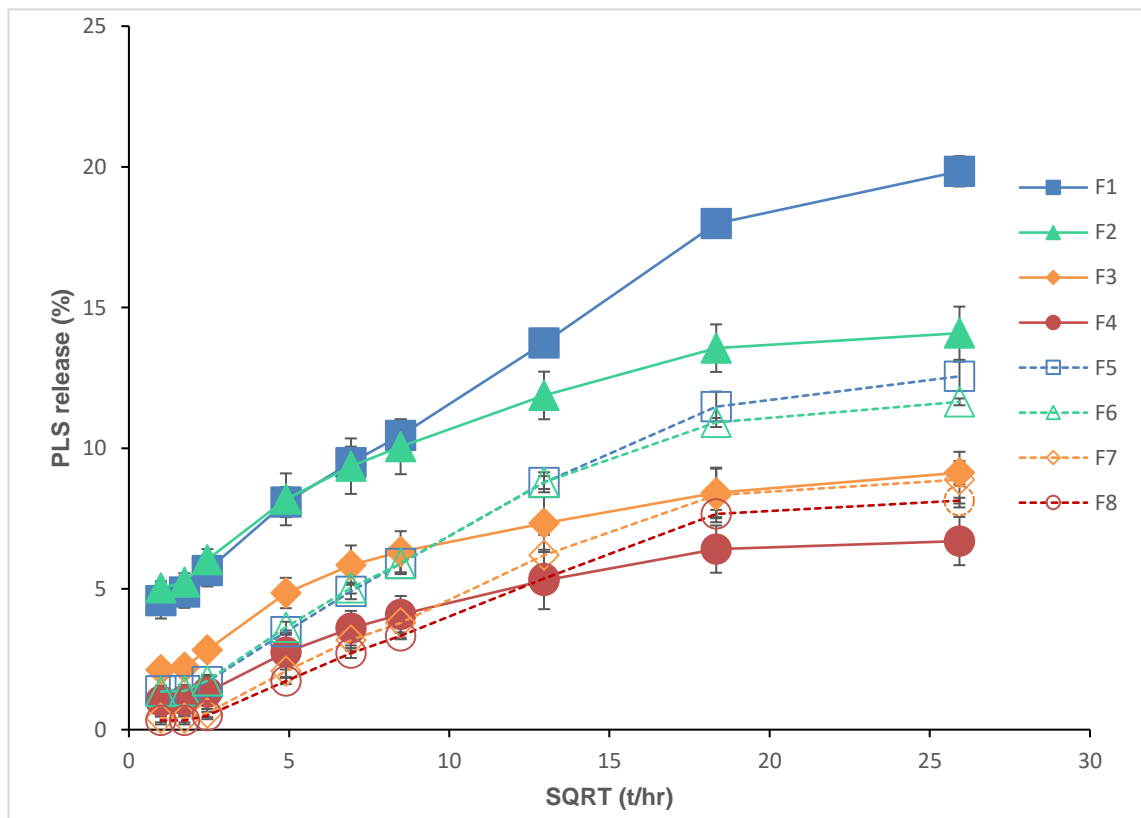
Figure 3-20 Cumulative PolyLysine release percentage versus SQRT of time at 37°C. Solid fill marker is high PLR, Blue/Green is high PLS, Square/Diamond high MCP. Error bars are 95% CI (n=3)

Factorial analysis of PLS release in grams (Figure 3-21) showed that increasing any of the variables resulted in an increase in PLS release and that there were positive interaction effects between PLR and PLS or between PLR and MCP. The percentage

effect was calculated using Equation 2-25. It showed that formulations with higher PLR and PLS caused a 51% and 375% increase in final PLS release in grams. It also showed that higher MCP increased PLS release by 35%. There was also a positive interaction effect of 25% between PLR and PLS (a_{12} term). Factorial analysis of PLS release percentage showed similar effect of variables but not as strong due to taking the total content of PLS in the discs into consideration.
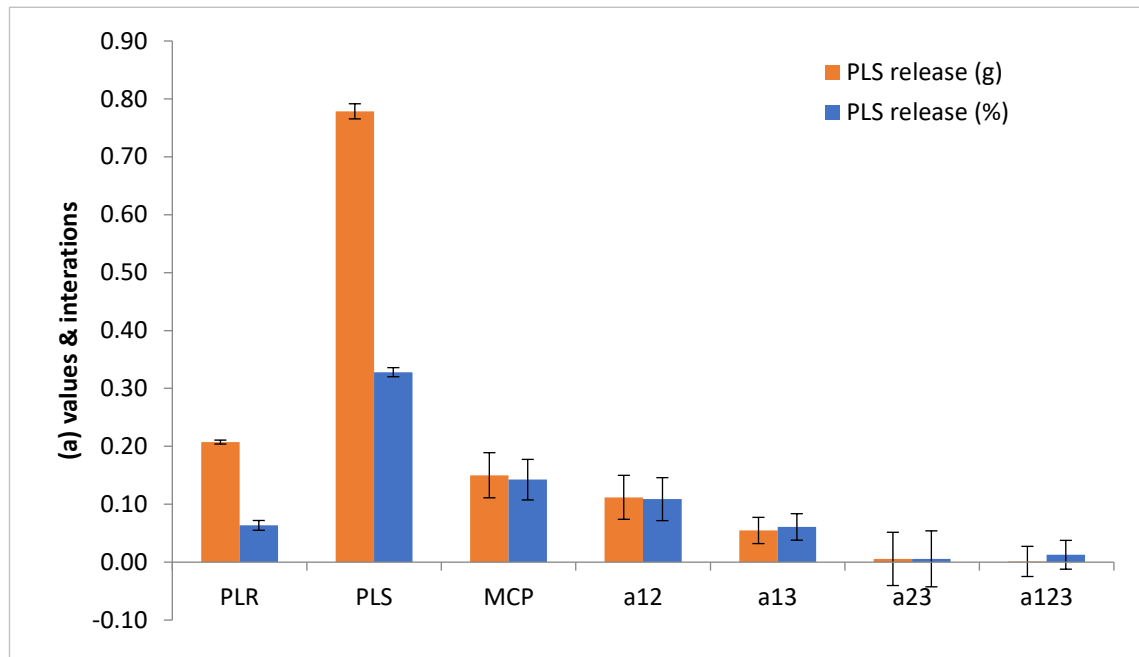
Figure 3-21 Factorial Analysis (a values and interactions) of PolyLysine release (in grams and as a percentage) after 2 months,. a1 is PLR, a2 is PLS and a3 is MCP

3.6.3 Mechanical tests (flexural strength and modulus)

3.6.3.1 Three-point bending flexural strength and modulus

All formulations exhibited flexural strength ≥80MPa with an average value of 90MPa, while the commercial composite z250 had significantly higher flexural strength (157MPa, $p = 9.3*10^{-13}$ to $3.7*10^{-10}$) (Figure 3-22).

MCP (wt%)	8	4	8	4	8	4	8	4	
PLS (wt%)	5		2		5		2		
PLR (w/w)	5				3				z250
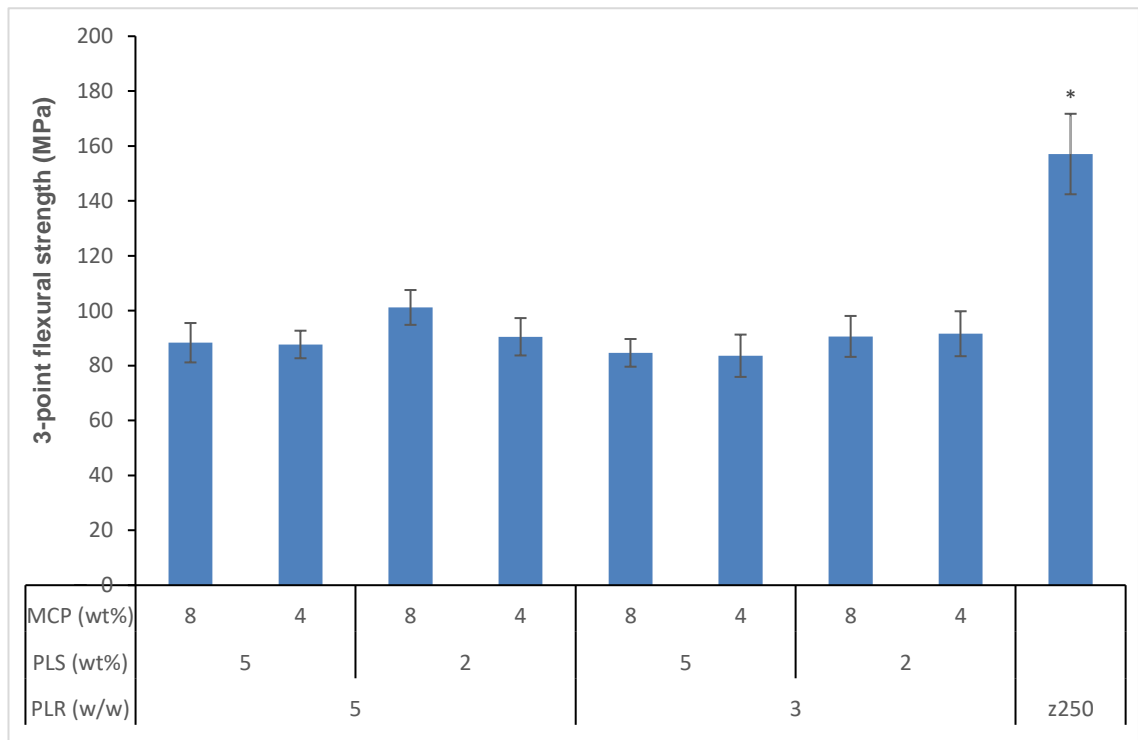
*Figure 3-22 Three point bending flexural strength (MPa) of all 8 formulations and z250 as a control after 1 day in water at 37°C. Crosshead speed was 0.75 mm/min. * indicates control is significantly different from all groups. Error bars are 95% CI (n=5)*

Modulus of elasticity was greater than 5GPa for all formulations. Furthermore, those with higher PLR and lower PLS gave higher results and were comparable to the commercial z250 (Figure 3-23).

MCP (wt%)	8	4	8	4	8	4	8	4	
PLS (wt%)	5		2		5		2		
PLR (w/w)	5				3				z250
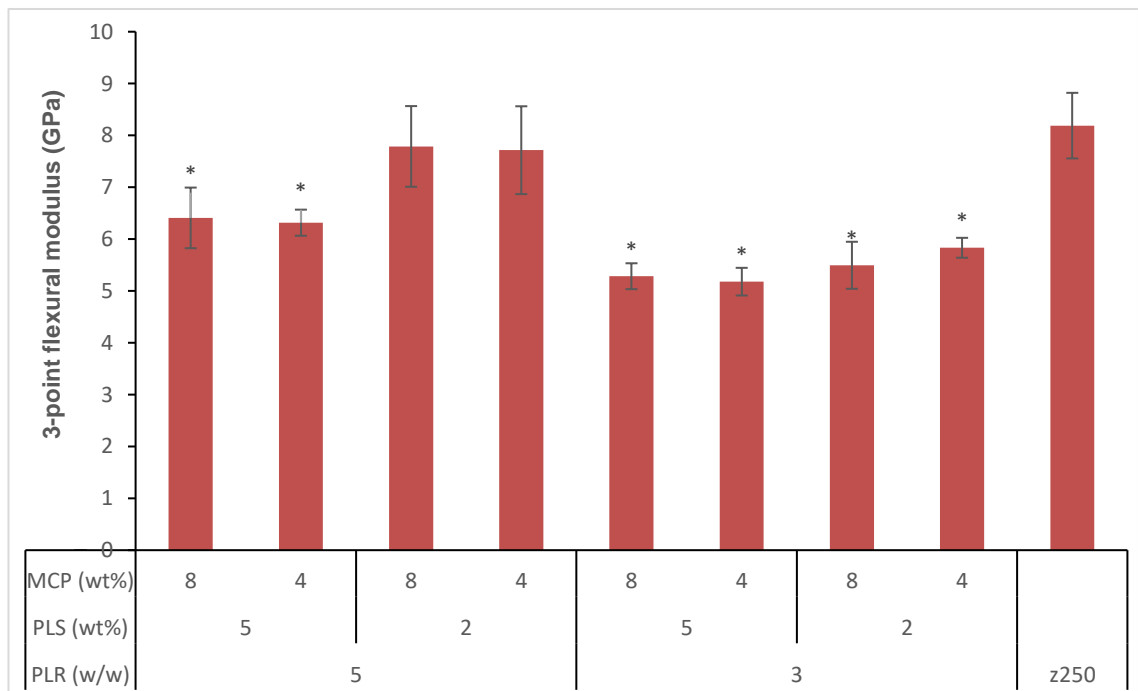
*Figure 3-23 Three point bending flexural modulus (GPa) of all 8 formulations and z250 as a control after 1 day in water at 37°C. Crosshead speed was 0.75 mm/min. * indicates significant difference from control. Error bars are 95% CI (n=5)*

Factorial analysis showed that the variables (PLR, PLS and MCP) had negligible effect on flexural strength (Figure 3-24). However, the modulus increased with higher PLR and decreased with higher PLS content. Using Equation 2-25 and Equation 2-26, higher PLR increased the modulus by 28.9% whilst higher PLS content decreased it by 12.5%.
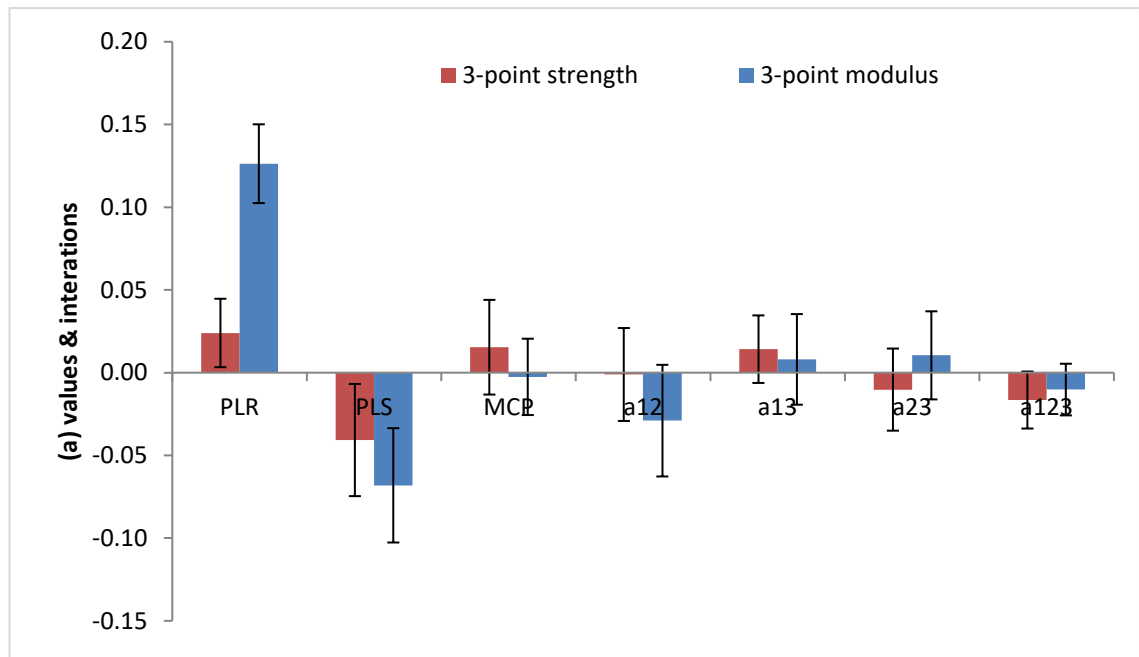
Figure 3-24 Factorial Analysis (a values and interactions) of three-point flexural strength and modulus. a1 is PLR, a2 is PLS and a3 is MCP

3.6.3.2 *Biaxial flexural strength and modulus*

Biaxial flexural strength results are shown in Figure 3-25 and Figure 3-26. All formulations showed at least 80MPa strength when tested after being left dry for 24 hours. Upon immersion in water and incubating at 37°C, the flexural strength peaked and then started going down until it levelled off after 3m of immersion. The same trend was noticed with all experimental composites (PLR 5:1 and 3:1) and z250, which reached a plateau after 1 month. The commercial group (z250) flexural strength was significantly higher than that of all experimental formulations at any given time point ($p = 1.8*10^{-3}$ to $1.4*10^{-13}$).
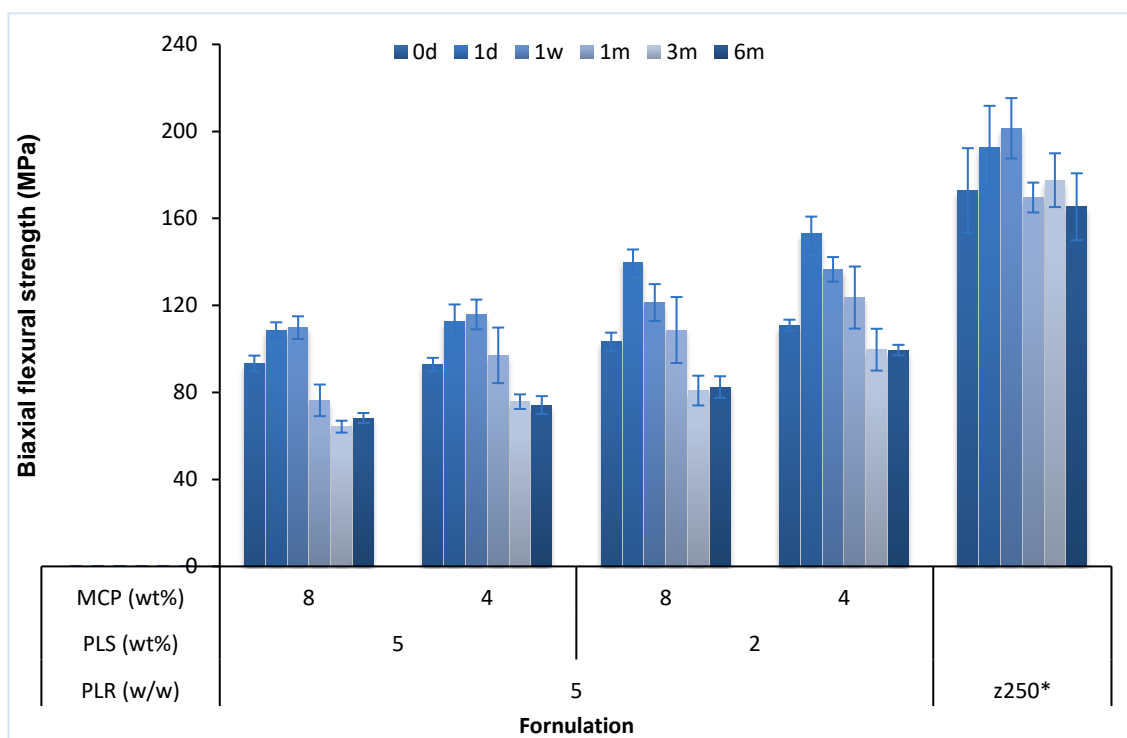
Figure 3-25 **Biaxial Flexural strength** *(MPa) of formulations of PLR* **5:1** *in comparison to z250 at different times after incubating in water at 37°C. Crosshead speed was 1 mm/min. * indicates control is significantly different from all groups while a letter indicates the groups that are significantly different from the control at the same time point. Error bars are 95% CI (n=8)*
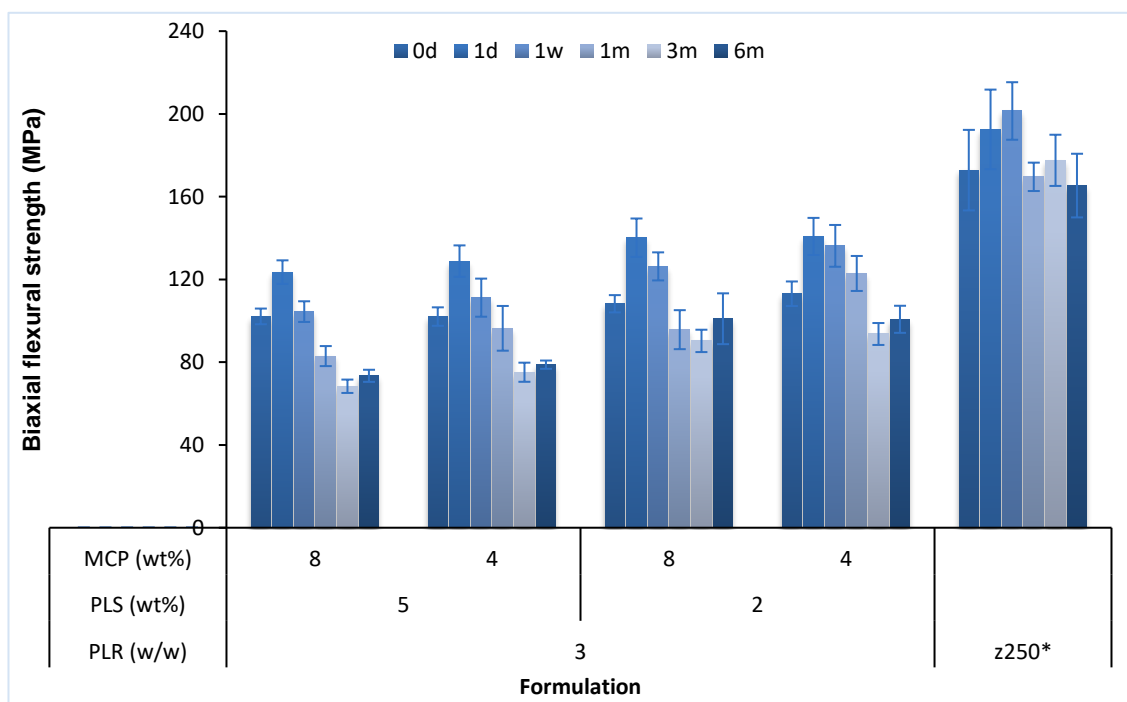
Figure 3-26 **Biaxial Flexural strength** *(MPa) of formulations of PLR* **3:1** *in comparison to z250 at different times after incubating in water at 37°C. Crosshead speed was 1 mm/min. * indicates control is significantly different from all groups while a letter indicates the groups that are significantly different from the control at the same time point. Error bars are 95% CI (n=8)*

Factorial analysis of flexural strength data (Figure 3-27) showed that the greatest change was caused by increasing the PLS content, followed by the MCP content, especially with increased incubation timing. Increasing both additives (PLS and MCP) caused the

flexural strength to decrease. Using Equation 2-25, lower PLS content caused an 11.7% increase in flexural strength initially but this reached 28% from 1 month onwards. Decreasing the MCP content caused a maximum increase in flexural strength of 22% at 1m but the benefit declined thereafter.
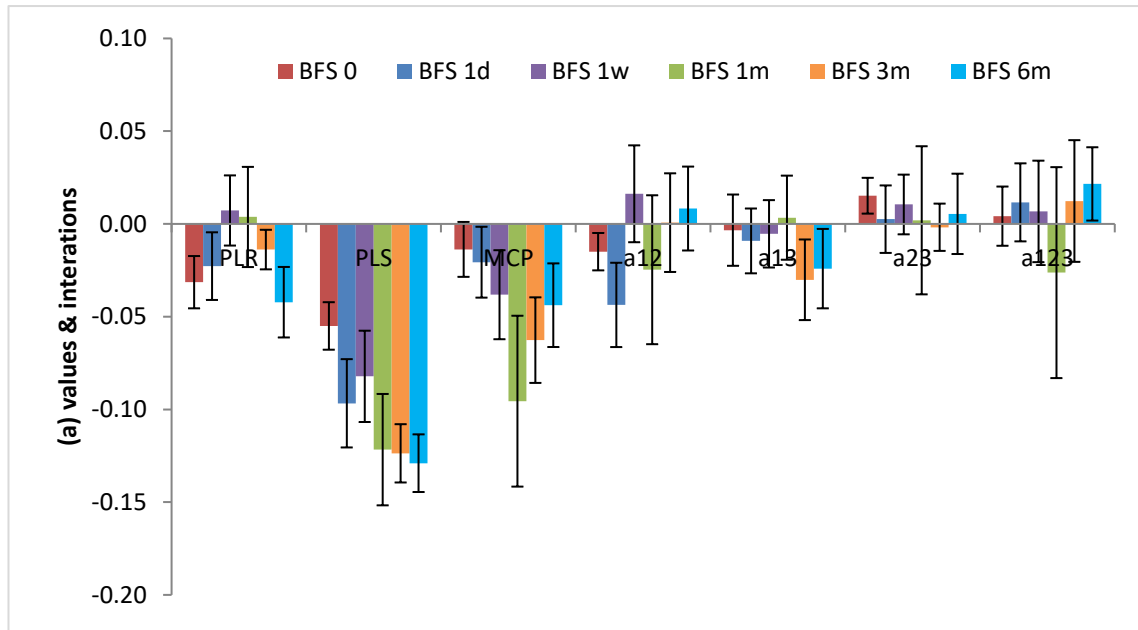
Figure 3-27 Factorial Analysis (a values and interactions) of biaxial flexural strength at different time points. a1 is PLR, a2 is PLS and a3 is MCP

The biaxial flexural modulus showed a downwards trend over time in water with higher PLS and MCP content but could peak over time with lower additive levels. Conversely, modulus of z250 was more stable over time and significantly higher than for all experimental formulations (p= $2.4*10^{-3}$ to $2.9*10^{-2}$). Full results are shown in Figure 3-28 and Figure 3-29 and significant difference from the commercial z250 is indicated.
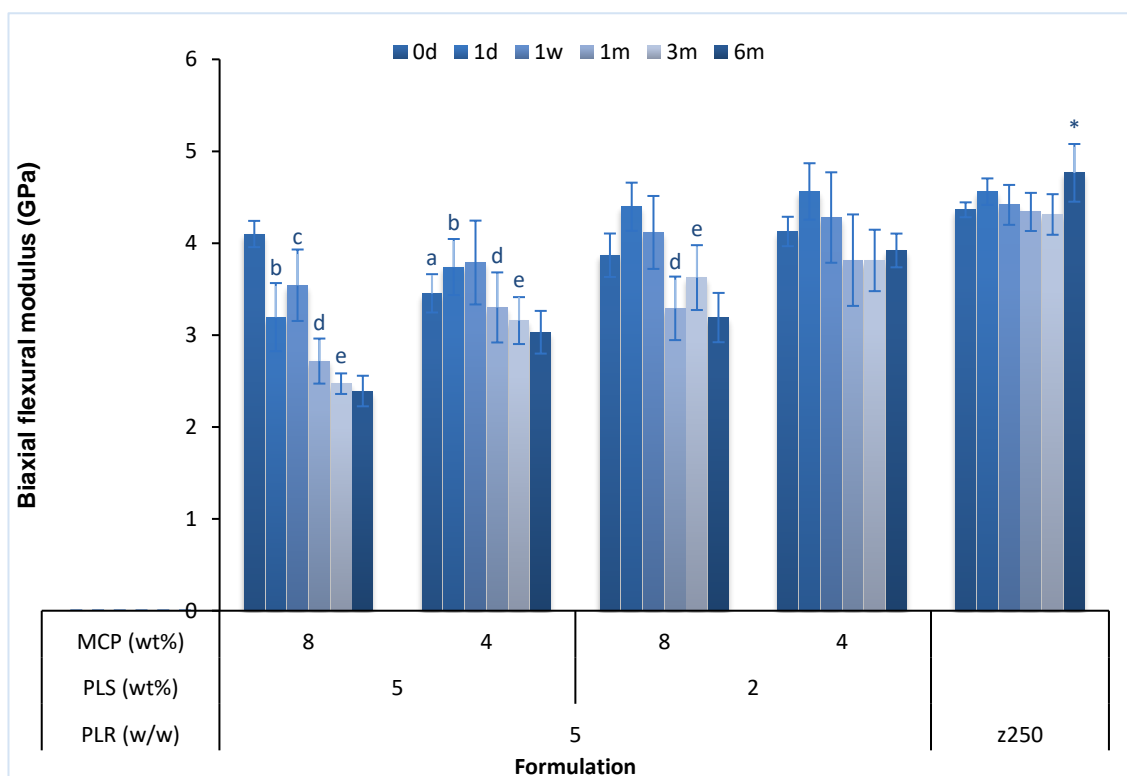
Figure 3-28 **Biaxial Flexural modulus** *(GPa) of formulations of PLR* **5:1** *in comparison to z250 at different times after incubating in water at 37°C. Crosshead speed was 1 mm/min. * indicates control is significantly different from all groups while a letter indicates the groups that are significantly different from the control at the same time point. Error bars are 95% CI (n=8)*
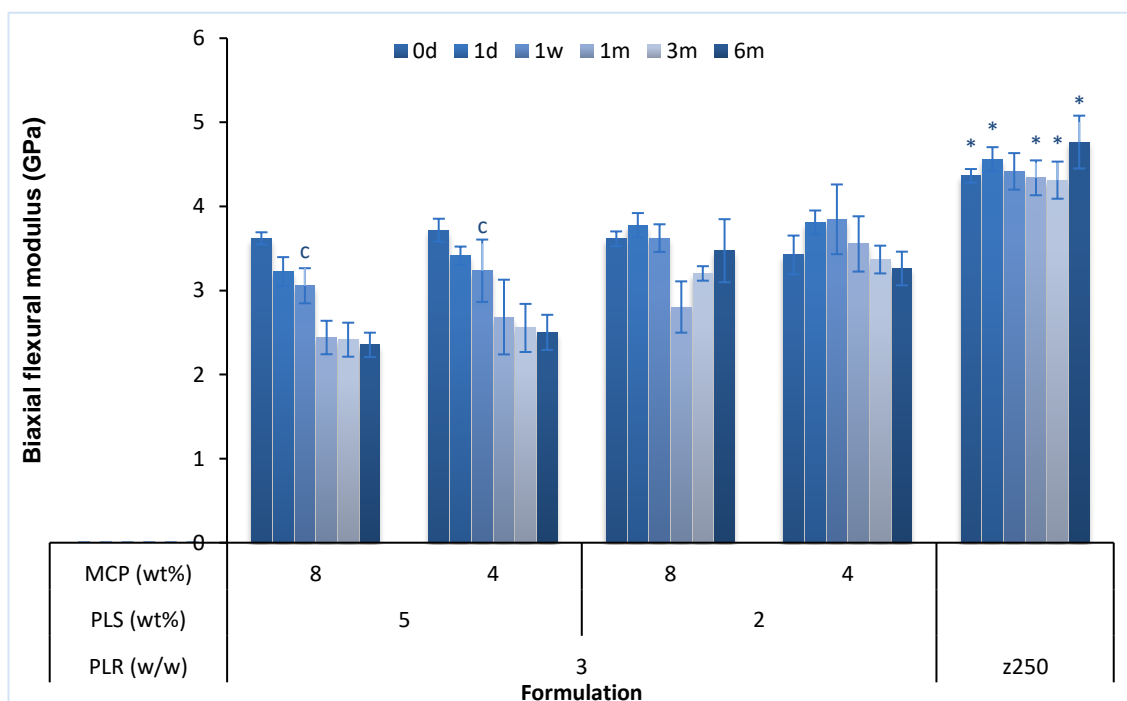
Figure 3-29 **Biaxial Flexural modulus** *(GPa) of formulations of PLR* **3:1** *in comparison to z250 at different times after incubating in water at 37°C. Crosshead speed was 1 mm/min. * indicates control is significantly different from all groups while a letter indicates the groups that are significantly different from the control at the same time point. Error bars are 95% CI (n=8)*

Factorial analysis of biaxial flexural modulus results (Figure 3-30) showed that both additives (PLS and MCP) had caused the modulus to decrease. This effect was more noticeable after 1 month of incubation in water. It also showed that higher PLR caused a consistent increase in the modulus. Using Equation 2-25 and Equation 2-26, it was noticed that the flexural modulus increased by 10-15% with higher PLR throughout the test. Similar to the flexural strength, the flexural modulus increased by 22.2% with lower PLS from day 1 and the increase reached 33.4% at 3 months. The lower MCP content increased the modulus by 21.6% after 1 month.
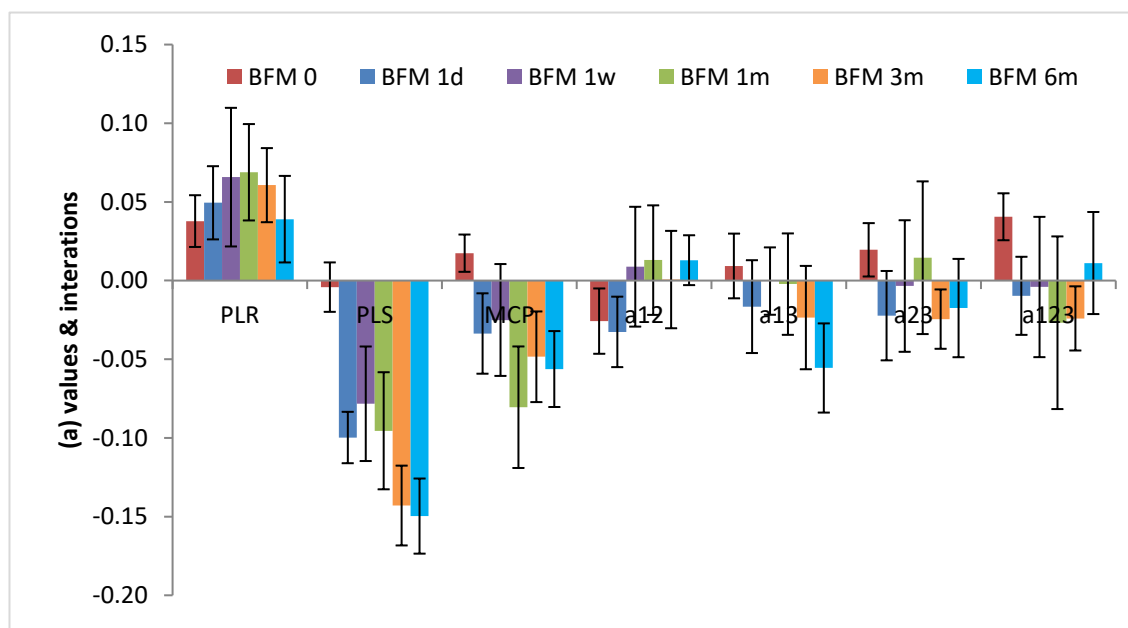
Figure 3-30 Factorial Analysis (a values and interactions) of biaxial flexural modulus at different time points. a1 is PLR, a2 is PLS and a3 is MCP

The average toughness (area under the force versus displacement curve) for dry versus 1m water stored samples is provided in Table 3-4. Full results are in Figure 12-1, Appendix C.

Table 3-4 Average value of toughness (J.m^{-3}) (area under Force versus Displacement curve)

	Dry	**1 month in water at 37°C**
All 8 formulations	87.2 ± 14.3	133.2 ± 21.0
z250	120.9 ± 34.3	98.4 ± 7.2
N.B. Detailed results are in Figure 12-1, Appendix C		

Factorial analysis of toughness results (Figure 3-31) showed that it was majorly affected by the PLR. Using Equation 2-26, a 30-50% increase in toughness was noticed with lower PLR and the highest effect was noticed before 3 months.
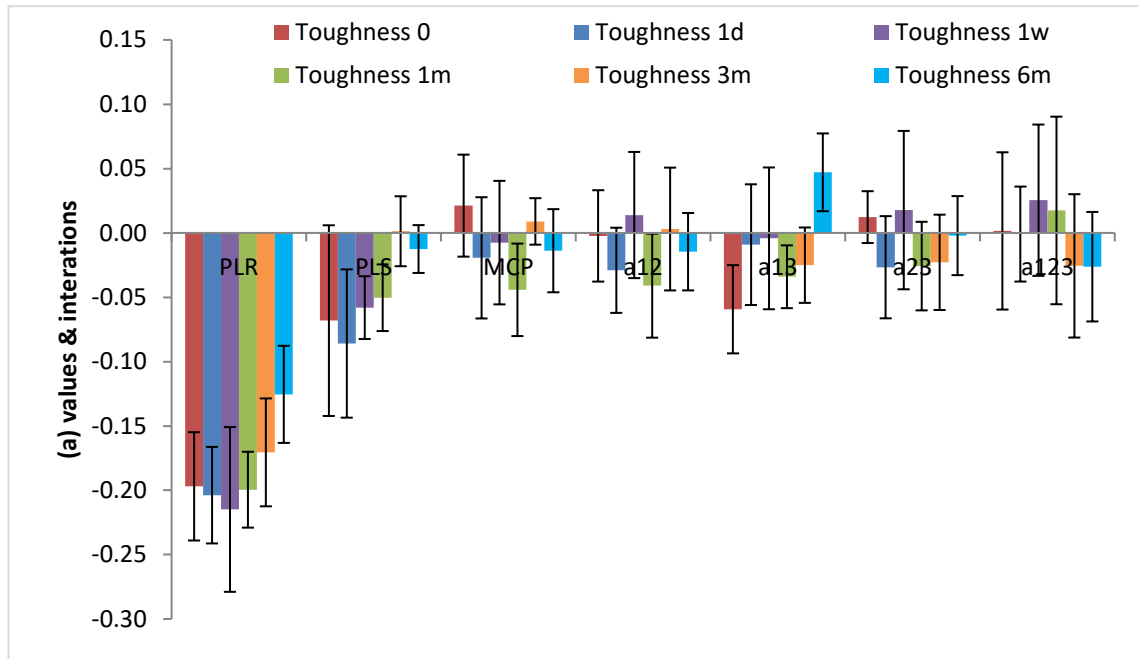
Figure 3-31 Factorial Analysis (a values and interactions) of toughness of experimental composites at different time points. a1 is PLR, a2 is PLS and a3 is MCP

3.6.3.3 Fracture healing observations

SEM images showed precipitation of minerals at the crack zone upon immersing the cracked discs in SBF. Figure 3-32 shows in the left column precipitation of minerals at the crack zone of an F4 disc (PLR5, low PLS, low MCP) that survived a mechanical test upon immersion for 1 week in water and was subsequently immersed in SBF (at 37°C) for 2 months and imaged with SEM. The bottom right image shows an F1 disc (PLR5, high PLS, high MCP) that survived a mechanical test after 1 month in water, and then was immersed in SBF for 3 months. It appeared totally covered with minerals (Figure 3-32).

Minerals precipitation was confirmed with EDX mapping, which showed higher concentration of Ca and P at the crack zone while the Si was more concentrated in areas where no precipitation was noticed (Figure 3-33).

F4 (4% MCP)
-1w in water
-BFS test
-2m in SBF

F1 (8% MCP)
-1m in water
-BFS test
-3m in SBF
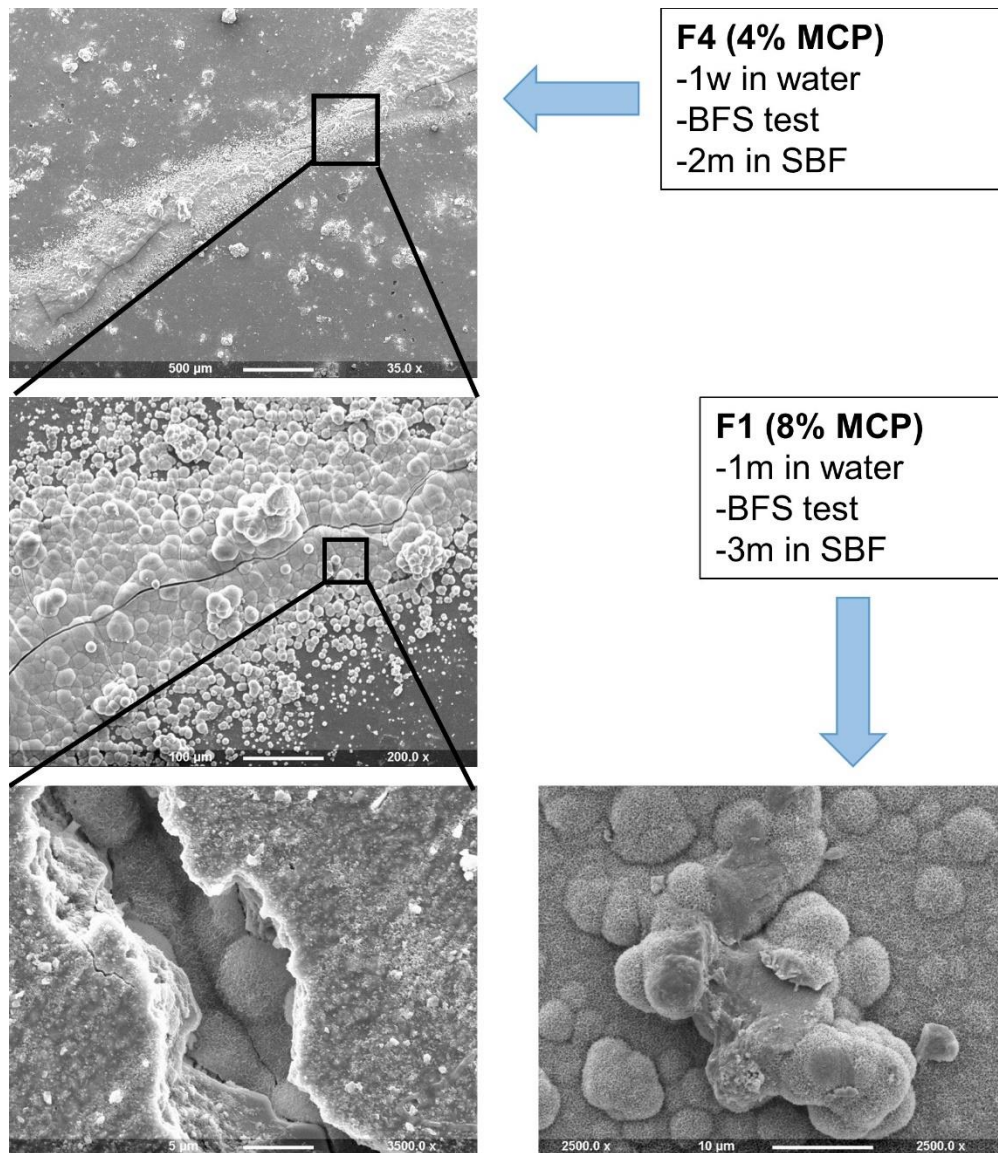
Figure 3-32 Fracture healing observations showing remineralisation of discs cracked during the biaxial flexural strength test.

Ca
P
Si
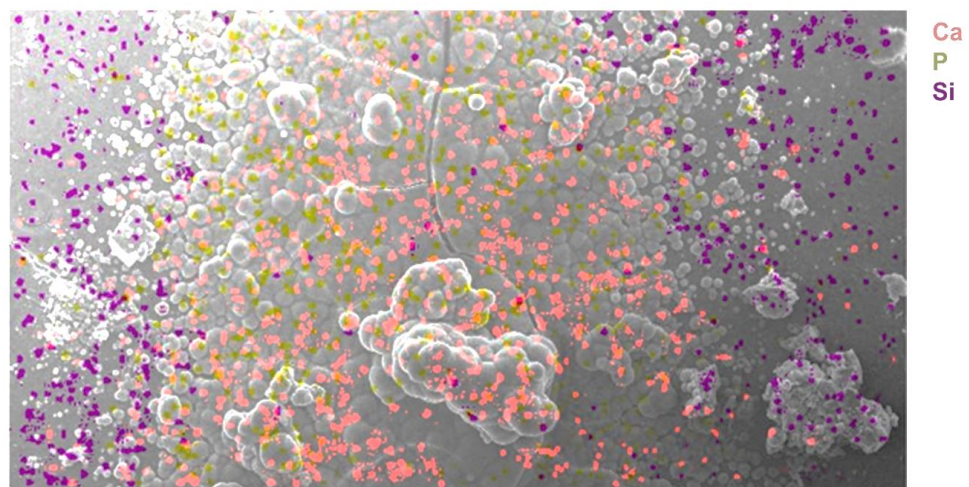
Figure 3-33 EDX map of the self-healed cracked disc (F4) upon immersing in SBF for 2 months. Calcium and Phosphate ions were highly concentrated at the crack zone while Si dominated the surface not covered with minerals

3.7 Discussion

3.7.1 Light-curing kinetics of the pastes

When using different thicknesses of F7, results showed that the thicker the sample the longer the time needed to achieve a conversion higher than 50%. When the delay time exceeded the light-curing time, no monomer conversion on the lower surfaces was observed as seen with the 3mm thick sample cured for 10s only. Adding 50/reaction rate to the delay time, gives the minimum light-curing time necessary to reach 50% monomer conversion. For example, with 4mm thick samples of F7 (2%/s rate of reaction and 17s delay time), the minimum time needed to achieve 50% conversion is (25+17=42s) (Figure 3-1). The results are in good agreement with a previous study that showed a linear decrease in conversion with depth and calcium phosphate (CaP) content (Aljabo et al., 2015).

The delay time reflects the inhibition time from the beginning of the light-curing process until monomer conversion in the lower layer (in contact with the ATR diamond) was triggered. Increased thickness caused an increase in delay time and a decrease in rate of reaction. This is due to the time needed to bleach the photo initiator in upper layers of the sample, which are closer to the light gun. This might be also explained by the Beer-Lambert law which predicts an exponential decline in light intensity with depth due to absorbance due to the photo initiator. Additionally, the light is scattered due to mismatch in refractive indices of the composite monomer and filler particles which can further reduce light levels at greater depth.

The resin composite cytotoxicity is known to be affected by residual free monomers. Unreacted monomers will leach out upon absorption of water (Caughman et al., 1991; Stanislawski et al., 1999; Goldberg, 2008; Mohd Zainal Abidin et al., 2015). Achieving higher monomer conversion will be beneficial in reducing cytotoxicity of the proposed formulations and increasing mechanical strength. A benefit of greater cure depth is that the proposed formulation can be placed in thicker layers (bulk fill).

The choice of monomers used in these proposed formulations are the main reason behind the high level of monomer conversion. Composites containing UDMA are expected to have higher monomer conversion in comparison to those containing Bis-GMA (Filtek z250). More flexible monomers with low glass transition temperature will result in higher conversion. It was reported that glass transition temperatures of TEGDMA, UDMA and Bis-GMA were -83, -354 and -8°C, respectively (Sideridou et al., 2002).

Factorial analysis showed none of the variables to have major effect on monomer conversion, except for 3% increase in conversion with lower PLR. This disagrees with Panpisut et al. who found the phosphate filler to decrease the final monomer conversion by 10%. It may be due to the use of higher MCP content (10%) in addition to using Tristrontium phosphate, which may have caused a greater mismatch in refractive index (Panpisut et al., 2016). Less viscous formulations (lower PLR) showed a higher conversion and that was in agreement with Garoushi et al., who proved composites of lower filler content have higher light transmission ability resulting in higher conversion (Garoushi et al., 2016).

As mentioned in (3.5.1), accelerated ageing was achieved by storing the pastes at 60°C incubator for 6 months. The equivalent room temperature time was calculated using Arrhenius model (ASTM, 2016):

$$Real\ Time\ (RT) = Accelerated\ Ageing\ Time\ (AAT) \times Q_{10}{}^{(t_{AA}-t_{RT})/10} \qquad \text{Equation 3-1}$$

Q_{10} is the ageing factor. As a first approximation it can be assumed to equal 2 (i.e. reaction rate doubles for every 10°C increase in temperature). t_{AA} is the accelerated ageing temperature (60°C in the reported test) and t_{RT} is the ambient temperature (23°C). Hence, ageing the pastes for 6 months at 60°C equates to 6.5 years at RT. ISO 11607 reports that the most acceptable method to test stability is through real time ageing (BSI, 2017). However, due to time limitation, this study used the accelerated ageing method to optimise a final formulation where further real time ageing can then be assessed.

The results showed that ageing did not affect delay time or rate of reaction but decreased the monomer conversion by 5%. The hydrophilicity of PLS and MCP might cause water sorption into the pastes during the ageing process. Low level of polymerisation and hydrolysis of UDMA N-H group (due to water sorption) might explain the slight changes in spectra of aged versus non-aged pastes. Therefore, the pastes may suffer precipitation of components and resulting in non-homogeneous pastes. The cloudiness of nonhomogeneous pastes and maybe water sorption over time will cause an increase in refractive index differences and more scatter of the light ending up with lower monomer conversion at greater depths. Although discolouration of the pastes during ageing might also cause a reduction in light penetration, colour changes were not noticed after ageing (with naked eyes). D`Alpino et al. study also showed z250 to be stable after being aged at 37°C for 12 weeks, which equals 9 months in real time (D'Alpino et al., 2015).

3.7.2 Interaction of the cured discs with water

3.7.2.1 Water sorption and solubility

Many of the experimental formulations failed to achieve water sorption and solubility values lower than those recommended by ISO and the results were significantly higher than the commercial material (BSI, 2009). ISO 4049 standard is for polymer-based restorative materials that have no function other than filling the cavity. In conventional composites water sorption and solubility have only detrimental effects. Conversely, in the new formulations, however, these results need further examination to ensure their effects are primarily beneficial. The experimental composites with the novel additives (PLS, MCP) will cause higher water sorption and solubility and it is desirable to release these components and have the optimum therapeutic effect. In terms of the commercial material z250, the results were in good agreement with other studies (Misilli and Gonulol, 2017). Distortion and irreproducibility in water solubility values, however, has also been previously reported (Muller et al., 2017). In some materials absorbed water cannot be easily removed since it binds to hydrophilic components in the composite structure. This can cause large errors in the standard water sorption and solubility tests.

Higher PLR of the pastes equates to more PLS and MCP which may dissolve and be replaced with water. With higher PLR water may replace more PLS and MCP, but will then evaporate when the discs are reconditioned, leaving empty voids and causing higher solubility and water sorption results. Conversely, however, lower PLR could also enhance water sorption due to expanding the resin matrix phase (Oysaed and Ruyter, 1986; Ortengren et al., 2001; Toledano et al., 2003). Results in the current study suggest that the monomer phase expansion is more important in enhancing water sorption than the loss of the filler phase based on factorial analysis (Figure 3-13).

3.7.2.2 Mass and Volume change and acidity (H^+ release)

Lowering PLR had a small effect on increasing mass and volume change. This might be explained by the expansion of polymers matrix (unlike the fillers) causing water to be pulled into it encouraged by the hydrophilic PLS and MCP and leading to higher water sorption. PLS hydrophilicity encourages water sorption and with its release is replaced by water of comparable density. The water expands the surrounding polymer matrix. With more polymers, this expansion is increased. This will consequently provoke MCP dissolution leading together to higher mass and volume change and higher H^+ release. Mass change reaches a maximum level before volume change. In fact, mass change starts to go down at later times with formulations of higher PLS and MCP content. This might be due to dense MCP filler being replaced by less dense brushite crystals

combined with phosphate ion release. However, the volume change never goes down again as the polymer matrix is already expanded by water sorption. The mass and volume change results are strongly related to water sorption and solubility since the interaction with water includes absorbing water and releasing components (PLS and MCP). Similar effect of calcium phosphate (CaP) on mass and volume change was noticed in a previous study (Aljabo et al., 2015).

The apatite precipitation is proportional to time and MCP content (Aljabo et al., 2016b). MCP reacts to form brushite crystals with high porosity that expands the material and matrix and releases phosphoric acid. Phosphoric acid may interact with PLS to form a complex that promotes apatite precipitation from simulated dentinal fluid. In previous studies related to remineralising bone cements and dental composites (Mehdawi et al., 2009; Aljabo et al., 2015; Abou Neel et al., 2016; Aljabo et al., 2016b; Panpisut et al., 2016), it was shown that MCP reacts with water to form brushite and phosphoric acid. The brushite then turns into apatite which reacts with phosphoric acid to form calcium deficient hydroxyapatite. The tooth responds to mild acid attacks from bacteria (or phosphoric acid) by forming tertiary dentine (sclerotic dentine), which might be beneficial in protecting the pulp (Liu et al., 2013; Chen et al., 2016). Furthermore, this might enhance the effect of the restoration in remineralising remnant caries. Phosphoric acid, unlike citric or nitric acid, forms insoluble species rather than chelating calcium which renders the tooth more soluble (West et al., 2001).

3.7.2.3 PolyLysine release

Polylysine is an FDA approved agent that has been used as a food preservative. Polylysine is a highly water-soluble agent. It therefore encourages water sorption which subsequently enables the release of the agent. F1 and F2 showed an initial burst release of PLS which might be explained by the agent being released out of the surface of these samples with higher content of PLS and PLR. This is particularly beneficial to kill bacteria in the cavity allowing a healthier self-healing process. A burst release from formulations with higher PLR and PLS was also found by Panpisut et al.(Panpisut et al., 2016). Diffusion rate of a component from within a matrix might be affected by several factors (temperature, concentration difference, diffusion distance and diffusing material). Fick`s first law also states that diffusion is proportional to concentration gradient and it is a time-dependant process. Based on that, difference in concentration between the disc and the storage solution is higher with discs of high PLR and PLS content and therefore will encourage higher release of PLS. This might explain the burst release of PLS that was noticed with F1 and F2, in addition to the high particle contact at the surface of the dry samples.

General understanding of discs interactions with water (at 1 week):

When discs are soaked in water, they start absorbing water and releasing components (PLS and MCP). Water sorption will cause the weight to increase while the solubility will decrease the weight. The average mass change percentage due to water sorption and solubility was stated previously in Table 3-2. It was also proved that the PLS can be released and hence can be responsible for some of the mass loss, which can be calculated using Equation 3-2:

$$Mass\ loss\ (\%) = \frac{R_{ppm} \times V \times 10^{-6}}{m}$$
Equation 3-2

where R_{ppm} is the PLS release at 1 week into 1mL storage solution (V) (acquired from PLS calibration curve using HPLC) and m is the mass of the sample (g). The results of mass loss percentage caused by PLS release at 1 week are shown in Figure 3-34.
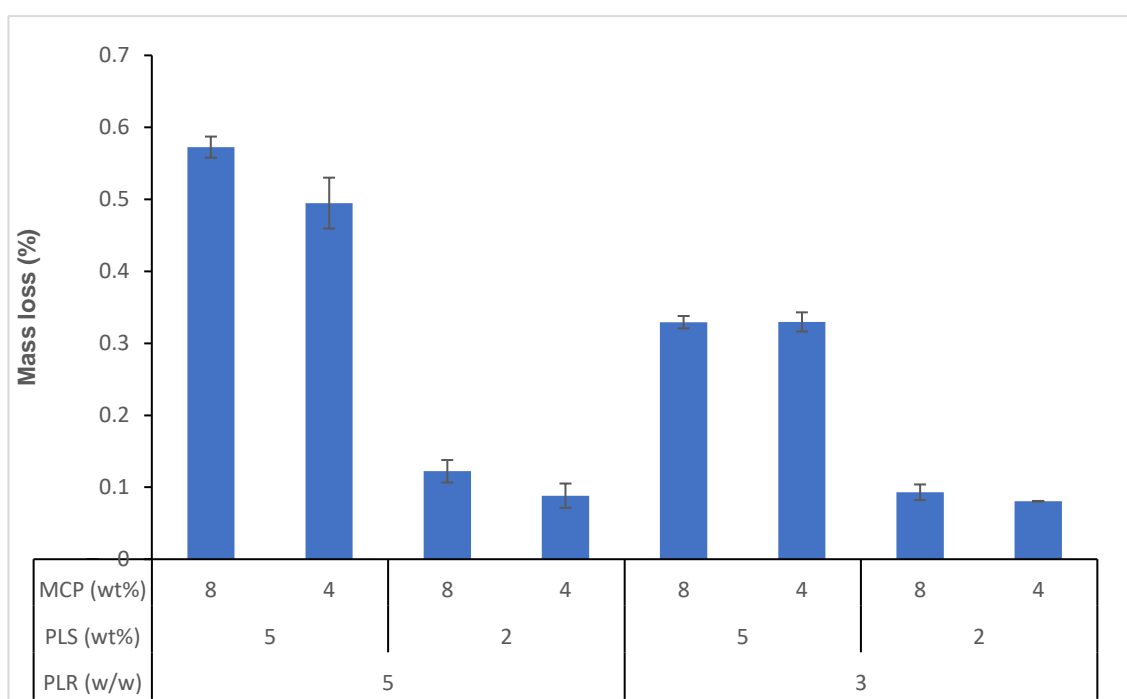
Figure 3-34 Mass loss percentage caused by PLS release at 1 week

Deducting the mass loss caused by PLS release from the total mass loss (calculated from water solubility results) provides the anticipated mass loss due to ion release from the MCP. The results are shown in Figure 3-35.
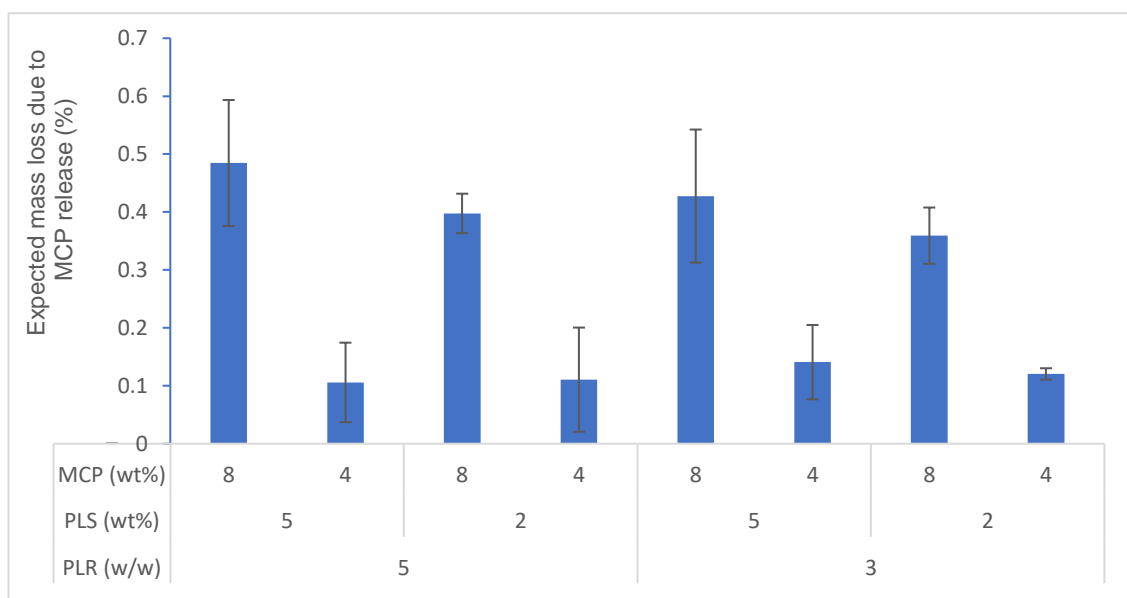
Figure 3-35 Expected mass loss due to MCP release at 1 week

Factorial analysis of these expected results (Figure 3-35) showed that MCP content is the major factor affecting the rest of the mass loss (295% increase with higher MCP content) which overlaps with the factorial analysis of acidity of solutions where discs were soaked (stated in 3.6.2.2). Therefore, the assumption of the acidity result (1 mole of H^+ per 1 mole of MCP) is reasonable.

3.7.3 Mechanical tests (flexural strength and modulus)

3.7.3.1 *Three-point bending flexural strength and modulus*

The commercial material showed significantly higher flexural strength in comparison to the proposed formulations and the results were comparable to similar studies (Chung et al., 2004; Thomaidis et al., 2013). Mechanical properties are majorly affected by the glass filler content, which explains higher modulus values when the PLR was increased. This was also in agreement with other studies (Manhart et al., 2000; Kim et al., 2002; Kumar and Sangi, 2014). Adding PLS caused a decrease in flexural strength. Panpisut et al results agree with the current research in that they also found the PLS and phosphate fillers to decrease flexural strength and modulus (Panpisut et al., 2016). This might be due to:

- lack of bonding between PLS/ MCP and the polymer phase,
- lower monomer conversion,
- hydrophilicity of these additives which increases the water sorption and leads to polymer to plasticise,

- and less homogenous material in comparison to those containing glass only (Ferracane, 2006).

3.7.3.2 Biaxial flexural strength and modulus

Comparing three-point bending with biaxial methods to test flexural strength shows that the biaxial method gives more reproducible and slightly higher values than the ISO method (Chung et al., 2004).

The additives in the formulations (PLS, MCP) can be released from within the discs at different times following water sorption and thus affect the mechanical properties of the discs. The early release of PLS (shown in PLS release test) led to a decrease in flexural strength and modulus starting one day after immersion in water. Discs will absorb water when immersed in water which will cause the polymers matrix to expand. This might reach a critical level where the polymer chain free energy no longer increased with further water sorption and the mechanical strength started to go down. Conversely, MCP had a delayed effect (after 1 month) that may be due to slower leaching of the agent. Aljabo et al. study showed a similar effect of CaP on flexural strength and modulus of a remineralising dental composite after 1 month of immersion in SBF (Aljabo et al., 2015; Aljabo et al., 2016b). Panpisut et al. results showed the same trend as they noticed a reduction in flexural strength and modulus with higher PLS and phosphate fillers (Panpisut et al., 2016). Results of this test were consistent with other studies that showed a decrease in flexural strength and modulus of composites after increased times of storage in water. That was explained by the dissolved unreacted monomers resulting in less dense samples, regardless of any reactive components. They also showed an increased strength in the first 24 hours due to continued reaction (monomer conversion) (Yap et al., 2002; Panahandeh et al., 2017). However, with the experimental formulations, the monomer conversion was high, and the unreacted monomers may not be a realistic explanation for the reduced strength. Interaction with water (hydrophilic components; PLS and MCP) and the polymers structure upon that interaction are more important factors.

Toughness increased with incubation in water due to the materials showing a wider plastic phase after reaching the yield point (end of elasticity).

As stated before, the MCP needs more time than PLS to leach out and show its remineralising effect. Therefore, the discs that were immersed in SBF for 3 months showed the surface to be totally covered with minerals in comparison to the 2 months ones that showed remineralisation at the crack zone only. Additionally, those discs which showed higher minerals precipitation, had a higher content of MCP, which might have

been the major factor affecting remineralisation. The precipitation started in the crack zone as it may have ensured a better attachment surface for the HA globules and it may also be explained by a higher concentration of minerals release in that zone. The influence of MCP content on remineralising was also stated in a previous study where higher MCP resulted in thicker layers of minerals covering the composite discs (Aljabo et al., 2015). This property will be beneficial in self-repairing any future cracks in the body of the restoration, close the gaps between the restoration and the tooth structure, remineralise any remaining carious tissues and help fight against recurrent caries.

3.8 Conclusion

The results of the tests in this chapter showed that:

- The minimum light-curing time needed is 20s for 2mm and 3mm samples to achieve at least 60% or 50% monomer conversion, respectively. For 4mm thickness samples, 40s light-curing time is needed.
- Delay time is higher in formulations of higher PLR.
- Rate of reaction is higher in formulations of lower PLR
- Monomer conversion is higher than 60% even with samples of 4mm thickness
- Increased thickness causes an increase in delay time and a decrease in rate of reaction.
- Ageing has small effects on light-curing kinetics. The PLS causes a 5% decrease in monomer conversion with 4mm aged samples.
- The additives (PLS and MCP) cause an increase in water sorption and solubility, mass and volume change and H^+ release.
- All formulations are able to release PLS. Formulations of higher PLR and PLS content show higher percentage of PLS release and initial burst release.
- Flexural strength of the experimental formulations after one day of soaking in water is higher than 80MPa, regardless of the method (three-point bending or biaxial).
- The additives (PLS and MCP) cause a reduction in flexural strength but it levels off after 3 months of soaking in water.
- Discs of experimental formulations show more plastic than elastic behaviour with increased times of incubation in water (when flexural strength is tested).
- Experimental formulations show the ability to promote minerals precipitation.

The following table (Table 3-5) summarises the major effect of variables (PLR, PLS, MCP) on the tested properties.

Table 3-5 Summary of variables effect on different properties of the proposed experimental formulations

	PLR	PLS	MCP
Increased	PLS release	PLS release	PLS release
	Water solubility	Mass change	Volume change
	Biaxial flexural modulus	Volume change	H^+ release
		H^+ release	Water sorption and solubility
		Water sorption and solubility	
Decreased	Water sorption	Biaxial flexural strength	Biaxial flexural strength
	Toughness	Biaxial flexural modulus	Biaxial flexural modulus
		Toughness	
		Conversion (4mm)	

4 Creating Caries-like Model to Check Sealing, Penetration and Resin Tags Formation

Thesis structure

Chapter 1:
literature review

Chapter 2:
Materials and methods

Chapters related to the first eight formulations

Chapter 3:
Basic properties of the first eight experimental formulations

Chapter 4:
Resin tags formation

light curing kinetics, intercations of the discs with water and mechanical properties

Creating caries-like collagen discs to check ability to penetrate

Chapters related to the final formulations
F9 and F10

Chapter 5:
Summary of chapters 3, 4 and the basic properties of F9, F10

Chapter 6:
Adhesion to tooth structure
(F9, F10)

Chapter 7:
The effect of the novel additives, MCP and PLS

Self-etch, cavity adaptation, tags formation, microleakage and shear bond strength

Remineralising effect and MMP inhibition

Chapter 8:
General conclusion

Chapter 9:
Future work

4.1 Abstract

Aims:

The purpose of the work presented in this chapter was to create a standardised caries-like model (collagen mesh) from human dentine then test the ability of the experimental formulations to form resin tags within this mesh.

Materials and methods:

Human dentine discs of different thicknesses were immersed in phosphoric acid (35%), demineralising remineralising buffer solutions or 4M formic acid. The resultant discs were checked using SEM/EDX and Raman spectroscopy and compared to natural caries. Mass change of these discs was also recorded.

The caries-like model was used and experimental formulations along with adjusted formulations (without 4META, PPGDMA, PLS or MCP) were applied on top of it and light-cured. Subsequently, the collagen was dissolved away by immersing specimens in NaOCl for two days and the adhesion interface scanned under SEM/EDX. The area covered by tags at the interface was measured by means of image analysis software.

Results:

Human dentine discs of 2mm thickness demineralised by immersion in formic acid 4M exhibited total loss of minerals and ~70% mass loss after 2 days. SEM/EDX results confirmed the loss of minerals and the maintenance of collagen structure. Raman spectroscopy showed a comparable composition of these discs to infected dentine.

All eight experimental formulations had the ability to penetrate into the collagen mesh and form resin tags. The length of these tags ranged from 15μm to 68μm and the coverage area varied from 35% to a maximum of 84% of the adhesion interface. Formulations of lower PLR, higher PLS and MCP showed better results. 4META and PPGDMA also helped increase this property.

Conclusion:

Formic acid 4M totally demineralised human dentine discs of 2mm thickness which subsequently resembled the naturally carious dentine.

All experimental formulations penetrated into the collagen mesh forming resin tags. Lower PLR and higher PLS and MCP all played a positive role boosting the tags coverage area.

4.2 Introduction

When caries progress into dentine, bacterial acids dissolve tooth minerals and different layers can be identified based on the level of demineralisation and collagen structure (Mazzoni et al., 2015b; Dorri et al., 2017a). These layers are mainly the infected and the affected dentine. The outer layer (infected) is highly carious, rich with bacteria and totally collapsed collagen unlike the inner layer (affected) which still contains some minerals and maintained structure of collagen. The dental pulp responds to carious attack by forming a mineral-rich third layer (translucent layer) to defend itself from irreversible damage (Fusayama et al., 1966; Fusayama and Terachima, 1972; Anderson et al., 1985; Angker et al., 2004).

Affected dentine can be saved and remineralise if properly sealed with a restorative material that can precipitate minerals at the interface. The main key factor for this to succeed is interlocking with carious dentine to limit microleakage at the interface and eliminate any residual bacteria in the cavity by trapping and starving it in a confined environment.

Restorative materials, which are currently used, require removal of both infected and affected dentine layers to place the filling in a caries free cavity.

In this chapter, creating a model that resembles the affected dentine in terms of structure is addressed. This model was used to assess the ability of the experimental formulations to form resin tags.

Forming resin tags would be beneficial in two ways:

- It will prove the ability of the experimental formulations to self-adhere to and interlock with carious dentine without the need for acid etching and the complicated bonding steps.
- Consequently, the proposed method of application of these materials would be an atraumatic restorative technique without the need for total caries removal which will enable a simpler and pain-free treatment.

4.3 Hypothesis

The null hypothesis is:

- There is no significant difference between the proposed experimental formulations and commercial comparators (Filtek z250, Activa, Fuji IILC and Fuji IX) in terms of forming resin tags (penetration) using a caries-like model.

4.4   Aims and objectives

The aim of the study in this chapter was to:

- Create a caries-like model (collagen mesh) by demineralising sound discs obtained from the top third of the coronal dentine of human permanent teeth and comparing it to different zones of naturally carious dentine.
- Test the ability of different experimental formulations to penetrate and form tags using the caries-like model, detect the composition of these tags and the role of variables (4META, PPGDMA, PLR, PLS and MCP) in forming tags.

4.5 Materials and methods

4.5.1 Demineralising dentine to create caries-like standardised model

Sound extracted human permanent teeth (molars and premolars) were collected and cleaned of any tissue remnants attached to the root, then soaked in Thymol 1% for 2 days before storing in fresh water in the fridge. Water was replenished every couple of weeks and teeth were used within 6 months of extraction.

Before cutting the teeth, they were mounted upright in a plastic mould with roots only immersed in epoxy resin (7:1 resin to curing agent ratio) and left for 24 hours to allow the resin to set before removing samples from the mould. Samples were then placed in a cutting machine (Leica SP1600) and had the occlusal enamel cut off. Cutting thickness was then set to 2mm of coronal dentine. Carious discs or discs with pulp horns apparent were discarded. Obtained discs were then polished using a grinding machine (Struers Ltd., Denmark) with 2000-grit abrasive paper. The resultant discs were composed of dentine surrounded by a ring of enamel. Discs were stored in deionised water in the fridge.

Preparing demineralising solutions:

- Formic acid (4M): 31.8mL of acid was added to 50mL of deionised water carefully and then topped with water to a final volume of 200mL (Besinis et al., 2014).
- Phosphoric acid 37%: 96% phosphoric acid solution was diluted to a final concentration of 37% by adding 77mL of the acid to 50mL of deionised water. Final volume was adjusted to 200mL with deionised water.
- Buffer solutions (pH cycling) (Marquezan et al., 2009; Buzalaf et al., 2010; Lenzi et al., 2015):
  - The demineralising solution contained 2.2mM $CaCl_2$, 2.2mM NaH_2PO_4, and 50mM acetic acid to adjust the pH to 4.8.
  - The remineralising solution contained 1.5mM $CaCl_2$, 0.9mM NaH_2PO_4, and 0.15M KCl to adjust the final pH to 7.

Demineralising protocol:

Each dentine disc was immersed in 15mL of a selected demineralising solution (n=3) for the following times on a shaker plate (Biometra WT16, speed 10):

- Formic acid 4M for 2 days using 0.5mm, 1mm or 2mm discs
- Phosphoric acid 37% for 2 days using 2mm discs

- Buffer solutions for 2 weeks using 2mm discs: samples were alternated in between the two solutions (2 days in demineralising solution/ 1 day in remineralising solution) for 14 days (solutions were replenished every cycle).

The discs were then thoroughly washed and vortexed to remove any acid remnants. Scanning Electron Microscopy (SEM) (Phillip XL-30, Eindhoven, The Netherlands), was used to image the resulting discs.

Additionally, mass change of the 2mm discs immersed in formic acid (n=13) over 48 hours was recorded. EDX (Inca X-Sight 6650 detector, Oxford Instrument, UK) and Raman spectroscopy (Horiba Jobin Yvon, Paris, France) were also used to compare the disc chemistry with that of sound and carious enamel and dentine. These tests were run to detect removal of all the minerals, and make sure the discs were pure collagen mesh.

4.5.2 Tags formation with the collagen mesh model

The ability of all eight experimental formulations to penetrate into the collagen mesh created with formic acid (4.5.1) was tested. The commercial comparators used were Filtek z250, Activa, Fuji II LC and Fuji IX. Additionally, the experimental formulations F1 and F2 were adjusted by taking out the PLS, MCP, 4META or PPGDMA to assess the effect these components have on tags formation.

Composite pastes were placed in a metal circlip (10*1mm). Blot dried collagen discs (caries-like dentine) was then laid on top of the paste and slightly pressed down until the disc was properly embedded in composite (n=3). Composite pastes were then light-cured for 40s on each side (except Fuji IX). Subsequently, each sample was immersed in 10mL sodium hypochlorite (NaOCl) 15% for 2 days to totally dissolve the collagen. This created composite discs with an imprint of the collagen discs.

Samples were then coated and imaged through SEM to check the length of resin tags and total tagged area using image analysis software (ImageJ, Fiji). The tags represent the quality and the ability of different composite formulations to penetrate into collagen in a way that mimics the clinical environment.

The areas covered with tags were noticed to be darker in colour (dark grey) than the tags free areas (light grey) after coating with Gold/Palladium. As a result, samples were imaged with a magnifier (x40) and images were analysed through ImageJ software to check the percentage of area covered by tags (Figure 4-1).

| SEM images of the interface upon dissolving the collagen | Analysed images based on greyscale (darker colour gives higher peaks) | Image of the sample coated for SEM scanning | Image analysed to calculate tagged area (dark grey) |
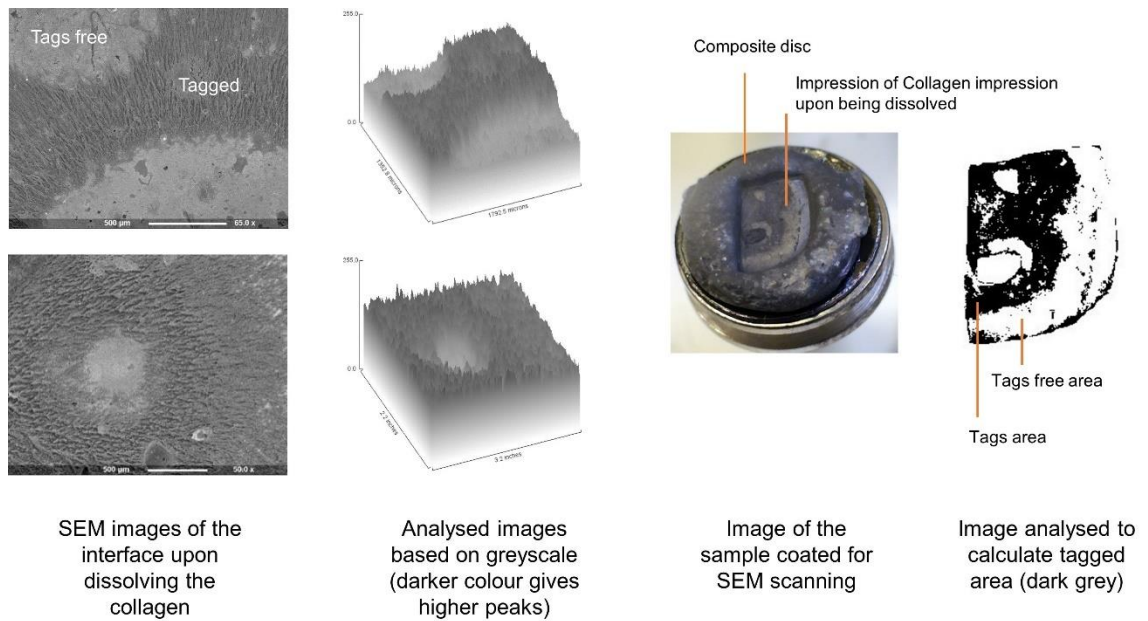
Figure 4-1 Method of detecting tagged area at the collagen/restoration interface. Dark and light grey areas were identified as tagged or tags free, respectively. Image analysis was used to calculate the percentage of dark grey area to the total adhesion surface

The steps followed in ImageJ software to analyse the images were as follows: a scale was set according to the diameter of the holding metal stud (12.6mm), any deformities in the disc (especially noticed near the pulp horns area) were measured and deducted from the total area of collagen imprint (adhesion interface area). Images were transformed into 8-bit and threshold applied (to change different grey shades into defined black and white). The threshold area was then measured which represents the area covered by the tags. The percentage of tagged area was calculated.

4.6   Results

4.6.1   Demineralising dentine to create caries-like standardised model

Figure 4-2 shows example SEM images of the discs obtained from human teeth following immersion in different demineralising solutions. Discs which were immersed in buffer solutions (alternately, 2 days in demineralising solution, 1 day in remineralising solution for two weeks) showed poor structure of opened dentinal tubules, enamel did not dissolve, and discs remained hard. Using phosphoric acid 37% as a demineralising solution for 2 days showed the same results as with the buffer solutions with one unique finding under SEM. It was the precipitation of minerals (in brushite form) in the enamel region.

Conversely, using formic acid 4M for 2 days, gave 2mm discs of non-collapsed dentine. These had widely opened dentinal tubules when scanned with SEM. The enamel was totally dissolved, and the resultant discs were flexible (easily bent). However, the 0.5 and 1mm thick discs showed the collagen structure to be degraded and the tubules to be occluded due to the collapsed collagen mesh.
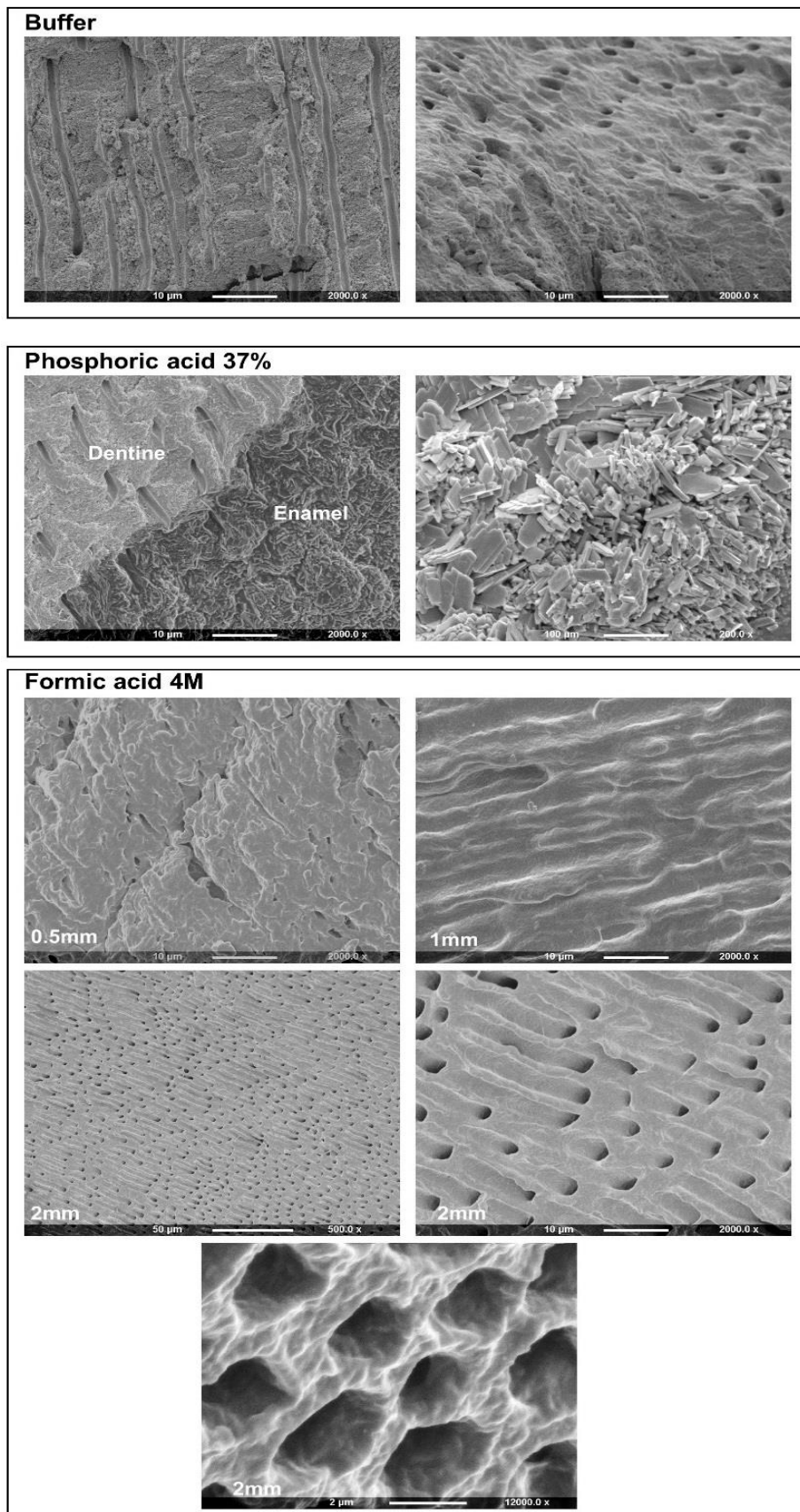
Figure 4-2 SEM images of dentine discs upon soaking in Buffer solutions (2 days in demineralising solution, 1 day in remineralising solution for two weeks), phosphoric acid 37% (for two days) or Formic acid 4M (for two days)

The 2mm discs that were demineralised using formic acid showed no mineral content (Ca, P) on the surface or in the bulk when scanned with EDX.

The mass change of discs upon immersion in formic acid (2mm discs) showed a linear decrease in mass versus square root of time until 24 hours and then levelled off. The mass loss recorded after 24 hours of soaking was 74% and it increased to 75% only after a further 24 hours (Figure 4-3). Drying these discs showed a final mass loss of 79% indicating a collagen disc water content of 4/25*100=16%.
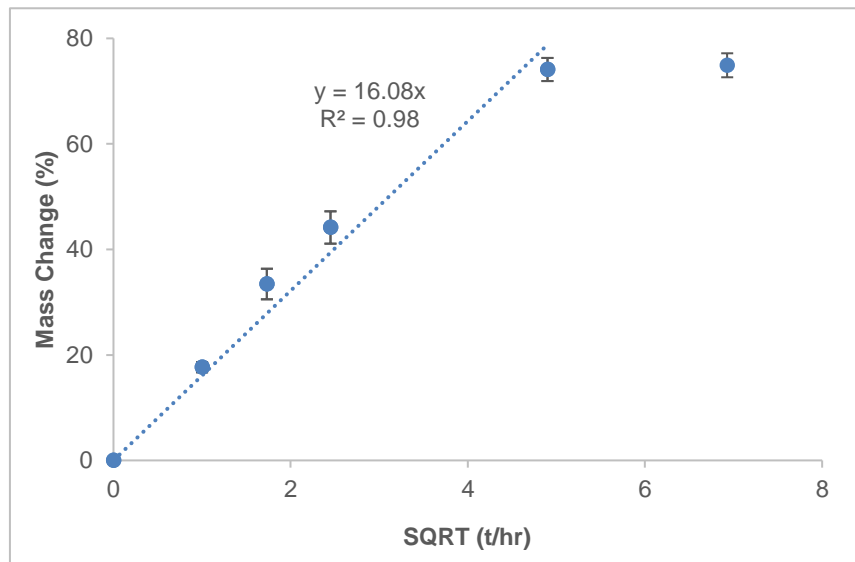
Figure 4-3 Dentine discs mass change percentage versus SQRT of time upon immersion in formic acid. Mass change is proportional to SQRT of time until one day then levels off. Error bars are 95% CI (n=13)

Raman spectra of sound enamel, different zones of carious dentine (surface, body of lesion and the translucent layer) and the collagen mesh (2mm discs demineralised over 48 hours using formic acid) showed the following major characteristics (Figure 4-4):

- Sound enamel had a higher peak at 960cm^{-1} (phosphate PO_4^{-3} peak) and weaker carbonate peak at 1085cm^{-1}
- Dentine had distinguishing CH peaks at about 1470 and 2900cm^{-1}
- Dentine also gave strong amide I and III peaks at 1250 and 1670cm^{-1}
- The phosphate peak (960cm^{-1}), which represents the mineral content (hydroxyapatite), decreased relative to the collagen peaks in the order; enamel > sound dentine > translucent layer > body and surface of the carious dentine lesion as well as the collagen mesh.
- Amide peaks (due to collagen) could be difficult to obtain from the surface of carious dentine due to high fluorescence. Collagen peaks were better maintained in the body of the lesion, the translucent layer and the collagen mesh.
- Raman spectrum of the collagen mesh was most like those from the body of the carious dentine lesion.
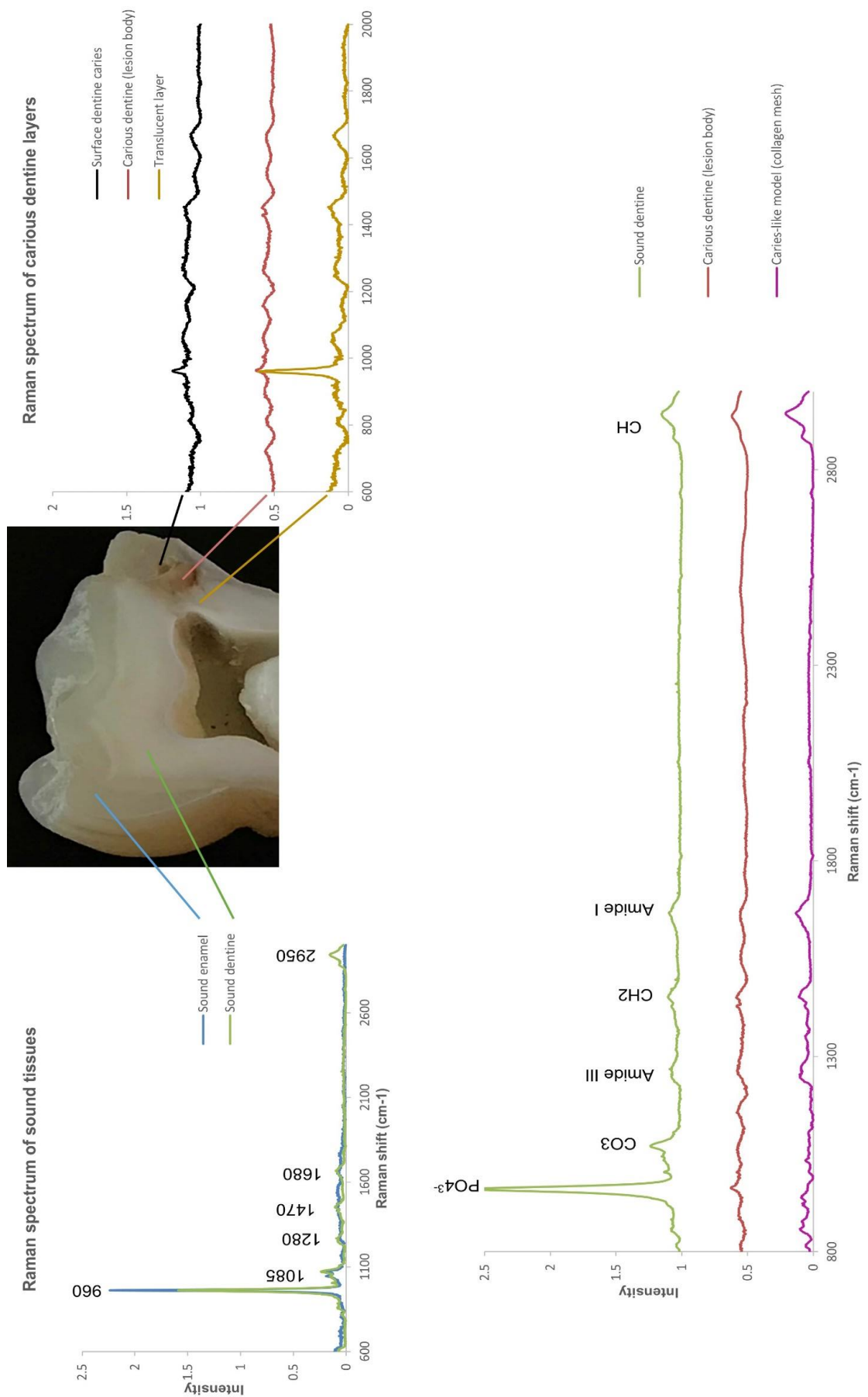
Figure 4-4 Average Raman Spectra of sound enamel and dentine, carious dentine layers and caries-like model (collagen mesh). n=3

4.6.2 Tags formation with the collagen mesh model

The following figure (Figure 4-5) shows SEM images of the interface (composite discs/ collagen mesh) following dissolving the collagen to detect composite penetration into the mesh. It shows resin tags formation of the two formulations with 5% PLS and 8% MCP (PLR 5 or 3) followed by the effect of removing the PLS, MCP, 4META or PPGDMA.
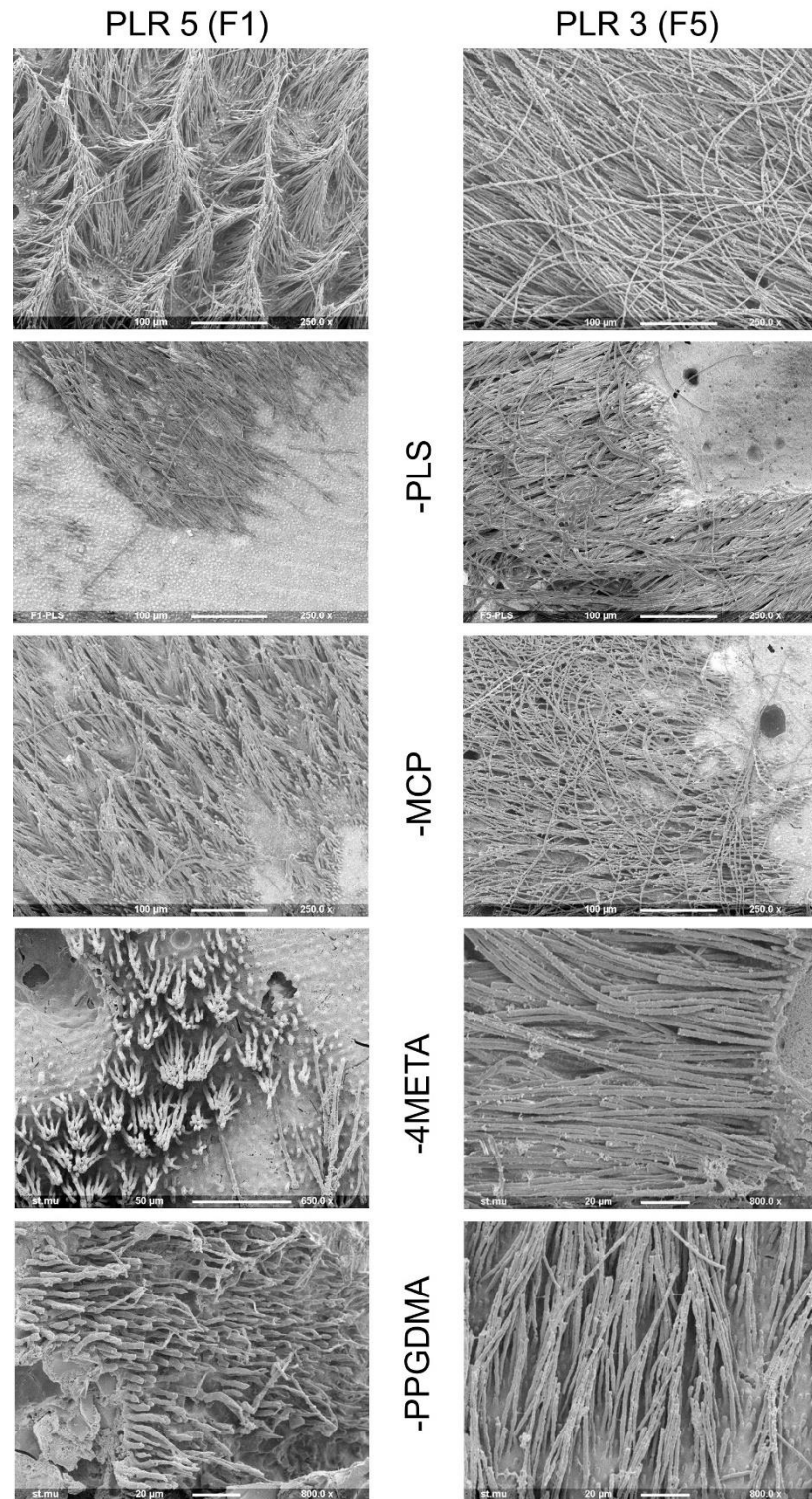
Figure 4-5 SEM images of tags formation with collagen mesh (ability to penetrate) of F1 (PLR5) and F5 (PLR3) in comparison to the adjusted fomulations by taking out PLS, MCP, 4META or PPGDMA

The average tags length formed within the collagen mesh by formulations of different PLR and with or without the addition of 4META and PPGDMA was measured (Figure 4-6). The results showed that the average length was 68μm for formulations of lower PLR (3:1), about 400% longer than what was achieved with formulations of higher PLR (5:1), 15μm length. Taking out 4META or PPGDMA did not seem to affect the tags length significantly.
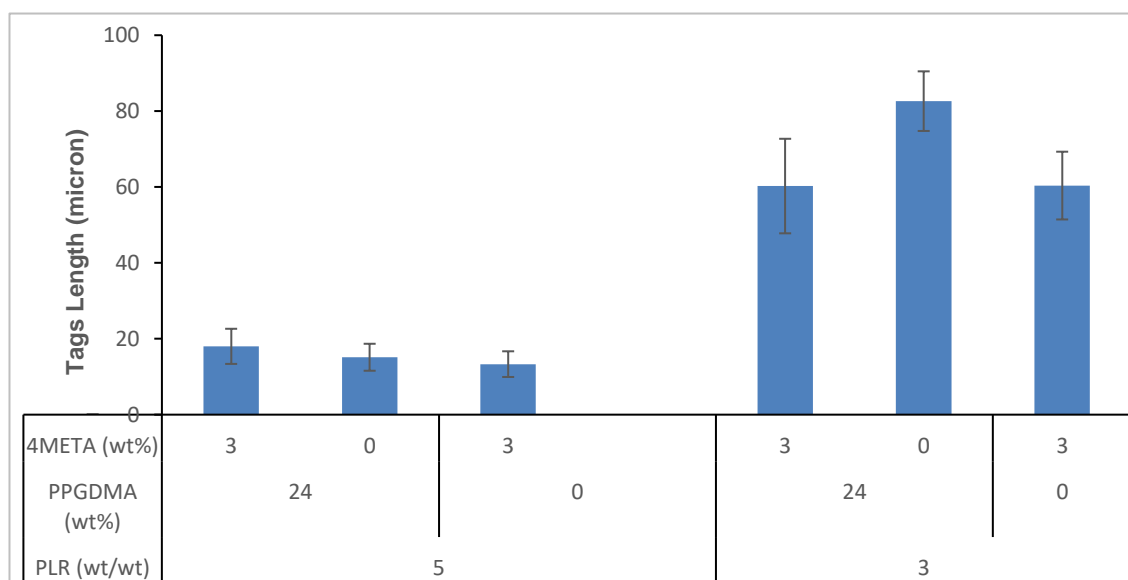
Figure 4-6 Length of tags penetration into the collagen mesh of formulations with 5% PLS and 8% MCP (PLR 5 or 3) in comparison to adjusted formulations (without 4META or PPGDMA). Error bars are 95% CI (n=15)

The area covered by tags using these formulations was also measured. The results are shown in Figure 4-7. The original formulations of F1 and F5 showed the highest results at 77% and 84%, respectively. Adjusted formulations with no PLS or MCP content showed the lowest results, but this will be reported in more details later in this section. However, factorial analysis also showed that taking out 4META or PPGDMA caused a decrease in tags coverage area (Figure 4-8). This effect was calculated using Equation 2-26 and it showed a 34% and 9% decrease in tags coverage area if 4META or PPGDMA were taken out, respectively.
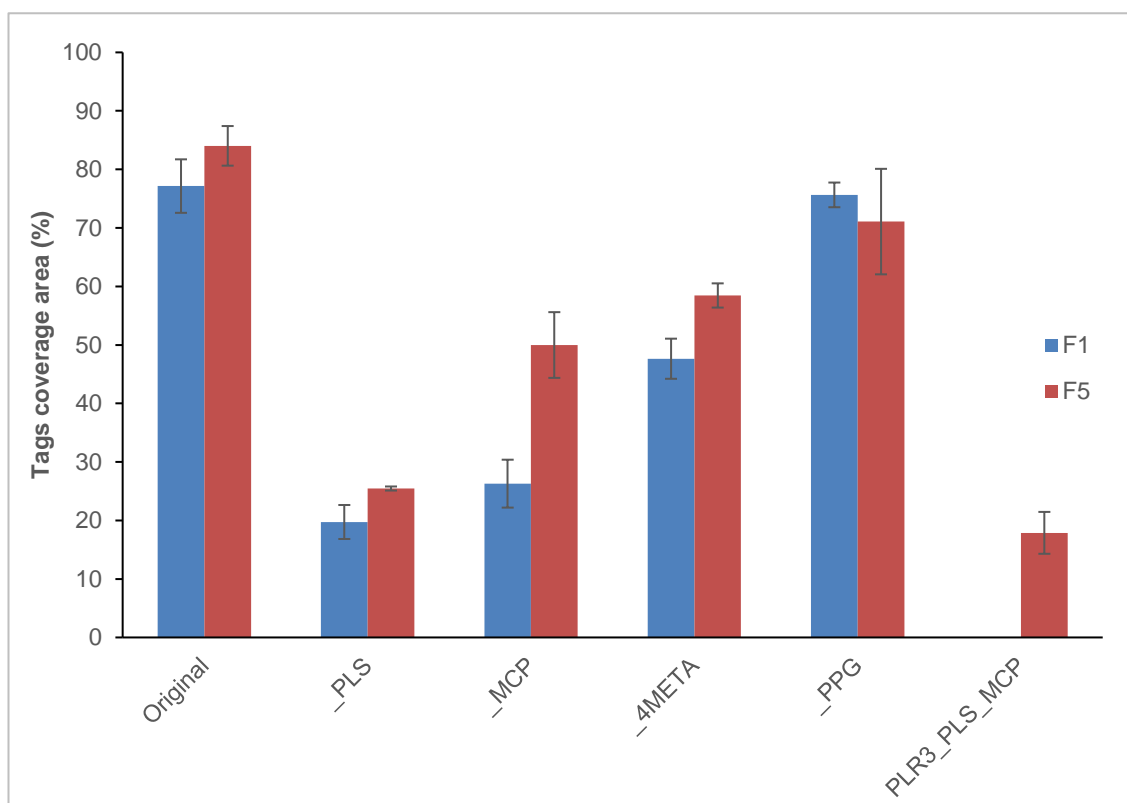
Figure 4-7 Tags coverage area of F1 (PLR5) and F5 (PLR3) in comparison to the adjusted formulations by taking out PLS, MCP, 4META, PPGDMA or PLS and MCP. Error bars are 95% CI (n=3)
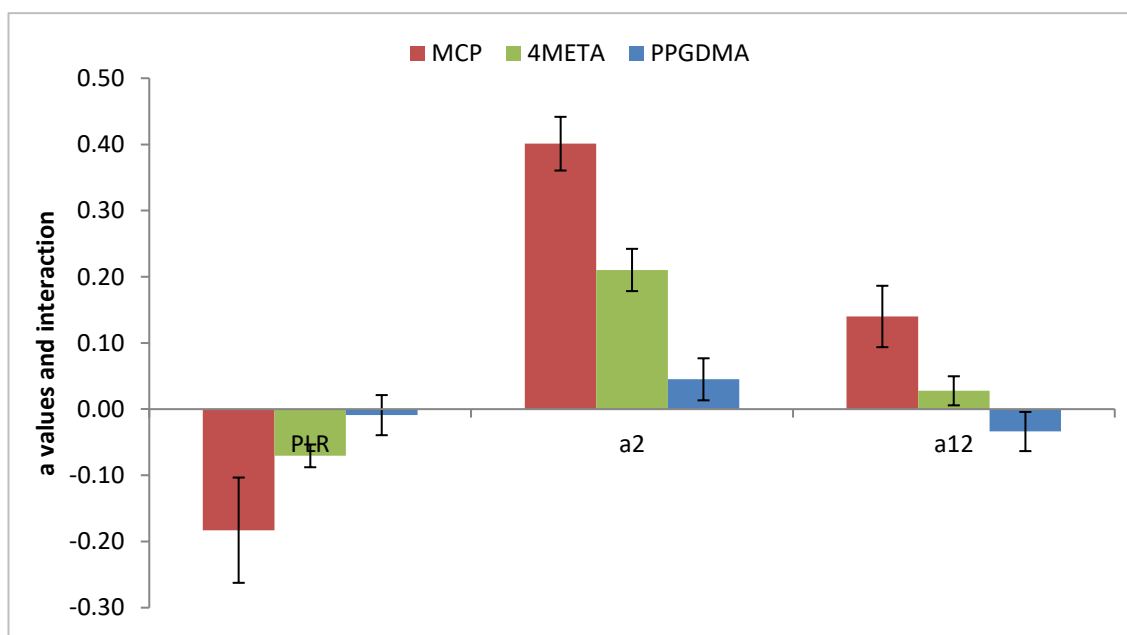
Figure 4-8 Factorial Analysis (a values and interactions) of tags coverage area amongst the adjusted formulations. a1 is PLR, a2 is MCP, 4META or PPGDMA

Looking further into the tags coverage area achieved by all eight experimental formulations, the results varied from 35% to a maximum of 84% (Figure 4-9). Increasing PLR caused a small decrease in coverage whilst within formulations of the same PLR there was also a downwards trend with lower PLS and MCP content. All images and

binary (thresholded) images which were used to acquire this data are shown in Appendix D.

MCP (wt%)	8	4	8	4	8	4	8	4
PLS (wt%)	5		2		5		2	
PLR (w/w)	5				3			
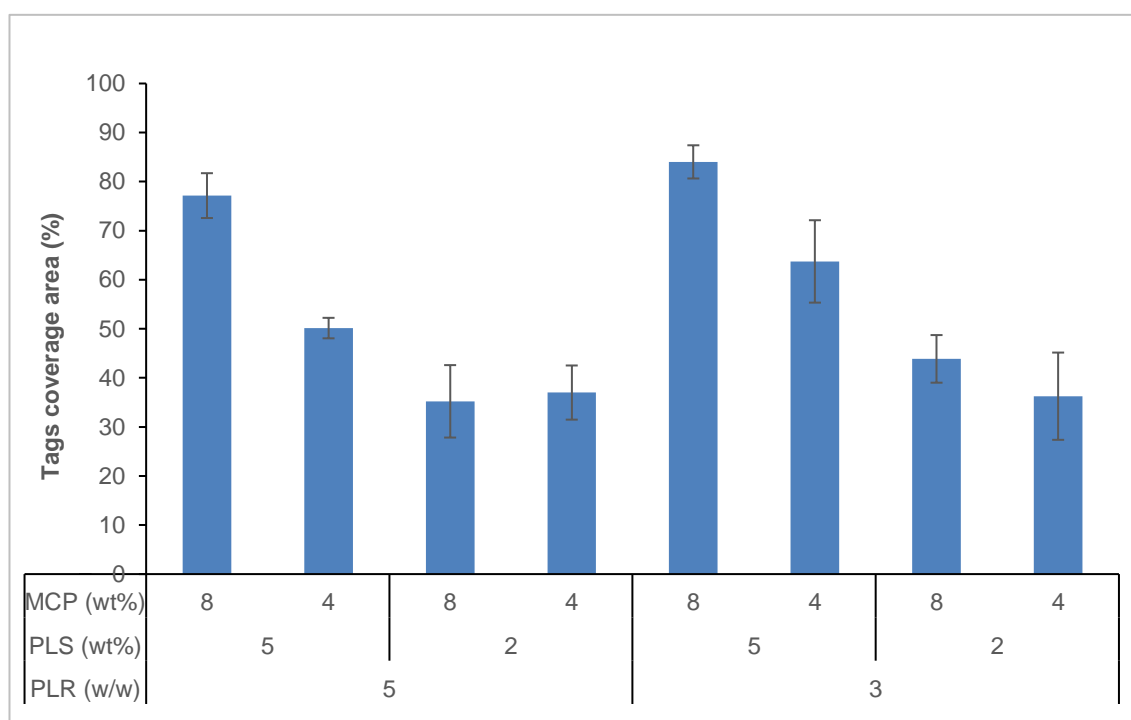
Figure 4-9 Tags coverage are of the experimental formulations. Error bars are 95% CI (n=3)

The commercial comparator z250 showed 55% tagged area (only when used with a bonding agent, otherwise no tags formed), while Activa showed 39% of the collagen mesh as covered by tags. Fuji IILC showed no tags formation with the collagen mesh while Fuji IX was not suitable for the test method as it degraded and collapsed when specimens were immersed in sodium hypochlorite (Figure 4-10).
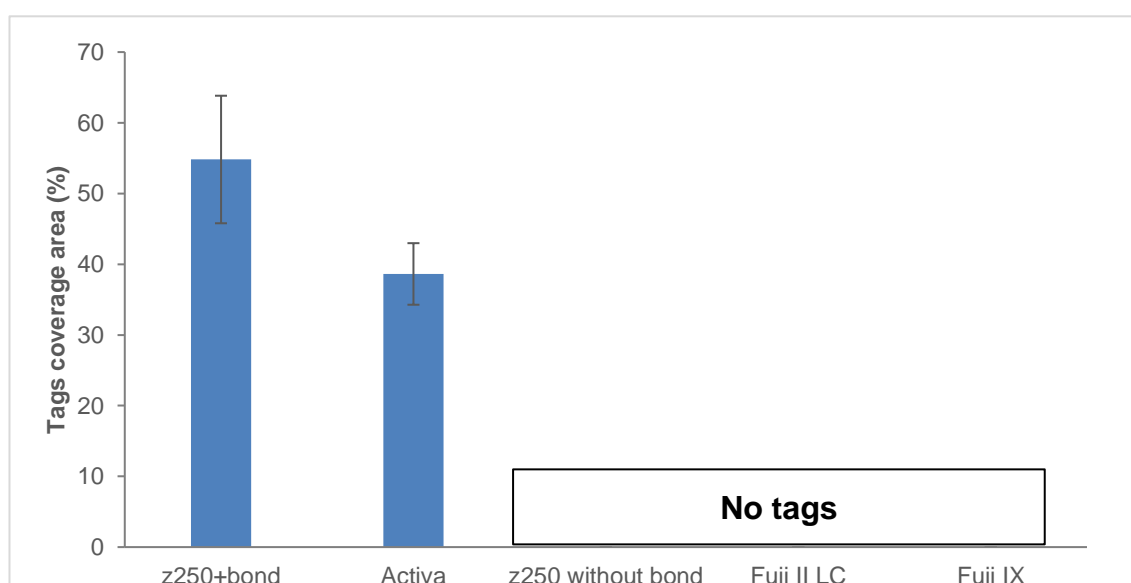
Figure 4-10 Tags coverage area of the commercial comparators. Error bars are 95% CI (n=3)

Fixing PLS at 5% and reducing the MCP content (from 8% to 4% to 0%) or fixing MCP at 8% and reducing the PLS content (from 5% to 2% to 0%) caused a linear decrease in the area covered by the tags. The gradient with varying MCP was PLR dependent and steeper with higher PLR. Conversely, PLR had lesser effect when PLS was varied (Figure 4-11).
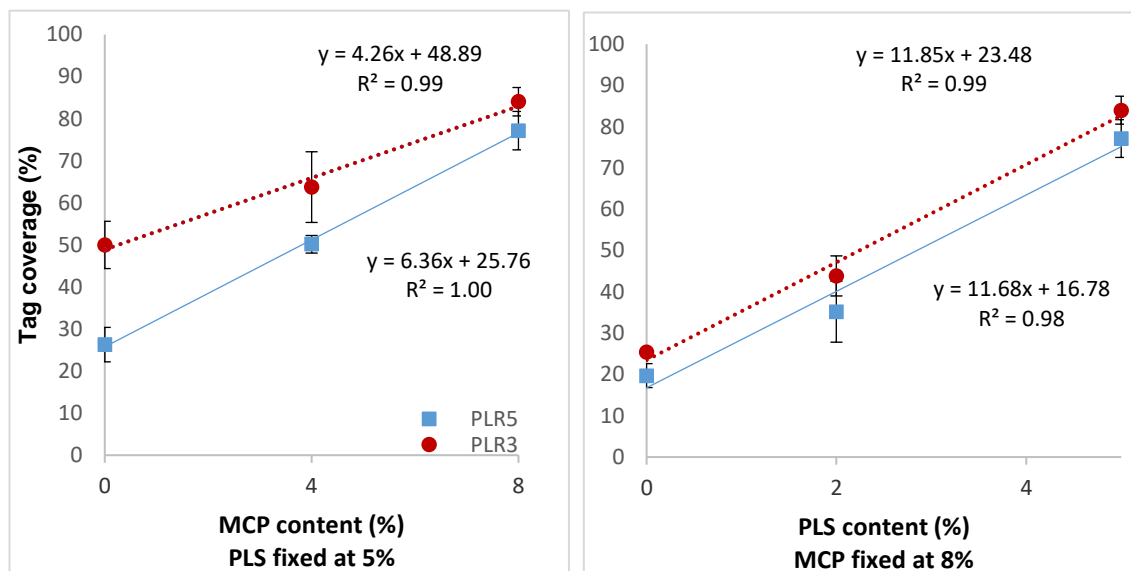
Figure 4-11 Effect of MCP and PLS content on tags coverage area amongst fomulations of PLR 5 or 3. Error bars are 95% CI (n=3)

Factorial analysis of tags coverage area (Figure 4-12) showed that the major variable that increased the tags coverage area was increasing the PLS content followed by the MCP content. PLR effect was smaller than its error bar and therefore considered experimentally insignificant. Using Equation 2-25 showed that increasing the PLS or MCP content resulted in 79% or 24% higher results. The analysis also showed that there was an interaction effect between PLS and MCP and between all three variables together, which was reflected in 10-15% increase in the area covered by the tags.
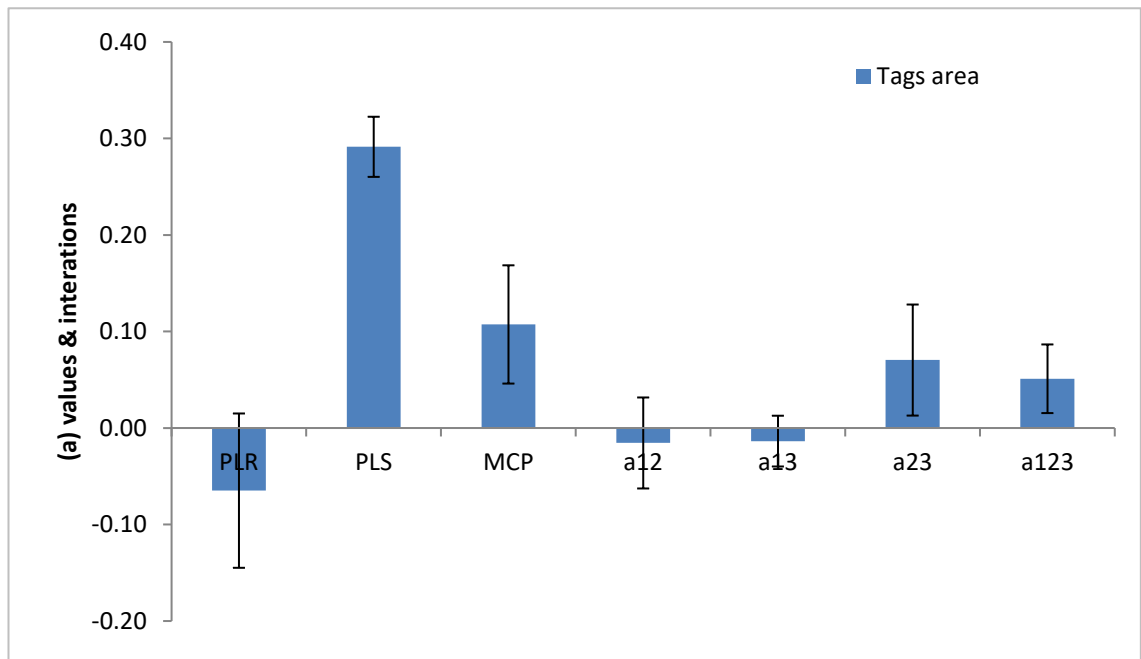
Figure 4-12 Factorial Analysis (a values and interactions) of tags coverage area of the original experimental formulations. a1 is PLR, a2 is PLS and a3 is MCP

EDX analysis of the tags formed by all experimental formulations in comparison to the surface of the composite discs is shown in Figure 4-13. The element composition showed higher Barium (Ba) and Silica (Si) on the surface of the discs. Resin tags showed higher Carbon (C) and Nitrogen (N) content. The ratio C:N was about 3:1 in all formulations on average.
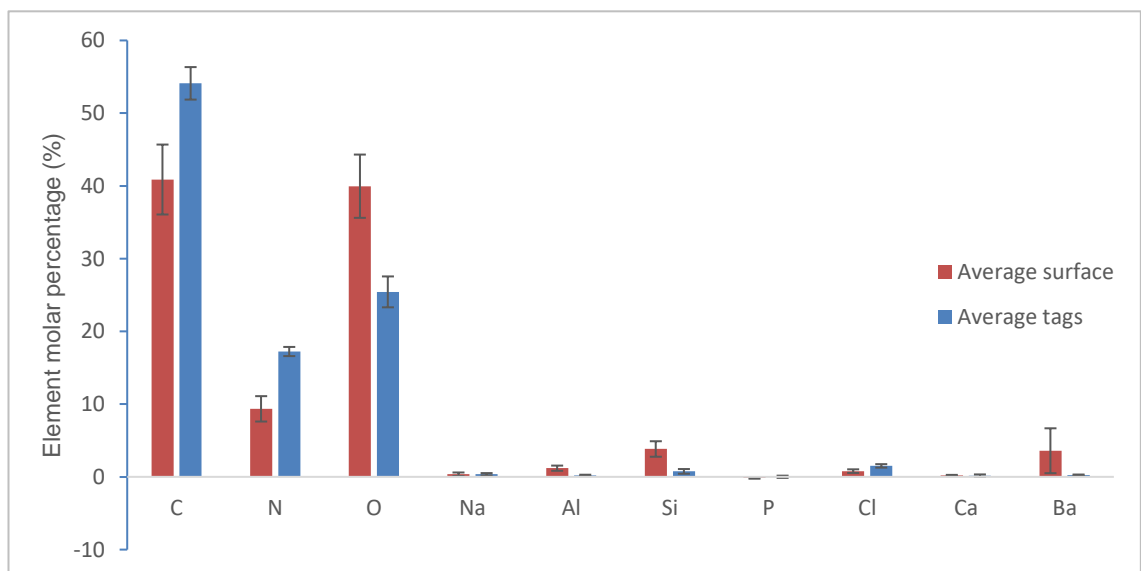
Figure 4-13 Element composition of tags and surface of the experimental formulations (molar percentage). Error bars are 95% CI (n=8)

4.7 Discussion

4.7.1 Demineralising dentine to create caries-like standardised model

Attempts to create a caries-like model to be used as a substrate for studies have previously included three main different methods of dentine demineralisation: chemical (using acids), bacterial or buffer solutions. The microbiological method resulted in a very soft structure comparable with naturally carious infected dentine. Conversely, a chemical method using lactic acid gave only superficial (~500µm) reduction in hardness (Marquezan et al., 2009). In this case the surface structure was more like caries affected dentine. The results from pH cycling varied massively with different reported protocols (Sousa and Silva, 2005; Buzalaf et al., 2010; Yang et al., 2011; Pacheco et al., 2013; Besinis et al., 2014; Abou Neel et al., 2016).

Why was formic acid (4M) the optimal demineralising method?

With phosphoric acid, the pH was only relatively low (2.55). At this pH, phosphoric acid can form minerals such as Dicalcium Phosphate Dihydrate (brushite, DCPD) instead of totally dissolving the enamel (Johnsson and Nancollas, 1992; West et al., 2001). This reaction can be explained by the following equation:

$$7H_3PO_4 + Ca_5(PO_4)_3OH \rightarrow 5Ca(H_2PO_4)_2 + H_2O \qquad \text{Equation 4-1}$$
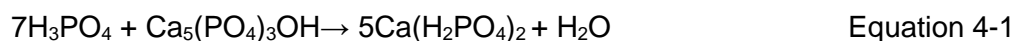
This prevented further reaction by blocking the dentinal tubules. A previous study showed that pH cycling or using acidified gel induced superficial demineralisation resembling affected dentine whilst a microbiological method created a structure more similar to infected dentine (Marquezan et al., 2009). However, unlike with formic acid use, none of the methods used in previous studies could demineralise more than 500µm deep of dentine surface (de Carvalho et al., 2008; Marquezan et al., 2009; Pacheco et al., 2013).

Formic acid, being able to demineralise thicker discs of dentine can be explained by it having the lowest pH (1.4) amongst the used solutions. The acid dissociation constant (K_a value) determines its strength; the higher the K_a value, the stronger the acid. K_a values of the used acidic solutions (with formic acid being at 1.8×10^{-4} in between acetic acid, 1.8×10^{-5}, and phosphoric acid, 7.1×10^{-3}) can also play a role in the demineralisation process. Additionally, calcium formate salts are more soluble than some of the calcium phosphates. Formic acid is known to be one of the highest cariogenic acids produced by bacteria in dental plaque. The efficacy of formic acid in creating caries-like model was

expected and it was in good agreement with other studies (Eggert and Germain, 1979; Odajima and Onishi, 1998).

Why 2mm dentine discs and how was total demineralisation confirmed?

Mass loss is diffusion controlled and the gradient depends on thickness. Therefore, thinner discs were expected to be totally demineralised, but they showed collapsed collagen mesh. This might be due to enzyme-related degradation. The percentage of weight loss that happened in the 2mm discs with formic acid is consistent with the level of inorganic content (minerals) in dentine (70%) plus a small amount from the thin layer of enamel. The loss of peak at $960cm^{-1}$ in the Raman spectrum reflects the loss of HA which was also confirmed by EDX. These results were in good agreement with other studies (in terms of detecting or losing HA peak in Raman spectrum and tracing Ca and P atoms in EDX) where sound dentine, collagen mesh and natural or artificial caries created were scanned through different methods (Xu et al., 1997; Tramini et al., 2000; Pacheco et al., 2013; Salehi et al., 2013).

4.7.2 Tags formation with the collagen mesh model

Resin bonding to sound dentine requires an adhesive agent that contains hydrophilic components (such as 4META or HEMA) that will penetrate into pre-etched tooth surface and hydrophobic components that will link the restorative material to the bonding layer (Trevor Burke et al., 2017). It was found that thinning that adhesive layer (bonding agent) by means of air blowing could reduce future nanoleakage by keeping this layer, which is responsible for future failure and recurrent of the disease due to solubility, to the minimum (Chen et al., 2014).

However, this bonding interface is not stable, and its degradation will lead to future nanoleakage and failure. Many methods have been reported in order to limit this effect, but none of them was sufficient to solve this problem. These methods included for example:

- chemical bonding to calcium ions (e.g. using 10MDP in self-etch adhesives),
- inhibiting the enzymes (MMPs) responsible for collagen degradation at the interface (e.g. using CHX) (Femiano et al., 2016),
- or ensuring high bond strength by selectively etching the enamel, even with self-etch adhesive systems. The reason being the lower ability of these systems to demineralise enamel and create appropriate rough surface for bonding (Matos et al., 2017).

Using the minimally invasive restorative technique will mean removal of infected dentine only and saving the affected dentine, especially in proximity to the pulp. Bonding to caries affected dentine, however, is more challenging and etching of this layer is questionable due to its low content of minerals. Additionally, bonding strength to this layer was reported to be lower and have less longevity due to the activity of MMPs (Pinna et al., 2015). The microtensile bond strength to primary teeth (which is the aim of the proposed experimental formulation) was shown to be lower in comparison to that to permanent teeth only upon storing in water for one year (up to two years). This might be due to higher organic content in primary teeth resulting in higher content of protease enzyme and thus more degradation of the bonding interface (F. Z. Soares et al., 2017).

Whilst tags formation does not reflect higher bond strength, microtags in the lateral dentinal tubules might be crucial for that purpose (J. C. Ferreira et al., 2017). Resin tags length might be beneficial in limiting microleakage and stabilising interlocked dentine. The average value of resin tags length observed in one study was higher with more flowable composites (about 10μm) (Prabhakar et al., 2011; Prabakar et al., 2018). The trend is in good agreement with this study as in achieving longer tags with less viscous and more hydrophilic formulations although the studied experimental formulations showed significantly longer tags (up to 80μm).

Less viscous materials tend to penetrate deeper into tooth structure, especially when coupled with sealant (de Menezes and Chevitarese, 1994). Increasing composite fluidity may have enabled faster flow into dentinal tubules. Consequently, an increase in tags length with formulations of lower PLR (3:1) was noticed. The adhesive monomer (4META) had negligible effect on the flow and thus did not affect tag length but it increased the area covered by the tags. This might be due to the acidic groups in the monomer interacting with the positively charged amino acids in the collagen mesh, while the positively charged PolyLysine interacted with the negatively charged amino acids causing a similar effect. Additionally, the PLS might have interacted with non-collagenous proteins, especially the phosphophoryn (PP) and chondroitin sulphate which are highly concentrated around the tubules. This interaction might have encouraged the composite paste to be pulled into the dentinal tubules. Hydrophilicity of MCP and the ability to produce Calcium ions and phosphoric acid are also possible explanations of MCP improving the area covered by tags.

EDX analysis of resin tags formed with different experimental formulations showed a C:N ratio of 3:1, which means the PLS was able to penetrate into the tubules (based on the chemical formula of the agents used in the formulations):

UDMA/PPGDMA= 3/1

3*UDMA($C_{23}N_2O_8$) + PPGDMA($C_{29}O_{10}$)= $C_{98}N_6O_{34}$= $C_{16}N_1O_{6\rightarrow}$ Polymer C:N ratio is 16:1.

While the PLS ($C_6H_{12}N_2O)_n$ has C:N ratio of 3:1. However, the results did not show an effect of PLS content. This might be explained by the release and degradation of PLS from resin tags during samples preparation (soaking in NaOCl for 2 days) which resulted in similar values amongst different formulations. The presence of the PLS in the resin tags will be effective in delivering its antibacterial effect into deeper layers of remaining caries-affected dentine.

.

4.8   Conclusion

The results of the tests in this chapter showed that:

- Formic acid 4M is the most suitable acid solution used to totally demineralise human dentine discs of 2mm thickness.
- The resultant discs (using formic acid) resemble the naturally carious dentine when checked under Raman spectroscopy. Hence, a caries-like model of collagen mesh was created.
- All experimental formulations have the ability to penetrate into the collagen mesh forming resin tags which might be able to interlock and stabilise carious dentine. The commercial materials z250 (without bonding agent), Fuji IX and Fuji II LC did not exhibit this ability while z250 (with bond) and Activa formed shorter resin tags.
- Formulations of lower PLR show longer resin tags
- Taking out 4META or PPGDMA cause a 34% or 9% decrease in resin tags area, respectively
- Increasing the PLS or MCP content result in 79% or 24% increase in tags area, respectively.

5   The Optimised Final Formulation

Thesis structure

Chapter 1:

literature review

Chapter 2:

Materials and methods

Chapters related to the first eight formulations

Chapter 3:

Basic properties of the first eight experimental formulations

Chapter 4:

Resin tags formation

light curing kinetics, intercations of the discs with water and mechanical properties

Creating caries-like collagen discs to check ability to penetrate

Chapters related to the final formulations F9 and F10

Chapter 5:

Summary of chapters 3, 4 and the basic properties of F9, F10

Chapter 6:

Adhesion to tooth structure (F9, F10)

Chapter 7:

The effect of the novel additives, MCP and PLS

Self-etch, cavity adaptation, tags formation, microleakage and shear bond strength

Remineralising effect and MMP inhibition

Chapter 8:

General conclusion

Chapter 9:

Future work

5.1 Abstract

Aims:

The purpose of the work presented in this chapter was to compare the light-curing kinetics, mechanical properties, water sorption and solubility and radio-opacity of the two versions of the final formulation (F9 and F10) prepared in-house or by a manufacturer.

Materials and methods:

Light-curing kinetics (delay time, rate of reaction and monomer conversion) of 2mm thick samples were tested by FTIR spectroscopy at 37°C. Biaxial flexural strength and modulus after 1 day of immersion in water were measured by a universal testing machine (Shimadzu, Japan). Water sorption and solubility and radio-opacity tests were performed in accordance with ISO 4049-2009 and ISO 13116-2014, respectively. Samples of 1 and 2mm thickness were X-rayed alongside an aluminium step-wedge to check radio-opacity. Results were compared to F5 wherever possible and the commercial comparators used were Filtek z250, Activa, Fuji IX and Fuji II LC.

Results:

Delay time (~6.5s), rate of reaction (~3.8%/s) and monomer conversion (>75%) results were comparable between F9 and F10. The biaxial flexural strength was ~120MPa and the modulus ~3.4GPa. Water sorption values were just above 40μg/mm^3 while the solubility results varied massively based on the light-curing method. The formulations were radio-opaque (1mm samples = 1.8mm aluminium thickness).

Conclusion:

The optimised final formulations (F9 and F10) were comparable to each other in terms of light-curing kinetics, mechanical properties, water sorption and solubility and radio-opacity. These results were within the expected deviation from F5 due to reducing the PLS content from 5% to 4%

5.2 Introduction

5.2.1 Summary of previous results and the rationale behind the final composition

Lab test results of all eight experimental composites discussed in chapters 3 and 4 are summarised in Table 5-1. In addition, biocompatibility and antibacterial properties assessed by Dr Caitriona O`Rourke and Dr Adam Day are provided. These were obtained using composite discs prepared as in (2.1.5). Biocompatibility was assessed using fluorescence intensity of human dental pulp stem cells and human gingival fibroblasts upon immersing in medium in which the composite discs were immersed. The antibacterial effect was assessed using three different concentrations of *Streptococcus mutans* inoculum (10^6, 10^7 and 10^8 CFU/mL). Methods and results are shown in detail in Appendix E.

Table 5-1 shows that all formulations were biocompatible and comparable in terms of stability and achieving more than 50% monomer conversion. F1 (PLR 5:1) and F5 (PLR 3:1), both with higher PLS (5%) and MCP (8%), had the best antibacterial and remineralising properties in addition to highest tags area on collagen mesh. However, they suffered high water sorption and solubility due to the hydrophilicity of the additives (PLS and MCP). F1 was viscous while F5 was more flowable and both can be packaged in compules to be used more comfortably with paediatric patients. Different packaging compules for the low viscosity formulation were assessed by 5 specialists. The questionnaire, results and the design of the preferred compule is shown in Appendix F.

As a result, a decision was made to choose F5 as a final optimised formulation with the PLS content reduced to 4%. This formulation (F5) showed better sealing of carious dentine and deep penetration by forming resin tags that covered most of the interface and was of about 200μm long (see Appendix D). Reducing the PLS content might also help comply better with ISO 4049-2009 requirements of water sorption and solubility.

Table 5-1 Summary of lab test results of the experimental formulations

	PLR	PLS (%)	MCP (%)	MC>50% Up to 4mm (bulk fill)	Stability with ageing	Water sorption <45µg/mm³	Water solubility <7.5µg/mm³	PLS release	3-point bending strength >80MPa at 1 day	Remineralising effect	Tags area with collagen mesh	Biocompatibility	Antibacterial effect 10⁶ CFU/mL	10⁷ CFU/mL	10⁸ CFU/mL
F1	5	5	8	✓	✓	✗	✗	High	✓	High	77%	✓	✓	✓	✗
F2	5	5	4	✓	✓	✓	✗	High	✓	Low	50%	✓	✓	✓	✗
F3	5	2	8	✓	✓	✓	✗	Low	✓	High	35%	✓	✓	✗	✗
F4	5	2	4	✓	✓	✓	✓	Low	✓	Low	37%	✓	✓	✓	✗
F5	3	5	8	✓	✓	✗	✗	High	✓	High	84%	✓	✓	✓	✗
F6	3	5	4	✓	✓	✗	✗	High	✓	Low	63%	✓	✓	✓	✗
F7	3	2	8	✓	✓	✓	✗	Low	✓	High	43%	✓	✓	✗	✗
F8	3	2	4	✓	✓	✓	✓	Low	✓	Low	36%	✓	✓	✗	✗

5.2.2 The final formulation (F9/F10) composition and paste preparation

The composition of the final formulation is detailed in Table 5-2. As mentioned in the previous paragraph, this has PLR 3:1 and contained 4% PLS and 8% MCP (i.e. very similar to F5 except slightly lower PLS content).

Table 5-2 Composition of the final optimised formulation

						PLR
Monomer	UDMA (72%)	PPGDMA (24%)	CQ (1%)	4META (3%)		
Ratio	3 :	1				
	96%					3:1
Powder	Nano-glass (8.8%)	0.7µ glass (26.4%)	7µ glass (52.8%)	MCP (8%)	PLS (4%)	
Ratio	1 :	3 :	6			
	88%					

This formulation **F9** was mixed using a speed mixer (DAC600.2 CM51, Synergy Devices Ltd.) by Wendy Xia. The procedure was as follows:

1. Powder phase (225g) was mixed at 1000 rpm for 30s (no vacuum)
2. Monomers (75g) were added to the premixed powder phase
3. Powder and liquid were mixed together again at 2300 rpm for 15s (no vacuum)
4. Vacuum was applied for 3 mins (no mixing) to reduce pressure down to 20 mbar
5. Mixing again at 1800 rpm for 30s (17 mbar)

The manufacturer "Schottlander" also had the same composition manufactured by DMG (Lot no. 783139, DMG, Germany) and filled in compules with movable red tip (**F10**), which allows better access to cavity and easy application. The mixing method has not been exposed by this manufacturer.

5.3 Hypothesis

The null hypothesis is:

- The two different versions of the final formulation (F9 and F10) are not identical and will show different results in terms of light-curing kinetics, mechanical strength, water sorption and solubility and radio-opacity.

5.4 Aims and objectives

The aim of this chapter was to evaluate the basic properties of the final formulation in its two different versions (F9 and F10). The objectives were to check if they provide results as expected from previous studies and if there are any discrepancies in the results between the two versions. The tests included:

- Light-curing kinetics
- Mechanical properties; biaxial flexural strength and modulus
- Water sorption and solubility
- Radio-opacity

Additionally, these results were compared to F5 wherever possible.

5.5 Materials and methods

5.5.1 Light-curing kinetics

The method of measuring light curing kinetics is detailed in (2.2.1). The lab work was performed by Dr Wendy Xia.

Discs of 2mm thickness were evaluated and were light-cured for 40s. The temperature of ATR-FTIR was set at 37°C in this method, contrary to chapter 3 where studies were undertaken at room temperature.

5.5.2 Mechanical properties (Biaxial flexural strength and modulus)

The methods followed to evaluate biaxial flexural strength and modulus upon immersion in water for 1 day are stated in (2.2.3). The lab work was performed by Dr Wendy Xia.

5.5.3 Water sorption and solubility

Water sorption and solubility was recorded using the method detailed in (2.2.2.1). Light-curing the discs (n=5), which were 16mm in diameter and 1mm thick, was varied in this chapter as follows:

- F9: similar to previous method (wide light-gun tip, 40s on each side, rotation movement).
- F10: wide light-gun tip, 40s at 5 overlapping exposure windows on each side (total 400s, 200s on each side).
- F10, Activa, Fuji II LC and z250: 20s at 5 overlapping exposure windows on each side (total 200s, 100s on each side).
- Fuji IX: no need for light-curing, discs were left over night in between the acetate sheets at room temperature before detaching from the metal circlips to ensure complete reaction.

5.5.4 Radio-opacity

The method followed for determining the radio-opacity is detailed in (2.2.4). It follows the instructions of ISO 13116:2014 except two different thicknesses of discs (1 and 2mm) were used instead of the one thickness required by ISO (1mm).

Composite discs were prepared as in (2.1.5). Materials used were F10 (Lot# 782332, DMG, Germany). Filtek z250 (shade B3, 3M ESPE), Fuji II LC (shade A2, Fuji) and Activa Kids (Pulpdent, USA) (Figure 5-1).

Additionally, F10 was applied into two carious primary teeth after slight excavation of soft caries to check radio-opacity in comparison to enamel and dentine (not required by ISO). One of the teeth was ground down to 1.7mm thickness (parallel to the long axis of the tooth) while the other tooth was kept as a whole.

An average result was taken out of the three repetitions of X-ray (as stated previously in the methods chapter).
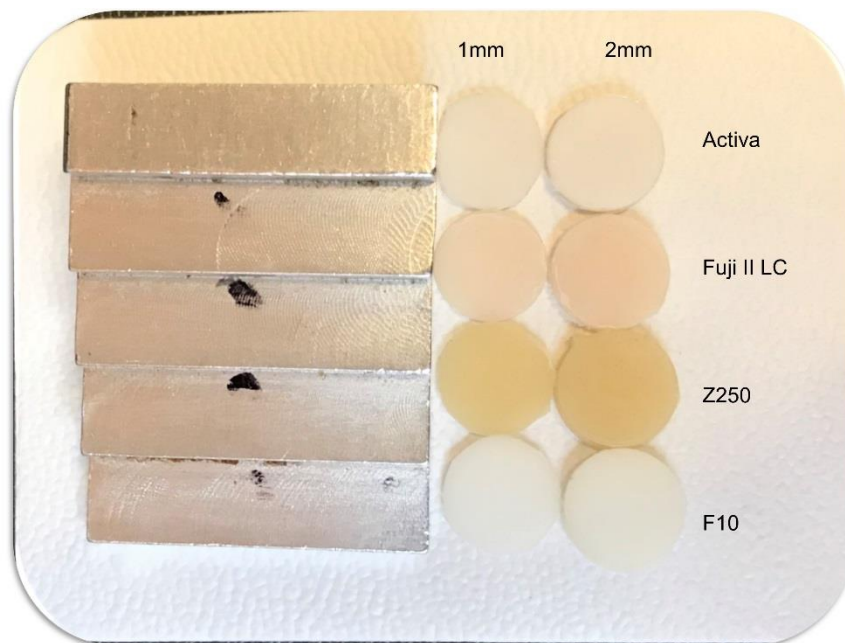
Figure 5-1 Radio-opacity test. X-ray images of two thicknesses of different materials were taken and analysed in comparison to the aluminium step-wedge.

.

5.6 Results

5.6.1 Light-curing kinetics

Figure 5-2 shows the results of Light curing kinetics (delay time, rate of reaction and final monomer conversion) of 2mm thickness samples of the optimised formulations (F9 and F10) in comparison to F5. Delay time was not significantly different between formulations and was about 7s for all. Rate of reaction of F5 (2.5%/s) was significantly lower when compared to F9 (p = 0.008) and F10 (p = 0.003). The same was noticed with final monomer conversion values where F5 showed significantly lower conversion of 66.3% in comparison to F9 (79.6%) and F10 (76%) (p = 0.0001 and 0.001, respectively). F9 and F10 curing kinetics were not significantly different from each other.
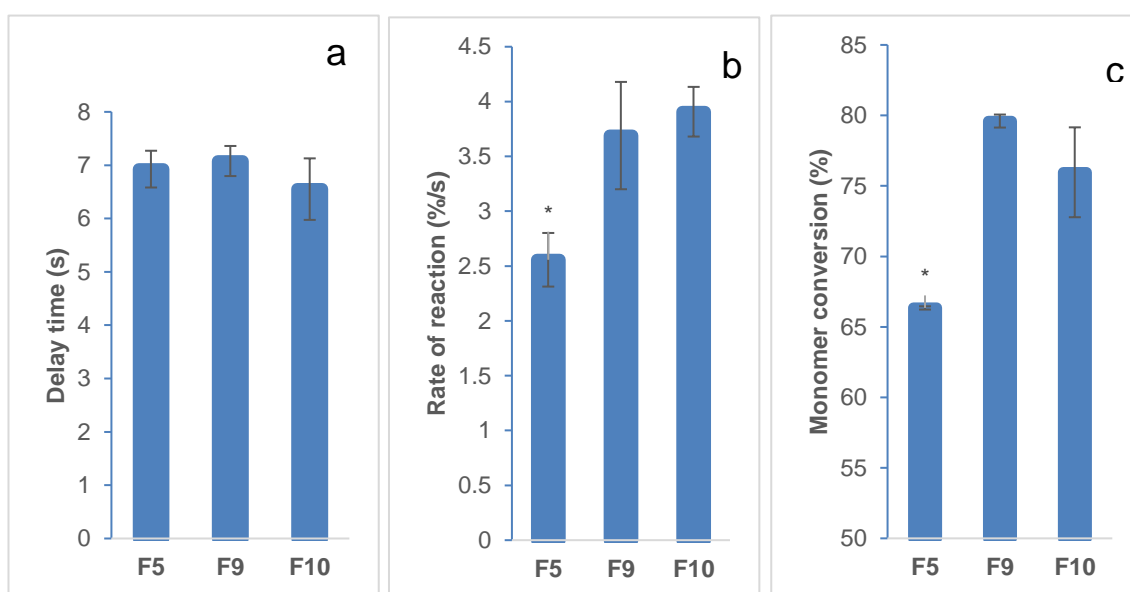
*Figure 5-2 Delay time (a), rate of reaction (b) and monomer conversion (c) of the optimised formulation (F9 and F10 tested at 37°C by Dr Wendy Xia) in comparison to F5 (tested at 25°C by the author). Sample thickness is 2mm and curing time is 20s. * indicates significant difference from other groups (p<0.05). Error bars are 95% CI (n=3).*

5.6.2 Mechanical properties (Biaxial flexural strength and modulus)

Biaxial flexural strength and modulus results are shown in Figure 5-3. The biaxial flexural strength was consistent amongst groups (121 MPa) while the biaxial flexural modulus of F5 (3.2GPa) was significantly lower than F9 (3.55GPa) (p = 0.046). F9 and F10 were insignificantly different from each other in terms of strength and modulus.
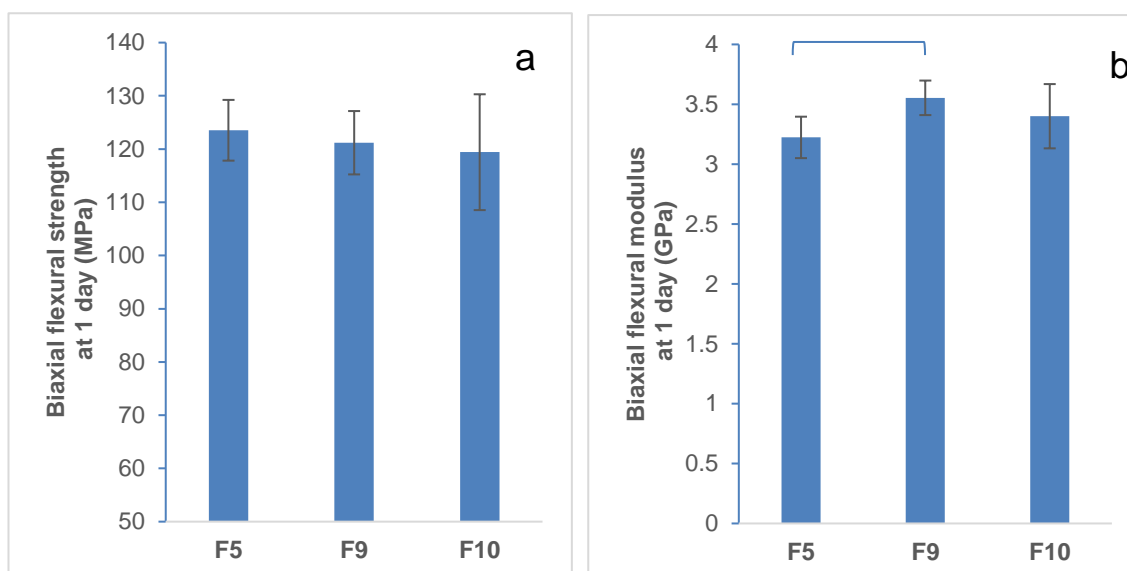
Figure 5-3 Biaxial flexural strength (a) and biaxial flexural modulus (b) of the optimised formulation (F9 and F10 assessed by Dr Wendy Xia) in comparison to F5 (tested by the author) after one day of immersion in water at 37°C. The blue bar indicates statistically significant difference between F5 and F9 (p<0.05). Error bars are 95% CI (n=8)

5.6.3   Water sorption and solubility

The water sorption and solubility test method is detailed in 2.2.2.1. The light-curing method was not the same for all of the groups shown in Figure 5-4. The details of different conditions are mentioned in 5.5.3.

The water sorption value recommended by ISO 4049-2009 for composites should be ≤40µg/mm^3. Water sorption results (blue bars in Figure 5-4) were as follows. Fuji II LC and Fuji IX water sorption results (167µg/mm^3 and 122µg/mm^3, respectively) were significantly higher while z250 (22.7µg/mm^3) was significantly lower than all other groups. Activa water sorption (37.3µg/mm^3) was comparable to F9 and F10, significantly lower than the glass ionomers and significantly higher than z250. Amongst the experimental formulations (F5, F9 and F10), F5 showed significantly higher water sorption (55.2µg/mm^3) in comparison to F9 (41.65µg/mm^3) and F10 (43.7µg/mm^3) (p = 0.0002 and 0.001, respectively). Increasing light-curing time of F10 (from 20s to 40s at 5 points on each side of the disc) showed comparable results (45.5µg/mm^3 to 43.7µg/mm^3). Both were close to but slightly exceeded the ISO maximum for composites of 40µg/mm^3.

The water solubility value recommended by ISO 4049-2009 for composites should be ≤7.5µg/mm^3. Water solubility results (orange bars in Figure 5-4) showed that z250, Fuji II LC and Fuji IX had significantly lower water solubility values. However, these values were negative indicative of insufficient drying or bound water. F10, when cured for 40s at 5 points on each side, showed significantly lower solubility (2µg/mm^3) in comparison

to F5 (13µg/mm^3) and F9 (14µg/mm^3) (p = 2*10^{-8} and 8*10^{-9}, respectively), however, it was comparable to Activa (2.5µg/mm^3).
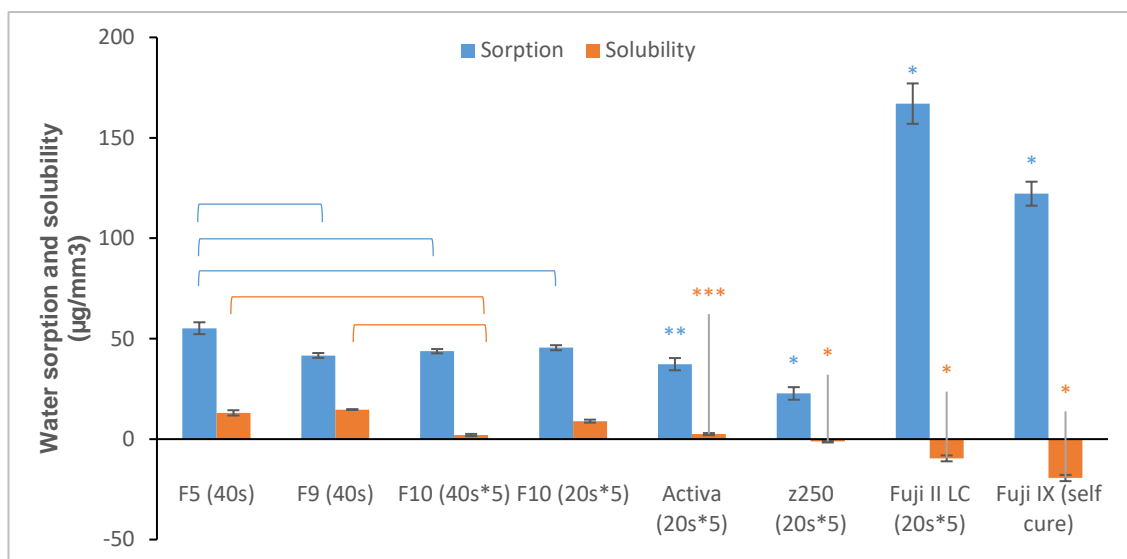
*Figure 5-4 Water sorption and solubility results of the optimised formulation (F9 and F10) in comparison to F5 and commercial comparators. Light curing method is stated in between brackets. The blue/orange bars indicate significant water sorption/solubility difference amongst the experimental formulations. * indicates significant difference from all other groups, ** significant difference from all except F9 and F10, *** significant difference from all except F10. Error bars are 95% CI (n=5)*

5.6.4 Radio-opacity

Radio-opacity of the optimised formulations (F9 and F10) in comparison to commercial comparators (Activa, Fuji II LC and z250) using 1mm and 2mm thickness discs was evaluated. Figure 5-5 shows a representative X-ray of these discs alongside an aluminium step-wedge (ranging from 3mm to 16mm). F9, F10 and Activa look comparable to each other, while z250 and Fuji II LC look more radio-opaque.
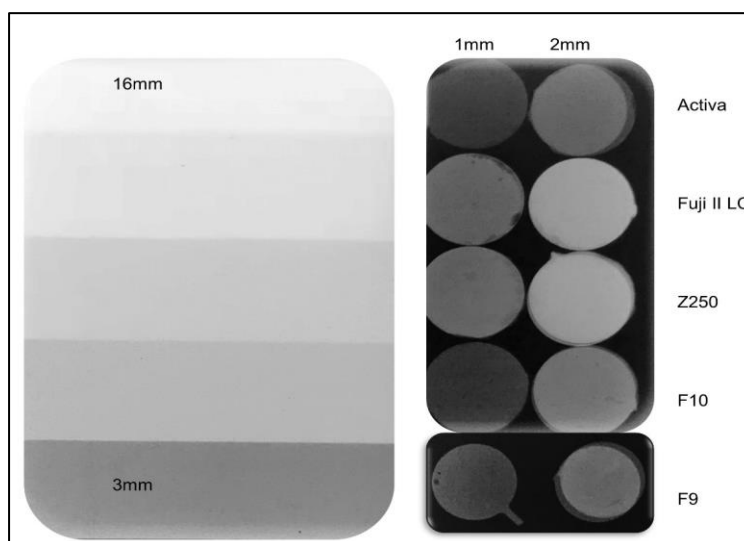
Figure 5-5 Radio-opacity of 1 and 2mm discs of different materials in comparison to the aluminium step-wedge (on the left)

Figure 5-6 shows a carious primary tooth filled with F10 after manual excavation of soft caries then X-rayed as a whole or upon grinding down to 1.7mm thickness to standardise radio-opacity. The restoration appeared to be distinctive. It was more radiopaque than dentine (carious and sound) but comparable to enamel.
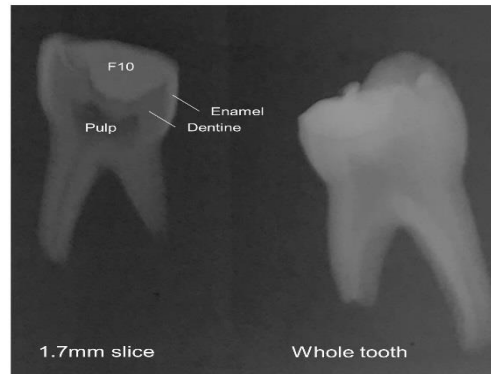
Figure 5-6 X-ray of primary tooth filled with F10 upon slight removal of carious dentine using ART technique

Quantifying results of three X-rays (similar to the one in Figure 5-5), resulted in values of radio-opacity in comparison to aluminium equivalent thickness (mm). For 1mm discs, Figure 5-7 shows that F9, F10 and Activa had comparable aluminium equivalent thickness of about 1.8mm while z250 and Fuji II LC were more radio-opaque (3.3mm and 3.8mm aluminium equivalent thickness, respectively). With 2mm discs, Activa, F9 and F10 were also comparable (4mm to 5mm aluminium equivalent thickness) while z250 and Fuji II LC were again more radio-opaque (5.7mm and 6.4mm, respectively).
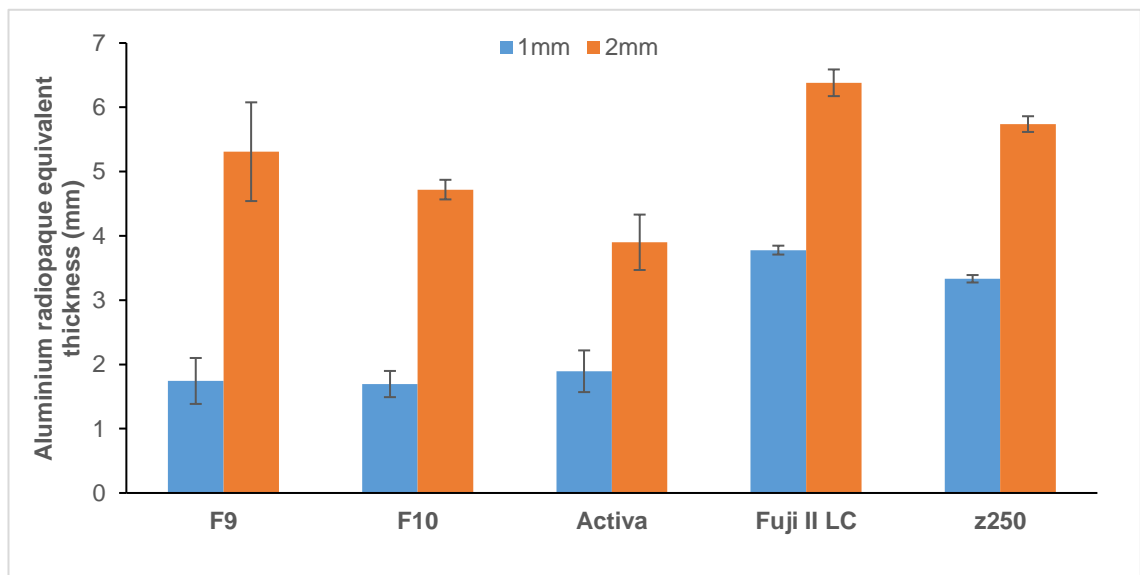
Figure 5-7 Aluminium radiopaque equivalent thickness of 1 and 2mm discs of F9, F10, Activa, Fuji II LC and z250. Error bars are 95% CI (n=3)

All materials used (regardless of the thickness) were considered radio-opaque since their values of aluminium equivalent thickness were higher than 1mm.

5.7 Discussion

5.7.1 Light-curing kinetics

Based on the factorial analysis performed for the initial experimental 8 formulations, PLS content is not expected to affect light curing kinetics (delay time, rate of reaction and final monomer conversion) of samples of 1mm thickness made with fresh pastes (see Figure 3-3, Figure 3-4 and Figure 3-6). Results showed that delay time was not affected by the reduction of PLS content from 5% to 4% as expected. However, both rate of reaction and final monomer conversion were significantly higher with F9 and F10. This might be explained by the difference in experiment conditions. While F5 was tested at 24°C, F9 and F10 light curing kinetics were tested at 37°C. Results of this work agree with a previous study by Price et al who stated an increase in rate of reaction of Tetric EvoCeram (Bis-GMA, Bis-EMA and UDMA monomer system) by 106% when temperature was increased from 22°C to 35°C (Price et al., 2011).

Reaction rates are often described by Equation 5-1 known as the Arrhenius equation (Peacock and Calhoun):

$$R = A^{\frac{-E_a}{R_g T}}$$

Equation 5-1

where R is rate of reaction, A is the pre-exponential factor, R_g is ideal gas constant and T is temperature. This indicates, the rate of reaction increases with higher temperature and lower activation energy which means faster achievement of higher conversion while the light-cure unit is still on. This might be important when the critical level of 50% monomer conversion need to be reached during the light-curing without depending on the dark-curing phase. Generally a doubling in rate for every 10°C rise in temperature is typical (Hiemenz and Lodge, 2007; Price et al., 2015).

Higher temperature also leads to increased mobility of free monomers and higher conversion before the polymer rubber to glass transition which slows and ultimately terminates the reaction (Trujillo et al., 2004; Palin et al., 2014). Enhancing conversion above 50% is important to ensure no cytotoxic free monomers remain. Above 50%, increased conversion improves crosslinking between polymer chains which is important for mechanical properties improvement. The new results are in good agreement with AlShaafi et al. who found that resin composites showed higher degree of conversion and Knoop hardness when curing temperature was 33°C instead of 23°C (AlShaafi, 2017). Results also agree Price et al who also found higher final degree of conversion when temperature was increased from 22°C to 35°C (Price et al., 2011). It was also found that

upon curing a composite, increased heat treatment can significantly increase final degree of conversion (Ferracane and Condon, 1992; Par et al., 2014).

5.7.2 Mechanical properties (Biaxial flexural strength and modulus)

Decreasing the PLS content was observed to increase biaxial flexural strength and modulus at 1 day (based on factorial analysis shown in Figure 3-27 and Figure 3-30). Results, however, showed no significant difference between F5, F9 and F10 in terms of strength while F9 only had significantly higher biaxial flexural modulus when compared to F5 at 1 day. Lack of significant difference might be explained by the minor reduction in PLS content. Figure 3-21 in section 3.6.2.3 showed that reducing the PLS content from 5% to 2% caused 22% increase in strength and modulus. Assuming a linear decline in strength with PLS content, a 1% change in PLS content will only result in about 7% change in mechanical properties at 1 day. This predicated value might not be enough to cause significant changes in results and therefore the optimised formulations showed consistent figures when compared to F5.

Since the proposed formulation is intended to be used for paediatric patients, occlusal forces are expected to be lower than with permanent restorations. However, the material shows mechanical properties somewhere between the resin modified glass ionomers (RMGI) and the resin composites (closer to the resin composites). Although a cavity that involves more than one surface of the tooth is not indicated for direct intracoronal restoration but rather a full coverage of the crown (Waggoner, 2015), it is still a widely used restorative option in clinics. The available materials (resin bonded composites, compomers, RMGI and GI) suffer from functional failure when used in class II cavities in primary teeth (22% failure rate for GI and higher for the rest of materials over 2 years) (Sengul and Gurbuz, 2015). The proposed formulation might perform better than the available options due to its adhesive and remineralising properties with the reduced sensitivity to bonding technique by eliminating acid etching and bonding steps.

5.7.3 Water sorption and solubility

When discs are immersed in water, they start absorbing water and releasing any active ingredients in their composition (soluble components). The mass of these discs increases due to water sorption (m2) in comparison to the initial dry weight (m1) due to the water mass absorbed being higher than the release of these components. When discs are dried up again after 1 week of immersion in water, the mass (m3) goes down unless the water absorbed is bound with the disc structure and cannot be released. In

that case the water solubility values will be negative and careful interpretation must be applied (Muller et al., 2017).

Results showed that glass ionomers (Fuji IX and Fuji II LC) have had the highest water sorption values in comparison to all other materials, while they showed negative solubility values. The commercial composite z250 showed the lowest sorption results due to its rigid structure and almost no solubility due to its composition which contains no soluble components. The results were in good agreement with other studies (Kumar and Sangi, 2014; Zankuli et al., 2014; Misilli and Gonulol, 2017).

The optimised final formulation (F10) was comparable to the commercial comparator Activa in terms of water sorption and solubility when it was cured for 40s at 5 points on each side of the disc. However, water solubility results of the optimised formulation have differed when the curing time was varied. Longer light-curing periods at multiple points reduced the solubility as it may have led to higher monomer conversion and a more rigid disc. This was also addressed by Castro et al who proved that there is a negative relationship between light-curing time (5, 10, 20, 40, and 60s) and water sorption and solubility values (Castro et al., 2013).

F5 showed significantly higher results of water sorption and solubility when compared to F9 and F10. This is explained by the higher content of PLS which is hydrophilic and will be released into water as proved previously in section 3.6.2.1 (Figure 3-13) and section 3.6.2.3, where it was shown that higher PLS caused a 77% and 99% increase in water sorption and solubility, respectively. Many other studies agree there is a significant positive relationship between hydrophilicity of the composition and its water sorption values and that increased sorption and solubility might affect the mechanical properties of the restoration and its durability (Ito et al., 2005; Malacarne et al., 2006; Yiu et al., 2006). However, it was proven in a previous chapter that the mechanical properties of the proposed formulations stabilise after 3 months of soaking in water without further deterioration and that they are of adequate strength (see section 3.6.3.2).

The solubility values of the proposed formulations fall beyond the maximum recommended by ISO. However, the ISO 4049 was set for materials that are rigid and plays no role but restoring cavities without the release of any components. If anything leached from such composites, it would be the unreacted monomers which counts for the toxicity of the material. Therefore, the values set by ISO for such materials were very low to limit cytotoxicity caused by released monomers. The benefits of PLS and MCP release were discussed previously in chapter three and they are more important than water solubility values as long as this would not affect the stability of these restorations in the oral cavity.

5.7.4 Radio-opacity

Radio-opacity of restorative dental materials is of great value to be able to differentiate between the materials and dentine (sound or carious). This allows clinicians to follow up their restorative work, detect interfacial gaps and overhanging, remineralising of carious dentine, recurrent caries and pulpal response by dentinal bridge formation. For a dental material to be considered radio-opaque, it should achieve a radio-opacity value of at least 1mm aluminium equivalent or higher. Therefore, all tested materials are considered radio-opaque. The final optimised formulation radio-opacity was comparable to that of Activa, while Fuji II LC and z250 were more radio-opaque. These results were comparable to other studies (Tsuge, 2009; Yasa et al., 2015; Yildirim et al., 2017).

Thicker samples showed higher values of aluminium equivalent (more radio-opaque). This is due to the distance the photons of an X-ray have to travel through, resulting in higher absorption of these photons and hence less of them reaching the X-ray film. This can be also explained by Beer-Lambert law. As mentioned in 2.2.4, the absorbance effect is the most important in dental X-rays. Higher atomic number of the components of the material X-rayed will result in higher absorption and higher radio-opacity.

The X-ray image of a tooth restored with F10 showed easy differentiation between the material and dentine (carious or sound) to an acceptable degree from a clinical point of view. This is due to radio-opacity value higher than that of human dentine (which equals 1.01mm of aluminium thickness) and comparable to that of enamel (which equals 1.89mm aluminium thickness) (Yildirim et al., 2017).

5.8   Conclusion

The results of the tests in this chapter showed that:

- The optimised final formulations (F9 and F10) were comparable to each other in terms of
    - o   Light-curing kinetics
    - o   Biaxial flexural strength
    - o   Water sorption and solubility
    - o   Radio-opacity
- The shift in values of these properties from F5 was either expected or justified (due to change in PLS content or experiment conditions).
- The optimised formulations showed sufficient monomer conversion (more than 75%) and biaxial flexural strength (120MPa) and modulus (3.5GPa) and they were radio-opaque.
- Water sorption and solubility values were very cure-dependent.
- The final formulations (F9 and F10) radio-opaque. Their radio-opacity was comparable to Activa, but lower than z250 and Fuji II LC.

6 Adhesion to Tooth Structure (Final Formulation)

Thesis structure

Chapter 1:
literature review

Chapter 2:
Materials and methods

Chapters related to the first eight formulations

Chapter 3:
Basic properties of the first eight experimental formulations

Chapter 4:
Resin tags formation

light curing kinetics, intercations of the discs with water and mechanical properties

Creating caries-like collagen discs to check ability to penetrate

Chapters related to the final formulations
F9 and F10

Chapter 5:
Summary of chapters 3, 4 and the basic properties of F9, F10

Chapter 6:
Adhesion to tooth structure
(F9, F10)

Chapter 7:
The effect of the novel additives, MCP and PLS

Self-etch, cavity adaptation, tags formation, microleakage and shear bond strength

Remineralising effect and MMP inhibition

Chapter 8:
General conclusion

Chapter 9:
Future work

6.1 Abstract

Aims:

The purpose of the work presented in this chapter was to test the ability of the final formulations (F10) to adhere to tooth structure by checking the ability to self-etch enamel, adapt to cavity walls, form tags within collagen mesh or carious dentine, limiting microleakage at the adhesion interface and the shear bond strength to bovine enamel and dentine.

Materials and methods:

F10 was applied to the enamel surface for different times (up to 2 mins) and compared to surfaces treated with 35%phosphoric acid under SEM. Class V cavities were then drilled into sound primary teeth and filled with F10, z250, Activa, Fuji IX or Fuji II LC according to the manufacturer`s instructions. These restored cavities were looked at using XCT (n=1) or aged for one day then stained with Methylene blue before cross-sectioning and checking depth of dye penetration. F10 alongside the same commercial comparators were applied to the collagen mesh or to naturally carious dentine then cross-sectioned and looked at under SEM/CLSM/EDX to check resin tags formation and composition. They were also applied to exposed bovine enamel and dentine surfaces to check shear bond strength following ISO 29022:2013 instructions.

Results:

F10 roughened the enamel surface but gave non identical acid etching pattern when compared with phosphoric acid. In terms of adaptation, XCT scans showed that F10 was comparable to z250 (with etch and bonding agent) and outperformed all other commercial materials which exhibited gaps at the adhesion interface. The same pattern was observed in microleakage test. Only F10, z250 (with bond) and Activa managed to form resin tags within collagen mesh but only F10 within natural caries. The coverage area was higher with F10 (62%) and tags were composed of polymers and maybe PLS. Shear bond strength to bovine dentine was very low while to enamel was ~2.5MPa and comparable to Fuji IX and Fuji II LC. When enamel was etched, F10 shear bond strength went up to 11.5MPa and was comparable to z250 (applied with acid etching and bond)

Conclusion:

The optimised final formulation, despite the simplified single-step application, could exhibit the ability to roughen enamel surface and adapt very well to cavity walls without gap formation. It was also proven that when applied to collagen mesh or to carious dentine, it could form resin tags of >200μm long. These helped limit microleakage at the adhesion interface and enabled outperformance when compared with commercial materials.

6.2   Introduction

In order to simplify the application method of a restorative material and potentially eliminate the use of the complex bonding systems, adhesive monomers should be added to the material. While most of the attempts addressed in literature incorporated such monomers in the bonding systems, only few tried incorporating them into the restorative materials itself (such as Vertise flow from Kerr and Fusio liquid dentin from Pentron clinical). Adding these monomers to the bonding system will only eliminate the etching step. On the other hand, the materials which incorporated GPDM as an adhesive monomer are flowable and not designed to restore the whole cavity due to their mechanical limitations (Ferracane, 2011; Yuan et al., 2015).

Hydrophilic bonding agents are usually used to guarantee good bond strength between tooth structure and the hydrophobic restorative resin material. However, the flowability of the experimental formulation in addition to the hydrophilic components (PLS and MCP) and the acidic monomer (4META) should help bonding to tooth structure without the need for etch and bond.

Adhesion to tooth structure can be tested through many routes. The ones chosen in this chapter are self-etching enamel, cavity adaptation, tags formation, microleakage and shear bond strength. Achieving good results in comparison to commercial materials will prove the ability to apply this material in a simple single-step method.

6.3   Hypothesis

The null hypothesis is:

- The optimised formulations cannot self-etch enamel, adapt to cavity walls, form tags within carious dentine, limit microleakage or bond to tooth structure.

6.4   Aims and objectives

The aim of the tests in this chapter was to evaluate the ability of the optimised formulations to adhere to tooth structure by assessing their ability to:

- self-etch enamel prior to light-curing,
- adapt to cavity walls,
- form tags within carious dentine or the collagen mesh model,
- limit microleakage at the material/tooth interface
- bond to enamel and dentine.

6.5 Materials and methods

6.5.1 Self-etching property

The ability of the optimised formulation to self-etch enamel was evaluated using phosphoric acid gel 35% (3M, ESPE) as a control. Flat enamel surface was obtained by grinding down the buccal surface of human permanent tooth using 500 grit-abrasive paper then ultra-sonication for 5 minutes to ensure removal of any debris. Surfaces were blot dried and F10 was applied for 20s, 40s, 60s, 90s or 120s. To remove F10, samples were washed using pure acetone and vortexed for 1 minute followed by vigorous washing in water for another minute. The same procedure was followed for discs etched with phosphoric acid. Discs were blow-dried and sputter coated to enable visualisation under SEM.

6.5.2 Cavity adaptation (XCT)

Five Class V cavities were prepared into one primary molar as in (2.2.5.1) in a single tooth. Each of these sound cavities, which was 2mm in diameter and 2mm depth, was restored with a different restorative material (n=1). Additionally, the proximal carious surface of the same tooth was filled with F10 upon manual excavation of the very soft caries (infected dentine). Restoration methods of the sound cavities were material dependent as follows:

- F10 (Lot# 783139, DMG, Germany): directly without acid etching or bonding. Filling was light cured for 20s.
- Fuji II LC: directly without acid etching or bonding. Filling was light cured for 20s.
- Fuji IX: directly without acid etching or bonding or light-curing.
- Activa: only acid etching for 10s then thoroughly wash and dry (5s using an air syringe) following manufacturer instructions. Filling was light cured for 20s.
- Z250: acid etching (30s enamel, 15s dentine) with phosphoric acid 35% gel (Universal etchant, 3M ESPE) then thoroughly washing and drying. Then bonding agent (Universal Scotchbond adhesive, 3M ESPE) was applied and light-cured for 20s following manufacturer`s instructions. Filling was light cured for 20s.

Tooth was then scanned by means of XCT to check adaptation of different materials to cavity walls by evaluating the gap formed between the filling and the tooth structure at the interface. The detailed method of scanning is mentioned in (2.2.5.2).

The scan was repeated after 3 months of soaking in deionised water to detect any changes at the adhesion surface.

6.5.3 Tags formation

The ability of the two versions of the final formulation (F9 and F10) to penetrate into collagen mesh (prepared as in 4.5.1 using formic acid) in comparison to commercial comparators (z250 with bond, Activa, Fuji II LC, Fuji IX) was assessed as in (4.5.2) using SEM and ImageJ software package. Percentage of adhesion interface covered with tags is reported.

Additionally, the composition of these tags formed by the optimised formulation was checked by means of Raman spectroscopy and EDX in comparison to the main body of the restoration. This would allow identifying the components that managed to penetrate into the dentinal tubules.

Finally, confocal laser microscopy (CLSM) was also used to visualise resin tags formation with either collagen mesh or carious primary teeth, which were excavated manually using a spoon excavator to remove totally demineralised dentine (infected dentine). The tested materials were the optimised formulation (F10), Activa, Fuji II LC, Fuji IX or z250 with bonding agent. These restored discs or cavities were sliced to expose the interface. Rhodamine B dye was applied for 2 minutes at the interface then washed thoroughly with deionised water for 1 minute. Samples were always saved in deionised water at room temperature if not being scanned. Interface was scanned under CLSM using an oil objective lens (x60) using the red fluorescence channel. The laser microscope settings for Rhodamine B were 568nm excitation and emission through 600-630nm filter. The Z motor was used to scan different levels at the interface and the saved scans were mounted as Z project with the aid of ImageJ software package. Three dimensional projects were also created to aid visualisation and can be viewed in the attached CD-ROM on the cover of the thesis. 2D images of these videos are shown in results.

6.5.4 Microleakage with sound enamel and dentine

Cavities were prepared as in (2.2.5.1) and restored with the final formulation (F9 or F10), Activa, Fuji II LC, Fuji IX or z250 following the manufacturer`s instructions as in (6.5.2). Sample number varied based on the availability of human teeth and is detailed in the results section.

6.5.5 Shear bond strength

ISO 29022:2013 instructions were followed. Details of tooth preparation, exposing bonding surface and testing procedure are detailed in (2.2.5.3). The following only explains steps followed to apply restoration buttons onto the exposed surfaces.

Bonding procedures:

Potted bovine incisors were kept in water at room temperature for 4 hours before applying restorations. Teeth were divided into 7 groups (n=10) and composite buttons applied as follows:

- Z250: acid etching (30s enamel, 15s dentine) with phosphoric acid 35% gel (Universal etchant, 3M ESPE) then thoroughly washing and drying. Then bonding agent (Universal Scotchbond adhesive, 3M ESPE) was applied on etched surface and rubbed for 20s, air-spread for 5s then light-cured for 10s (Demiplus, Kerr, ~1500mW/cm^2 light intensity). Composite button was applied on top (using a metal ring of approximately 3mm diameter and 2mm height) using the commercial composite Filtek z250 (3M, ESPE)
- Activa: only acid etching for 10s then thoroughly wash and dry (5s using the air syringe) following manufacturer instructions. Filling was light cured for 20s.
- Fuji II LC: directly without acid etching or bonding. Filling was light cured for 20s.
- Fuji IX: directly without acid etching or bonding or light-curing.
- F9: directly without acid etching or bonding then was light cured for 20s.
- F10: directly without acid etching or bonding then was light cured for 20s.
- F10 with acid etching (phosphoric acid gel 35%) for 30s (enamel) or 15s (dentine). Bonding surface was then thoroughly washed and dried, and the restoration applied and light-cured for 20s

Samples were put back into water once restored then incubated at 37°C for 1 day before testing shear bond strength.

6.6 Results

6.6.1 Self-etching property

SEM images of buccal enamel surfaces of permanent teeth which were exposed to F10 showed increased surface roughness with longer application times (Figure 6-1 and Figure 6-2). However, this etching pattern was not similar to the one noticed with phosphoric acid. Samples etched with phosphoric acid showed the structure of enamel prisms while those exposed to F10 roughened uneven surface in comparison to untreated enamel. The pattern was not consistent through the whole surface, however.
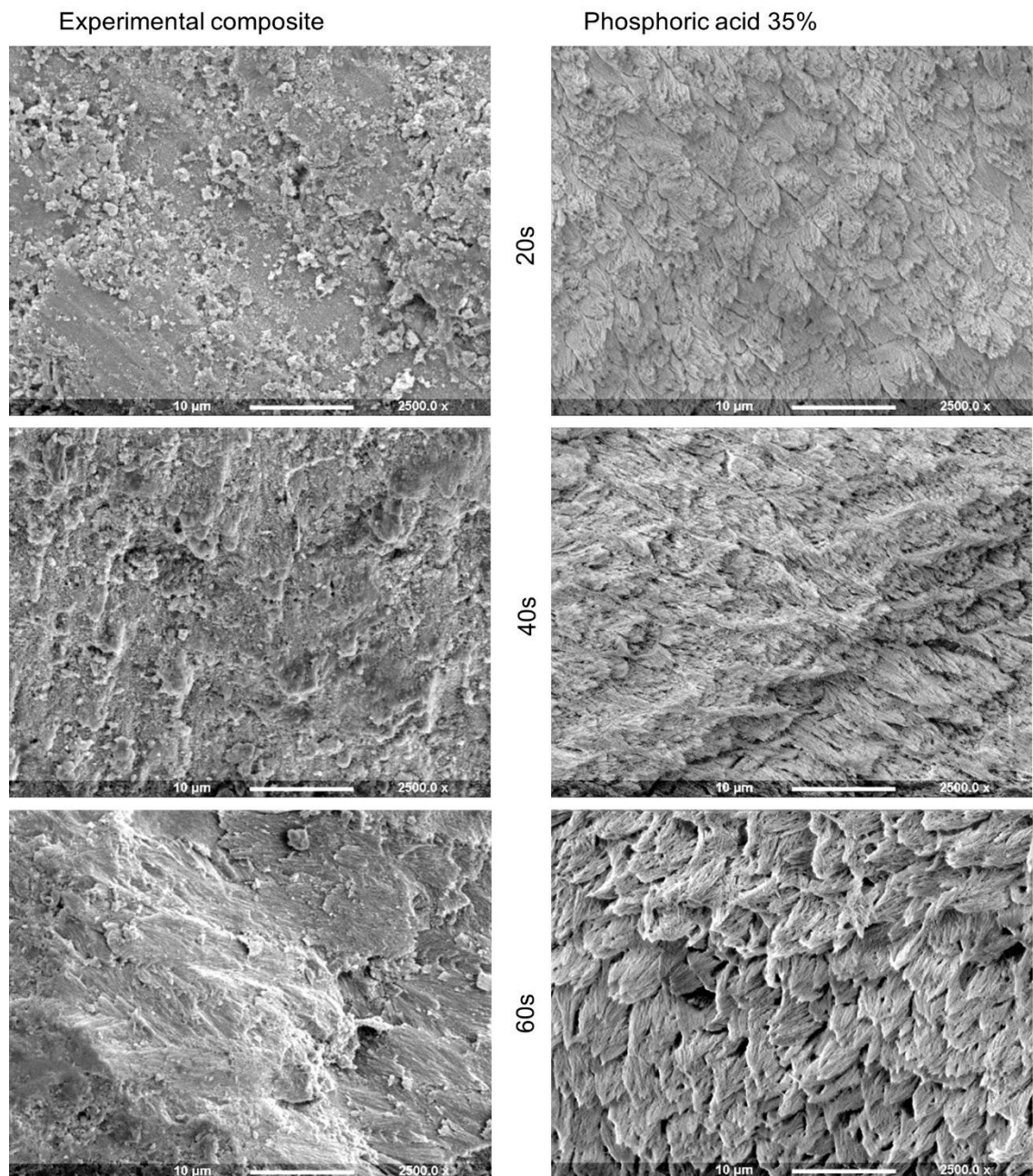
Figure 6-1 SEM images of enamel surface upon applying F10 (left column) or phosphoric acid gel 35% (right column) for different times (20s to 120s) and then washing it away using pure acetone or water, respectively.

164

90s

120s

Untreated enamel
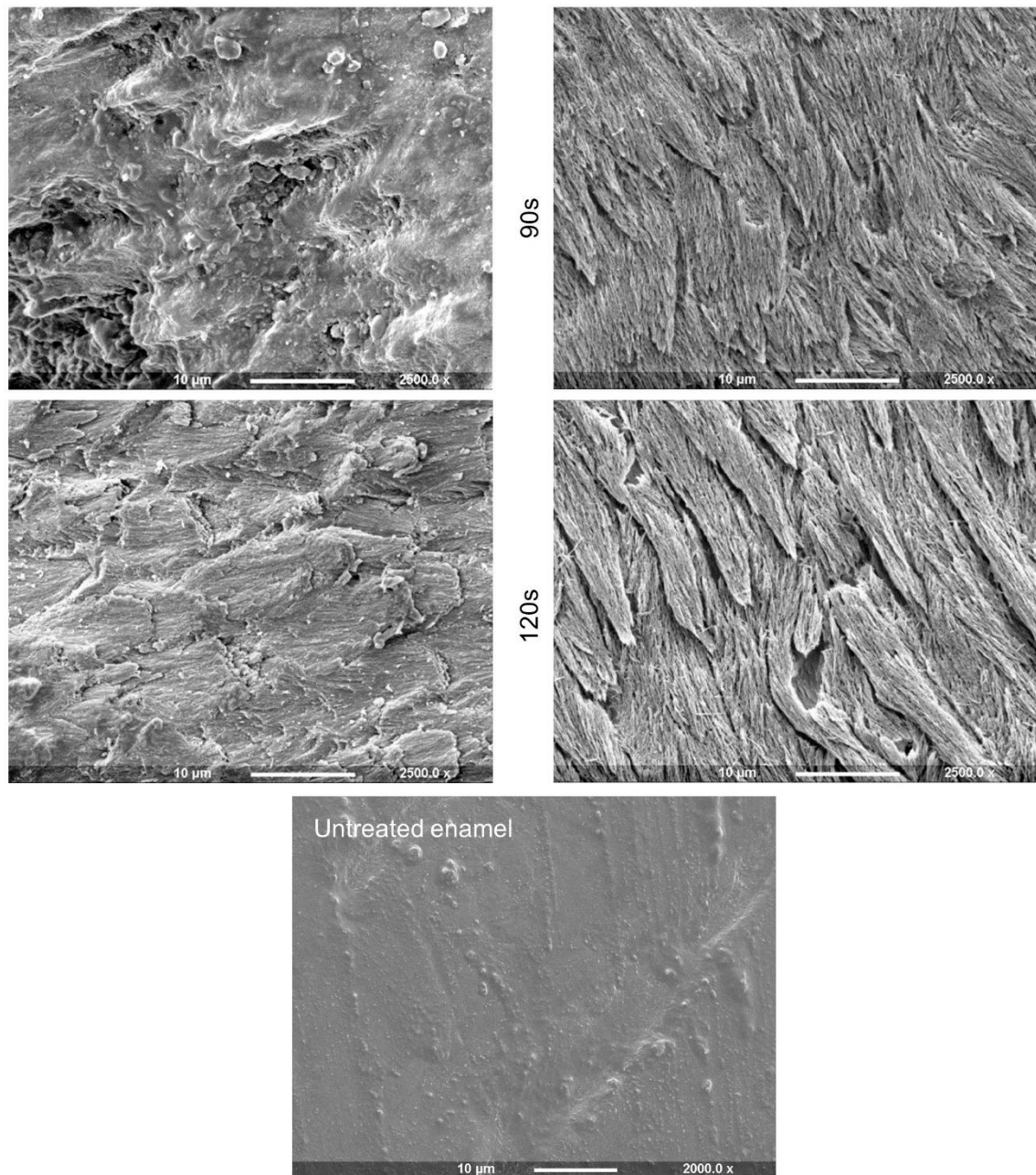
Figure 6-2 SEM images of enamel surface upon applying F10 (left column) or phosphoric acid gel 35% (right column) for different times (20s to 120s) and then washing it away using pure acetone or water, respectively

6.6.2 Cavity adaptation (XCT)

Figure 6-3 shows representative XCT initial scans of a primary tooth filled with different restorative materials (F10, z250, Activa, Fuji IX and Fuji II LC). The selected images represent the worst scan for each material (where the gap between the material and tooth structure is the widest). Cavity adaptation was evaluated by checking the gap formed at the interface between the filling and tooth structure (enamel/dentine). The images and videos (in the attached CD-ROM on the cover of the thesis) showed that F10 had the ability to adapt to cavity wall (whether it was carious or sound) and it was

comparable to z250. Activa, Fuji IX and Fuji II LC, however, were less adaptable to cavity walls and formed gaps of 20µm, 25µm and 120µm, respectively.

The scans after 3 months showed no visible changes or increase in the gap at the interface.
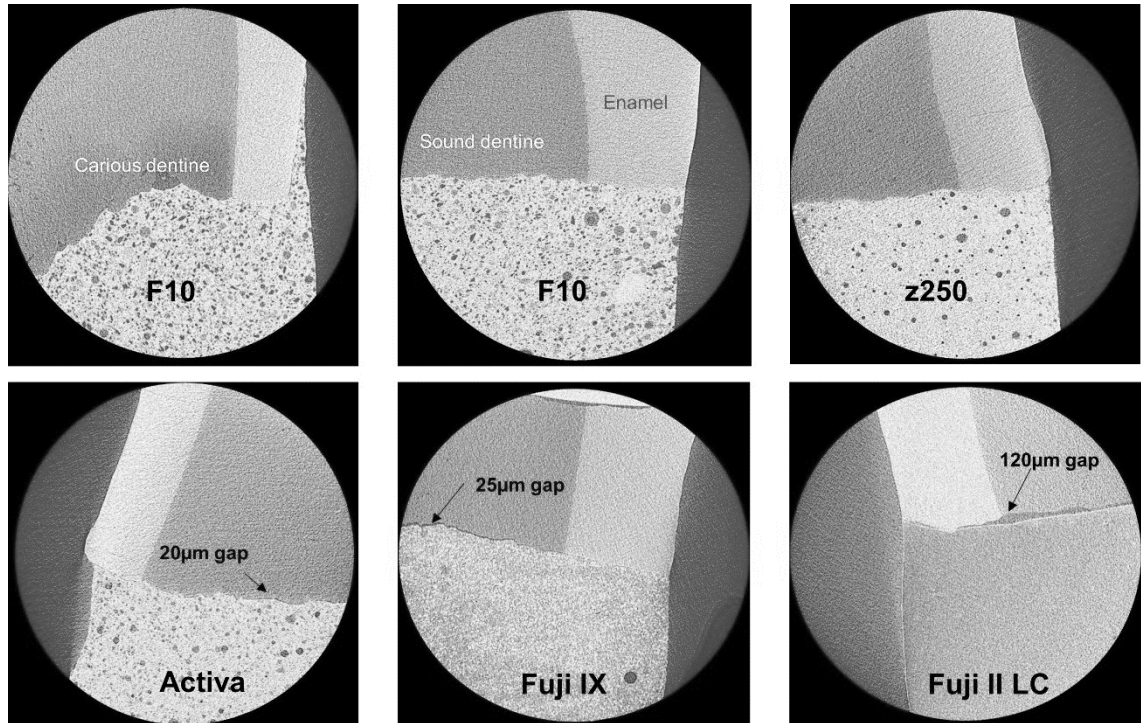
Figure 6-3 Representative single scan of XCT results showing adaptation of different materials (F10, z250, Activa Fuji IX and Fuji II LC) to cavity walls (enamel and dentine). F10 showed good adaptation despite the single step application technique, while Activa, Fuji IX and Fuji II LC showed variable thickness of gap and less ability to adapt to cavity.

Three dimensional models were processed based on the previous scans for each restoration to try and visualise the whole field of scan. 3D Slicer software was used for that purpose. The 3D models are shown in Figure 6-4 (representative images) and in full in the attached CD-ROM. The results were consistent with what was noticed previously (F10 = z250 < Activa < Fuji IX< Fuji II LC) but the gap volume could not be measured due to incompatibility between the files extension and the software.
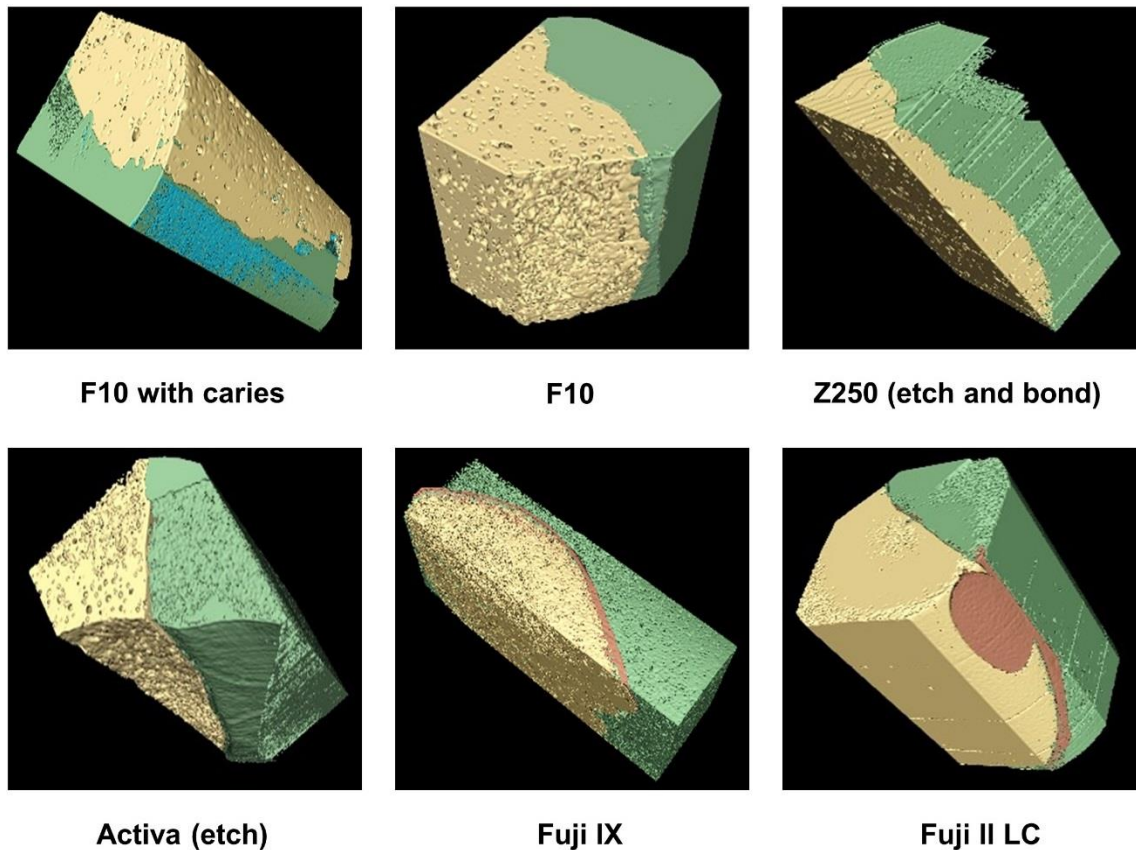
Figure 6-4 3D models build-up of XCT scans of cavities restored with different martials (using 3D slicer software). Material in yellow, tooth structure in green, gap in brown and caries in blue.

6.6.3 Tags formation

The ability to penetrate and form tags was evaluated using two different substrates; collagen mesh or naturally carious dentine. Raman spectroscopy was used to analyse the composition of the resin tags.

6.6.3.1 Tags with collagen mesh model

The ability to penetrate and form tags with collagen mesh was evaluated by SEM and CLSM then quantified using ImageJ software.

Figure 6-5 shows SEM scans of resin tags formed with collagen mesh upon application of different restorative materials (F9, F10, Activa or z250 with bond). Fuji II LC did not show tags while Fuji IX was not suitable for this method as the samples were totally collapsed upon immersion in sodium hypochlorite to dissolve collagen and expose tags. F9 and F10 showed an extensive network of tags formed within collagen mesh in comparison to Activa and z250.
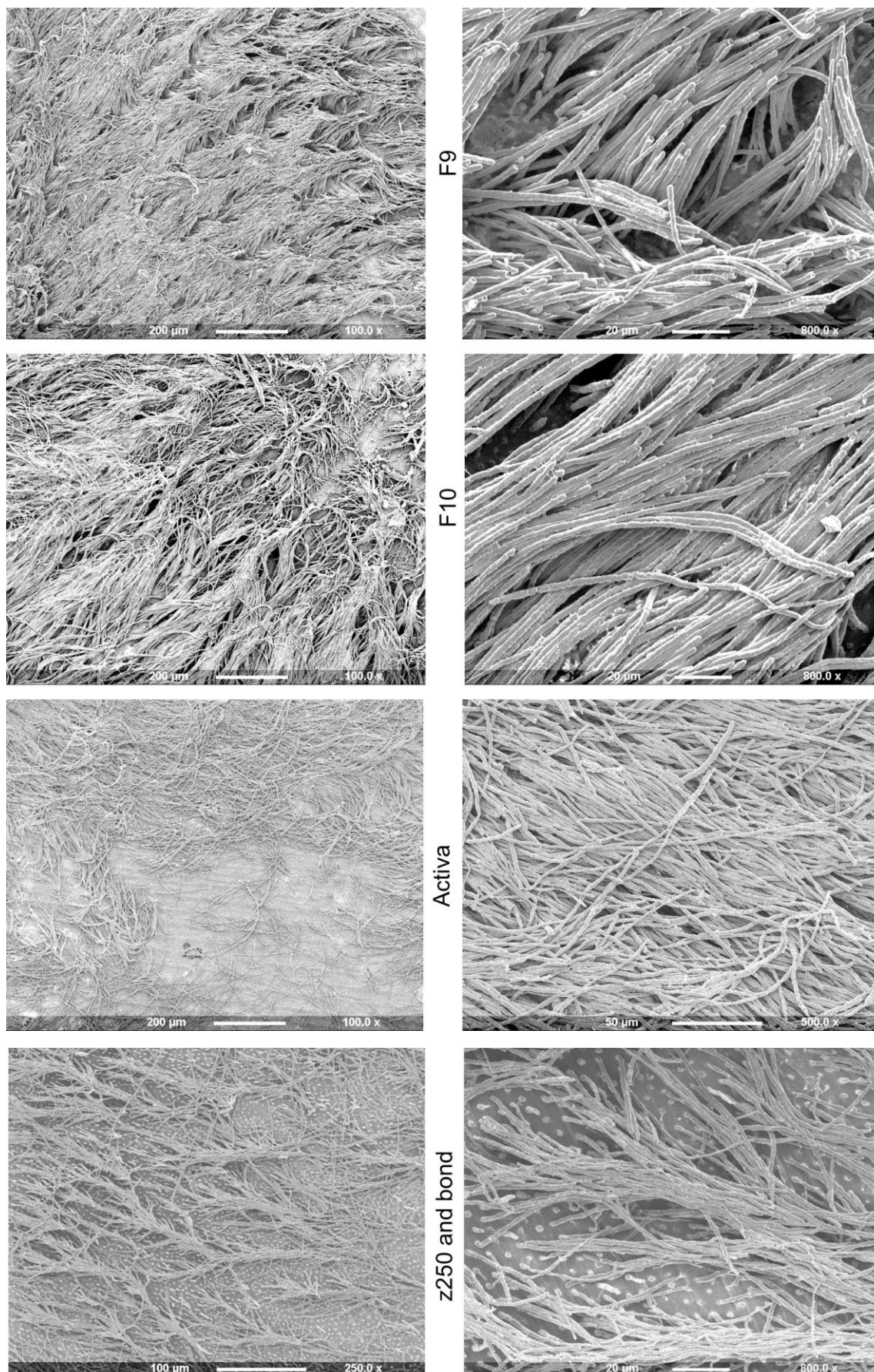
Figure 6-5 SEM images of resin tags formation with collagen mesh (ability to penetrate) using F9, F10, Activa or z250. n=3

The CLSM scans results (Figure 6-6) were comparable to those of SEM. However, Fuji IX and Fuji II LC were suitable for this method as it did not require dissolving the collagen but only grinding down the samples to expose the material/collagen interface. Tags formed using F10 were much longer in comparison to these of z250. Fuji IX and Fuji II LC did not show any evidence of tags formation.

| F10 | z250 and bond | Fuji IX | Fuji II LC |
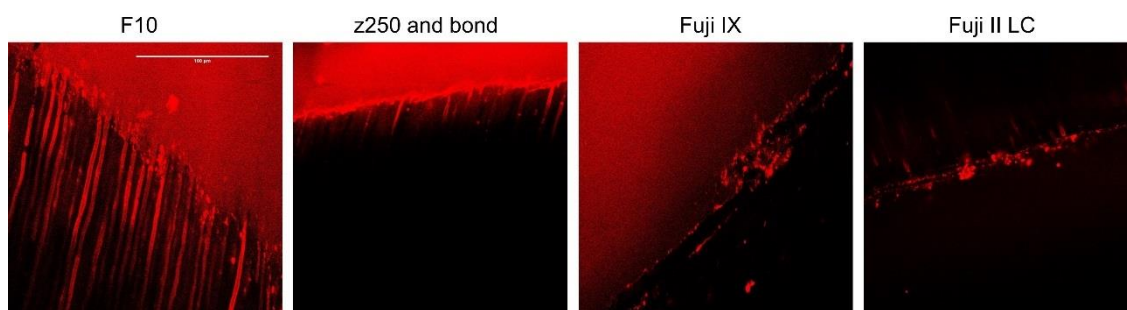
Figure 6-6 CLSM images of resin tags formation with collagen mesh using F10, z250, Fuji IX or Fuji II LC. n=3

The percentage area covered by these tags at the interface was quantified using the method detailed in 4.5.2. The results are shown in Figure 6-7. F5 showed significantly higher value of 84% of the interface covered with tags (p = 0.04 to 0.001) followed by F9 and F10 (63%), which were comparable to z250 with bonding agent (55%). Activa had significantly lower results than all other groups showing a percentage coverage of 39% (p = 0.034 to 0.001).
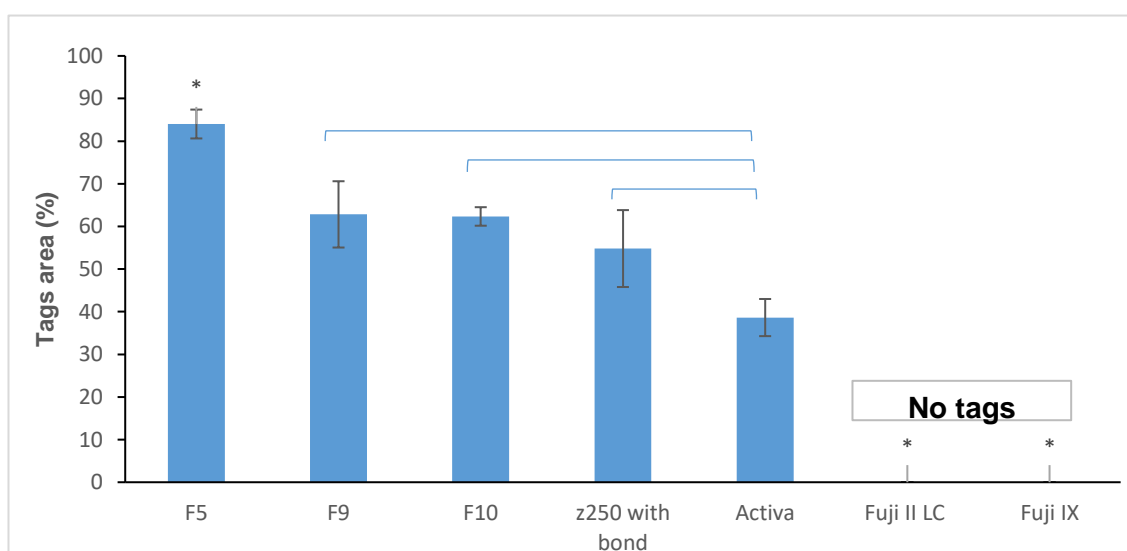
*Figure 6-7 Tags coverage area at the adhesion interface with the collagen mesh using F5, F9, F10, z250, Activa, Fuji IX or Fuji II LC. * indicates significant difference from all other groups while the blue bars indicate significant difference within groups. Error bars are 95% CI (n=3).*

Composition of these resin tags was analysed through Raman spectroscopy and EDX. Raman spectra of tags in comparison to PLS and the cured polymers in the liquid phase of the composition are shown in Figure 6-8. The figure shows good overlap of the resin tags peaks with those of the cured polymers and the loss of C=C peak at 1640cm^{-1}. PLS

amide peaks and N-H and C-O peaks (1575cm^{-1} and 1680cm^{-1}) were not apparent in the tags spectrum. However, there were many shared peaks with UDMA/ PPGDMA (see Table 2-5) in chapter 2.
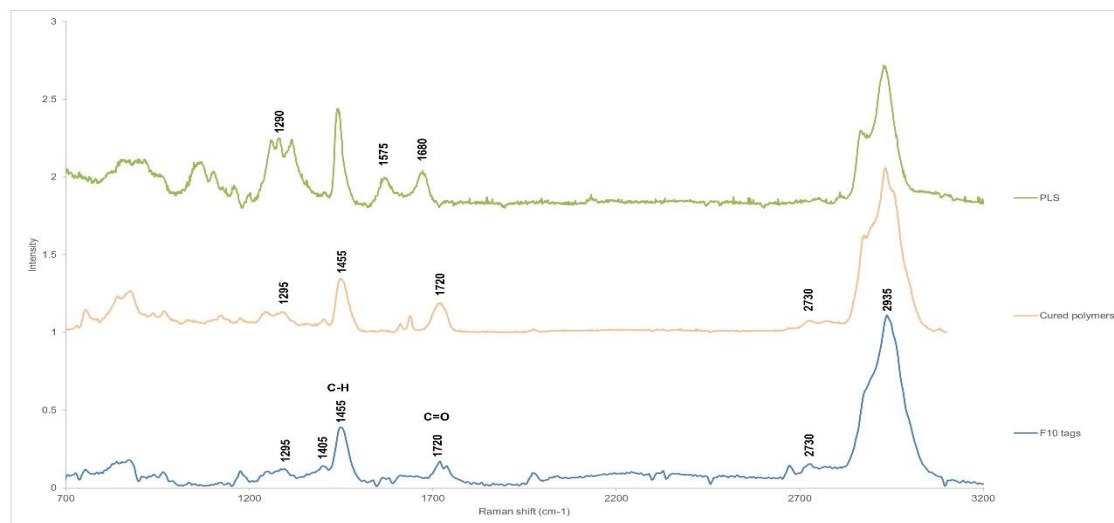
Figure 6-8 Raman spectra of F10 resin tags in comparison to PLS and the cured polymers of liquid phase

EDX map for an area of F10 resin tags adjacent to tags-free area was acquired (Figure 6-9). Nitrogen (N), Phosphate (P) and Calcium (Ca) showed no difference in distribution between the tags and the body of the composite. Silica (Si) and Oxygen (O) appeared to be higher in the tags-free area. Carbon (C) appeared very distinctively higher in the resin tags such that they can be even visualised through the map.
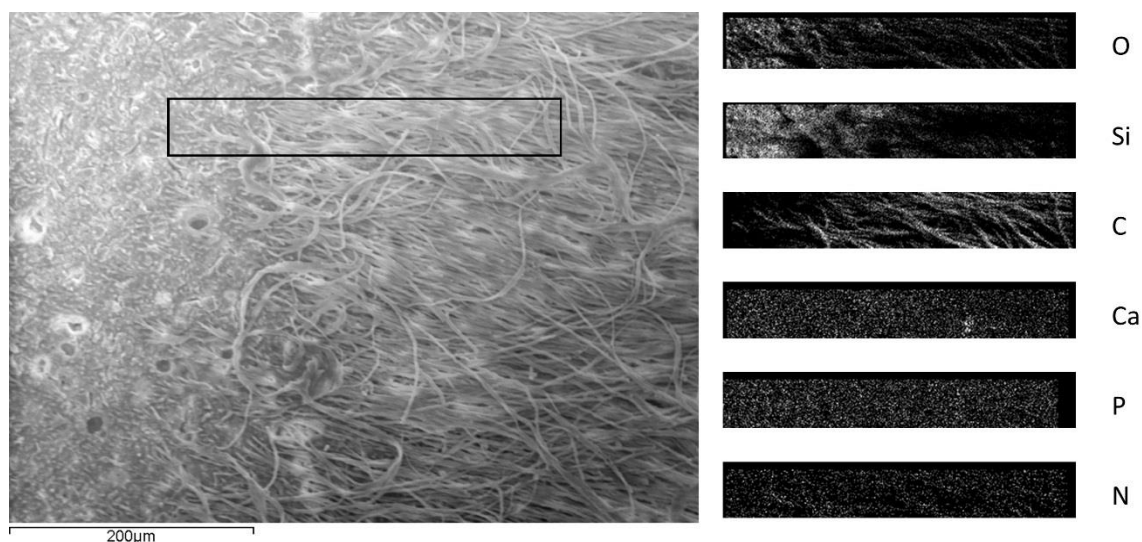
Figure 6-9 EDX map of tags formed by F10 in comparison to an area free of tags on the composite disc

6.6.3.2 Tags with carious dentine

The ability to penetrate and form tags with naturally carious dentine was evaluated using CLSM following grinding down of the samples to expose the interface (carious dentine/ restoration).

F10, z250 with bond, Activa, Fuji IX and Fuji II LC were used as restorative materials. F10 showed best penetration and ability to form resin tags within carious dentine (Figure 6-10). All other materials (z250 with bond, Activa, Fuji IX, Fuji II LC) showed no evidence of resin tags presence at the interface.
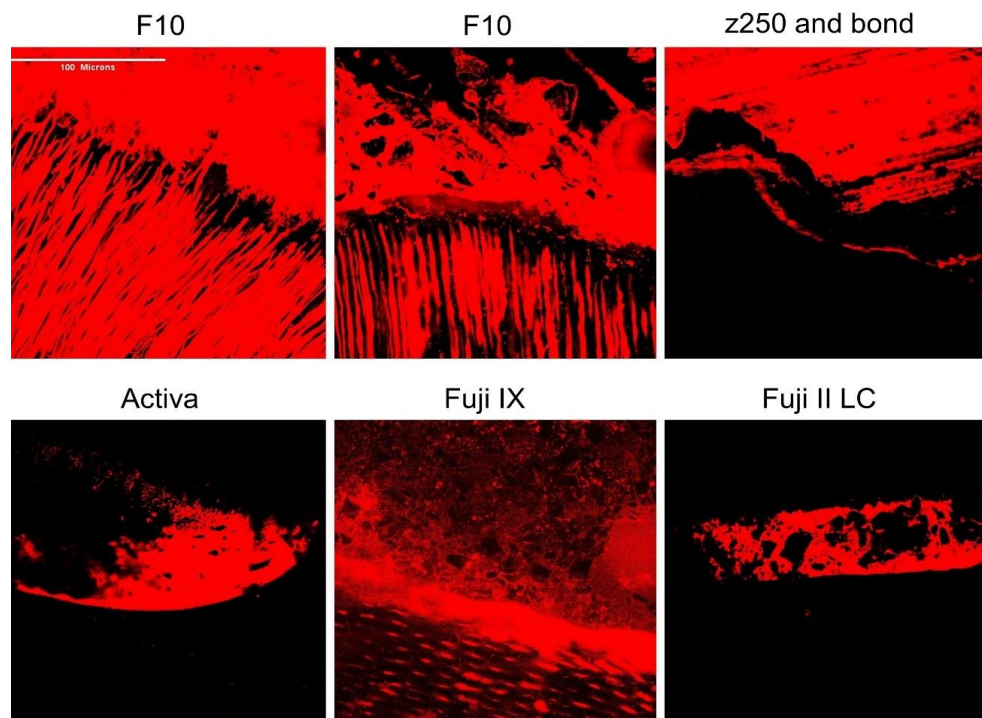
Figure 6-10 CLSM images of resin tags formation with caries dentine using F10, z250, Activa, Fuji IX or Fuji II LC. Filling material is shown on top part of the image and carious dentine on the lower part. n=3

6.6.4 Microleakage with sound enamel and dentine

Sample number was not consistent in this test due to limited availability of human primary teeth. For each group, the sample number is the sum of numbers inside its pie chart.

6.6.4.1 *Microleakage with sound enamel*

Figure 6-11 shows the microleakage results associated with enamel with different restorative materials used as per manufacturer`s instructions. The darker the pie chart, the more extensive the microleakage. F9, F10 and z250 (with etch and bond) showed less microleakage in comparison to other commercial comparators (Activa, Fuji IX and Fuji II LC). Statistical analysis (ordinal regression and Kruskal-Wallis pairwise comparisons) showed that F9, F10 and z250 were comparable to each other and significantly different from all other commercial comparators.
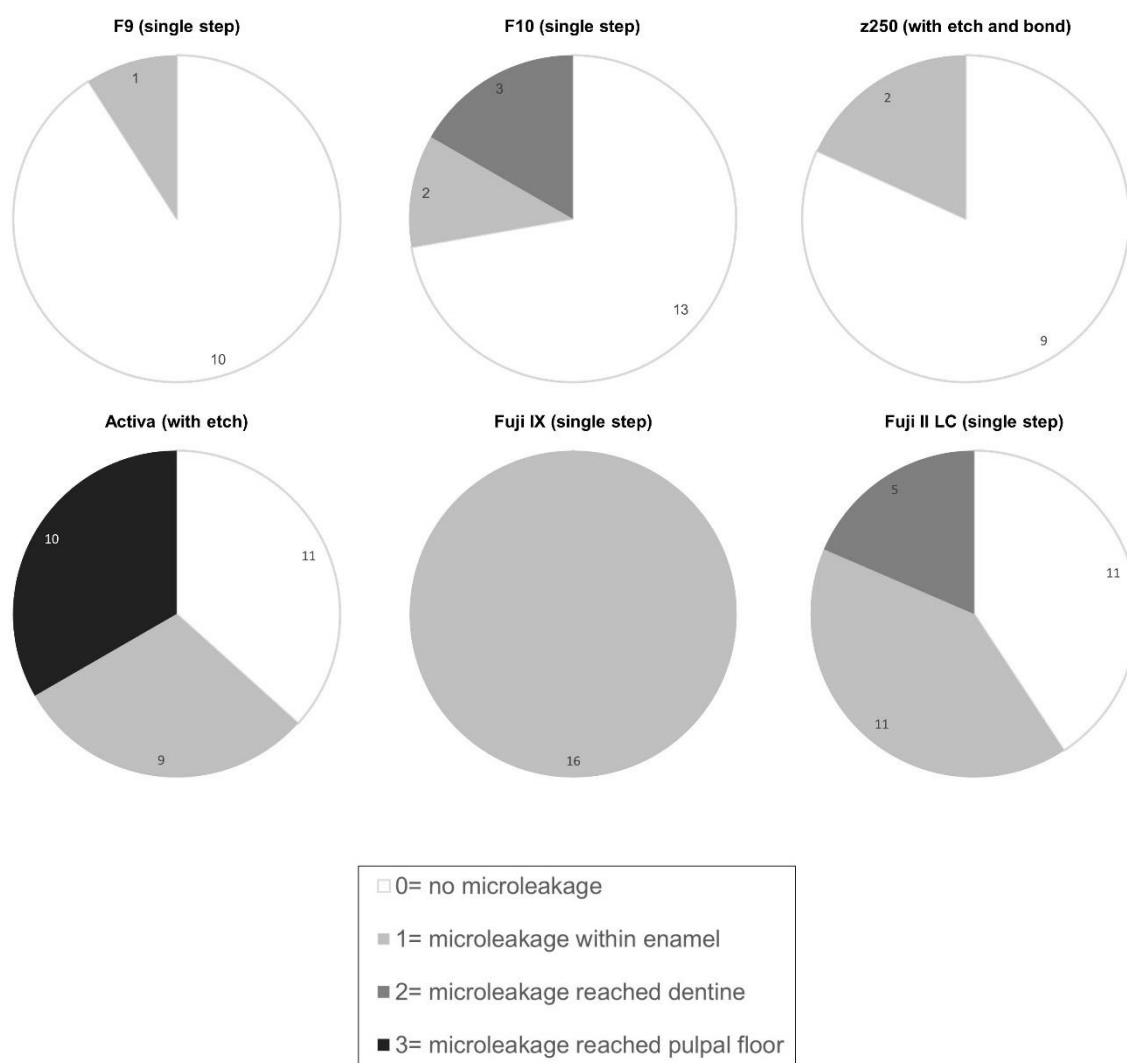
Figure 6-11 Adhesion to sound enamel upon immersion in water for 24 hours at 37°C: Microleakage test results within adhesion interface using F9, F10, z250, Activa, Fuji IX and Fuji II LC. The darker the pie chart, the more extensive the dye penetration, and the worse is the adhesion. Sample number varied and for each group it is the sum of the numbers in the pie chart.

6.6.4.2 Microleakage with sound dentine

Figure 6-12 shows the microleakage results associated with dentine using different restorative materials. Again, F9 and F10 showed less microleakage in comparison to other commercial comparators and even better than z250. Statistical analysis (ordinal regression and Kruskal-Wallis pairwise comparisons) showed that F9, F10 and z250 were comparable to each other and significantly different from all other commercial comparators.
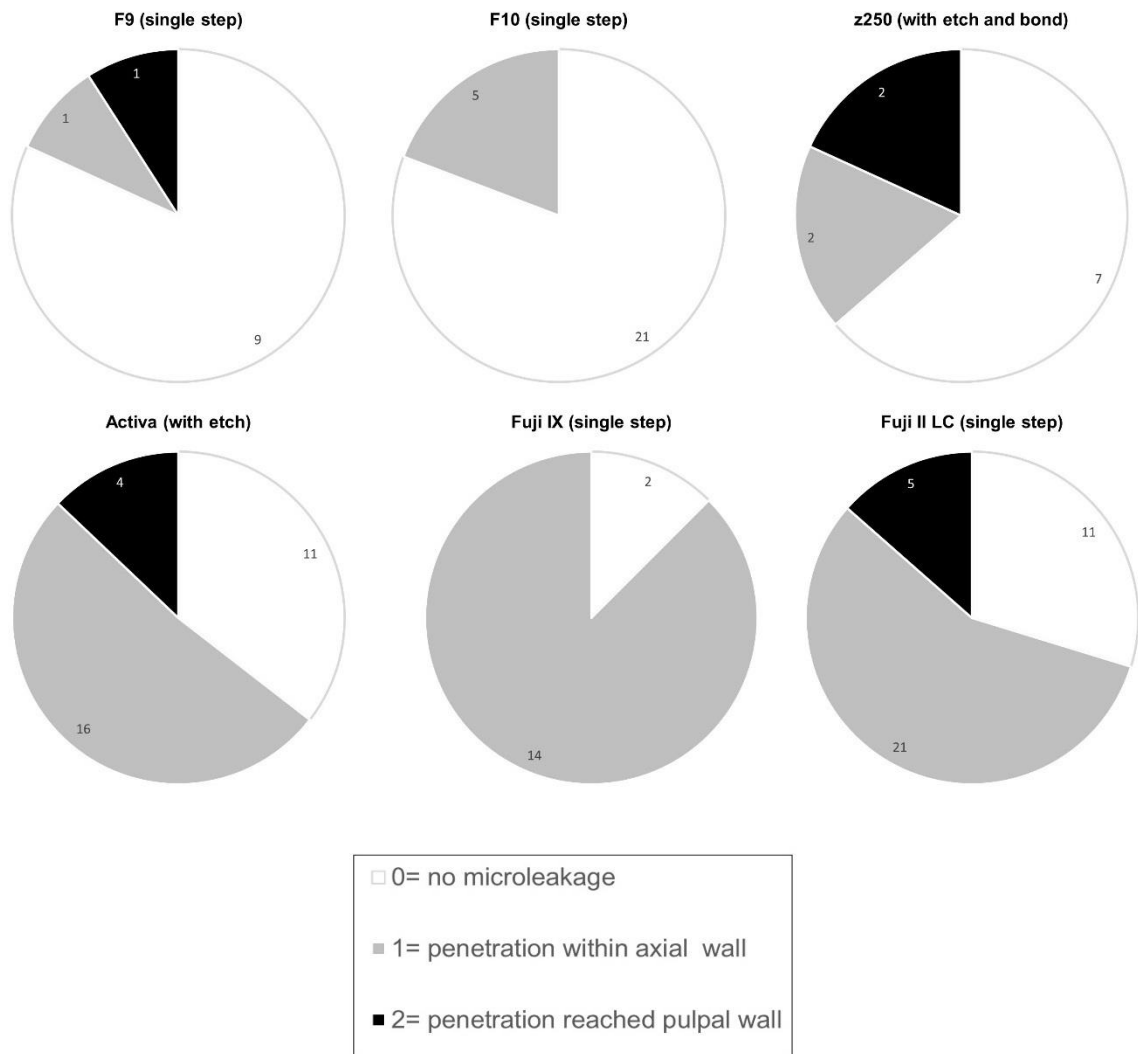
Figure 6-12 Adhesion to sound dentine upon immersion in water for 24 hours at 37°C: Microleakage test results within adhesion interface using F9, F10, z250, Activa, Fuji IX and Fuji II LC. The darker the pie chart, the more extensive the dye penetration, and the worse is the adhesion. Sample number varied and for each group it is the sum of the numbers in the pie chart.

6.6.5 Shear bond strength

Figure 6-13 shows the shear bond strength to bovine enamel and dentine following immersing the samples in water at 37°C for 24 hours. The optimised formulations (F9 and F10) managed to achieve a bond to untreated enamel but failed to bond to dentine.

Pre-treating the enamel and dentine with phosphoric acid gel 35% (for 30s or 15s, respectively) only boosted the ability of F10 to bond to enamel but not dentine.

Values of shear bond strength to enamel were comparable for F9, F10, Fuji Ix and Fuji II LC (2.6, 2.8, 4.5, 4.3MPa, respectively). Activa recorded a shear bond strength of 6.8MPa to enamel and was not significantly different from Fuji IX and Fuji II LC. When acid etch was used with F10 to pre-treat enamel, the formulation achieved higher bond strength (11.5MPa) and was comparable to z250 with etch and bonding agent (14.7MPa).

Shear bond strength to dentine was comparable amongst F9, F10, Activa and Fuji II LC as they all failed to achieve proper adhesion. Fuji IX and z250 however, were significantly higher than other groups ($p = 0.045$ to $5*10^{-6}$) (and significantly different from each other as well, $p = 3*10^{-4}$) and they achieved 4.6MPa and 12.2MPa shear bond strength to dentine, respectively.
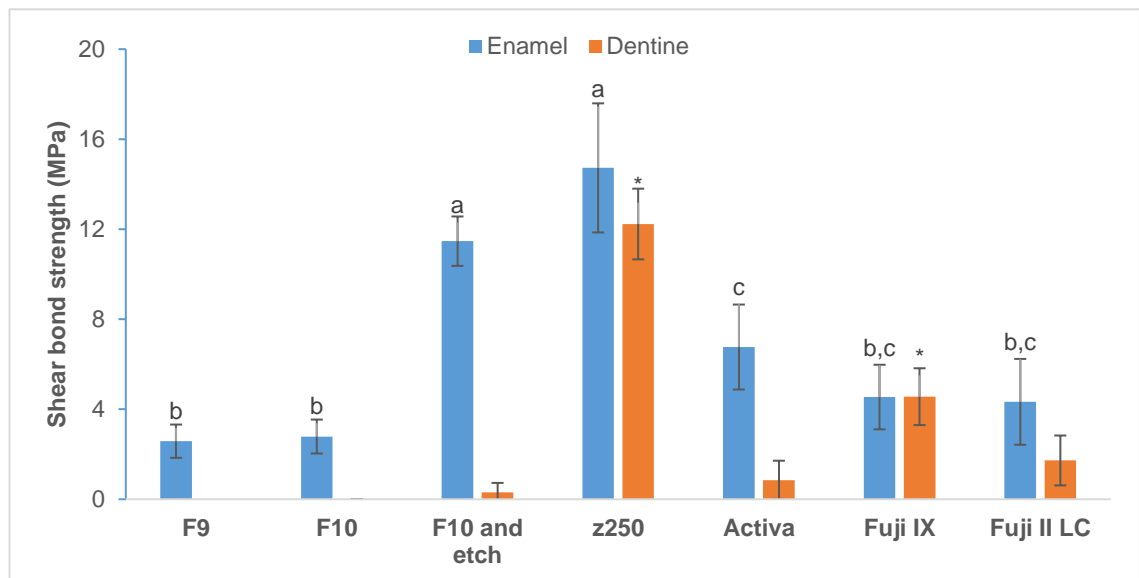
*Figure 6-13 Shear bond strength test results of F9, F10 (with or without acid etch), z250, Activa, Fuji IX and Fuji II LC to sound bovine enamel and dentine. Specimens were tested upon 24 hours immersion in water at 37°C. * indicates significant difference from all other groups. Groups holding the same letter (a, b or c) are not significantly different from each other. Error bars are 95% CI (n=10).*

6.7 Discussion

6.7.1 Self-etching property

Different acid etching protocols have been suggested in the literature. However, with the acceptance of the total etch technique (etching enamel and dentine simultaneously), phosphoric acid 37% for 15s has been the preferred one to avoid over-etching dentine and creating a thick hybrid layer that is difficult to be penetrated by resins. Etching enamel can end up with different etching patterns. Enamel, which is made up of prisms, can demonstrate one of three patterns; demineralised edges or centres of the prisms or a mix of both. While these patterns are not of clinical significance (does not affect bond strength) and a uniform pattern cannot always be achieved, the purpose of etching is just to roughen and increase the surface area, regardless of the pattern produced (Hobson and McCabe, 2002; Ireland and Sherriff, 2006; Zhu et al., 2014).

F10 was not able to create an etching pattern similar to that of phosphoric acid when applied up to 2 minutes. However, the surface morphology has definitely changed upon application and it was noticed that the enamel got rougher with increasing application time. The enamel discs were relatively humid when the paste was applied. Therefore, when the F10 paste was applied, it was in contact with water. Based on the results in section 3.6.2.2, the experimental formulations of high PLS and MCP content showed a considerable release of H^+ moles from cured discs into water.

Equation 2-14 shows that MCP can form phosphoric acid when in water. The concentration of the formed acid might not be as high as the commercial gel (35%). However, it was enough to roughen the surface. Additionally, this property might be beneficial in breaking down some hydroxyapatite crystals which will act as precursors for future remineralisation of affected tissues.

6.7.2 Cavity adaptation (XCT)

ISO 11405:2015 (BSI, 2015) states that to test adhesion to dentine, measuring the gap between the tooth and the restorative material might be used as a method. Other methods include microleakage and shear bond strength. However, the ISO methods measure the gap in one plane upon grinding down the restoration parallel to its surface. Conversely, using non-destructive XCT scans allows an overview of the whole interface of filling/tooth and the maximum forming gap to be measured. Then with 3D models, this gap can be visualised.

Cavity adaptation is affected by the ability of the material to flow into the cavity (wettability) and adapting to all walls (Braga and Ferracane, 2004). Additionally, the

175

stress generated by polymerisation shrinkage upon curing can lead to gaps forming at the interface if the bond strength to the tooth structure was not sufficient and the higher the stress the bigger the gaps and worse is the following microleakage (Ferracane and Mitchem, 2003; Alomari et al., 2007; Han and Park, 2017; Han et al., 2019). These gaps can play a major role in the recurrence of the disease by allowing microleakage and creating an optimal environment for bacteria to grow in. On the other hand, if the bond strength was adequate but the stress generated was too high, this might lead to further problems like cuspal deflection and enamel fracture (C. J. Soares et al., 2017; Enochs et al., 2018).

It was also of interest to scan the restorations again after 3 months to check their stability. The optimised final formulation showed water solubility values that exceeded the maximum recommended by ISO. The release of active components will level off upon 2 months of immersion in water. Hence, the high water solubility would have been expected to cause some defects in the restoration, especially at the interface. However, all tested materials showed consistent results after 3 months without any major increase in gaps.

Despite the simplified application method of F10 which entitled a single-step without preconditioning dentine or the use of any adhesive agent, it showed no gaps with sound or carious dentine. These results were similar to z250 that was applied upon acid etching and applying bonding agent. Activa and Fuji IX showed a 20-25μm gap while the resin modified glass ionomers was the worst with up to 120μm gap.

6.7.3 Tags formation

When a commercial restoration is applied into a cavity, it needs prior steps to ensure micro-retention by penetrating into the tooth structure. These steps usually include acid etch and bonding agent application. The acid etch will remove about 10μm of the tooth surface, including the smear layer (~2μm) and prepare dentine to receive the bonding agent which will penetrate and form resin tags. This layer of bonding agent / exposed collagen is called the hybrid layer. Increased etching time will create thicker demineralised layer but that is not always beneficial unless the restoration integrates with the whole thickness. Total etch systems exhibited thicker hybrid layer in comparison to self-etch systems. Although resin penetration is not limited to the demineralised thickness, the tags length is higher with deepest demineralisation (Iwaku et al., 1981; Arrais and Giannini, 2002; Sato and Miyazaki, 2005; Sundfeld et al., 2005; Baweja et al., 2007; Prabhakar et al., 2011; Ramesh Kumar et al., 2011; Mithiborwala et al., 2012; Rahal et al., 2012; Adiga et al., 2013)

The ability of a restorative material to penetrate into caries affected dentine might be beneficial in many ways. It will enable better interlocking with the diseased tissue and consequently limiting microleakage and recurrent disease. It will also cause remnant caries to arrest and provide a favourable environment for remineralisation. Additionally, it will enable the use of such material in an atraumatic restorative technique (ART) without the need for total caries removal and the use of complicated etch and bond procedures.

All experimental formulations showed the ability to penetrate into naturally carious dentine despite the simplified single-step technique. The commercial comparators (z250, Activa, Fuji IX and Fuji II LC) did not form tags with carious dentine. In literature, the average length reported of resin tags formed by adhesive agents ranged between 10-60μm. Glass ionomers are known to bond chemically and hence it was expected not to detect resin tags. Composite resins on the other hand, require the application of etch and bond on sound dentine and hence not much data available about their ability to penetrate carious dentine. F10, however, exhibited >200μm long resin tags with a simple single-step application on carious dentine without any prior conditioning of the tooth substrate.

The hydrophilic components in the experimental formulations (PLS and MCP) are mainly responsible for this property. This was proved previously with the factorial analysis (see Figure 4-12) and discussed thoroughly in section 4.7.2. As mentioned there, PLS (positively charged) might have interacted with non-collagenous proteins, especially the phosphophoryn (PP) and chondroitin sulphate which are highly concentrated around the tubules. This interaction might have encouraged the composite paste to be pulled into the dentinal tubules.

Based on the linear relationship between PLS content and the area covered by tags (Figure 4-11), it was expected that reducing the PLS content from 5% to 4% will result in a formulation that is able to cover 63.5% of the adhesion interface with tags. This is in good agreement with the tested optimised final formulations (F9 and F10) which showed 62% tags coverage area.

The resin tags formed within collagen and caries affected dentine with the proposed formulation were much longer than those reported in literature with some other commercial materials where it did not exceed 20-30μm even with dentine pre-treatment (Giachetti et al., 2005; Rosa et al., 2015). The enamel etching protocol (time and concentration of phosphoric acid) showed some importance in the length of the resulting tags where it went down from 22μm to 5μm when concentration of phosphoric acid was decreased from 35% to 3% (Shinchi et al., 2000). Although F10 was not tested in terms

of forming tags within enamel, its self-etching, microleakage and cavity adaptation results proved a good seal was achieved with the cavity edges.

The ability of a material to form tags is widely affected by its flowability and hydrophilicity. The higher the filler content or the lower the monomer phase, the less flowable the material is. Therefore, the PLR plays a major role in flowability and the length of the resulting resin tags (Prabhakar et al., 2011; Prabakar et al., 2018). On the other hand, PLS and MCP, as mentioned previously, have improved this property due to being hydrophilic components. Based on that, the components that were expected to be detected in the resin tags are the polymers and the PLS basically. Raman spectra proved that the composition of these tags is majorly made of polymers. The tags spectra which showed no presence of the C=C peak at $1640cm^{-1}$ proves that these tags were polymerised and penetrating into collagen did not inhibit or affect the light-curing kinetics. EDX showed that this composition contained no silica and was dominated by Carbon. The PLS was not detected in Raman spectroscopy or EDX and this might be explained by the sample preparation method. To expose these resin tags the samples were soaked in aqueous solution of sodium hypochlorite for about two days. The fine diameter of these resin tags is 5µm on average. This very thin structure, if it contained any PLS, it will be expected to be released very easily and rapidly.

6.7.4 Microleakage with sound enamel and dentine

Testing microleakage into the adhesion interface (tooth/restoration) is another method of testing adhesion to tooth structure set by ISO 11405:2015 (BSI, 2015).

Although the final optimised formulations (F9 and F10) were applied in a simple single step method without the use of acid etch, they showed limited microleakage and were comparable to z250 which was applied upon acid etching and bonding. Activa and glass ionomers showed extensive microleakage. Cavity adaptation results (see 6.6.2) showed bigger gaps formed at the adhesion interface when Activa, Fuji IX or Fuji II LC were used to restore cavities. This might explain why these materials exhibited higher dye penetration at the adhesion interface when the microleakage test was performed. Additionally, the ability of F10 to self-etch enamel might have participated in its reduced microleakage values when applied without preconditioning of enamel. Gaps at the interface and their causes and effects on following results were previously discussed in sections 6.7.2.

6.7.5 Shear bond strength

Bovine teeth were used to perform this test instead of human teeth to reduce variability in results since many factors affect human teeth and render them not an ideal substrate.

Shear bond strength to bovine dentine was very low for all materials except z250 (with acid etch and bond) and Fuji IX. These results were comparable to other studies (Fritz et al., 1996; Hibino et al., 2004; Carvalho et al., 2011). All the materials that were applied with a single-step method (F9, F10, Fuji IX and Fuji II LC) showed comparable bond strength to bovine enamel. Activa (with etch) and z250 (with acid and etch) bonded much better to bovine enamel.

Using acid etch before applying F10 increased bond strength to enamel (comparable to z250) but not dentine. This is in good agreement with many other studies that showed that some materials bond better to enamel when etched while the bond strength to dentine decreases with longer etching times (Xuan and Wang, 2015; Tsujimoto et al., 2017; Buyuk and Kucukekenci, 2018). The acid etch will create a rough enamel surface and massively increase the bonding surface area resulting in higher bond strength and this was reflected in the results.

Bond strength might also be negatively affected by higher monomer conversion and the stress resulting from polymerisation shrinkage as stated previously in this section (Kanehira et al., 2006).

Bonding to enamel is more important than dentine since it forms the edge of the cavity (cavosurface) and forms the first line of defence against bacterial attacks and recurrent disease. Additionally, bonding to dentine is usually much more difficult and always shows lower values in comparison to enamel because of the lower mineral content. Consequently, this was the theory behind the novel method of selective etching which recommends etching the enamel only and not depend on any bond strength with the dentine.

6.8 Conclusion

The results of the tests performed in this chapter showed that the optimised final formulation can (without the use of acid etching or bonding agent) adhere to tooth structure by:

- Self-etching enamel and creating rough surface,
- Adapting very well to cavity walls without forming any gaps,
- Penetrating and forming resin tags within collagen mesh and carious dentine,
- Limiting microleakage at the adhesion interface (tooth/restoration),
- And bonding to bovine enamel (better with acid etching) but not dentine.

It also showed that it had superior results to all other commercial comparators used in terms of adapting to cavity walls, forming resin tags and limiting microleakage at the adhesion interface.

7   Remineralising Effect and Inhibiting Matrix Metalloproteinase (MMP) in Carious Dentine

Thesis structure

Chapter 1:
literature review

Chapter 2:
Materials and methods

Chapters related to the first eight formulations

Chapter 3:
Basic properties of the first eight experimental formulations

Chapter 4:
Resin tags formation

light curing kinetics, intercations of the discs with water and mechanical properties

Creating caries-like collagen discs to check ability to penetrate

Chapters related to the final formulations
F9 and F10

Chapter 5:
Summary of chapters 3, 4 and the basic properties of F9, F10

Chapter 6:
Adhesion to tooth structure (F9, F10)

Chapter 7:
The effect of the novel additives, MCP and PLS

Self-etch, cavity adaptation, tags formation, microleakage and shear bond strength

Remineralising effect and MMP inhibition

Chapter 8:
General conclusion

Chapter 9:
Future work

7.1 Abstract

Aims:

The purpose of the work presented in this chapter was to test the ability of F10 to stabilise the adhesion interface when applied to carious or caries-like dentine by precipitating minerals (remineralisation) and limiting the enzymatic degradation (MMP activity).

Materials and methods:

Light-cured F10, Activa or Fuji II LC discs (n=3) were applied to collagen mesh discs and stored in SBF at 37ºC incubator for 5 months when they were detached and scanned under CLSM and SEM to detect remineralisation. Carious primary tooth was also restored with F10 and immersed in AS while SBF was pumped through the pulp chamber for 6 months. Subsequently, it was cross-sectioned and looked at under CLSM.

PLS solutions of different concentrations (0.1 to 1000mM) were prepared and added to gelatin substrate and collagenase (EnzCheck Gelatinase/Collagenase Assay Kit, Molecular Probe). A known MMP inhibitor (Phenanthroline monohydrate) was used as a positive control). The fluorescence was checked under a microplate reader until 4 days. Collagen substrate conjugated with fluorescein was applied at the collagen mesh surface or in a carious dentine cavity then restored with F10 or other commercial comparators. The interface was then exposed and scanned under CLSM at 2 and 14 days to check if the collagen was broken down by MMP activity and became fluorescent.

Results:

Collagen mesh discs that were in contact with F10 showed total occlusion of dentinal tubules at the interface and a precipitation of mineral layer, unlike with Activa and Fuji II LC. This surface was also less green-fluorescence under CLSM.

Higher PLS concentration was correlated to less enzymatic activity. The fluorescence at the adhesion interface almost disappeared at 14 days (0-1% of the scanned field area) when the discs were restored with F10 and this was significantly lower than all other commercial comparators which exhibited higher fluoresce values.

Conclusion:

The optimised final formulation F10 could precipitate minerals at the adhesion interface and stabilise caries affected tissue which can enhance the remineralising process. It also inhibited the MMP activity, maybe by interlocking dentine and/ or PLS release.

7.2 Introduction

For the affected dentine to be saved, the restorative material must have some key characteristics. One of these is interlocking with carious dentine and cavity-sealing ability. The ability of the final optimised formulation to do so was proved in chapter 6. The other two are the ability to precipitate minerals and limit the enzymatic deproteinisation process at the interface.

Remineralising carious tissues at the interface is beneficial to restore mineral content in this partially demineralised tissue (affected dentine). Many attempts have been made to produce calcium and phosphate ion-releasing composites to prevent progress and remineralise dental caries (Xu et al., 2009; L. Zhang et al., 2016).

Auto-fluorescence of demineralised dentine was used as an indicator of minerals content (or remineralisation) of the collagen mesh model created in chapter 4. There are different theories for carious dentine green auto-fluorescence, but it is not widely understood. It is mainly described that "chromophores" are the reason behind auto-fluorescence. These chromophores fluoresce when they are either (van der Veen and ten Bosch, 1996):

- De-quenched: which means that when they are bound to both collagen and hydroxyapatite, their emittance is masked but when minerals are dissolved the fluorescence becomes stronger
- Chemically modified: this includes a possible reduction in the amount of amino acids (arginine, proline and hydroxyproline) as components of dentine organic matrix.

The current limitation of resin-composites apart from the complex bonding procedure is the failure related to the recurrent disease at the interface. Matrix metalloproteinase enzymes (MMPs) could be responsible for this failure in the long-term and for the progress of disease in dentine. They are deproteinisation agents which when activated, will complete the role of the demineralising bacterial acids by breaking down the organic content of dentine (collagen) (Takahashi and Nyvad, 2016). Therefore, a material that can limit or inhibit this activity would be of great benefit.

As previously discussed in the introduction, these dentine and saliva enzymes get activated in an acidic environment created by bacterial acids during carious attack or even by the acid-etching step prior to bonding procedure. This results in the degradation of the interface and the future failure of restorations. MMP-8 of the collagenase and MMP-9 of the gelatinase family are the most abundant enzymes in dentine, however,

many other MMPS have been proven to be present in carious dentine (Visse and Nagase, 2003; Chaussain-Miller et al., 2006; Boushell et al., 2011; Mazzoni et al., 2011; Mazzoni et al., 2015a; Tjaderhane et al., 2015; Femiano et al., 2016).

7.3 Hypothesis

The null hypothesis is:

- The optimised formulation can neither remineralise carious dentine nor inhibit the MMP activity at the interface (material/tooth).

7.4 Aims and objectives

The aim of this chapter is to evaluate two novel properties of the optimised formulation:

- The ability to remineralise demineralised dentine
- The ability to inhibit MMP activity at the adhesion interface

7.5 Materials and methods

7.5.1 Remineralising effect through the peristaltic pump model or the collagen mesh

To test the remineralising effect of F10 due to its content of MCP, two methods were optimised.

In the first one, cured composite discs of F10 (prepared as in 2.1.5) were placed in tight contact with collagen mesh discs of 2mm thickness (prepared as in 4.5.1 using formic acid). Activa and Fuji II LC were used as commercial comparators (n=3 for each group). The specimens were then placed in 10mL SBF and incubated at 37°C. SBF was replenished every two weeks to avoid contamination. After 6 months, samples were taken out, gently detached and the interface was scanned by means of CLSM then SEM to detect any precipitation of minerals on the collagen. CLSM settings were consistent for all samples and the plane with best focus and highest fluorescence signal was recorded.

The other method included using a freshly extracted carious primary tooth to mimic what might happen in the oral cavity. The tooth was cleaned and disinfected (using chloramine T 1% for 2 days) then the pulp removed through the apices after grinding them down to enlarge the foramens. Caries were manually excavated with a spoon excavator to remove the very soft highly infected dentine and leave the affected dentine. Cavity was restored with F10 and light-cured for 20s. Initial periapical X-ray was taken and then pipes were fit into the apices of the tooth to pump SBF into the pulp chamber using a peristaltic pump (Watson Marlow, UK). The flow rate of SBF was set at 7.8mL/min as it was found to be the optimal rate according to the pulp chamber size and the inner diameter of the pipes used to avoid building pressure and tubing detachment. SBF was replenished every two weeks to avoid contamination. Tooth was immersed externally in artificial saliva. Every month the tooth was X-rayed again until 5 months when the tooth was sectioned and scanned through CLSM to compare it to another tooth that had been restored the same way. No labelling probe was used as the collagen in dentine has its own green auto-fluorescence which is stronger with demineralised dentine.

7.5.2 Inhibiting MMP activity

The ability of the optimised formulations to inhibit MMP activity was evaluated using solutions of different PLS concentrations. Subsequently carious dentine substrate or collagen mesh substrate were restored with different materials and the interfaces scanned through CLSM.

7.5.2.1 Preparing solutions

Following a Molecular Probe protocol (EnzCheck Gelatinase/Collagenase Assay Kit, Molecular Probe), solutions where prepared as follows:

- Gelatin substrate from pig skin: This substrate is conjugated with fluorescein which releases fluorescence when broken down. The vial contents (1mg) were dissolved in 1mL of deionised water (concentration is 1mg/mL) and agitated in an ultrasonic water bath for 5 minutes to facilitate mixing.
- Collagen substrate: It is a highly quenched type I collagen that is heavily labelled with fluorescein and has more complicated structure in comparison to gelatin. When broken down by enzyme activity, it releases fluorescent peptides. The solution was prepared as with the Gelatin substrate.
- Reaction Buffer (10X): contains 50mL 0f 0.5M Tris-HCL, 1.5M NaCl, 50mM of $CaCl_2$ and 2mM of sodium azide, prepared to a pH of 7.6. It was diluted by a factor of 10 by adding 2mL of the stock solution to 18mL of deionised water (1X reaction buffer).
- Collagenase from *Clostridium histolyticum* (MMP-1): collagenase is more selective for collagen type-I (which is the abundant organic component of dentine). The vial contains 0.5mL (1000 units per mL). The stock solution was diluted to 0.2 unit per mL by adding 0.2μL of it to 1000μL of 1X reaction buffer.
- 1,10-Phenanthroline monohydrate is a general metalloproteinase inhibitor. Two concentrations were prepared by adding 9.9mg to 25μL of ethanol then 10mM solution was prepared by adding 10μL of this solution to 2mL of 1X reaction buffer. This solution was then serially diluted to two concentrations (0.2mM and 1mM).
- In addition, different concentrations of PLS were prepared (0.1, 1, 10, 100, 250, 500, 750, 1000mM)

7.5.2.2 Effect of different PolyLysine concentrations on collagenase activity

96 well-plates were used, and the total volume of reaction was 200μL as follows. In each well, 80μL of either PLS (0.1, 1, 10, 100, 250, 500, 750 or 1000mM) or Phenanthroline monohydrate (0.2 or 1mM) were mixed with 20μL of gelatin substrate (1mg/mL) and 100μL of either Collagenase (*Clostridium histolyticum,* 0.2U/mL) or 1X buffer as a control (n=3 in each group). Positive and negative controls were prepared by mixing 20μL of the gelatin substrate with either 80μL of 1X buffer and 100μL collagenase or with 180μL buffer, respectively. After mixing, the well plate was wrapped with double layers of foil to

protect from light and stored at room temperature (24°C). Fluorescence intensity was measured using a microplate reader (Flx800, BioTek) at 30min, 1hr, 3hr, 5hr, 1d, 2d, 3d and 4d. The absorption maximum was set at 495nm and the fluorescence emission maximum at 515nm. Background was corrected by subtracting the values of the corresponding controls (gelatin and inhibitor without collagenase enzyme) from the ones with full reaction components (inhibitor + gelatin + collagenase).

7.5.2.3 Matrix Metalloproteinase (MMP) activity at the interface between naturally carious dentine and different restorative materials (Appendix G)

Following removal of soft caries with a spoon excavator, 20μL of the collagen substrate was mixed with 80μL of 1X buffer to bring down the concentration to 200μg/mL. 5μL of this solution was added to a blot dried cavity and left for 5 minutes to enable it to soak in. The cavity was then restored using the final formulation F10 or one of the commercial materials (Fuji IX, Fuji II LC, z250 or Activa) (n=1). Bonding agent was only used with z250, while etchant was not used in any sample as the dentine was affected with caries and therefore already demineralised. Restorations were light-cured immediately for 20s and stored humid in a sealed pot with moist tissue in a 37°C incubator for 1d. Samples were trimmed down (perpendicular to the adhesion surface) to expose the interface then scanned through confocal laser microscopy (using the highest fluorescence settings possible without detecting the collagen green auto fluorescence). Samples were then stored in 2mL deionised water for 2 weeks at 37°C and scanned again.

7.5.2.4 Matrix Metalloproteinase (MMP) activity at the interface between collagen mesh and different restorative materials

Collagen mesh discs were prepared as in (4.5.1). 20μL of the solution prepared in 7.5.2.3 were added to a blot dried collagen disc and allowed to soak in for 5 minutes. Restoration was applied (1mm thickness) on the same surface following the same steps as before (n=3). A negative control of non-restored collagen mesh was used.

7.6   Results

7.6.1   Remineralising effect

7.6.1.1   With collagen mesh

The CLSM scans of the collagen mesh surface that had been in contact with the optimised formulation (F10) for 6 months in SBF at 37°C are shown in Figure 7-1. Activa and Fuji II LC were used as comparators. The scans show that collagen discs that have been in contact with F10 showed less auto fluorescence in comparison to those that had been in contact with Activa or Fuji II LC.
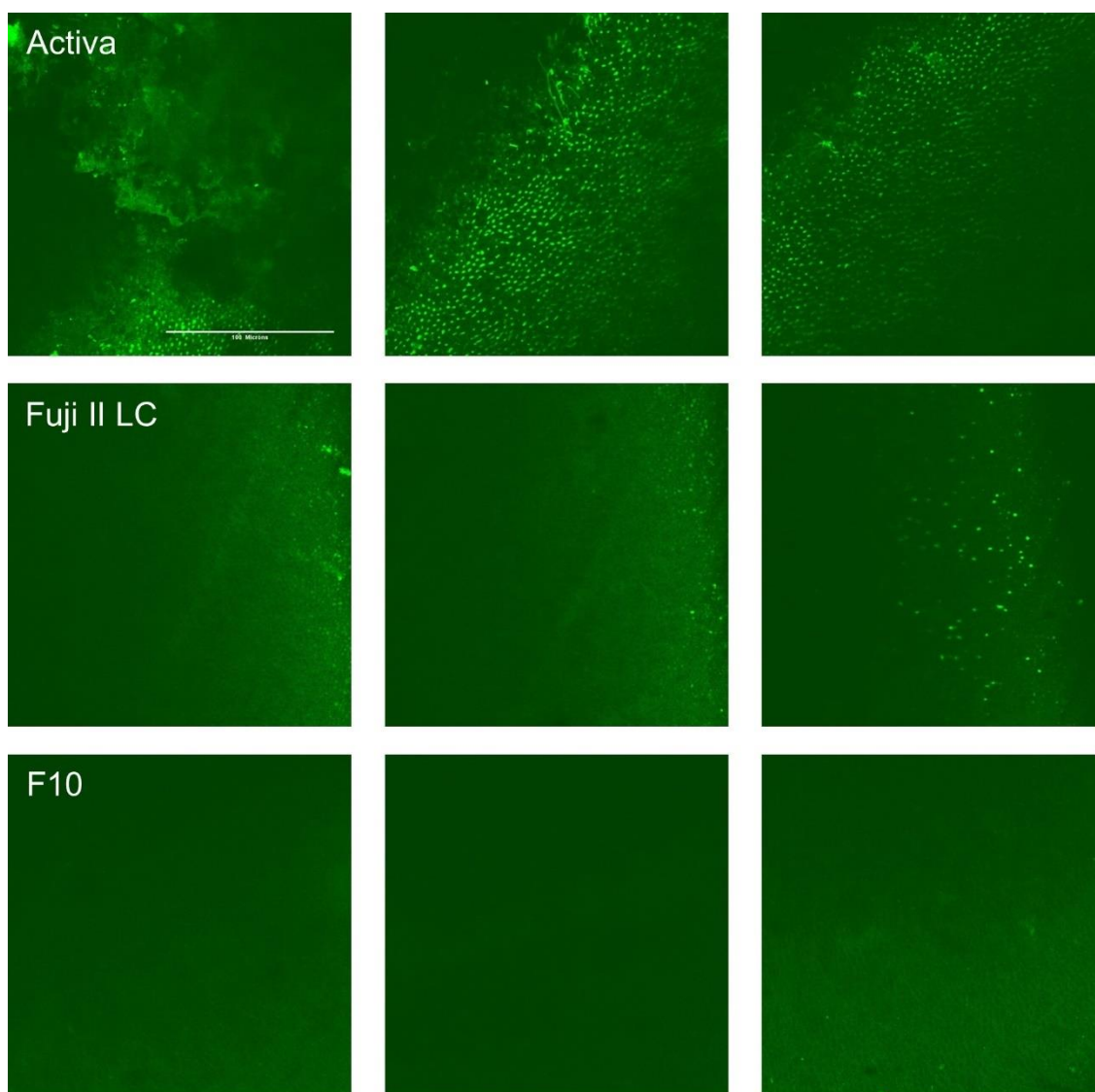
Figure 7-1 CLSM scans of the collagen mesh discs that were in contact with pre-cured Activa, Fuji II LC and F10 discs and incubated at 37°C in SBF for 6 months. Collagen that was in contact with F10 showed less fluorescence. (n=3)

These surfaces were coated and scanned under SEM, the images are shown in Figure 7-2. Collagen discs that were incubated with Activa or Fuji II LC showed no sign of minerals at the interface with widely opened dentinal tubules. However, those that were incubated with F10 showed an interface totally covered with minerals and the dentinal tubules totally occluded.
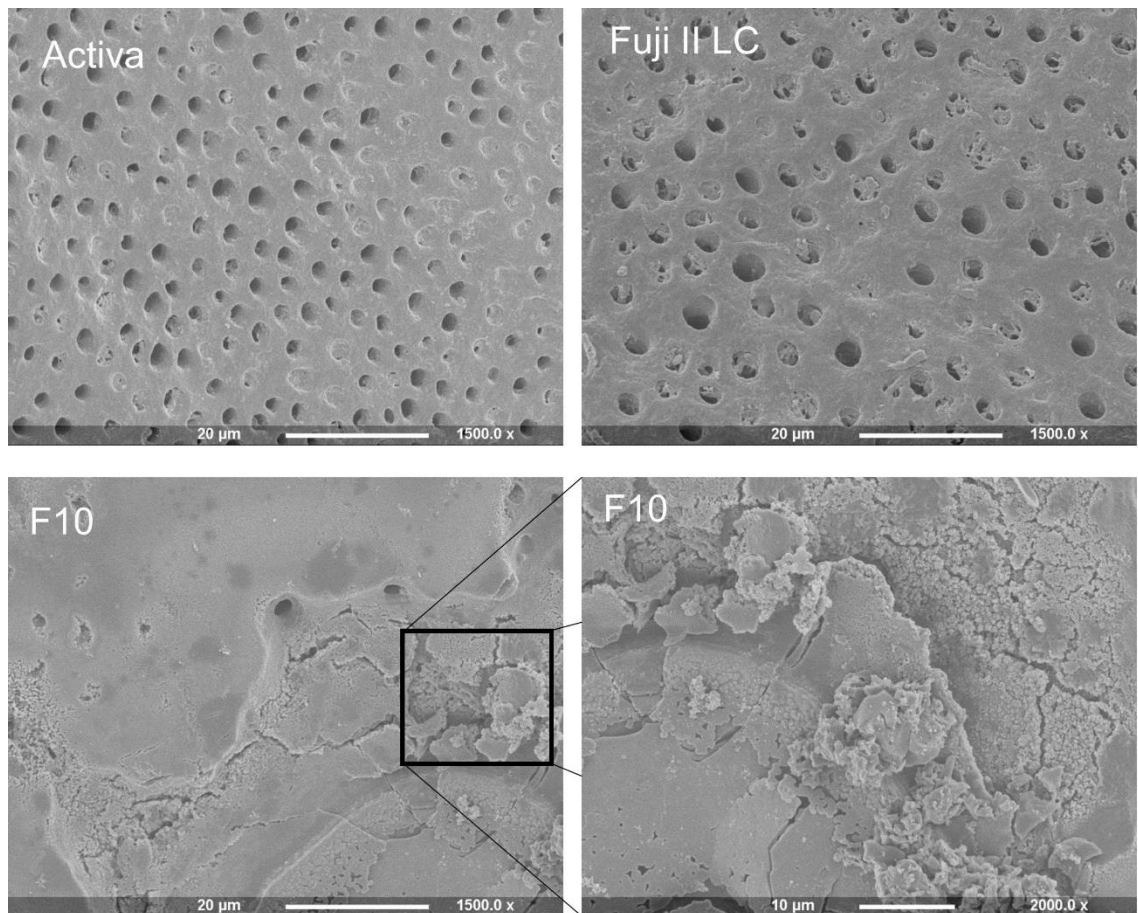
Figure 7-2 SEM images of the collagen mesh discs that were in contact with pre-cured Activa, Fuji II LC and F10 discs and incubated at 37°C in SBF for 6 months. Activa and Fuji II LC shows widely opened dentinal tubules while F10 covered the whole surface with a layer of minerals. (n=3)

7.6.1.2 With carious dentine (peristaltic pump model)

Figure 7-3 shows monthly X-ray images of the carious primary tooth that was restored with F10 using atraumatic technique upon being immersed in AS and having SBF pumped through its pulp chamber continuously for 5 months. The caries beneath the restoration (appearing more radiolucent) did not show any signs of progression or regression. They appeared to be stable or at least the method was not able to detect significant changes.
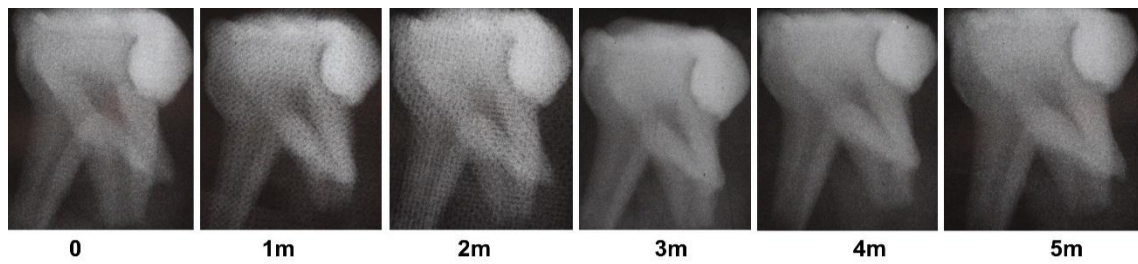
Figure 7-3 X-ray images sequence (up to 5 months) of a carious primary tooth that was restored atraumatically with F10 then immersed in AS and had SBF pumped through its pulp chamber.

The tooth was cross sectioned longitudinally at the end of the 5-month experiment and the CLSM scan of the restoration / carious dentine interface is shown in Figure 7-4. Carious dentine showed highest fluorescence, which was reduced with sound dentine. In comparison to freshly restored tooth, the auto fluorescence of the carious dentine at the interface seemed to be reduced up to a thickness of 10-20 microns.
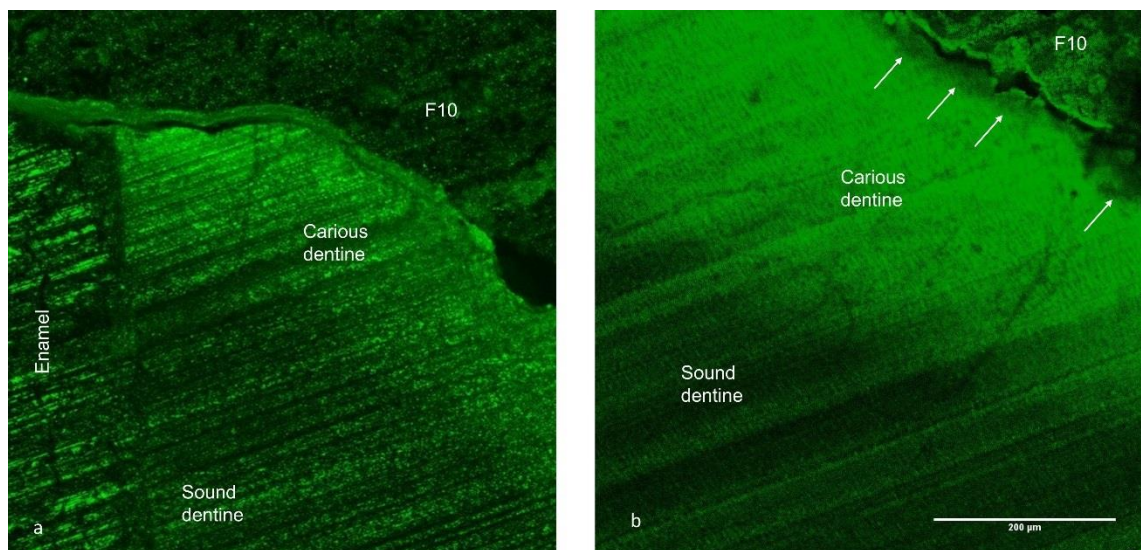
Figure 7-4 CLSM scan of restoration / carious dentine interface of (a) freshly restored tooth and (b) upon immersing in AS and having SBF pumped through the pulp chamber for 5 months. Both teeth were restored using F10 with atraumatic technique.

7.6.2 Inhibiting MMP activity

7.6.2.1 Effect of different PolyLysine concentrations on collagenase activity

Figure 7-5 shows increased fluorescence and thus increased MMP activity as a function of time for all PLS solutions, the negative control (no inhibitor) and the positive control (0.2mM Phenanthroline monohydrate). The positive controls showed the least fluorescence (higher MMP inhibition effect), especially with 1mM concentration. All PLS solutions, except for the lowest 0.1mM concentration, showed fluorescence results in between the negative and positive controls. These results decreased with higher

concentration of PLS. Negative correlation between PLS concentration and fluorescence was proved by statistical analysis (Pearson correlation) within each time-point. The value of this correlation was always negative and decreased with longer times (stronger correlation). Correlation results are shown in Table 7-1.
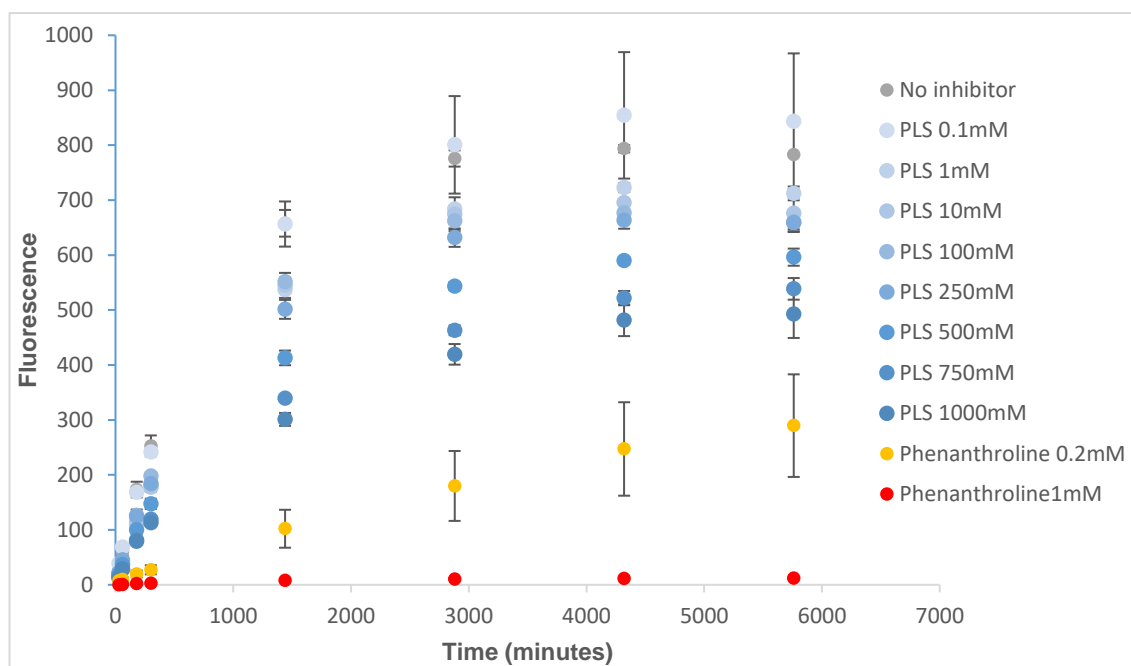
Figure 7-5 MMP activity measured by fluorescence in a microplate reader using different concentrations of PLS solutions (0.1mM to 1000mM) to check inhibition effect. No inhibitor samples were used as a negative control and Phenanthroline (0.2mM or 1mM) as a positive control. Error bars are 95% CI (n=3).

Table 7-1 Pearson correlation between PLS concentration and fluorescence (MMP activity) at different time-points

Time	Pearson correlation
0.5 hour	-0.58
1 hour	-0.62
3 hours	-0.78
5 hours	-0.88
1 day	-0.94
2 days	-0.93
3 days	-0.88
4 days	-0.84

7.6.2.2 Matrix Metalloproteinase (MMP) activity at the interface between naturally carious dentine and different restorative materials

Results of this pilot study are shown in Appendix G.

7.6.2.3 Matrix Metalloproteinase (MMP) activity at the interface between collagen mesh and different restorative materials

Figure 7-6 shows representative CLSM images of the interface (collagen mesh/ restoration). F10 showed the least fluorescence which disappeared totally after 14 days, unlike when PLS was taken out of the formulation.
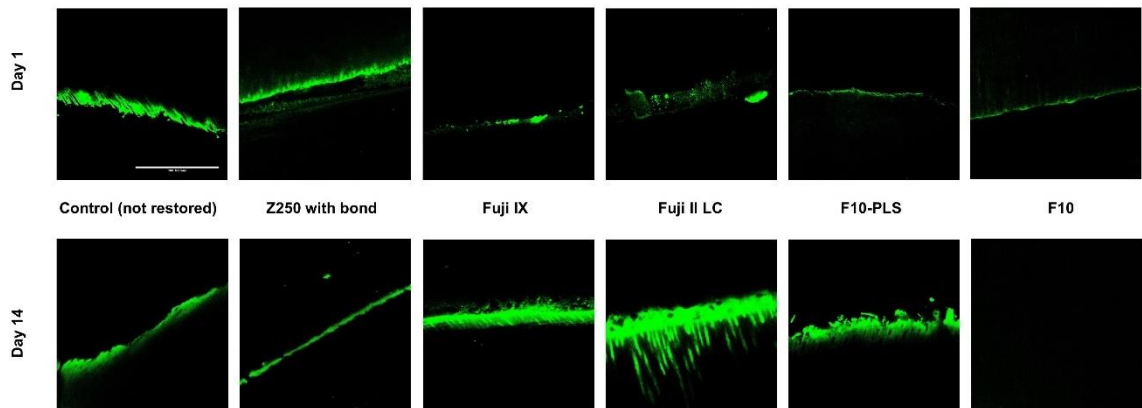
Figure 7-6 CLSM images of MMP activity(in green) after 1 day and 14 days at the adhesion interface of z250, Fuji IX, Fuji II LC, F10 without PLS and F10 with collagen mesh as a substrate. Non restored collagen disc was used as a negative control. Field width is 200 microns, scale bar is 100 microns, n=3

Quantifying these images (through ImageJ software) resulted in the data shown in Figure 7-7. It shows again that F10 had significantly lower MMP activity (less than 1% at any time) in comparison to all other commercial groups (p = 0.01 to 8.3*10^{-8}). The values were significantly higher when PLS was taken out of the optimised formulation, especially after 14 days (5.9%) where it was comparable to Fuji IX and Fuji II LC (4.6% and 3.2%, respectively). Activa and z250 results were in the middle (significantly lower than Fuji IX and Fuji II LC, and significantly higher than F10) after 14 days of incubation.
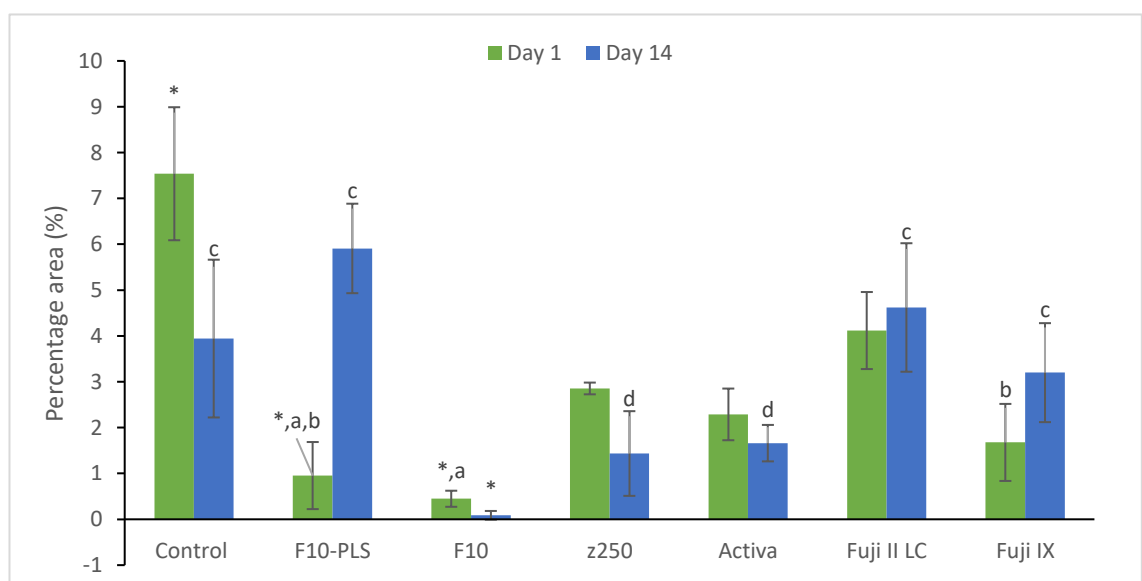
*Figure 7-7 MMP activity by area percentage (green fluorescence quantification of CLSM images) using collagen mesh as a substrate at 1 day and 14 days. n=1. * indicates significant difference from all other groups unless they share the same letter (a, b, c or d). Error bars are 95% CI (n=3).*

7.7 Discussion

7.7.1 Remineralising effect through the peristaltic pump model or the collagen mesh

F10 managed to form a conspicuous layer of minerals at the interface with collagen mesh. This layer, that appeared to cover the whole surface of collagen, was not observed when Activa or Fuji II LC were used, and the dentinal tubules did not look occluded. CLSM scans also showed that the collagen mesh that was incubated in contact with F10 showed considerably less auto fluorescence in comparison to the commercial comparators. However, it was not clear if this precipitation has occurred only at the interface or went deep down into the collagen mesh.

Due to the organic content in dentine, especially the collagen, it can be excited with the confocal laser and give some green fluorescence without the need to use any staining probe. This auto fluorescence increases when dentine is demineralised by a carious attack because of exposing more collagen fibrils and might be explained by the interaction between the collagen and the bacteria matrix which might create a refined fluorescent matrix (Banerjee et al., 2004). Therefore, the strength of fluorescence can be linked to the level of mineral content in dentine. This is in good agreement with the findings of Banerjee et al who found that highly carious dentine have a stronger auto fluorescence signal in comparison to less carious dentine and that sound dentine and enamel did not show that signal (Banerjee et al., 1999; Banerjee et al., 2010). They have also managed to relate the strength of the auto fluorescence signal to the microhardness of dentine.

In literature, using the 405nm laser induced auto fluorescence showed a unique spectral pattern between 450nm and 800nm. The demineralised dentine gave higher emission (stronger peak) at 529nm when excited at 488nm. The spectral range between 550nm and 600nm provides the least overlap between different zones of carious lesions and might be the most useful method to identify these zones (van der Veen and ten Bosch, 1995; Joseph et al., 2015; Son et al., 2016; Ko et al., 2017).

In the peristaltic pump model, the aim was to mimic the conditions in the oral cavity. A few complications hindered the method but were manageable. For example, the pulp chamber got frequently blocked and had to be flushed and cleaned with saline irrigation and some debridement. X-ray images were not of great value as it was not always possible to get a repetitive image with exactly the same contrast and brightness to compare the greyscale of the carious layer beneath the restoration. Another drawback was the removal of the pulp, pulp cells (especially odontoblasts) might play important role in remineralisation and protecting the pulp from irreversible damage. Based on the

CLSM scans however, F10 has managed to remineralise a very thin layer of about 10-20μm. When compared to silver diamine fluoride (SDF) for example, which can arrest caries up to 150μm deep, F10 appears less able to remineralise caries. However, in a study by Mei et al, this thickness was not achieved till after 2 years of applying SDF (Mei et al., 2014). This layer might actually be thicker in clinical conditions due to the reasons mentioned before about the pump model complications. Additionally, this layer might be beneficial to block the adhesion interface against future bacterial attacks, microleakage and recurrent of the disease.

The ability of F10 to precipitate minerals, at least at the interface, can be explained by the MCP content. This hydrophilic component (MCP) can form phosphoric acid when in water (Equation 2-14), which might be the reason behind creating an environment of optimal pH for brushite to form and then mature into hydroxyapatite. The storage solution (SBF) might have also played an important role in the remineralisation process as a source of minerals (Atmeh et al., 2015). This was observed in a pilot study of teeth restored with F10 and immersed in SBF for shorter periods (see Chapter 9). These observations might suggest that some kind of guided tissue remineralisation has occurred, especially at the interface (Tay and Pashley, 2008). The amount of remineralisation (thickness and occluding dentinal tubules, looks more promising in comparison to a Casein phosphopeptide-amorphous calcium phosphate (CPP-ACP) containing paste (Cao et al., 2013). Remineralising results must be interpreted carefully before claiming the ability of a formulation to repair caries and induce biomimetic remineralisation process through adding bioactive fillers. Minerals can easily precipitate at collagen fibres when that collagen is immersed in a calcium/phosphate rich medium.

7.7.2 Inhibiting MMP activity

Within 3 days, PLS managed to limit the activity of MMP. However, it was not as effective as the positive control Phenanthroline monohydrate 1mM. Increased PLS concentrations showed higher efficacy against MMP. Although it is difficult to predict the concentration of PLS released into the interface, the collagen mesh and the naturally carious dentine models showed that it might be enough to inhibit MMP. These two models contain activated MMP enzymes. Low pH caused by natural caries process (bacterial acids) or the immersion in acid to demineralise the discs can result in the activation of the enzymes. These enzymes can also be activated during the acid etching process prior to applying a restoration. This could be responsible for future degradation and nanoleakage at the interface, leading to recurrence of the disease and failure of the restoration.

The CLSM scans also showed that upon 2 weeks of incubation of restored teeth or collagen mesh with different materials, MMP activity almost disappeared in F10 samples followed by z250< F10 without PLS< Activa< Fuji IX< Fuji II LC. This sequence looks very comparable to the microleakage and cavity adaptation results. Therefore, the ability to seal the interface and bond well to tooth structure might also play an important role in limiting the MMP activity. The effect of good sealing on inhibiting MMP activity was also addressed in literature (Osorio et al., 2012; Kuhn et al., 2016). It was proved that infiltrating into dentine and achieving better interlocking can inhibit MMPs.

Research showed that MMPs which are host-derived enzymes are most abundant and active in carious dentine alongside with cysteine cathepsins. This distribution of MMP is mainly due to the role they play in caries progression and therefore any subsequent failure at the adhesion interface (Nascimento et al., 2011; Vidal et al., 2014; Mazzoni et al., 2015a; Femiano et al., 2016; Scaffa et al., 2017). It has been argued that all-in-one (one step) bonding systems show less ability to inhibit MMP activity and that this was related to their inferior performance because of MMP associated collagen degradation at the hybrid layer (Apolonio et al., 2017).

Many attempts have been introduced to limit or inhibit the MMP activity. Some of these included adding inhibitors to the bonding systems (such as chlorhexidine, BB94 and GM6001) or crosslinking collagen (Almahdy et al., 2012; Montagner et al., 2014; Almahdy et al., 2015; Seseogullari-Dirihan et al., 2016). Most of these studies showed good results with enhanced bonding strength to tooth structure in the long term due to limiting the degradation at the interface. However, the results were very dependent on the adhesive system used (self-etch or etch-and-rinse) with preference for the non-simplified systems.

While the chlorhexidine for example works as an endogenous inhibitor of collagenolytic enzyme, F10 (containing PLS) might have a similar or a different mechanism. Biomimetic remineralisation was also introduced as a way to inhibit MMP, which may have played a more important role in the proposed final formulation (F10) (Perdigao et al., 2013; Mazzoni et al., 2015a). The mechanism needs to be studied more thoroughly and in depth.

7.8 Conclusion

The results of the tests performed in this chapter showed that the optimised final formulation F10 can:

- Precipitate minerals at the adhesion interface and stabilise caries affected tissue which can enhance the remineralising process.
- Inhibit the MMP activity within 3 days due to the ability to seal and interlock dentine and/ or PLS release.

8 Summary and General Conclusion

Thesis structure

Chapter 1:
literature review

Chapter 2:
Materials and methods

Chapters related to the first eight formulations

Chapter 3:
Basic properties of the first eight experimental formulations

Chapter 4:
Resin tags formation

light curing kinetics, intercations of the discs with water and mechanical properties

Creating caries-like collagen discs to check ability to penetrate

Chapters related to the final formulations
F9 and F10

Chapter 5:
Summary of chapters 3, 4 and the basic properties of F9, F10

Chapter 6:
Adhesion to tooth structure (F9, F10)

Chapter 7:
The effect of the novel additives, MCP and PLS

Self-etch, cavity adaptation, tags formation, microleakage and shear bond strength

Remineralising effect and MMP inhibition

Chapter 8:
General conclusion

Chapter 9:
Future work

Through the work presented in this thesis, it can be concluded that:

The results of the tests in chapter 3 showed that the proposed experimental formulations can be used as bulk fill with light-curing time of 40s being sufficient to cure 4mm thick samples. Higher PLR caused an increase in delay time but a decrease in rate of reaction. The pastes were stable upon ageing. In terms of cured disc interactions with water, it was proved that the hydrophilic additives (PLS and MCP) caused an increase in water sorption and solubility, mass and volume change and H^+ release. Formulations of higher PLR and PLS content showed higher initial burst and percentage release of PLS. Flexural strength of the experimental formulations after one day of soaking in water was higher than 80MPa. Whilst the additives (PLS and MCP) caused a reduction in flexural strength it levelled off after 3 months of soaking in water. It was also shown that the formulations are able to promote minerals precipitation.

The aim of chapter 4 was to create a model that resembles carious dentine in terms of loss of minerals but maintains the structure of the collagen framework. This was achieved by using formic acid 4M, which totally demineralised human dentine discs of 2mm thickness. All experimental formulations were able to penetrate into the collagen mesh forming resin tags which might be able to interlock and stabilise carious dentine. Formulations of lower PLR gave longer resin tags. Increasing the PLS or MCP content, however, resulted in an increase in collagen area covered by tags.

Chapter 5 discussed the selection of an optimised formulation based on the previous work and compared two versions of it (in-house and commercially supplied). The tests showed that both formulations were comparable in terms of:

- o Light-curing kinetics
- o Biaxial flexural strength
- o Water sorption and solubility
- o Radio-opacity

Furthermore, any shift in values of these properties compared with F5 was either expected or justified (due to slight change in PLS content or experiment conditions).

The optimised formulations showed high monomer conversion (more than 75%) and acceptable biaxial flexural strength (120MPa) and modulus (3.5GPa). Furthermore, they were radio-opaque.

In chapter 6, various tests were performed to test adhesion to tooth structure in different ways. The results showed that the optimised final formulation can (without the use of acid etching or bonding agent) adhere to tooth structure by:

- Self-etching enamel thereby creating a rough surface,

- Adapting very well to cavity walls without forming any gaps,
- Penetrating and forming resin tags within collagen mesh and carious dentine,
- Limiting microleakage at the adhesion interface (tooth/restoration),
- And bonding to bovine enamel (better with acid etching) although not dentine.

Furthermore, the optimised formulation had superior results to all other commercial comparators investigated in terms of adapting to cavity walls, forming resin tags and limiting microleakage at the adhesion interface.

Chapter 7 focused on more innovative work to open the door for further studies. The results of the tests performed in that chapter showed that the optimised final formulation can:

- Precipitate minerals at the adhesion interface and stabilise caries affected tissue which can enhance the remineralising process.
- Inhibit the MMP activity within 3 days due to its ability to seal and interlock dentine and/ or release PLS.

It can be concluded that this project was successful in providing the data needed to make a decision towards a final formulation after years of hard work in the lab and carry it forward to clinical trials.

9 Future work

Thesis structure

Chapter 1:
literature review

Chapter 2:
Materials and methods

Chapters related to the first eight formulations

Chapter 3:
Basic properties of the first eight experimental formulations

Chapter 4:
Resin tags formation

light curing kinetics, intercations of the discs with water and mechanical properties

Creating caries-like collagen discs to check ability to penetrate

Chapters related to the final formulations
F9 and F10

Chapter 5:
Summary of chapters 3, 4 and the basic properties of F9, F10

Chapter 6:
Adhesion to tooth structure (F9, F10)

Chapter 7:
The effect of the novel additives, MCP and PLS

Self-etch, cavity adaptation, tags formation, microleakage and shear bond strength

Remineralising effect and MMP inhibition

Chapter 8:
General conclusion

Chapter 9:
Future work

There is no perfectly complete work in science. Every research should open the door for more investigations to acquire better knowledge. Based on the work presented in this thesis, the following areas can be recommended for future projects:

- Clinical trials are needed as part of regulations before releasing a product. It can be done in many phases. Shorter periods are required in the beginning to look for any adverse reactions or safety issues (see Appendix H). Then longer periods for long-term stability and longevity of these restorations. These teeth when ready to be extracted can be analysed in the lab in many different ways with special interest to look at the interface (gaps, resin tags, remineralising, MMP activity, analyse content of the filling in comparison to discs that has not been in the patient`s mouth etc.).

- At the same time, more lab work can be done in the following areas:
  - Bond strength is a complicated test with many variables affecting it. More work should be done to optimise a method to test bond strength to human teeth with a focus on sample preparation which plays a major role in the final results.
  - The possibility of developing a bonding agent to be used with the final formulation.
  - Further studies to develop understanding of how the paste interacts with tooth structure prior to curing. This might be crucial in changing application instructions.
  - The novel properties of this formulation might be useful if applied as a fissure sealant, perhaps upon adjusting the PLR to give a more flowable paste.
  - Increase the sample size and reanalyse the inhibitory effect of this formulation on MMP to understand how the PLS can limit MMP action.
  - Resin tags formed with the collagen mesh model were noticed to be distributed across the adhesion surface except in the centre (closer to pulp horns) (see Appendix D). More work is needed to understand the anatomy of that area and justify this finding.
  - The compatibility of the use of this formulation with other restorative materials (Zinc oxide and eugenol, composites…), to test the ability to adhere to these materials and check any polymerisation inhibitory effect. Adhesion of layers of the material can also be tested immediately or upon contamination with artificial saliva for different times (to repair fractures for example).
  - Remineralising effect with the use of appropriate stains with the help of CLSM to visualise remineralising pattern, depth and distribution at

different times (using the auto-fluorescence of carious dentine as an indicator).

o In a pilot study, it was observed that different teeth restored with F10 and immersed in SBF for up to 5 weeks could precipitate brushite at the interface. SEM observations of the carious dentine surface are shown in Figure 9-1. Increasing the sample number and quantifying remineralising effect should be determined in the future.
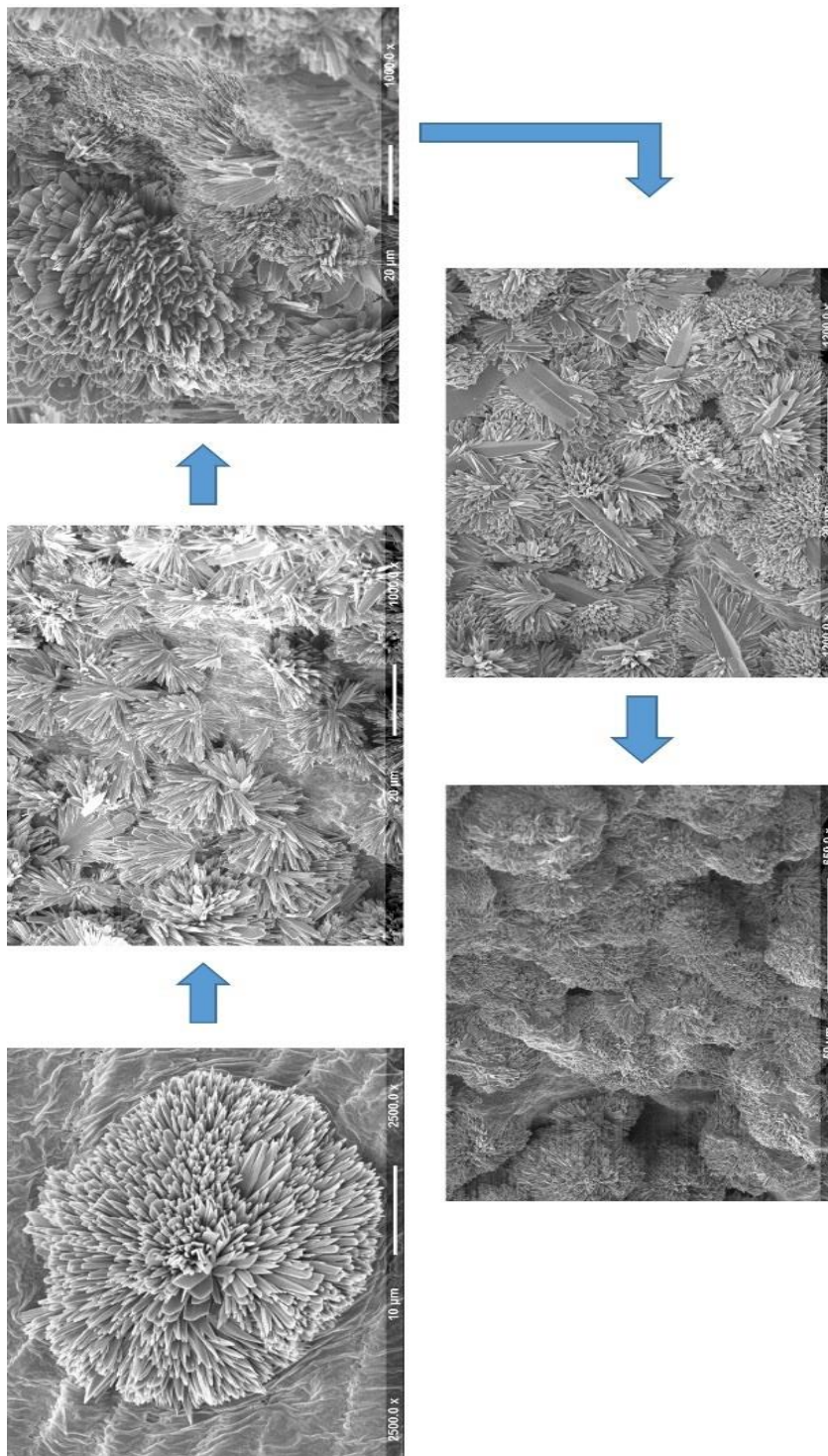
Figure 9-1 Different stages (weekly basis up to 5 weeks) of minerals precipitation at the adhesion interface of carious tooth restored with F10 and immersed in SBF at 37°C.

10 Appendix A

Light curing kinetics

Figure 10-1 Delay time of all experimental formulations (1mm and 4mm, aged at 60°C for 6 months or non-aged) compared to z250 as a control. Samples were light-cured for 40s at room temperature (24°C). Error bars are 95% CI (n=3)
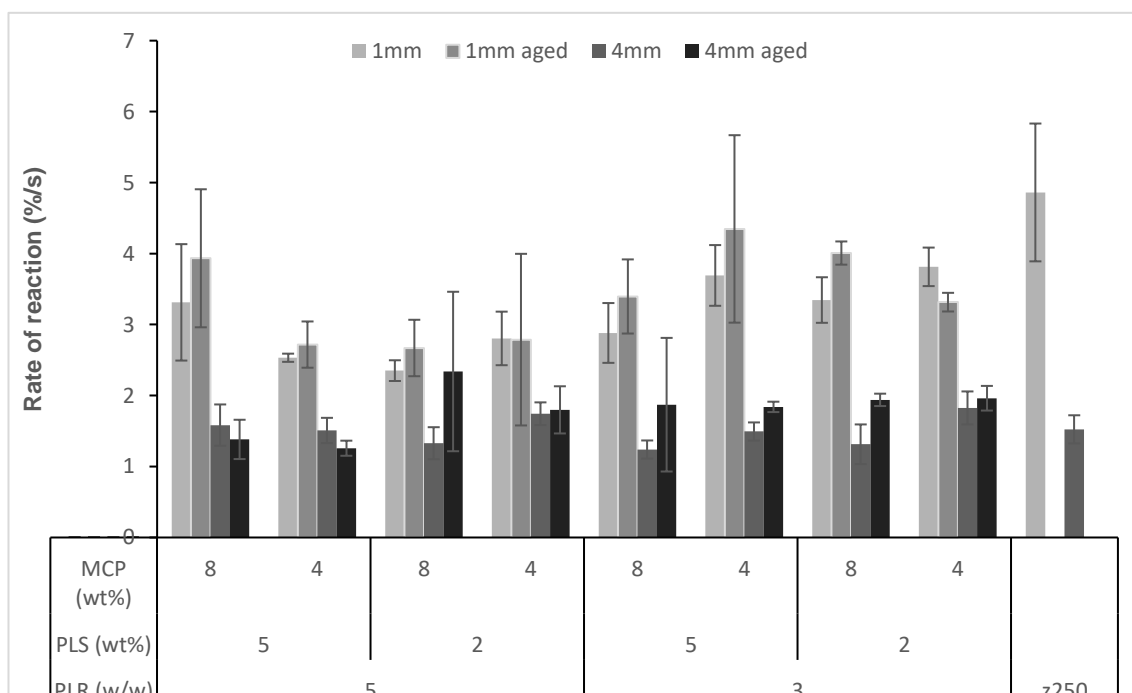
Figure 10-2 Rate of reaction of all experimental formulations (1mm and 4mm, aged at 60°C for 6 months or non-aged) compared to z250 as a control. Samples were light-cured for 40s at room temperature (24°C). Error bars are 95% CI (n=3)
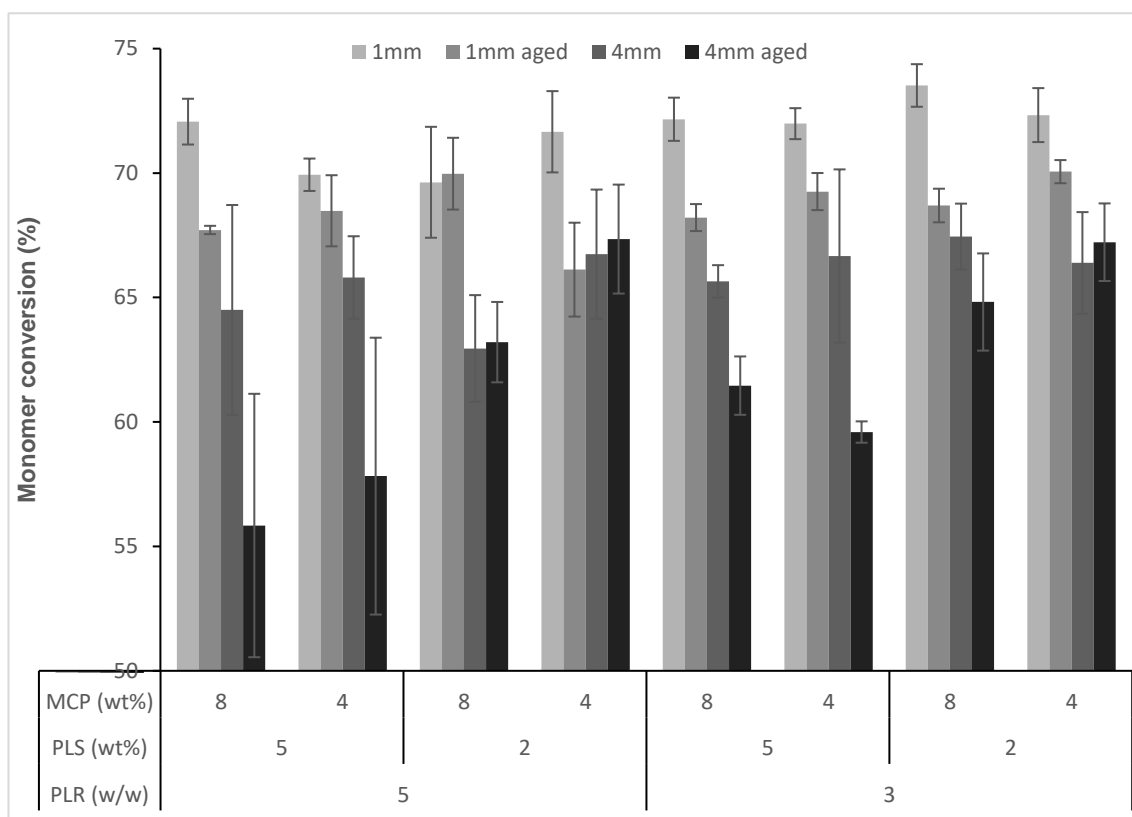
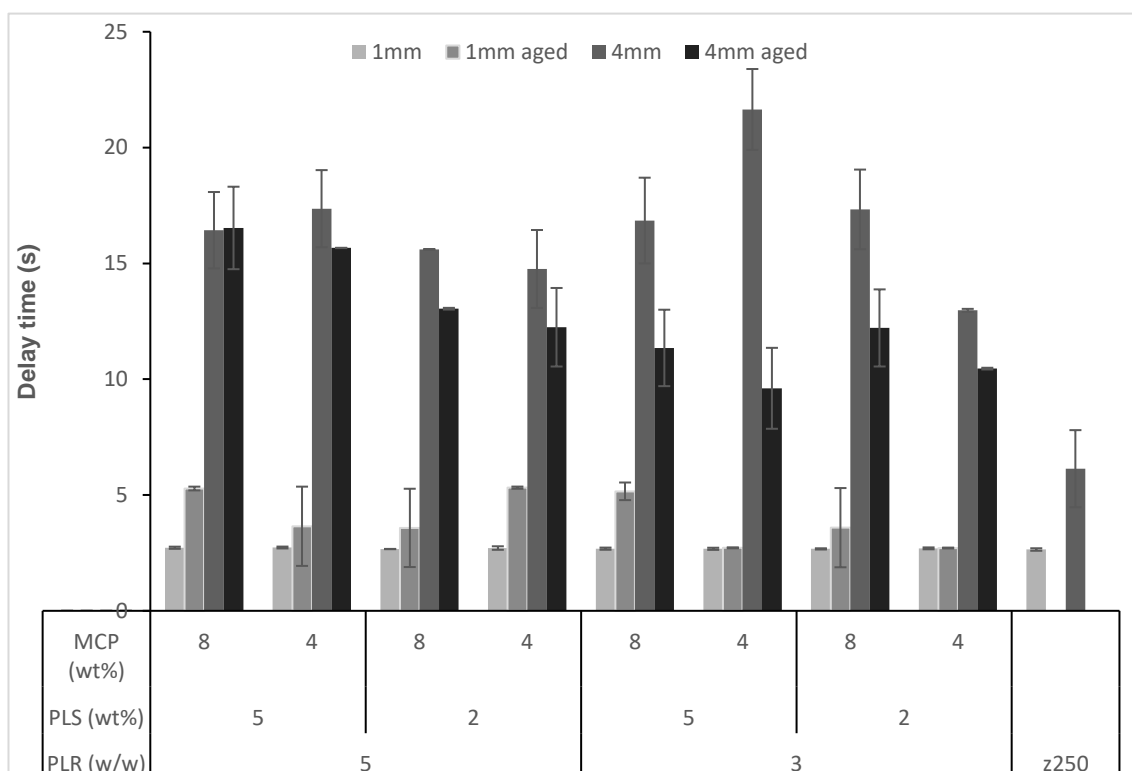*Figure 10-3 Monomer conversion of all experimental formulations (1mm and 4mm, aged at 60°C for 6 months or non-aged). Samples were light-cured for 40s at room temperature (24°C). Error bars are 95% CI (n=3)*
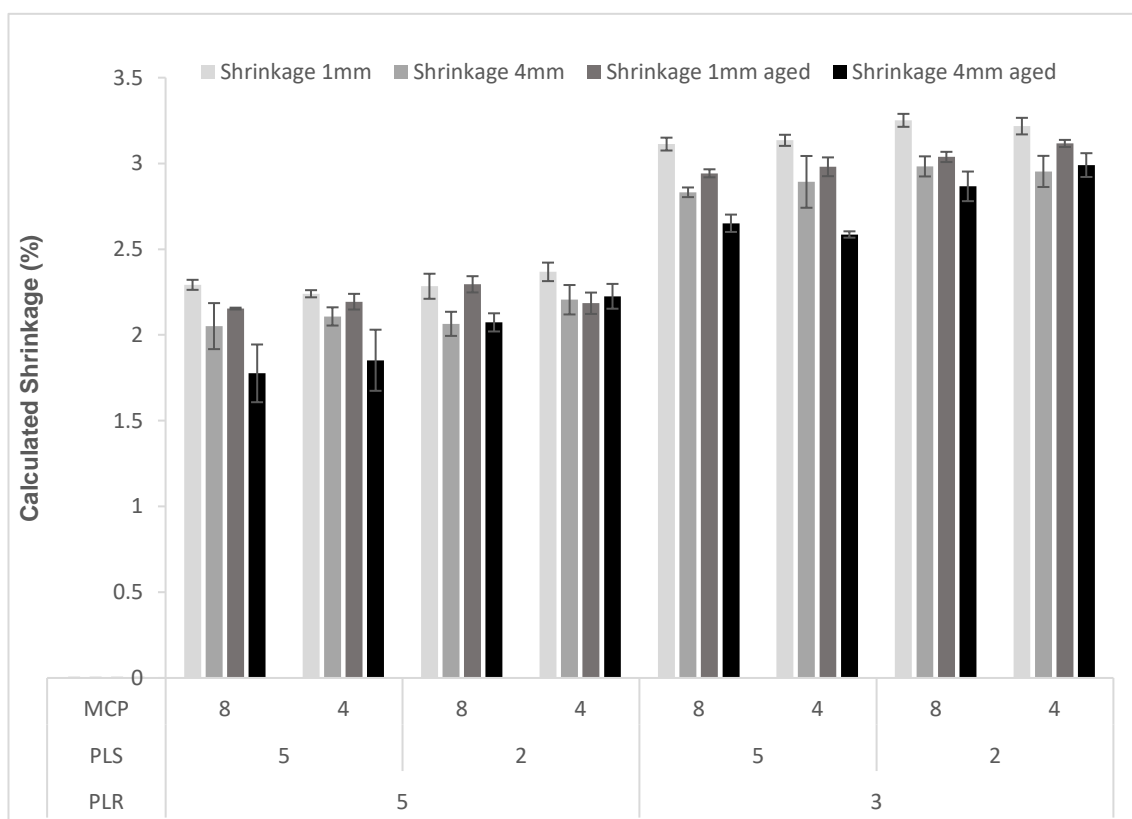
Figure 10-4 Calculated shrinkage of all experimental formulations (1mm and 4mm, aged at 60°C for 6 months or non-aged). Samples were light-cured for 40s at room temperature (24°C). Error bars are 95% CI (n=3)

11 Appendix B

## Interaction of the cured discs with water
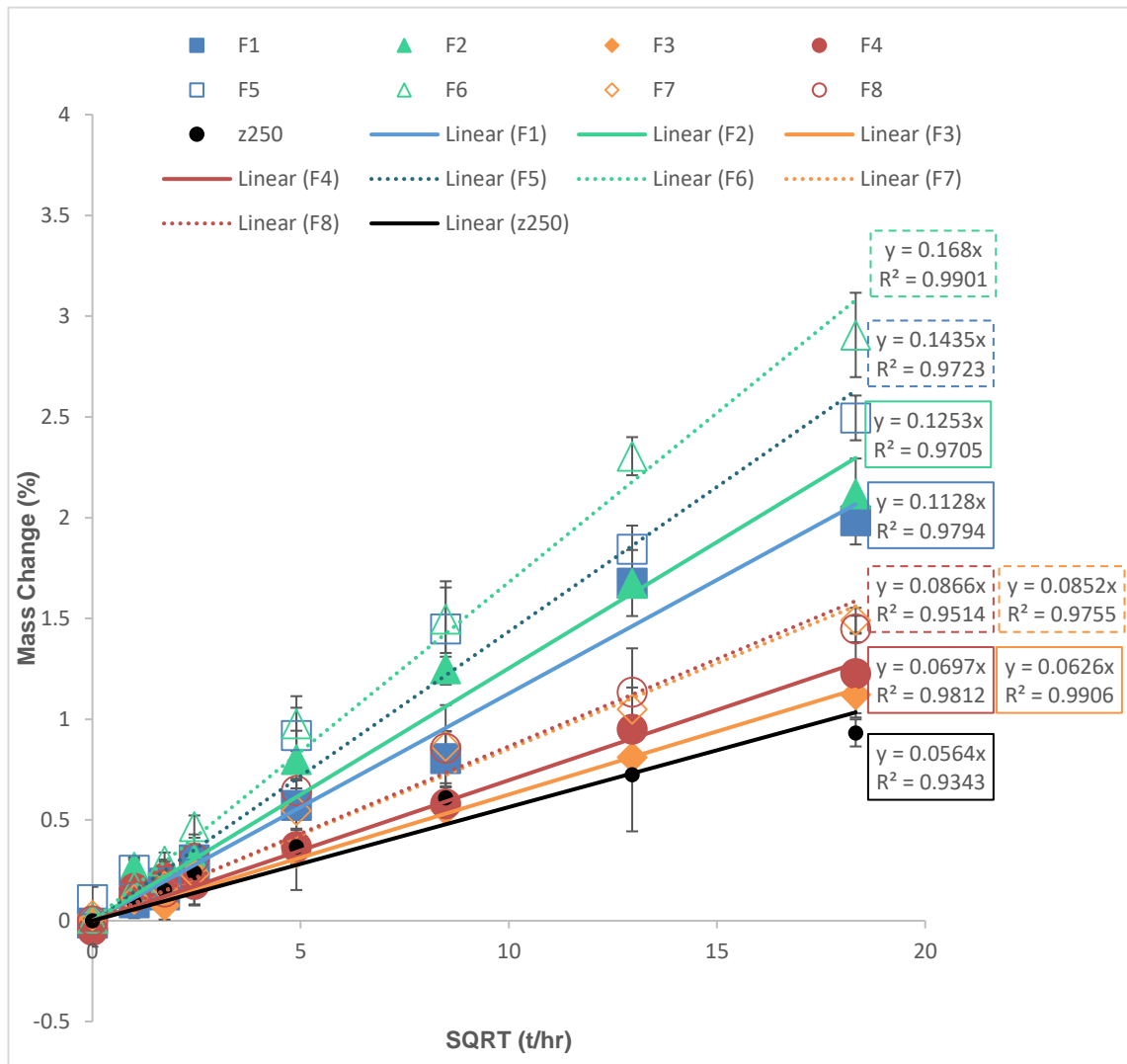
Figure 11-1 Mass change (%) versus SQRT of time for all experimental composites compared to z250. *Solid fill marker is high PLR, Blue/Green is high PLS, Square/Diamond high MCP. Linear trend lines are fitted on data up to two weeks (when mass started to level off). Error bars are 95% CI (n=3)*
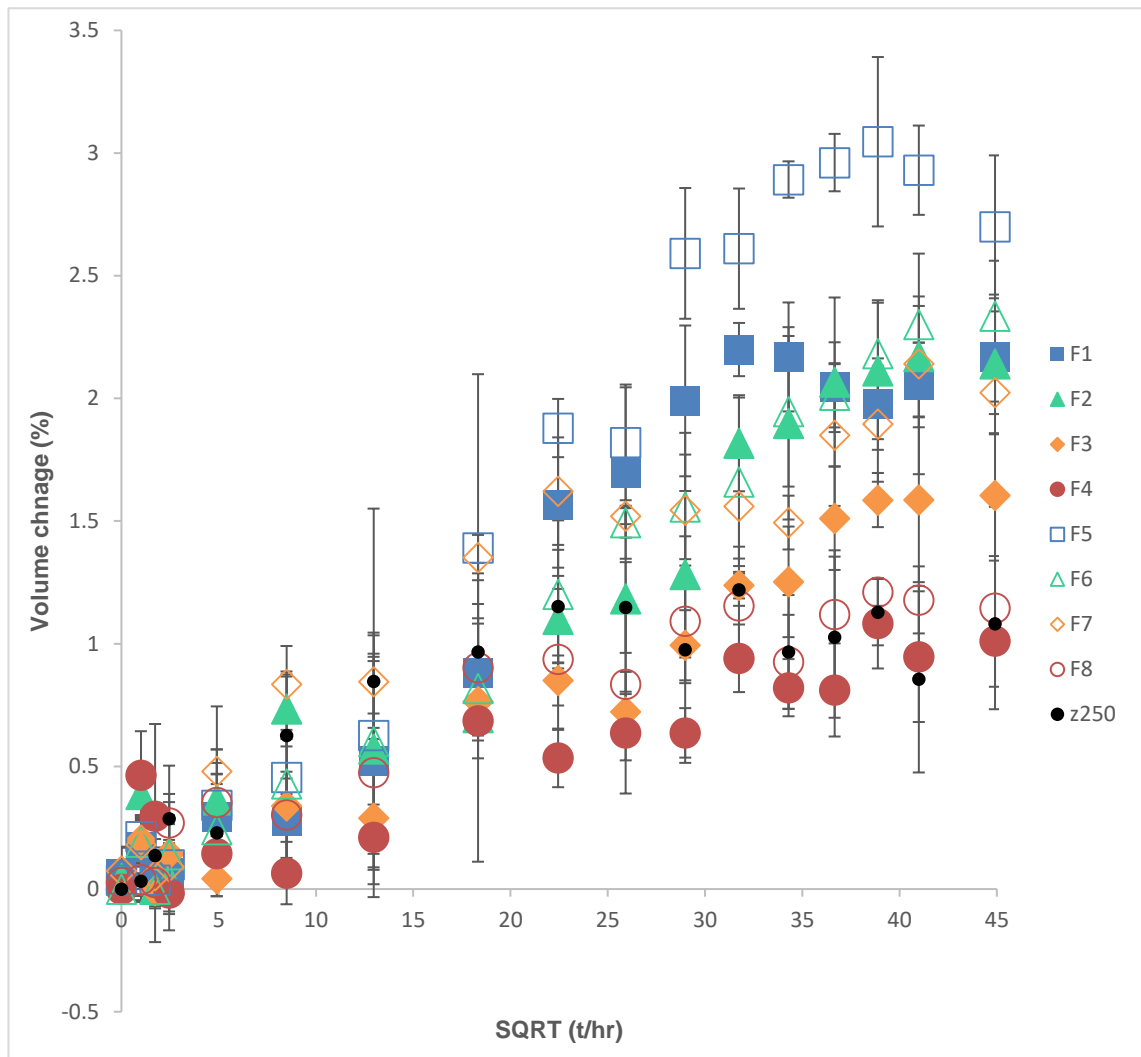
Figure 11-2 Volume change (%) versus SQRT of time for all experimental composites compared to z250.Solid fill marker is high PLR, Blue/Green is high PLS, Square/Diamond high MCP. Error bars are 95% CI (n=3)

12 Appendix C

Mechanical properties
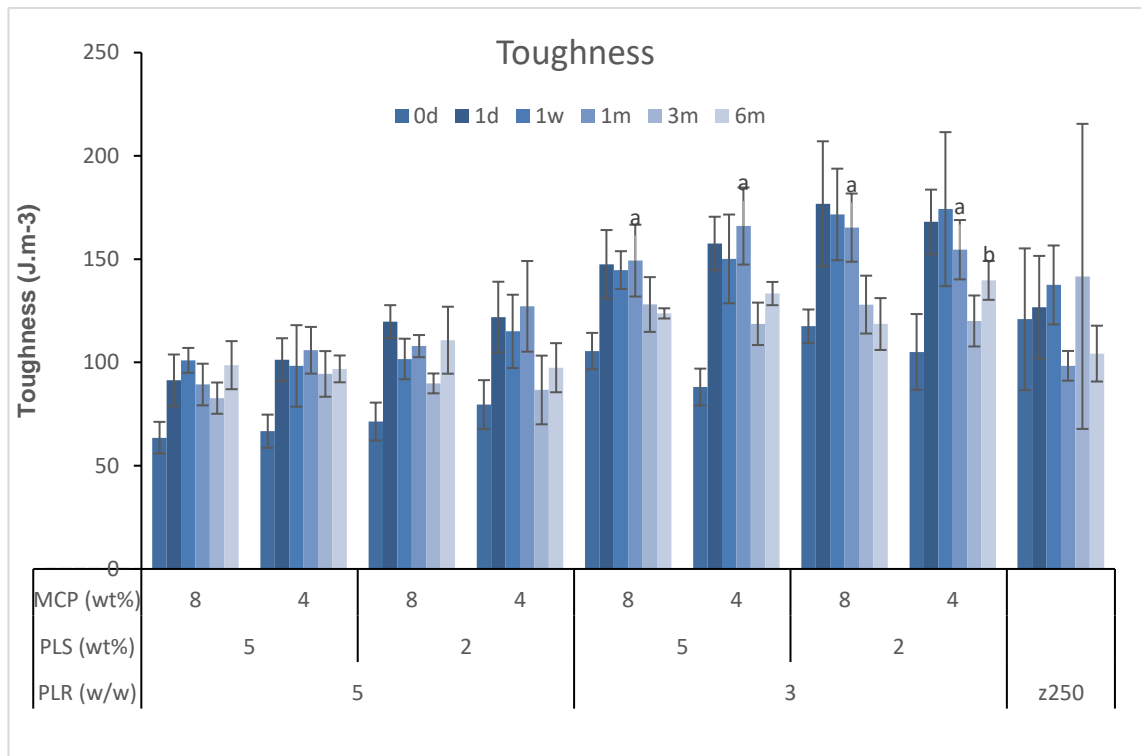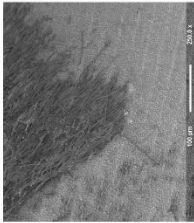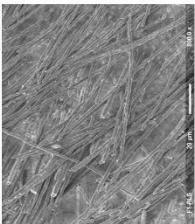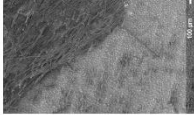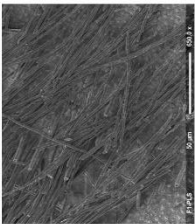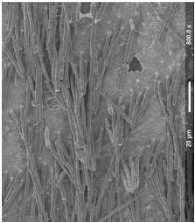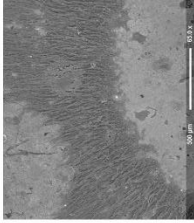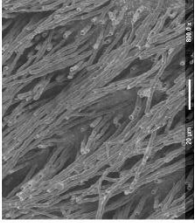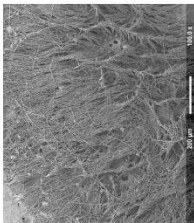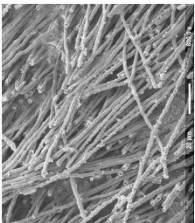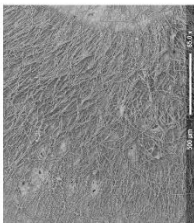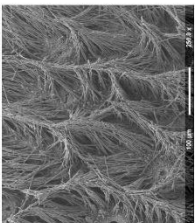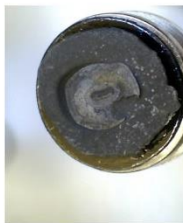
Figure 12-1 Toughness of all formulations in comparison to z250 at different times after incubating in water at 37°C. Crosshead speed was 1 mm/min. Groups carrying letters are significantly different from the control within the same time point. Error bars are 95% CI (n=8)

13 Appendix D

	F1	F1 without MCP	F1 without PLS
SEM			
Coated sample & Binary image			

208

F5 without PLS

F5 without MCP
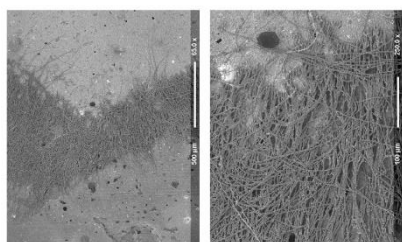
F5

SEM
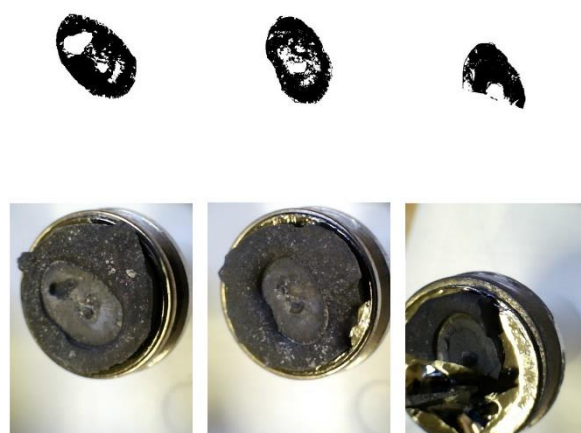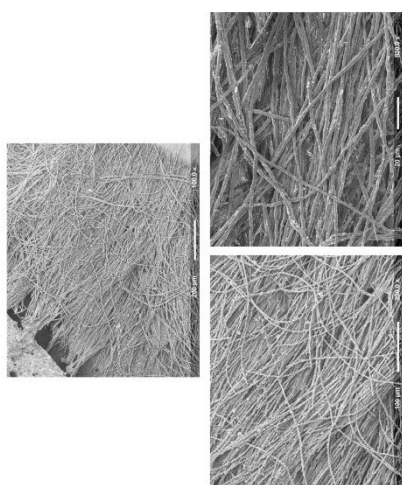
Coated sample

&

Binary image

F4
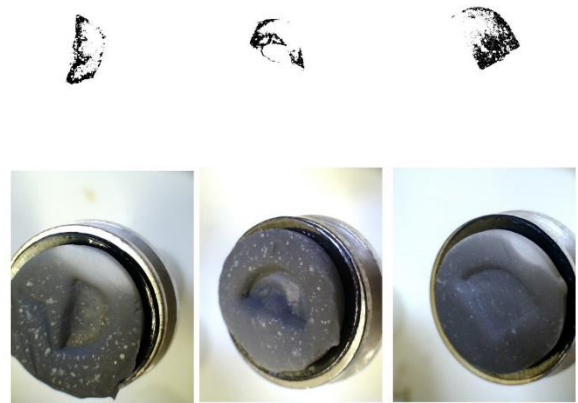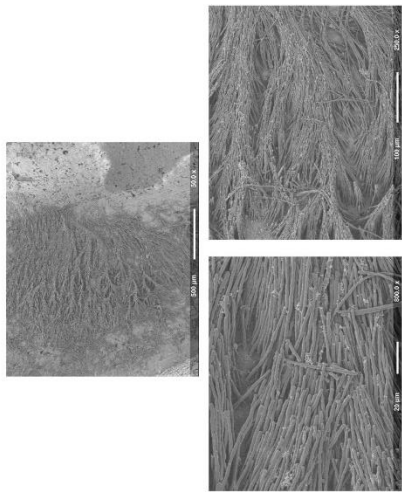
F3
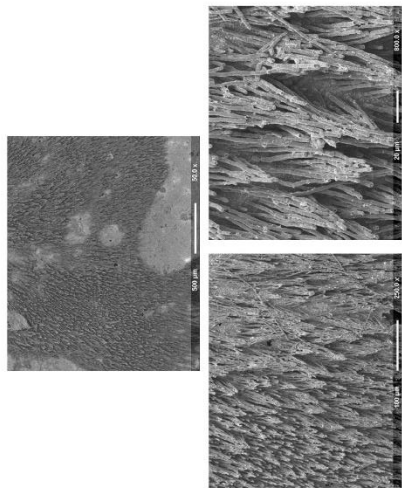
F2

SEM

Coated
sample

&

Binary
image

F8

F7

F6

SEM
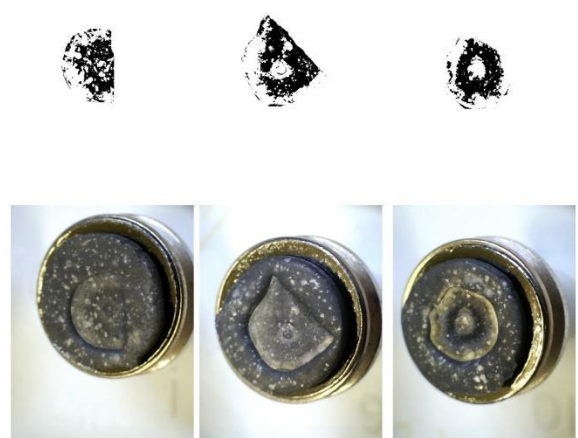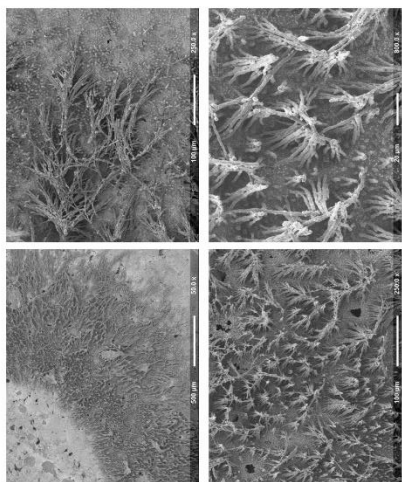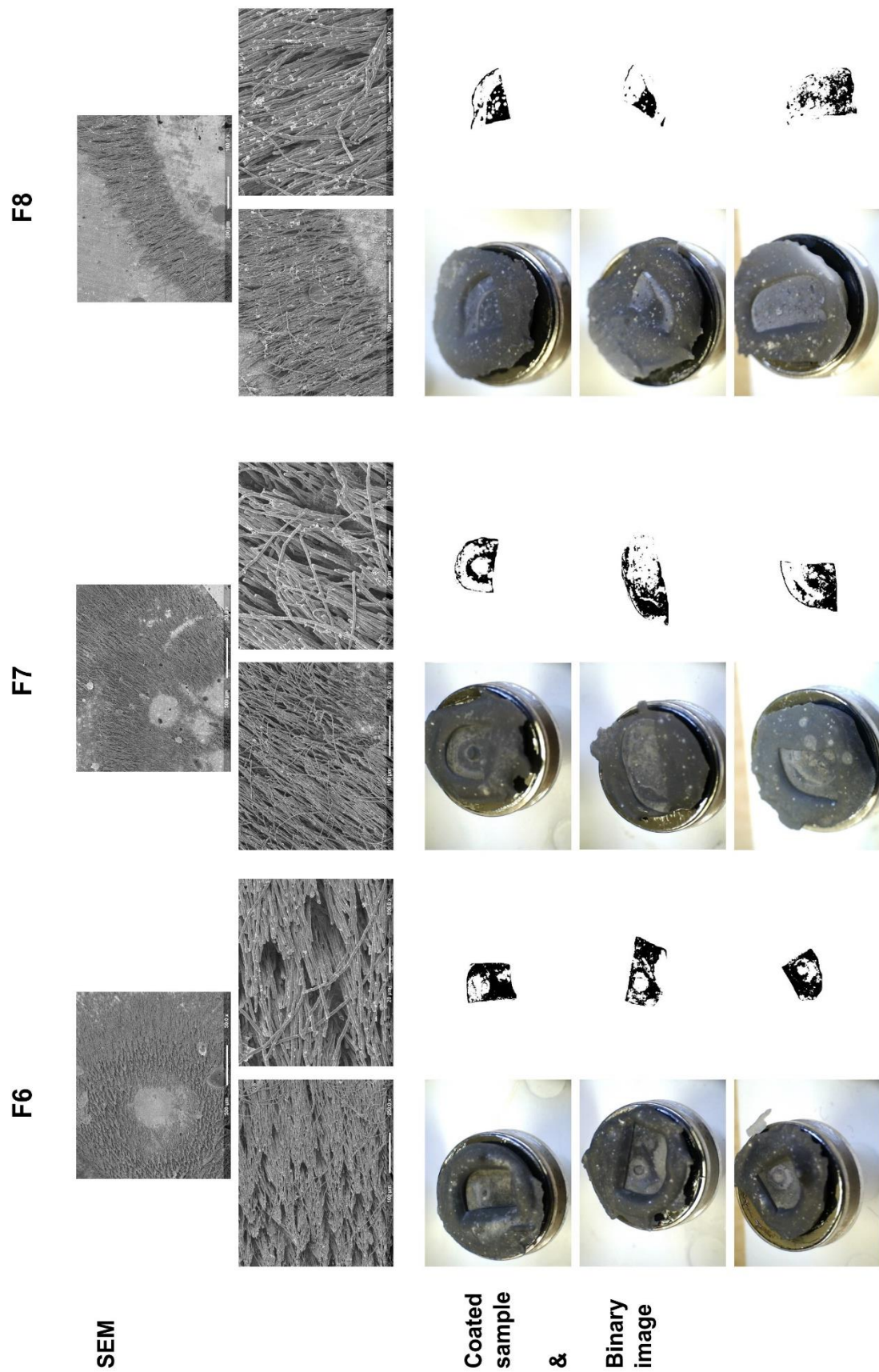
Coated
sample

&

Binary
image

Activa
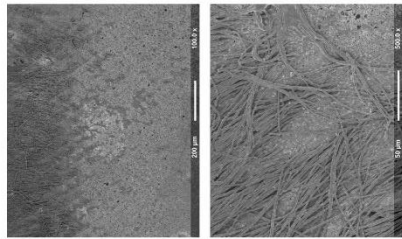
z250 and bond
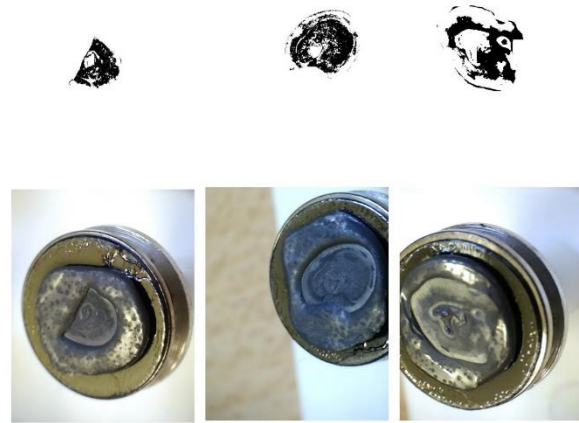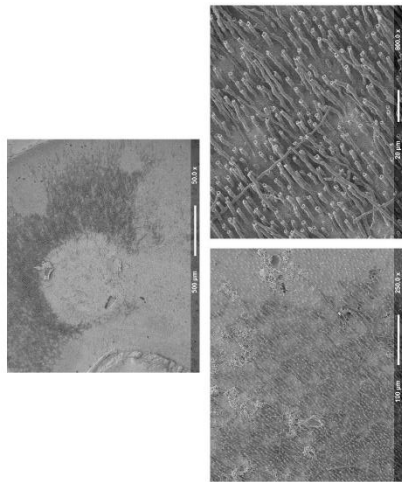
F10
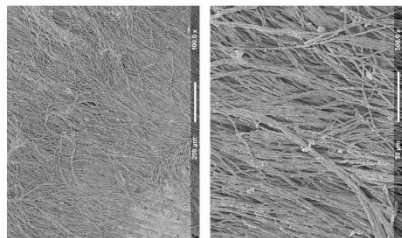
F9

SEM

Coated
sample

&

Binary
image

212
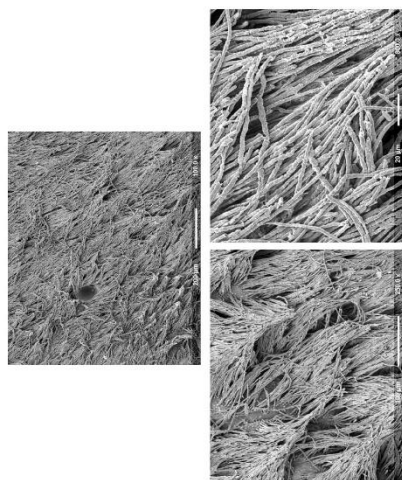
14 Appendix E

Biocompatibility and antibacterial effect

As reported by Dr Caitriona O`Rourke:

"Human dental pulp stem cells (hDPSCs) and human gingival fibroblasts (HGF1) were used to assess biocompatibility. Composite discs were incubated in cell culture medium for 24 hours under standard conditions (37°C, 95% air, 5% $CO2$ 95% relative humidity). hDPSCs were seeded at a density of 30,000 cells/cm^2 in a 96 well plate. After 24 hours, cell culture medium was replaced with medium in which the composite had been immersed and cells incubated for a further 24 hours. CellTiter 96® AQ_{ueous} One Solution Cell Proliferation Assay was used to determine cell viability. 20µl CellTiter was added to each well containing cells immersed in 100µl of culture medium. Following 90 minutes incubation under standard conditions, absorbance was measured at 490nm using Infinite M200 plate reader (Tecan, Männedorf, Switzerland). In all cases, a control that incorporated cells cultured on standard tissue culture plastic ware was included."
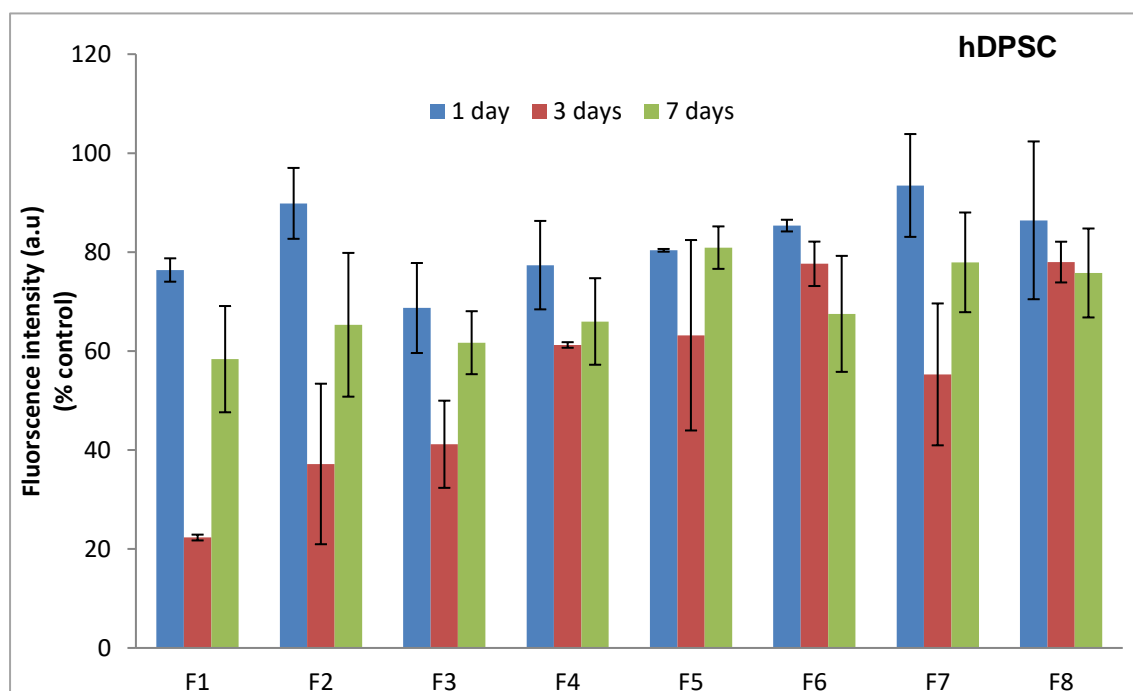
Figure 14-1 Biocompatibility test results of all formulations using human dental pulp stem cells hDPSC as fluorescence intensity percentage of control. Error bars are 95% CI (n=3). Data kindly provided by Dr Caitriona O`Rourke.
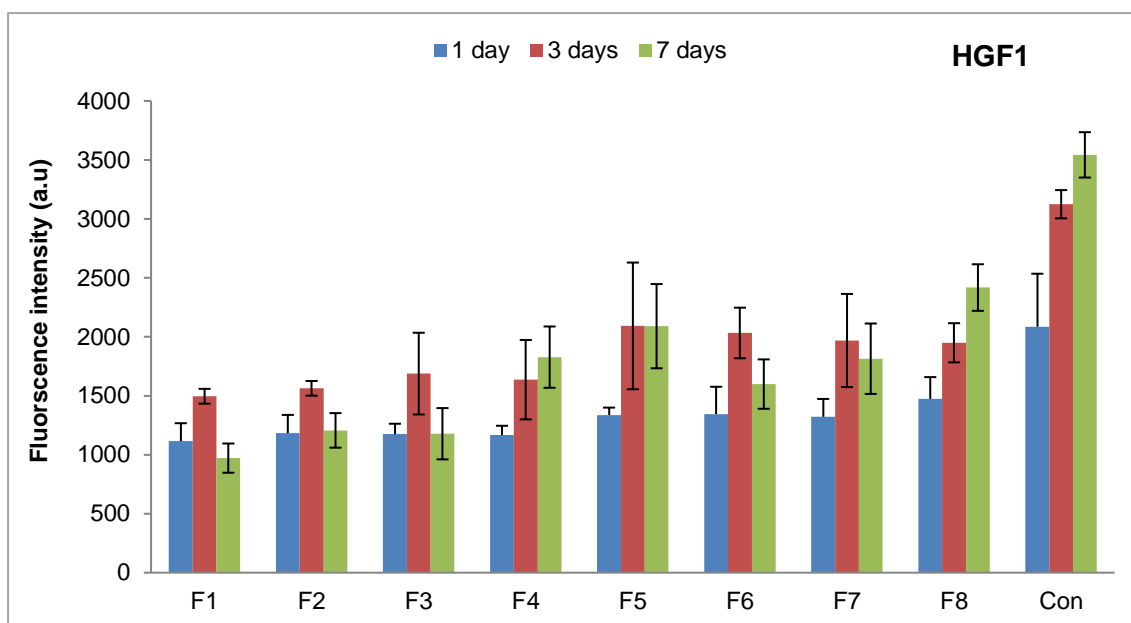
Figure 14-2 Biocompatibility test results of all formulations using human gingival fibroblasts HGF1 as fluorescence intensity in comparison to control. Error bars are 95% CI (n=3). Data kindly provided by Dr Caitriona O`Rourke.

As reported by Dr Adam Day:

"*Streptococcus mutans* (*S.mutans*, UA159) was sub cultured on brain heart infusion (BHI) agar plates (Oxoid, Basingstoke, UK) and incubated overnight at 37°C in an aerobic environment supplemented with 5% CO_2. One colony of *S.mutans* was inoculated in 10mL of sterile BHI broth and incubated overnight at 37°C in an aerobic environment supplemented with 5% CO_2. The overnight broth culture was diluted to an optical density at 600nm (OD_{600}) between 0.4 to 0.5 to give a concentration of ~1×10^9 CFU/mL. Each broth was serially diluted, and 50µl was plated on half a BHI agar plate and incubated for 2-4 days to allow colony forming units (CFU) to grow. After this time, colony counts were conducted by eye. Plates that were not countable by eye due to being too confluent (high density of colonies) were counted by photographing the plates and importing each image to ImageJ (image analysis software package) and counted using the multipoint counting tool. Colony counts were converted to colony-forming units per mL (CFU/mL). Inoculums of ~1×10^9 CFU/mL were further diluted 1:100 with sterile BHI broth. 1mL of this inoculum was added to each well of a 24 well plate containing the test discs (F1-F8), discs without PLS and without PLS or MCP (control discs), Z250 (commercial control), and wells without discs (inoculum only – positive controls) and left in an air incubator at 37 °C on a shaker (setting 2) for 24 hours. The initial inoculum was serially diluted, and the CFU/mL was determined as previously described. Following 24 hours, 50µL was removed from each well, serially diluted, plated on half an agar BHI plate and counted as previously described.

After 24 hours the inoculum, F3, F7, F8, control discs (without PLS or PLS and MCP), and commercial control discs had all increased by 2xlog$_{10}$. All discs containing 5% PLS and F4 containing 2% PLS were effective at inhibiting *S. mutans* growth after 24 hrs.
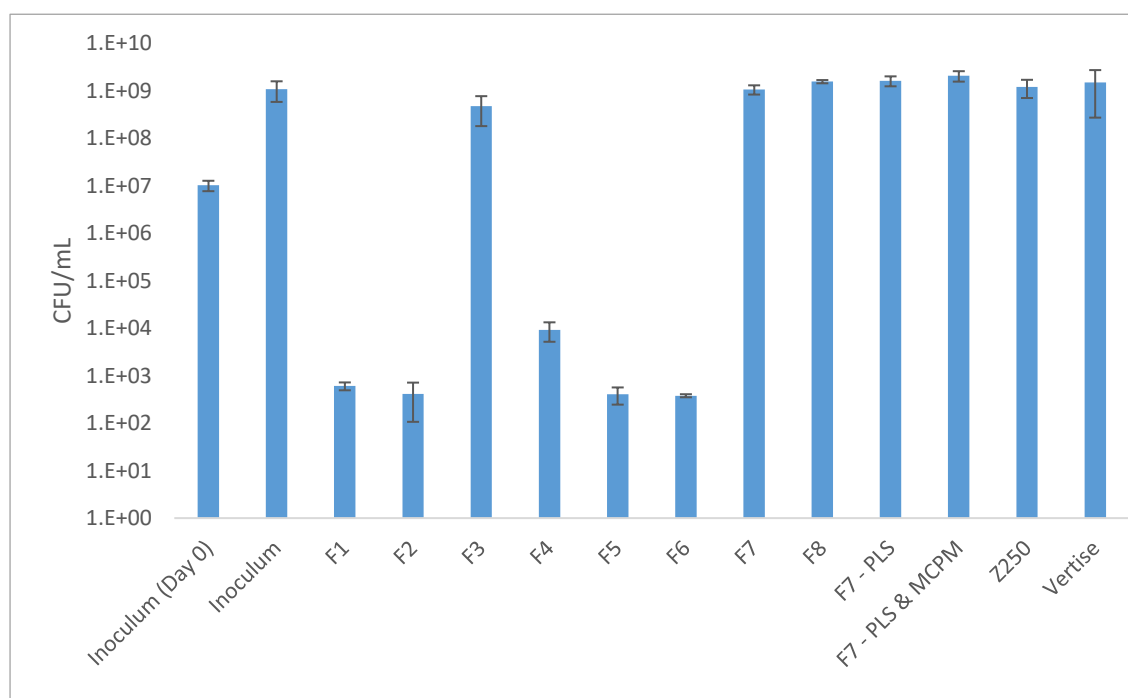
Figure 14-3 Antibacterial test results of all formulations in comparison to initial inoculum, commercial comparator or negative control of adjusted formulations (by taking out PLS or MCP). The bacteria used was S.mutans. Error bars are 95% CI (n=3). Data kindly provided by Dr Adam Day.

The experiment was conducted again following the same protocol but using an initial inoculum of ~1x10^6 or 1x10^8 CFU/mL to determine whether discs containing 2% PLS or 5% PLS, respectively, were effective at inhibiting *S. mutans* growth at this concentration.

It was found that all 2% PLS discs were effective at inhibiting *S. mutans* growth (10^6 CFU/mL) after 24 hrs. Inoculum, disc, and commercial controls all increased by 3xlog$_{10}$. At an initial inoculum concentration of 1x10^8 CFU/mL growth was not inhibited by any discs even those containing 5% PLS."

15 Appendix F

Comparison between compule tips ('black', 'move', 'needle')

EDI, 12th January 2018

Compule tip 'needle' (Figure 15-1, a)
Compule tip 'black' (Figure 15-1, b)
Compule tip 'move' (Figure 15-1, c)
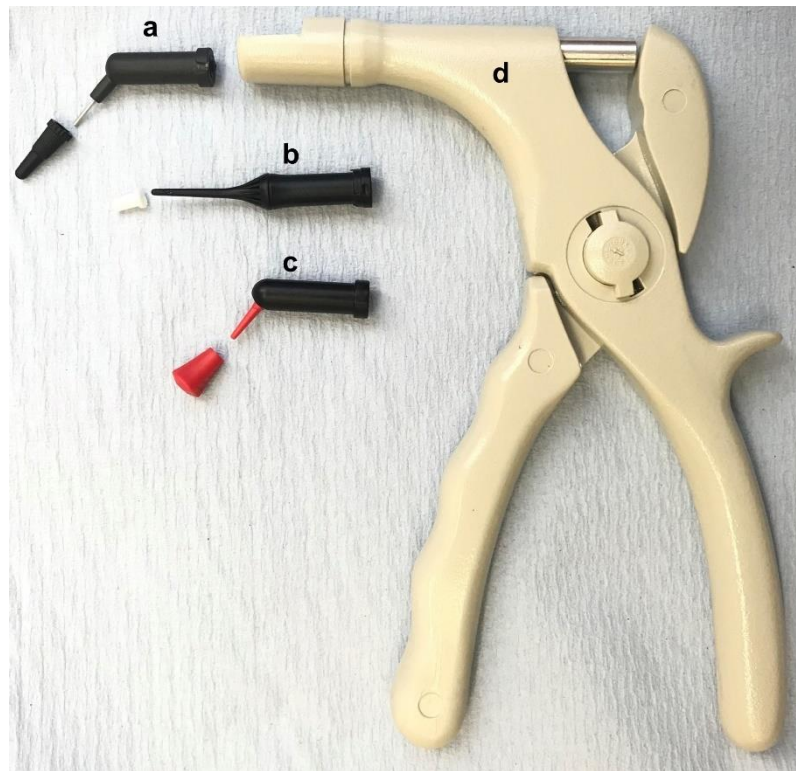
Figure 15-1 The three different packaging compules compared by the clinicians. (a) is the compule with the needle tip, (b) is the compule with the straight black tip and (c) is the compule with a red plastic tip that can be adjustable. d is the application gun.

Three tips were assessed by five dentists, Paul Ashley (Paediatric dentist and trial investigator), Nabih Alkhouri (PhD student and dentist) , Yucef Esmaoi (MSc student and Restorative dentist), Aspasia Katsimpali (DDent student and Paediatric Dentist), Zoi Tzelepi (DDent student and Paediatric Dentist) and Mohsin Chaudhury (Paediatric dentist with no connection to the project).

Tips were assessed by ejecting composite onto a paper pad. Dentists were asked for verbal feedback and to rate each tip from a scale of 1-5 where 1 = best and 5 = worst. Dentists were asked just to comment on the compule tip, not the handling properties of the composite.

Results

Score: 1, 2, 3, 4, 5 (1: excellent 5: worst)	P.A	N.A	Y.E	A.K	Z.T	M.C
Black tip compules	Score: 3	Score: 2 The nozzle width of both 'Black' and 'Needle' was small, this could incorporate more bubbles into the filling	Score: 2	Score: 2 Better than the needle capsule, run smoothly, still needs some pressure, may need a big mouth opening, because it is long due to the long tip and lots of material is wasted.	Score: 2 Material runs smoothly, but still takes longer to place it.	Score: 4 No flexibility of the tip
Move tip compules	Score: 1 Gives greater flexibility for material placement particularly on posterior teeth	Score: 1	Score: 3	Score: 1 Excellent handling, easy, no pressure, run smoothly, is thin enough for small cavities without looking scary.	Score: 1 Best performance, material running easily, tip is thin enough so the quantity of material can be well controlled.	Score: 3 Good for hard to reach areas
Needle tip compules	Score: 5 Could cause a needlestick? Looks frightening	Score: 2	Score: 4	Score: 4 Needs a lot of pressure. Look scary for children. Too thin so it takes time to fill with.	Score: 4 Needs a lot of pressure for the material to come through, takes longer to place it in the cavity.	Score: 2

Conclusion

The 'move' tip (c) was the most preferred by assessors.

………………………….………… ………………………………

……………………………….

Paul Ashley   Nabih Alkhouri

Figure 15-2 The selected packaging compule preferred by the clinicians with an adjustable angulation of the tip.

16 Appendix G

Matrix Metalloproteinase (MMP) activity at the interface between naturally carious dentine and different restorative materials

CLSM images of the interface (carious dentine/ restoration) are shown in Figure 16-1. The high green fluorescence at the interface indicates MMP activity. The interface was scanned at day 1 and day 14. These images were quantified using ImageJ software by calculating the average percentage of green area to the whole scan.
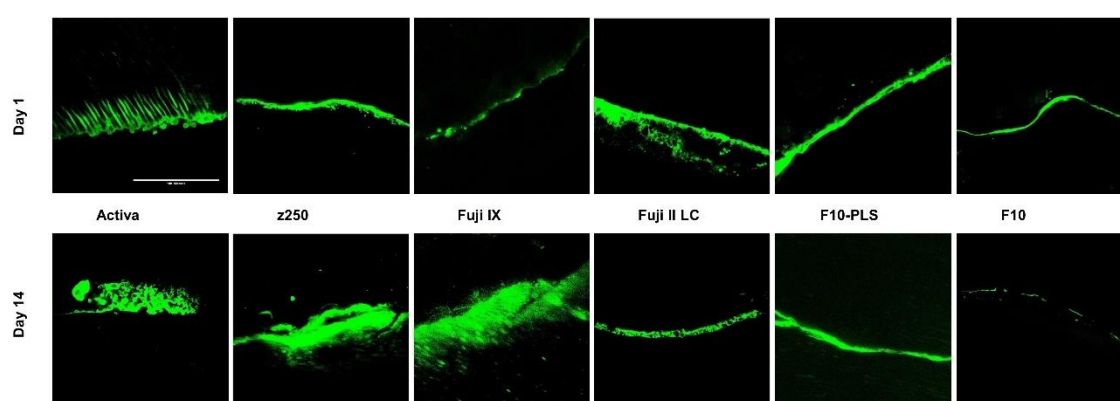
Figure 16-1 CLSM images of MMP activity(in green) after 1 day and 14 days at the adhesion interface of Activa, z250, Fuji IX, Fuji II LC, F10 without PLS and F10 with carious dentine as a substrate. Field width is 200 microns, scale bar is 100 microns, n=1

Quantitative data of the scans in Figure 16-1 are shown in Figure 16-2. Statistical analysis was not done as n=1. The bar chart shows that F10 had the lowest MMP activity at day 1 and this area decreased to only 0.27% after 14 days. The values were higher when PLS was taken out of the optimised formulation (about 4% average area). Fuji IX and z250 showed a considerable increase in MMP activity after 14 days although initially was comparable to F10. MMP activity went slightly down after 14 days with Activa and Fuji II LC but was still higher than F10.
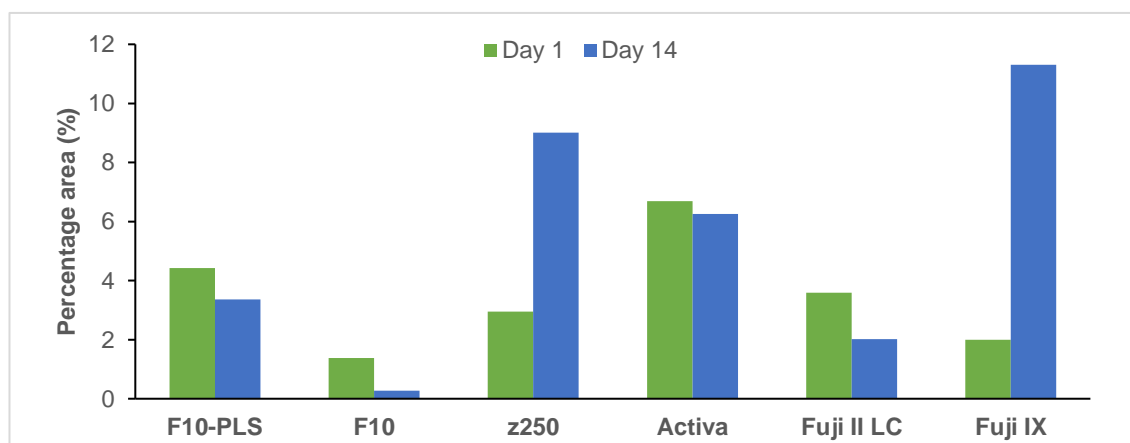
Figure 16-2 MMP activity by area percentage (green fluorescence quantification of CLSM images) using carious dentine as a substrate at 1 day and 14 days. n=1

17 Appendix H

A single site, single arm clinical trial (phase 1): Assessment of Safety

Paul Ashley, Wendy Xia, Nabih Alkhouri, Anne Young

- **Aims and objectives:**

The primary aim of the first phase of clinical trial was to look for adverse effects and evaluate the safety of using F10 to restore primary teeth that were indicated for extraction. These teeth were also used upon extraction to evaluate retention of restorations, placement procedure and resin tags formation within carious dentine.

- **Materials and methods:**

F10 compules (stored at 4ºC) were used for the clinical trial (see Figure 15-2, Appendix F).

Patients were recruited between January and June 2019 (n=7). Each patient had one primary molar (first or second, of ICDAS score 5 or 6) slightly excavated to remove the soft highly infected caries (ART technique). Then it was restored with F10 (by Prof Paul Ashley) in a single-step without the use of etch and bond. The restorations were light-cured for 40s.

All restorations were in the mouth for at least one month during which, adverse events were assessed immediately during placement, at 3 days (telephone call) and at the extraction appointment.

Extracted teeth were collected, cleaned and soaked in 1% Chloramine T for 3 days for disinfection (by Dr Wendy Xia) then stored at 4ºC in water until evaluated in the lab.

Periapical X-rays were obtained using a Planmeca Prox machine (Planmeca Oy, Helsinki, Finland) with the following settings: 70kV and 8mA for 0.1s. Teeth were x-rayed from the buccal side and imaged using a digital camera (Canon EOS 1300D) and a Nikon lens (AF Micro Nikkor, 55mm).

Two teeth were ground down mesiodiastally parallel to the long axis of the tooth from the buccal side using abrasive paper (grit no 220). When the adhesion interface was exposed, Rhodamine b (0.2% in isopropanol) was applied for 2 minutes then gently rinsed. CLSM was consequently used to scan the interface using an oil objective lens

(x60) and the Z motor to scan different levels. Acquired scans were analysed using ImageJ software package.

- **Results and Discussion**

The restorations were placed as an interim solution to restore function of the tooth until extracted. Each patient received one restoration for an occlusal distal cavity (of a first primary molar) or an occlusal mesial cavity (of a second primary molar).

Restoration placement procedure was rapid and simple (single step) following slight excavation without the use of an anaesthetic and hence lessened the duration of the procedure as well as reduced any distress of the child patient.

Adverse effects:

Following immediate evaluation after restoration placement and the evaluation at 3 days and at the extraction appointment, no adverse effects were present. No pain was reported in relation to the restored teeth as well although the pulp condition was not tested in advance.

Protocol violations

All patients were assigned for a planned extraction appointment one month after receiving the restoration. However, patients 3 and 4 had the restorations in place for longer than a month (up to 3 months with patient 3) due to rescheduling their appointments. Patient 6 decided to withdraw from the trial after material placement and did not want the filled tooth to be extracted. This patient is being kept under review during the follow up appointments until tooth exfoliation.

Radiographs and imaging

All restored cavities had a proximal box distally (in first molars) or mesially (in second molar). That was expected as this contact area between the molars is bigger and more difficult to clean in comparison to the one between the first molars and canines for example.

Representative images of the teeth upon extraction and the related X-rays are shown in Figure 17-1. F10 restorations were always detected in cavities. Although X-rays showed good adaptation to cavity walls, there was always a gap at the gingival wall in the proximal box. Additionally, despite the non-retentive cavity shape in some cases, the restoration remained intact until time of extraction which might be explained by good penetration and interlocking with carious dentine. This gap, however, would lead to greater food and bacteria accumulation in a difficult to clean location and resulting in continued progress of the disease.
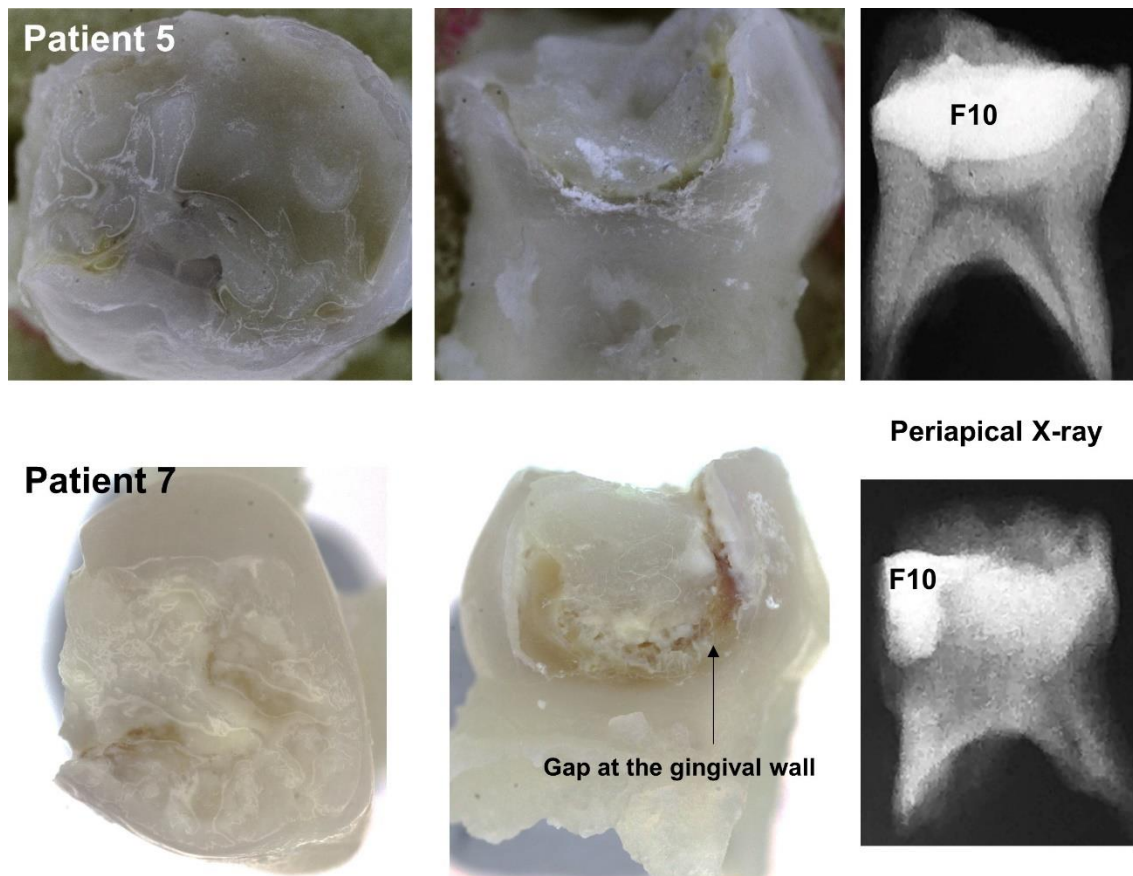
Figure 17-1 Representative light microscopy images of occlusal and proximal surfaces and radiographic images of patients 5 (top row) and patient 7 (lower row). There is good adaptation except at the gingival wall in the proximal box which suggests difficulty in placing or limited accessibility.

Therefore, adjusting the placement method is required, maybe by using a floss, a sectional matrix system or celluloid strips. Squeezing the composite paste starting from the deepest area on the gingival wall while pulling the nozzle upwards would also be beneficial. Method of placement was not optimised prior to the clinical trial for the following reasons; first it was the first time to test how the material acts in clinical scenarios and second the main aim was to evaluate safety only. These observations and amending the application method will be taken into considerations before commencing phase 2 of the clinical trials.

CLSM scans (Figure 17-2) also demonstrated the ability of F10 to penetrate into carious dentine, confirming the results previously obtained in the lab. When collagen structure was totally destructed, F10 also penetrated into gaps but not dentinal tubules since they may have collapsed (patient 2).
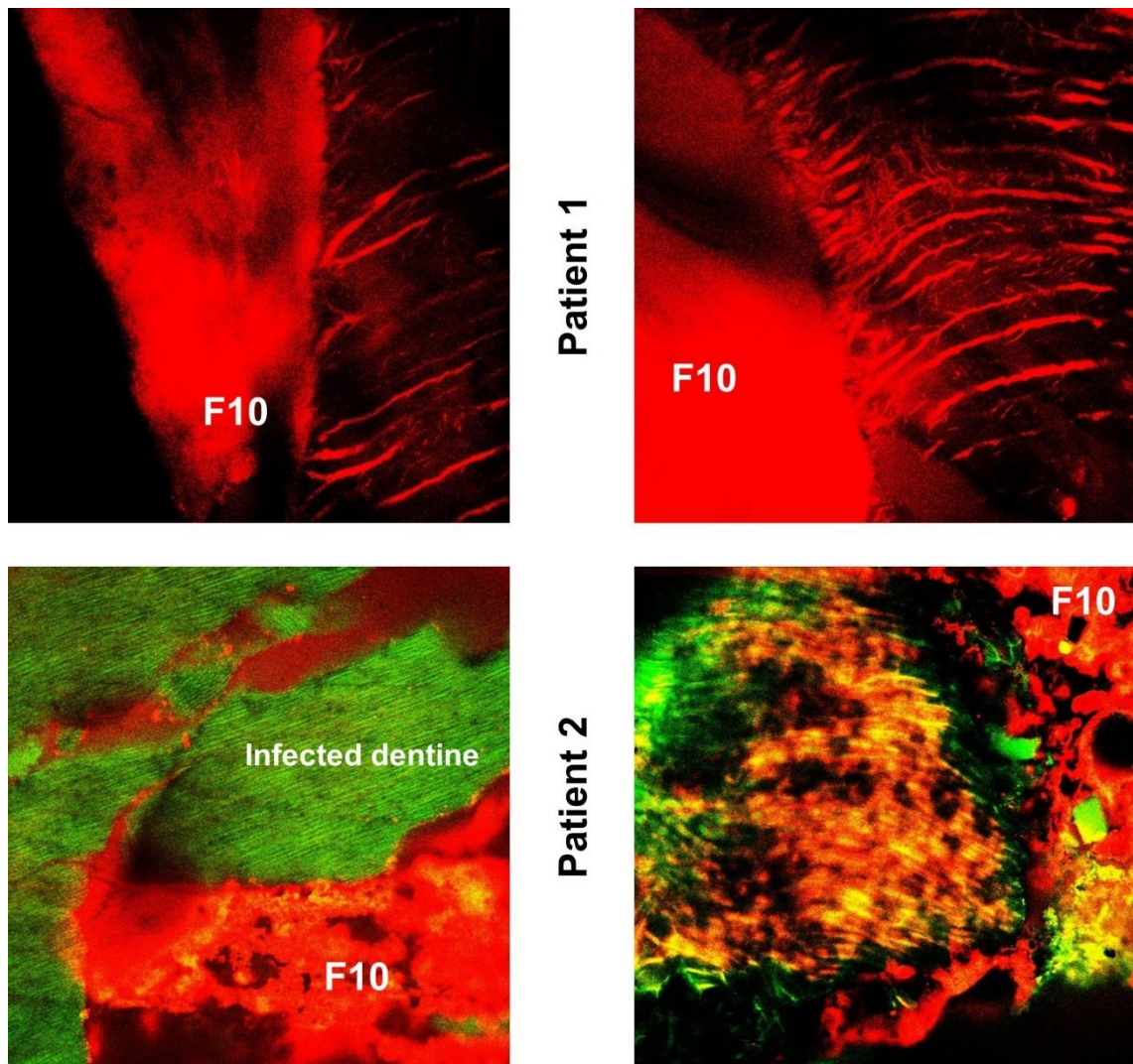
Figure 17-2 CLSM images of the adhesion interface in teeth extracted from patient 1 (top row) and patient 2 (bottom row). F10 formed resin tags when the collagen structure was somehow less destructed (patient 1) but also interlocked with badly carious dentine (patient 2)

Although F10 was optimised to be used in smaller cavities, where caries has not reached the pulp, selecting grossly carious teeth to be included in this trial was justified by the need to recruit teeth that were indicated for extraction anyway. This enabled lab investigations and acquiring more results from a small sample number.

- **Conclusions**

F10 was proven to:

- be fully safe to be used to treat children teeth using ART technique,
- have no significant or severe adverse effects,
- remain stable in the cavity even in cases where the tooth was underfilled,
- be able to penetrate into carious dentine and form resin tags.

The trial also showed the need to optimise the placement procedure to avoid gaps at the gingival wall in Class II cavities.

Bibliography

Abou Neel E. A., Aljabo A., Strange A., Ibrahim S., Coathup M., Young A. M., Bozec L. & Mudera V. 2016. Demineralization-remineralization dynamics in teeth and bone. *International journal of nanomedicine,* 11**,** 4743-4763.

Adiga S., Ataide I. & Fernades M. 2013. Comparative evaluation of etch pattern, the length of resin tags, and shear bond strength of all-in-one adhesive system on intact enamel with and without phosphoric acid pre-etching: An <i>in vitro</i> investigation. 4(3)**,** 106-113.

Aljabo A., Abou Neel E. A., Knowles J. C. & Young A. M. 2016a. Development of dental composites with reactive fillers that promote precipitation of antibacterial-hydroxyapatite layers. *Materials science & engineering. C, Materials for biological applications,* 60**,** 285-292.

Aljabo A., Abou Neel E. A., Knowles J. C. & Young A. M. 2016b. Development of dental composites with reactive fillers that promote precipitation of antibacterial-hydroxyapatite layers. *Materials science & engineering. C, Materials for biological applications,* 60**,** 285-92.

Aljabo A., Xia W., Liaqat S., Khan M. A., Knowles J. C., Ashley P. & Young A. M. 2015. Conversion, shrinkage, water sorption, flexural strength and modulus of re-mineralizing dental composites. *Dental materials : official publication of the Academy of Dental Materials,* 31(11)**,** 1279-89.

Almahdy A., Koller G., Festy F., Bartsch J. W., Watson T. F. & Banerjee A. 2015. An MMP-inhibitor modified adhesive primer enhances bond durability to carious dentin. *Dental materials : official publication of the Academy of Dental Materials,* 31(5)**,** 594-602.

Almahdy A., Koller G., Sauro S., Bartsch J. W., Sherriff M., Watson T. F. & Banerjee A. 2012. Effects of MMP inhibitors incorporated within dental adhesives. *Journal of dental research,* 91(6)**,** 605-11.

Alomari Q., Ajlouni R. & Omar R. 2007. Managing the polymerization shrinkage of resin composite restorations: a review. *SADJ : journal of the South African Dental Association = tydskrif van die Suid-Afrikaanse Tandheelkundige Vereniging,* 62(1)**,** 12, 14, 16 passim.

Alshaafi M. M. 2017. Factors affecting polymerization of resin-based composites: A literature review. *The Saudi dental journal,* 29(2)**,** 48-58.

Anderson M. H., Loesche W. J. & Charbeneau G. T. 1985. Bacteriologic study of a basic fuchsin caries-disclosing dye. *The Journal of prosthetic dentistry,* 54(1)**,** 51-5.

Angker L., Nockolds C., Swain M. V. & Kilpatrick N. 2004. Correlating the mechanical properties to the mineral content of carious dentine--a comparative study using an ultra-micro indentation system (UMIS) and SEM-BSE signals. *Archives of oral biology,* 49(5)**,** 369-78.

Anil S. & Anand P. S. 2017. Early Childhood Caries: Prevalence, Risk Factors, and Prevention. *Frontiers in pediatrics,* 5**,** 157.

Apolonio F. M., Mazzoni A., Angeloni V., Scaffa P. M., Santi S., Saboia V. P., Tay F. R., Pashley D. H. & Breschi L. 2017. Effect of a one-step self-etch adhesive on endogenous dentin matrix metalloproteinases. *European journal of oral sciences,* 125(2)**,** 168-172.

Arends J., Dijkman G. E. H. M. & Dijkman A. G. 1995. Review of Fluoride Release and Secondary Caries Reduction by Fluoridating Composites. 9(4)**,** 367-376.

Arrais C. A. & Giannini M. 2002. Morphology and thickness of the diffusion of resin through demineralized or unconditioned dentinal matrix. *Pesquisa odontologica brasileira = Brazilian oral research,* 16(2)**,** 115-20.

Asmussen E. & Peutzfeldt A. 2002. Long-term fluoride release from a glass ionomer cement, a compomer, and from experimental resin composites. 60(2)**,** 93-97.

Association L. G. 2016. Tackling poor oral health in children: local government's public health role. UK.

Astm 2016. Standard Guide for Accelerated Aging of Sterile Barrier Systems for Medical Devices. *ASTM F1980-16.* West Conshohocken, PA: ASTM International.

Atmeh A. R., Chong E. Z., Richard G., Boyde A., Festy F. & Watson T. F. 2015. Calcium silicate cement-induced remineralisation of totally demineralised dentine in comparison with glass ionomer cement: tetracycline labelling and two-photon fluorescence microscopy. *Journal of microscopy,* 257(2)**,** 151-60.

Attar N. & Önen A. 2002. Fluoride release and uptake characteristics of aesthetic restorative materials. 29(8)**,** 791-798.

Baldassarri M., Margolis H. C. & Beniash E. 2008. Compositional determinants of mechanical properties of enamel. *Journal of dental research,* 87(7)**,** 645-9.

Banerjee A., Cook R., Kellow S., Shah K., Festy F., Sherriff M. & Watson T. 2010. A confocal micro-endoscopic investigation of the relationship between the microhardness of carious dentine and its autofluorescence. *European journal of oral sciences,* 118(1)**,** 75-9.

Banerjee A., Gilmour A., Kidd E. & Watson T. 2004. Relationship between S. mutans and the autofluorescence of carious dentin. *American journal of dentistry,* 17(4)**,** 233-6.

Banerjee A., Sherriff M., Kidd E. A. & Watson T. F. 1999. A confocal microscopic study relating the autofluorescence of carious dentine to its microhardness. *British dental journal,* 187(4)**,** 206-10.

Baratieri L. N. & Ritter A. V. 2001. Four-year clinical evaluation of posterior resin-based composite restorations placed using the total-etch technique. *Journal of esthetic and restorative dentistry : official publication of the American Academy of Esthetic Dentistry ... [et al.],* 13(1)**,** 50-7.

Baweja P., Hemamalathi S., Velmurugan N. & Kandaswamy D. 2007. A confocal microscopic evaluation of the hybrid layer and resin tag formation of a total etch technique in comparison with self etching primers with three different pH. 10(3)**,** 104-111.

Bertassoni L. E. 2017. Dentin on the nanoscale: Hierarchical organization, mechanical behavior and bioinspired engineering. *Dental materials : official publication of the Academy of Dental Materials,* 33(6)**,** 637-649.

Besinis A., Van Noort R. & Martin N. 2014. Remineralization potential of fully demineralized dentin infiltrated with silica and hydroxyapatite nanoparticles. *Dental materials : official publication of the Academy of Dental Materials,* 30(3)**,** 249-62.

Bleicher F., Richard B., Thivichon-Prince B., Farges J.-C. & Carrouel F. 2015. Chapter 30 - Odontoblasts and Dentin Formation. *In:* Vishwakarma, A., Sharpe, P., Shi, S. & Ramalingam, M. (eds.) *Stem Cell Biology and Tissue Engineering in Dental Sciences.* Boston: Academic Press, 379-395.

Boushell L. W., Nagaoka H., Nagaoka H. & Yamauchi M. 2011. Increased matrix metalloproteinase-2 and bone sialoprotein response to human coronal caries. *Caries research,* 45(5)**,** 453-9.

Braga R. R. & Ferracane J. L. 2004. Alternatives in polymerization contraction stress management. *Critical reviews in oral biology and medicine : an official publication of the American Association of Oral Biologists,* 15(3)**,** 176-84.

Brignardello-Petersen R. 2017. Untreated dental caries associated with small worsening of oral health-related quality of life in 1- to 3-year-old children. *Journal of the American Dental Association (1939),* 148(9)**,** e130.

Bsi 2009. Polymer-based restorative materials. *BS EN ISO 4049:2009* British Standard Institution.

Bsi 2013a. Adhesion- Notch-edge shear bond strength. *BS EN ISO 29022:2013.* British Standard Institution.

Bsi 2013b. Polymerization shrinkage: Method for determination of polymerization shrinkage of polymer-based restorative materials. *BS EN ISO 17304:2013.* British Standard Institution.

Bsi 2014a. Implants for surgery- In vitro evaluation for apatite-forming ability of implant materials. *BS ISO 23317:2014.* British Standard Institution.

Bsi 2014b. Test method for determining radio-opacity of materials. *BS EN ISO 13116:2014.* British Standard Institution.

Bsi 2015. Testing of adhesion to tooth structure. *PD ISO/TS 11405:2015.* British Standard Institution.

Bsi 2017. Packaging for terminally sterilized medical devices. Requirements for materials, sterile barrier systems and packaging systems. *BS EN ISO 11607-1:2017.* British Standards Institution.

Buyuk S. K. & Kucukekenci A. S. 2018. Effects of different etching methods and bonding procedures on shear bond strength of orthodontic metal brackets applied to different CAD/CAM ceramic materials. *The Angle orthodontist,* 88(2)**,** 221-226.

Buzalaf M. A., Hannas A. R., Magalhaes A. C., Rios D., Honorio H. M. & Delbem A. C. 2010. pH-cycling models for in vitro evaluation of the efficacy of fluoridated dentifrices for caries control: strengths and limitations. *Journal of applied oral science : revista FOB,* 18(4)**,** 316-34.

Byrd T. O. 2016. Preventing Advanced Carious Lesions with Caries Atraumatic Restorative Technique. *The journal of evidence-based dental practice,* 16 Suppl**,** 84-90.

Cao C. Y., Mei M. L., Li Q. L., Lo E. C. & Chu C. H. 2015. Methods for biomimetic remineralization of human dentine: a systematic review. *International journal of molecular sciences,* 16(3)**,** 4615-27.

Cao Y., Mei M. L., Xu J., Lo E. C., Li Q. & Chu C. H. 2013. Biomimetic mineralisation of phosphorylated dentine by CPP-ACP. *Journal of dentistry,* 41(9)**,** 818-25.

Carvalho T. S., Van Amerongen W. E., De Gee A., Bonecker M. & Sampaio F. C. 2011. Shear bond strengths of three glass ionomer cements to enamel and dentine. *Medicina oral, patologia oral y cirugia bucal,* 16(3)**,** e406-10.

Castro F. L., Campos B. B., Bruno K. F. & Reges R. V. 2013. Temperature and curing time affect composite sorption and solubility. *Journal of applied oral science : revista FOB,* 21(2)**,** 157-62.

Caughman W. F., Caughman G. B., Shiflett R. A., Rueggeberg F. & Schuster G. S. 1991. Correlation of cytotoxicity, filler loading and curing time of dental composites. *Biomaterials,* 12(8)**,** 737-40.

Chaffee B. W., Rodrigues P. H., Kramer P. F., Vitolo M. R. & Feldens C. A. 2017. Oral health-related quality-of-life scores differ by socioeconomic status and caries experience. *Community dentistry and oral epidemiology,* 45(3)**,** 216-224.

Chaussain-Miller C., Fioretti F., Goldberg M. & Menashi S. 2006. The role of matrix metalloproteinases (MMPs) in human caries. *Journal of dental research,* 85(1)**,** 22-32.

Chen H. & Liu Y. 2014. Chapter 2 - Teeth. *In:* Shen, J. Z. & Kosmač, T. (eds.) *Advanced Ceramics for Dentistry.* Oxford: Butterworth-Heinemann, 5-21.

Chen J. H., Liu Y., Niu L. N., Lu S., Tay F. R. & Gao Y. 2014. A feasible method to eliminate nanoleakage in dentin hybrid layers. *The journal of adhesive dentistry,* 16(5)**,** 429-34.

Chen K. L., Yeh Y. Y., Lung J., Yang Y. C. & Yuan K. 2016. Mineralization Effect of Hyaluronan on Dental Pulp Cells via CD44. *Journal of endodontics,* 42(5)**,** 711-6.

Chen M.-H. 2010. Update on Dental Nanocomposites. 89(6)**,** 549-560.

Cheng L., Weir M. D., Xu H. H., Antonucci J. M., Lin N. J., Lin-Gibson S., Xu S. M. & Zhou X. 2012. Effect of amorphous calcium phosphate and silver nanocomposites on dental plaque microcosm biofilms. *Journal of biomedical materials research. Part B, Applied biomaterials,* 100(5)**,** 1378-86.

Cheng L., Zhang K., Weir M. D., Melo M. A., Zhou X. & Xu H. H. 2015. Nanotechnology strategies for antibacterial and remineralizing composites and adhesives to tackle dental caries. *Nanomedicine (London, England),* 10(4)**,** 627-41.

Cheng L., Zhang K., Zhang N., Melo M. a. S., Weir M. D., Zhou X. D., Bai Y. X., Reynolds M. A. & Xu H. H. K. 2017. Developing a New Generation of Antimicrobial and Bioactive Dental Resins. 96(8)**,** 855-863.

Choi K. K., Ferracane J. L., Hilton T. J. & Charlton D. 2000. Properties of Packable Dental Composites. 12(4)**,** 216-226.

Chung S. M., Yap A. U., Chandra S. P. & Lim C. T. 2004. Flexural strength of dental composite restoratives: comparison of biaxial and three-point bending test. *Journal of biomedical materials research. Part B, Applied biomaterials,* 71(2)**,** 278-83.

Clark W., Geneser M., Owais A., Kanellis M. & Qian F. 2017. Success rates of Hall technique crowns in primary molars: a retrospective pilot study. *General dentistry,* 65(5)**,** 32-35.

Cocco A. R., Rosa W. L., Silva A. F., Lund R. G. & Piva E. 2015. A systematic review about antibacterial monomers used in dental adhesive systems: Current status and further prospects. *Dental materials : official publication of the Academy of Dental Materials,* 31(11)**,** 1345-62.

Contreras V., Toro M. J., Elias-Boneta A. R. & Encarnacion-Burgos A. 2017. Effectiveness of silver diamine fluoride in caries prevention and arrest: a systematic literature review. *General dentistry,* 65(3)**,** 22-29.

Curzon M. E. J. & Duggal M. S. 2003. DENTAL DISEASE | Structure of Teeth. *In:* Caballero, B. (ed.) *Encyclopedia of Food Sciences and Nutrition (Second Edition).* Oxford: Academic Press, 1743-1746.

D'alpino P. H., Svizero Nda R., Arrais C. A., De Oliveira M., Alonso R. C. & Graeff C. F. 2015. Polymerization kinetics and polymerization stress in resin composites after accelerated aging as a function of the expiration date. *Journal of the mechanical behavior of biomedical materials,* 49**,** 300-9.

De Carvalho F. G., De Fucio S. B., Sinhoreti M. A., Correr-Sobrinho L. & Puppin-Rontani R. M. 2008. Confocal laser scanning microscopic analysis of the depth of dentin caries-like lesions in primary and permanent teeth. *Brazilian dental journal,* 19(2)**,** 139-44.

De Mattos Pimenta Vidal C., Leme-Kraus A. A., Rahman M., Farina A. P. & Bedran-Russo A. K. 2017. Role of proteoglycans on the biochemical and biomechanical properties of dentin organic matrix. *Archives of oral biology,* 82**,** 203-208.

De Medeiros Serpa E. B., Clementino M. A., Granville-Garcia A. F. & Rosenblatt A. 2017. The effect of atraumatic restorative treatment on adhesive restorations for dental caries in deciduous molars. *Journal of the Indian Society of Pedodontics and Preventive Dentistry,* 35(2)**,** 167-173.

De Menezes L. F. & Chevitarese O. 1994. Sealant and resin viscosity and their influence on the formation of resin tags. *The Angle orthodontist,* 64(5)**,** 383-8.

Dewaele M., Truffier-Boutry D., Devaux J. & Leloup G. 2006. Volume contraction in photocured dental resins: the shrinkage-conversion relationship revisited. *Dental materials : official publication of the Academy of Dental Materials,* 22(4)**,** 359-65.

Din 2010. Determination of the colourfastness of articles for common use- part 1: Test with artificial saliva. *DIN 53160-1:2010.* German Institute for Standardisation.

Dorri M., Martinez-Zapata M. J., Walsh T., Marinho V. C., Sheiham Deceased A. & Zaror C. 2017a. Atraumatic restorative treatment versus conventional restorative treatment for managing dental caries. *The Cochrane database of systematic reviews,* 12**,** Cd008072.

Dorri M., Martinez-Zapata M. J., Walsh T., Marinho V. C. C., Sheiham A. & Zaror C. 2017b. Atraumatic restorative treatment versus conventional restorative treatment for managing dental caries. (12).

Duangthip D., Chu C. H. & Lo E. C. 2016. A randomized clinical trial on arresting dentine caries in preschool children by topical fluorides--18 month results. *Journal of dentistry,* 44**,** 57-63.

Duangthip D., Wong M. C. M., Chu C. H. & Lo E. C. M. 2018. Caries arrest by topical fluorides in preschool children: 30-month results. *Journal of dentistry,* 70**,** 74-79.

Eggert F. M. & Germain J. P. 1979. Rapid demineralization in acidic buffers. *Histochemistry,* 59(3)**,** 215-24.

England P. H. 2018. National Dental Epidemiology Programme for England: oral health survey of five-year-old children. London, UK.

Enochs T., Hill A. E., Worley C. E., Verissimo C., Tantbirojn D. & Versluis A. 2018. Cuspal flexure of composite-restored typodont teeth and correlation with polymerization shrinkage values. *Dental materials : official publication of the Academy of Dental Materials,* 34(1)**,** 152-160.

Ertugrul F., Eltem R. & Eronat C. 2003. A comparative study of plaque mutans streptococci levels in children receiving glass ionomer cement and amalgam restorations. *Journal of dentistry for children (Chicago, Ill.),* 70(1)**,** 10-4.

Fda. 2004. *Agency Response Letter GRAS Notice No. GRN 000135* [Online]. FDA. Available: https://www.fda.gov/Food/IngredientsPackagingLabeling/GRAS/NoticeInventory/ucm153957.htm [Accessed].

Fdi 2014. FDI policy statement on dental amalgam and the Minamata Convention on Mercury: adopted by the FDI General Assembly: 13 September 2014, New Delhi, India. *World Dental Association.*

Federation F. D. I. W. D. 2014. FDI policy statement on dental amalgam and the Minamata Convention on Mercury: adopted by the FDI General Assembly: 13 September 2014, New Delhi, India. *International dental journal,* 64(6)**,** 295-6.

Femiano F., Femiano R., Femiano L., Jamilian A., Rullo R. & Perillo L. 2016. Dentin caries progression and the role of metalloproteinases: an update. *European journal of paediatric dentistry : official journal of European Academy of Paediatric Dentistry,* 17(3)**,** 243-247.

Feng L., Suh B. I. & Shortall A. C. 2010. Formation of gaps at the filler-resin interface induced by polymerization contraction stress: Gaps at the interface. *Dental materials : official publication of the Academy of Dental Materials,* 26(8)**,** 719-29.

Ferracane J. L. 1995. Current Trends in Dental Composites. 6(4)**,** 302-318.

Ferracane J. L. 2006. Hygroscopic and hydrolytic effects in dental polymer networks. *Dental materials : official publication of the Academy of Dental Materials,* 22(3)**,** 211-22.

Ferracane J. L. 2011. Resin composite—State of the art. 27(1)**,** 29-38.

Ferracane J. L. & Condon J. R. 1992. Post-cure heat treatments for composites: properties and fractography. 8(5)**,** 290-295.

Ferracane J. L. & Mitchem J. C. 2003. Relationship between composite contraction stress and leakage in Class V cavities. *American journal of dentistry,* 16(4)**,** 239-43.

Ferreira J. C., Pires P. T., De Azevedo A. F., Arantes-Oliveira S., Silva M. J. & De Melo P. R. 2017. Morphology of the Dentin-resin Interface yielded by Two-step Etch-and-rinse Adhesives with Different Solvents. *The journal of contemporary dental practice,* 18(10)**,** 947-958.

Ferreira M. C., Ramos-Jorge M. L., Marques L. S. & Ferreira F. O. 2017. Dental caries and quality of life of preschool children: discriminant validity of the ECOHIS. *Brazilian oral research,* 31**,** e24.

Folwaczny M., Loher C., Mehl A., Kunzelmann K. H. & Hickel R. 2001. Class V lesions restored with four different tooth-colored materials--3-year results. *Clinical oral investigations,* 5(1)**,** 31-9.

French-Mowat E. & Burnett J. 2012. How are medical devices regulated in the European Union? *J R Soc Med,* 105 Suppl 1(Suppl 1)**,** S22-S28.

Frencken J. E., Flohil K. A. & De Baat C. 2014. [Atraumatic restorative treatment in relation to pain, discomfort and dental treatment anxiety]. *Nederlands tijdschrift voor tandheelkunde,* 121(7-8)**,** 388-93.

Frencken J. E., Pilot T., Songpaisan Y. & Phantumvanit P. 1996. Atraumatic restorative treatment (ART): rationale, technique, and development. *Journal of public health dentistry,* 56(3 Spec No)**,** 135-40; discussion 161-3.

Fritz U. B., Finger W. J. & Uno S. 1996. Resin-modified glass ionomer cements: bonding to enamel and dentin. *Dental materials : official publication of the Academy of Dental Materials,* 12(3)**,** 161-6.

Fronza B. M., Rueggeberg F. A., Braga R. R., Mogilevych B., Soares L. E., Martin A. A., Ambrosano G. & Giannini M. 2015. Monomer conversion, microhardness, internal marginal adaptation, and shrinkage stress of bulk-fill resin composites. *Dental materials : official publication of the Academy of Dental Materials,* 31(12)**,** 1542-51.

Fugolin A. P. P. & Pfeifer C. S. 2017. New Resins for Dental Composites. *Journal of dental research,* 96(10)**,** 1085-1091.

Fusayama T., Okuse K. & Hosoda H. 1966. Relationship between hardness, discoloration, and microbial invasion in carious dentin. *Journal of dental research,* 45(4)**,** 1033-46.

Fusayama T. & Terachima S. 1972. Differentiation of two layers of carious dentin by staining. *Journal of dental research,* 51(3)**,** 866.

Gao S. S., Zhang S., Mei M. L., Lo E. C. & Chu C. H. 2016. Caries remineralisation and arresting effect in children by professionally applied fluoride treatment - a systematic review. *BMC oral health,* 16**,** 12.

Garoushi S., Vallittu P., Shinya A. & Lassila L. 2016. Influence of increment thickness on light transmission, degree of conversion and micro hardness of bulk fill composites. *Odontology,* 104(3)**,** 291-7.

Giachetti L., Bertini F., Scaminaci Russo D. & Rubino I. 2005. The extension of resin tags in etched dentin: a misinterpretation? *Minerva stomatologica,* 54(3)**,** 139-51.

Goldberg M. 2008. In vitro and in vivo studies on the toxicity of dental resin components: a review. *Clinical oral investigations,* 12(1)**,** 1-8.

Goldberg M., Kulkarni A. B., Young M. & Boskey A. 2011. Dentin: structure, composition and mineralization. *Frontiers in bioscience (Elite edition),* 3**,** 711-35.

Hamilton I. R. 1990. Biochemical Effects of Fluoride on Oral Bacteria. 69(2_suppl)**,** 660-667.

Han S. H. & Park S. H. 2017. Comparison of Internal Adaptation in Class II Bulk-fill Composite Restorations Using Micro-CT. *Operative dentistry,* 42(2)**,** 203-214.

Han S. H., Sadr A., Shimada Y., Tagami J. & Park S. H. 2019. Internal adaptation of composite restorations with or without an intermediate layer: Effect of polymerization shrinkage parameters of the layer material. *Journal of dentistry,* 80**,** 41-48.

He G. & George A. 2004. Dentin matrix protein 1 immobilized on type I collagen fibrils facilitates apatite deposition in vitro. *The Journal of biological chemistry,* 279(12)**,** 11649-56.

Hendre A. D., Taylor G. W., Chavez E. M. & Hyde S. 2017. A systematic review of silver diamine fluoride: Effectiveness and application in older adults. *Gerodontology,* 34(4)**,** 411-419.

Hesse D., De Araujo M. P., Olegario I. C., Innes N., Raggio D. P. & Bonifacio C. C. 2016. Atraumatic Restorative Treatment compared to the Hall Technique for occluso-proximal cavities in primary molars: study protocol for a randomized controlled trial. *Trials,* 17**,** 169.

Hibino Y., Kuramochi K., Harashima A., Honda M., Yamazaki A., Nagasawa Y., Yamaga T. & Nakajima H. 2004. Correlation between the strength of glass ionomer cements and their bond strength to bovine teeth. *Dental materials journal,* 23(4)**,** 656-60.

Hickel R., Roulet J. F., Bayne S., Heintze S. D., Mjor I. A., Peters M., Rousson V., Randall R., Schmalz G., Tyas M. & Vanherle G. 2007. Recommendations for conducting controlled clinical studies of dental restorative materials. Science Committee Project 2/98--FDI World Dental Federation study design (Part I) and criteria for evaluation (Part II) of direct and indirect restorations including onlays and partial crowns. *The journal of adhesive dentistry,* 9 Suppl 1**,** 121-47.

Hiemenz P. C. & Lodge T. P. 2007. *Polymer Chemistry*, CRC Press.

Higg W. A., Lucksanasombool P., Higgs R. J. & Swain M. V. 2001. Evaluating acrylic and glass-ionomer cement strength using the biaxial flexure test. *Biomaterials,* 22(12)**,** 1583-90.

Hiraki J., Ichikawa T., Ninomiya S., Seki H., Uohama K., Seki H., Kimura S., Yanagimoto Y. & Barnett J. W., Jr. 2003. Use of ADME studies to confirm the safety of epsilon-polylysine as a preservative in food. *Regulatory toxicology and pharmacology : RTP,* 37(2)**,** 328-40.

Hobson R. S. & Mccabe J. F. 2002. Relationship between enamel etch characteristics and resin-enamel bond strength. *British dental journal,* 192(8)**,** 463-8.

Hsieh Y.-S., Ho Y.-C., Lee S.-Y., Chuang C.-C., Tsai J.-C., Lin K.-F. & Sun C.-W. 2013. Dental optical coherence tomography. *Sensors (Basel),* 13(7)**,** 8928-8949.

Hyldgaard M., Mygind T., Vad B. S., Stenvang M., Otzen D. E. & Meyer R. L. 2014. The antimicrobial mechanism of action of epsilon-poly-l-lysine. *Applied and environmental microbiology,* 80(24)**,** 7758-70.

Innes N., Stewart M., Souster G. & Evans D. 2015. The Hall Technique; retrospective case-note follow-up of 5-year RCT. *British dental journal,* 219(8)**,** 395-400.

Innes N. P., Evans D. J., Bonifacio C. C., Geneser M., Hesse D., Heimer M., Kanellis M., Machiulskiene V., Narbutaite J., Olegario I. C., Owais A., Araujo M. P., Raggio D. P., Splieth C., Van Amerongen E., Weber-Gasparoni K. & Santamaria R. M. 2017. The Hall Technique 10 years on: Questions and answers. *British dental journal,* 222(6)**,** 478-483.

Innes N. P., Evans D. J. & Stirrups D. R. 2007. The Hall Technique; a randomized controlled clinical trial of a novel method of managing carious primary molars in general dental practice: acceptability of the technique and outcomes at 23 months. *BMC oral health,* 7**,** 18.

Innes N. P. T., Ricketts D., Chong L. Y., Keightley A. J., Lamont T. & Santamaria R. M. 2015. Preformed crowns for decayed primary molar teeth. (12).

Ireland A. J. & Sherriff M. 2006. An investigation into the use of an anaerobic adhesive with two commercially available orthodontic brackets. 22(2)**,** 112-118.

Ito S., Hashimoto M., Wadgaonkar B., Svizero N., Carvalho R. M., Yiu C., Rueggeberg F. A., Foulger S., Saito T., Nishitani Y., Yoshiyama M., Tay F. R. & Pashley D. H. 2005. Effects of resin hydrophilicity on water sorption and changes in modulus of elasticity. *Biomaterials,* 26(33)**,** 6449-59.

Iwaku M., Nakamichi I., Nakamura K., Horie K., Suizu S. & Fusayama T. 1981. Tags penetrating dentin of a new adhesive resin. *The Bulletin of Tokyo Medical and Dental University,* 28(2)**,** 45-51.

Johnsson M. S. & Nancollas G. H. 1992. The role of brushite and octacalcium phosphate in apatite formation. *Critical reviews in oral biology and medicine : an official publication of the American Association of Oral Biologists,* 3(1-2)**,** 61-82.

Joseph B., Prasanth C. S., Jayanthi J. L., Presanthila J. & Subhash N. 2015. *Detection and quantification of dental plaque based on laser-induced autofluorescence intensity ratio values*, SPIE.

Jurgensen N. & Petersen P. E. 2013. Promoting oral health of children through schools--results from a WHO global survey 2012. *Community dental health,* 30(4)**,** 204-18.

Kaminska A., Szalewski L., Batkowska J., Wallner J., Wallner E., Szabelska A. & Borowicz J. 2016. The dependence of dental caries on oral hygiene habits in preschool children from urban and rural areas in Poland. *Annals of agricultural and environmental medicine : AAEM,* 23(4)**,** 660-665.

Kanehira M., Finger W. J., Hoffmann M., Endo T. & Komatsu M. 2006. Relationship between degree of polymerization and enamel bonding strength with self-etching adhesives. *The journal of adhesive dentistry,* 8(4)**,** 211-6.

Kangwankai K., Sani S., Panpisut P., Xia W., Ashley P., Petridis H. & Young A. M. 2017. Monomer conversion, dimensional stability, strength, modulus, surface apatite precipitation and wear of novel, reactive calcium phosphate and polylysine-containing dental composites. *PloS one,* 12(11)**,** e0187757.

Kim J. H., Cho J., Lee Y. & Cho B. H. 2017. The Survival of Class V Composite Restorations and Analysis of Marginal Discoloration. *Operative dentistry,* 42(3)**,** E93-e101.

Kim K. H., Ong J. L. & Okuno O. 2002. The effect of filler loading and morphology on the mechanical properties of contemporary composites. *The Journal of prosthetic dentistry,* 87(6)**,** 642-9.

Kinney J. H., Marshall S. J. & Marshall G. W. 2003. The mechanical properties of human dentin: A critical review and re-evaluation of the dental literature. 14(1)**,** 13-29.

Klapdohr S. & Moszner N. J. M. F. C. C. M. 2005. New Inorganic Components for Dental Filling Composites. 136(1)**,** 21-45.

Ko C. C., Yi D. H., Lee D. J., Kwon J., Garcia-Godoy F. & Kwon Y. H. 2017. Diagnosis and staging of caries using spectral factors derived from the blue laser-induced autofluorescence spectrum. *Journal of dentistry,* 67**,** 77-83.

Kuhn E., Reis A., Campagnoli E. B., Chibinski A. C., Carrilho M. R. & Wambier D. S. 2016. Effect of sealing infected dentin with glass ionomer cement on the abundance and localization of MMP-2, MMP-8, and MMP-9 in young permanent molars in vivo. *International journal of paediatric dentistry,* 26(2)**,** 125-33.

Kumar N. & Sangi L. 2014. Water sorption, solubility, and resultant change in strength among three resin-based dental composites. *Journal of investigative and clinical dentistry,* 5(2)**,** 144-50.

Larsen T. & Fiehn N. E. 2017. Dental biofilm infections - an update. *APMIS : acta pathologica, microbiologica, et immunologica Scandinavica,* 125(4)**,** 376-384.

Lee S. Y., Chiu C. H., Boghosian A. & Greener E. H. 1993. Radiometric and spectroradiometric comparison of power outputs of five visible light-curing units. 21(6)**,** 373-377.

Lempel E., Toth A., Fabian T., Krajczar K. & Szalma J. 2015. Retrospective evaluation of posterior direct composite restorations: 10-year findings. *Dental materials : official publication of the Academy of Dental Materials,* 31(2)**,** 115-22.

Lenzi T. L., Soares F. Z. M., Tedesco T. K. & Rocha R. D. O. 2015. Is It Possible to induce Artificial Caries-affected Dentin using the Same Protocol to Primary and Permanent Teeth? 16(8)**,** 638-642.

Leprince J. G., Palin W. M., Vanacker J., Sabbagh J., Devaux J. & Leloup G. J. J. O. D. 2014. Physico-mechanical characteristics of commercially available bulk-fill composites. 42(8)**,** 993-1000.

Leung D., Spratt D. A., Pratten J., Gulabivala K., Mordan N. J. & Young A. M. 2005. Chlorhexidine-releasing methacrylate dental composite materials. *Biomaterials,* 26(34)**,** 7145-53.

Li F., Wang P., Weir M. D., Fouad A. F. & Xu H. H. 2014. Evaluation of antibacterial and remineralizing nanocomposite and adhesive in rat tooth cavity model. *Acta biomaterialia,* 10(6)**,** 2804-13.

Liang K., Weir M. D., Xie X., Wang L., Reynolds M. A., Li J. & Xu H. H. 2016. Dentin remineralization in acid challenge environment via PAMAM and calcium phosphate composite. *Dental materials : official publication of the Academy of Dental Materials,* 32(11)**,** 1429-1440.

Listl S., Galloway J., Mossey P. A. & Marcenes W. 2015. Global Economic Impact of Dental Diseases. *Journal of dental research,* 94(10)**,** 1355-61.

Liu Z., Jiang T., Wang Y. & Wang X. 2013. Fluocinolone acetonide promotes the proliferation and mineralization of dental pulp cells. *Journal of endodontics,* 39(2)**,** 217-22.

Loguercio A. D., Reis A., Barbosa A. N. & Roulet J. F. 2003. Five-year double-blind randomized clinical evaluation of a resin-modified glass ionomer and a polyacid-modified resin in noncarious cervical lesions. *The journal of adhesive dentistry,* 5(4)**,** 323-32.

Malacarne J., Carvalho R. M., De Goes M. F., Svizero N., Pashley D. H., Tay F. R., Yiu C. K. & Carrilho M. R. 2006. Water sorption/solubility of dental adhesive resins. *Dental materials : official publication of the Academy of Dental Materials,* 22(10)**,** 973-80.

Manhart J., Kunzelmann K. H., Chen H. Y. & Hickel R. 2000. Mechanical properties and wear behavior of light-cured packable composite resins. *Dental materials : official publication of the Academy of Dental Materials,* 16(1)**,** 33-40.

Marinho V. C. C., Higgins J. P. T., Sheiham A. & Logan S. 2004. Combinations of topical fluoride (toothpastes, mouthrinses, gels, varnishes) versus single topical fluoride for preventing dental caries in children and adolescents. (1).

Marinho V. C. C., Worthington H. V., Walsh T. & Chong L. Y. 2015. Fluoride gels for preventing dental caries in children and adolescents. (6).

Marinho V. C. C., Worthington H. V., Walsh T. & Clarkson J. E. 2013. Fluoride varnishes for preventing dental caries in children and adolescents. (7).

Marquezan M., Correa F. N., Sanabe M. E., Rodrigues Filho L. E., Hebling J., Guedes-Pinto A. C. & Mendes F. M. 2009. Artificial methods of dentine caries induction: A hardness and morphological comparative study. *Archives of oral biology,* 54(12)**,** 1111-7.

Marshall G. W., Jr., Marshall S. J., Kinney J. H. & Balooch M. 1997. The dentin substrate: structure and properties related to bonding. *Journal of dentistry,* 25(6)**,** 441-58.

Marshall Jr G. W., Marshall S. J., Kinney J. H. & Balooch M. 1997. The dentin substrate: Structure and properties related to bonding. 25(6)**,** 441-458.

Martins M. T., Sardenberg F., Bendo C. B., Abreu M. H., Vale M. P., Paiva S. M. & Pordeus I. A. 2017. Dental caries remains as the main oral condition with the greatest impact on children's quality of life. *PloS one,* 12(10)**,** e0185365.

Materials C. S. R. D. 2012. Chapter 2 - The Oral Environment. *In:* Sakaguchi, R. L. & Powers, J. M. (eds.) *Craig's Restorative Dental Materials (Thirteenth Edition).* Saint Louis: Mosby, 5-23.

Matos A. B., Trevelin L. T., Silva B., Francisconi-Dos-Rios L. F., Siriani L. K. & Cardoso M. V. 2017. Bonding efficiency and durability: current possibilities. *Brazilian oral research,* 31(suppl 1)**,** e57.

Mazzoni A., Papa V., Nato F., Carrilho M., Tjaderhane L., Ruggeri A., Jr., Gobbi P., Mazzotti G., Tay F. R., Pashley D. H. & Breschi L. 2011. Immunohistochemical and biochemical assay of MMP-3 in human dentine. *Journal of dentistry,* 39(3)**,** 231-7.

Mazzoni A., Tjaderhane L., Checchi V., Di Lenarda R., Salo T., Tay F. R., Pashley D. H. & Breschi L. 2015a. Role of dentin MMPs in caries progression and bond stability. *Journal of dental research,* 94(2)**,** 241-51.

Mazzoni A., Tjäderhane L., Checchi V., Di Lenarda R., Salo T., Tay F. R., Pashley D. H. & Breschi L. 2015b. Role of dentin MMPs in caries progression and bond stability. *J Dent Res,* 94(2)**,** 241-251.

Meereis C. T. W., Munchow E. A., De Oliveira Da Rosa W. L., Da Silva A. F. & Piva E. 2018. Polymerization shrinkage stress of resin-based dental materials: A systematic review and meta-analyses of composition strategies. *Journal of the mechanical behavior of biomedical materials,* 82**,** 268-281.

Mehdawi I., Neel E. A., Valappil S. P., Palmer G., Salih V., Pratten J., Spratt D. A. & Young A. M. 2009. Development of remineralizing, antibacterial dental materials. *Acta biomaterialia,* 5(7)**,** 2525-39.

Mehdawi I. M., Pratten J., Spratt D. A., Knowles J. C. & Young A. M. 2013. High strength re-mineralizing, antibacterial dental composites with reactive calcium phosphates. 29(4)**,** 473-84.

Mei M. L., Ito L., Cao Y., Lo E. C., Li Q. L. & Chu C. H. 2014. An ex vivo study of arrested primary teeth caries with silver diamine fluoride therapy. *Journal of dentistry,* 42(4)**,** 395-402.

Melo M. A., Guedes S. F., Xu H. H. & Rodrigues L. K. 2013. Nanotechnology-based restorative materials for dental caries management. *Trends in biotechnology,* 31(8)**,** 459-67.

Miletic V., Pongprueksa P., De Munck J., Brooks N. R. & Van Meerbeek B. J. C. O. I. 2017. Curing characteristics of flowable and sculptable bulk-fill composites. 21(4)**,** 1201-1212.

Milgrom P., Horst J. A., Ludwig S., Rothen M., Chaffee B. W., Lyalina S., Pollard K. S., Derisi J. L. & Mancl L. 2018. Topical silver diamine fluoride for dental caries arrest in preschool children: A randomized controlled trial and microbiological analysis of caries associated microbes and resistance gene expression. *Journal of dentistry,* 68**,** 72-78.

Misilli T. & Gonulol N. 2017. Water sorption and solubility of bulk-fill composites polymerized with a third generation LED LCU. *Brazilian oral research,* 31**,** e80.

Mithiborwala S., Chaugule V., Munshi A. K. & Patil V. 2012. A comparison of the resin tag penetration of the total etch and the self-etch dentin bonding systems in the primary teeth: An in vitro study. *Contemporary clinical dentistry,* 3(2)**,** 158-63.

Mohd Zainal Abidin R., Luddin N., Shamsuria Omar N. & Mohamed Aly Ahmed H. 2015. Cytotoxicity of Fast-set Conventional and Resin-modified Glass Ionomer Cement Polymerized at Different Times on SHED. *The Journal of clinical pediatric dentistry,* 39(3)**,** 235-40.

Montagner A. F., Sarkis-Onofre R., Pereira-Cenci T. & Cenci M. S. 2014. MMP Inhibitors on Dentin Stability: A Systematic Review and Meta-analysis. *Journal of dental research,* 93(8)**,** 733-43.

Muller J. A., Rohr N. & Fischer J. 2017. Evaluation of ISO 4049: water sorption and water solubility of resin cements. *European journal of oral sciences,* 125(2)**,** 141-150.

Namba N., Yoshida Y., Nagaoka N., Takashima S., Matsuura-Yoshimoto K., Maeda H., Van Meerbeek B., Suzuki K. & Takashiba S. 2009. Antibacterial effect of bactericide immobilized in resin matrix. *Dental materials : official publication of the Academy of Dental Materials,* 25(4)**,** 424-30.

Namgung C., Rho Y. J., Jin B. H., Lim B. S. & Cho B. H. 2013. A retrospective clinical study of cervical restorations: longevity and failure-prognostic variables. *Operative dentistry,* 38(4)**,** 376-85.

Nascimento F. D., Minciotti C. L., Geraldeli S., Carrilho M. R., Pashley D. H., Tay F. R., Nader H. B., Salo T., Tjaderhane L. & Tersariol I. L. 2011. Cysteine cathepsins in human carious dentin. *Journal of dental research,* 90(4)**,** 506-11.

Odajima T. & Onishi M. 1998. A study on the promotion and suppression of demineralization of human dental hard tissues and hydroxyapatite. *Connective tissue research,* 38(1-4)**,** 119-27; discussion 139-45.

Ortengren U., Wellendorf H., Karlsson S. & Ruyter I. E. 2001. Water sorption and solubility of dental composites and identification of monomers released in an aqueous environment. *Journal of oral rehabilitation,* 28(12)**,** 1106-15.

Osorio R., Yamauti M., Sauro S., Watson T. F. & Toledano M. 2012. Experimental resin cements containing bioactive fillers reduce matrix metalloproteinase-mediated dentin collagen degradation. *Journal of endodontics,* 38(9)**,** 1227-32.

Oysaed H. & Ruyter I. E. 1986. Water sorption and filler characteristics of composites for use in posterior teeth. *Journal of dental research,* 65(11)**,** 1315-8.

Pacheco L. F., Banzi E., Rodrigues E., Soares L. E., Pascon F. M., Correr-Sobrinho L. & Puppin-Rontani R. M. 2013. Molecular and structural evaluation of dentin caries-like lesions produced by different artificial models. *Brazilian dental journal,* 24(6)**,** 610-8.

Palin W. M., Hadis M. A., Leprince J. G., Leloup G., Boland L., Fleming G. J. P., Krastl G. & Watts D. C. 2014. Reduced polymerization stress of MAPO-containing resin composites with increased curing speed, degree of conversion and mechanical properties. 30(5)**,** 507-516.

Panahandeh N., Torabzadeh H., Naderi H. & Sheikh-Al-Eslamian S. M. 2017. Effect of water storage on flexural strength of silorane and methacrylate-based composite resins. *Restorative dentistry & endodontics,* 42(4)**,** 309-315.

Panpisut P., Khan M. A., Main K., Arshad M., Xia W., Petridis H. & Young A. M. 2019. Polymerization kinetics stability, volumetric changes, apatite precipitation, strontium release and fatigue of novel bone composites for vertebroplasty. *PloS one,* 14(3)**,** e0207965.

Panpisut P., Liaqat S., Zacharaki E., Xia W., Petridis H. & Young A. M. 2016. Dental Composites with Calcium / Strontium Phosphates and Polylysine. *PloS one,* 11(10)**,** e0164653.

Par M., Gamulin O., Marovic D., Klaric E. & Tarle Z. 2014. Effect of temperature on post-cure polymerization of bulk-fill composites. *Journal of dentistry,* 42(10)**,** 1255-60.

Pashley D. H. 1989. Dentin: A dynamic substrate - A review. 3(1)**,** 161-176.

Peacock A. J. & Calhoun A. Polymer Chemistry - Properties and Applications. Hanser Publishers.

Perdigao J., Reis A. & Loguercio A. D. 2013. Dentin adhesion and MMPs: a comprehensive review. *Journal of esthetic and restorative dentistry : official publication of the American Academy of Esthetic Dentistry ... [et al.],* 25(4)**,** 219-41.

Peres M. A., Macpherson L. M. D., Weyant R. J., Daly B., Venturelli R., Mathur M. R., Listl S., Celeste R. K., Guarnizo-Herreno C. C., Kearns C., Benzian H., Allison P. & Watt R. G. 2019. Oral diseases: a global public health challenge. 394(10194)**,** 249-260.

Peutzfeldt A. 1997. Resin composites in dentistry: the monomer systems. *European journal of oral sciences,* 105(2)**,** 97-116.

Pinna R., Maioli M., Eramo S., Mura I. & Milia E. 2015. Carious affected dentine: its behaviour in adhesive bonding. *Australian dental journal,* 60(3)**,** 276-93.

Prabakar J., John J., Arumugham I. M., Kumar R. P. & Sakthi D. S. 2018. Comparative Evaluation of the Viscosity and Length of Resin Tags of Conventional and Hydrophilic Pit and Fissure Sealants on Permanent Molars: An In vitro Study. *Contemporary clinical dentistry,* 9(3)**,** 388-394.

Prabhakar A. R., Murthy S. A. & Sugandhan S. 2011. Comparative evaluation of the length of resin tags, viscosity and microleakage of pit and fissure sealants - an in vitro scanning electron microscope study. *Contemporary clinical dentistry,* 2(4)**,** 324-30.

Price R. B., Ferracane J. L. & Shortall A. C. 2015. Light-Curing Units: A Review of What We Need to Know. *Journal of dental research,* 94(9)**,** 1179-86.

Price R. B., Whalen J. M., Price T. B., Felix C. M. & Fahey J. 2011. The effect of specimen temperature on the polymerization of a resin-composite. 27(10)**,** 983-989.

Rahal V., De Oliveira F. G., Briso A. L., Dos Santos P. H., Sundefeld M. L. & Sundfeld R. H. 2012. Correlation between hybrid layer thickness, resin tag length and microtensile bond strength of a self-etching adhesive system. *Acta odontologica latinoamericana : AOL,* 25(2)**,** 231-7.

Rai M., Yadav A. & Gade A. 2009. Silver nanoparticles as a new generation of antimicrobials. *Biotechnology advances,* 27(1)**,** 76-83.

Ramesh Kumar K. R., Shanta Sundari K. K., Venkatesan A. & Chandrasekar S. 2011. Depth of resin penetration into enamel with 3 types of enamel conditioning methods: a confocal microscopic study. *American journal of orthodontics and dentofacial orthopedics : official publication of the American Association of Orthodontists, its constituent societies, and the American Board of Orthodontics,* 140(4)**,** 479-85.

Reed B. B. 1997. Effect of resin composition of kinetics of dimethacrylate photopolymerization. 38**,** 108-109.

Reese S. & Guggenheim B. 2007. A novel TEM contrasting technique for extracellular polysaccharides in in vitro biofilms. *Microscopy research and technique,* 70(9)**,** 816-22.

Retrouvey J.-M., Goldberg M. & Schwartz S. 2012. Chapter 5 - Dental Development and Maturation, from the Dental Crypt to the Final Occlusion. *In:* Glorieux, F. H., Pettifor, J. M. & Jüppner, H. (eds.) *Pediatric Bone (Second Edition).* San Diego: Academic Press, 83-108.

Ricketts D., Lamont T., Innes N. P. T., Kidd E. & Clarkson J. E. 2013. Operative caries management in adults and children. (3).

Romero M. F., Haddock F. & Todd M. 2017. Combination of centripetal and successive layering techniques for a stress-reduced posterior direct composite restoration. *General dentistry,* 65(3)**,** 72-76.

Rosa A. J., Da Silva E. M. & Tostes M. A. 2015. Scanning electron microscopy analysis of microstructure of the adhesive interface between resin and dentin treated with papain gel. *Indian journal of dental research : official publication of Indian Society for Dental Research,* 26(1)**,** 77-81.

Rosatto C., Bicalho A., Veríssimo C., Bragança G., Rodrigues M., Tantbirojn D., Versluis A. & Soares C. J. J. O. D. 2015. Mechanical properties, shrinkage stress, cuspal strain and fracture resistance of molars restored with bulk-fill composites and incremental filling technique. 43(12)**,** 1519-1528.

Rothmund L., Reichl F. X., Hickel R., Styllou P., Styllou M., Kehe K., Yang Y. & Hogg C. 2017. Effect of layer thickness on the elution of bulk-fill composite components. *Dental materials : official publication of the Academy of Dental Materials,* 33(1)**,** 54-62.

Rueggeberg F. & Tamareselvy K. 1995. Resin cure determination by polymerization shrinkage. *Dental materials : official publication of the Academy of Dental Materials,* 11(4)**,** 265-8.

Ruff R. R. & Niederman R. 2018. Silver diamine fluoride versus therapeutic sealants for the arrest and prevention of dental caries in low-income minority children: study protocol for a cluster randomized controlled trial. *Trials,* 19(1)**,** 523.

Salehi H., Terrer E., Panayotov I., Levallois B., Jacquot B., Tassery H. & Cuisinier F. 2013. Functional mapping of human sound and carious enamel and dentin with Raman spectroscopy. *Journal of biophotonics,* 6(10)**,** 765-74.

Santamaria R. & Innes N. 2018. Sealing Carious Tissue in Primary Teeth Using Crowns: The Hall Technique. *Monographs in oral science,* 27**,** 113-123.

Sato M. & Miyazaki M. 2005. Comparison of depth of dentin etching and resin infiltration with single-step adhesive systems. *Journal of dentistry,* 33(6)**,** 475-84.

Scaffa P. M., Breschi L., Mazzoni A., Vidal C. M., Curci R., Apolonio F., Gobbi P., Pashley D., Tjaderhane L., Tersariol I. L., Nascimento F. D. & Carrilho M. R. 2017. Co-distribution of cysteine cathepsins and matrix metalloproteases in human dentin. *Archives of oral biology,* 74**,** 101-107.

Sengul F. & Gurbuz T. 2015. Clinical Evaluation of Restorative Materials in Primary Teeth Class II Lesions. *The Journal of clinical pediatric dentistry,* 39(4)**,** 315-21.

Seseogullari-Dirihan R., Apollonio F., Mazzoni A., Tjaderhane L., Pashley D., Breschi L. & Tezvergil-Mutluay A. 2016. Use of crosslinkers to inactivate dentin MMPs. *Dental materials : official publication of the Academy of Dental Materials,* 32(3)**,** 423-32.

Shima S., Matsuoka H., Iwamoto T. & Sakai H. 1984. Antimicrobial action of epsilon-poly-L-lysine. *The Journal of antibiotics,* 37(11)**,** 1449-55.

Shinchi M. J., Soma K. & Nakabayashi N. 2000. The effect of phosphoric acid concentration on resin tag length and bond strength of a photo-cured resin to acid-etched enamel. *Dental materials : official publication of the Academy of Dental Materials,* 16(5)**,** 324-9.

Sideridou I., Tserki V. & Papanastasiou G. 2002. Effect of chemical structure on degree of conversion in light-cured dimethacrylate-based dental resins. *Biomaterials,* 23(8)**,** 1819-29.

Sloan A. J. 2015. Chapter 29 - Biology of the Dentin-Pulp Complex. *In:* Vishwakarma, A., Sharpe, P., Shi, S. & Ramalingam, M. (eds.) *Stem Cell Biology and Tissue Engineering in Dental Sciences.* Boston: Academic Press, 371-378.

Soares C. J., Faria E. S. a. L., Rodrigues M. P., Vilela A. B. F., Pfeifer C. S., Tantbirojn D. & Versluis A. 2017. Polymerization shrinkage stress of composite resins and resin cements - What do we need to know? *Brazilian oral research,* 31(suppl 1)**,** e62.

Soares F. Z., Lenzi T. L. & De Oliveira Rocha R. 2017. Degradation of resin-dentine bond of different adhesive systems to primary and permanent dentine. *European*

archives of paediatric dentistry : official journal of the European Academy of Paediatric Dentistry, 18(2)**,** 113-118.

Son S.-A., Jung K.-H., Ko C.-C. & Kwon Y. H. 2016. *<!-- *** Custom HTML *** -->Spectral characteristics of caries-related autofluorescence spectra and their use for diagnosis of caries stage<strong />,* SPIE.

Son S.-A., Park J.-K., Seo D.-G., Ko C.-C. & Kwon Y. H. J. C. O. I. 2017. How light attenuation and filler content affect the microhardness and polymerization shrinkage and translucency of bulk-fill composites? 21(2), 559-565.

Sousa S. M. & Silva T. L. 2005. Demineralization effect of EDTA, EGTA, CDTA and citric acid on root dentin: a comparative study. *Brazilian oral research,* 19(3)**,** 188-92.

Stanislawski L., Daniau X., Lauti A. & Goldberg M. 1999. Factors responsible for pulp cell cytotoxicity induced by resin-modified glass ionomer cements. *Journal of biomedical materials research,* 48(3)**,** 277-88.

Stansbury J. W. 2000. Curing Dental Resins and Composites by Photopolymerization. 12(6)**,** 300-308.

Sundfeld R. H., Valentino T. A., De Alexandre R. S., Briso A. L. & Sundefeld M. L. 2005. Hybrid layer thickness and resin tag length of a self-etching adhesive bonded to sound dentin. *Journal of dentistry,* 33(8)**,** 675-81.

Surgery F. O. D. 2015. The state of children's oral health in England. UK: Faculty of Dental Surgery.

Takahashi N. & Nyvad B. 2016. Ecological Hypothesis of Dentin and Root Caries. *Caries research,* 50(4)**,** 422-31.

Tay F. R. & Pashley D. H. 2008. Guided tissue remineralisation of partially demineralised human dentine. *Biomaterials,* 29(8)**,** 1127-37.

Thomaidis S., Kakaboura A., Mueller W. D. & Zinelis S. 2013. Mechanical properties of contemporary composite resins and their interrelations. *Dental materials : official publication of the Academy of Dental Materials,* 29(8)**,** e132-41.

Tjaderhane L., Buzalaf M. A., Carrilho M. & Chaussain C. 2015. Matrix metalloproteinases and other matrix proteinases in relation to cariology: the era of 'dentin degradomics'. *Caries research,* 49(3)**,** 193-208.

Toledano M., Osorio R., Osorio E., Fuentes V., Prati C. & Garcia-Godoy F. 2003. Sorption and solubility of resin-based restorative dental materials. *Journal of dentistry,* 31(1)**,** 43-50.

Tramini P., Pelissier B., Valcarcel J., Bonnet B. & Maury L. 2000. A Raman spectroscopic investigation of dentin and enamel structures modified by lactic acid. *Caries research,* 34(3)**,** 233-40.

Trevor Burke F. J., Lawson A., Green D. J. B. & Mackenzie L. 2017. What's New in Dentine Bonding?: Universal Adhesives. *Dental update,* 44(4)**,** 328-30, 332, 335-8, 340.

Trujillo M., Newman S. M. & Stansbury J. W. 2004. Use of near-IR to monitor the influence of external heating on dental composite photopolymerization. 20(8)**,** 766-777.

Tsuge T. 2009. Radiopacity of conventional, resin-modified glass ionomer, and resin-based luting materials. *Journal of oral science,* 51(2)**,** 223-30.

Tsujimoto A., Fischer N., Barkmeier W., Baruth A., Takamizawa T., Latta M. & Miyazaki M. 2017. Effect of Reduced Phosphoric Acid Pre-etching Times on Enamel Surface Characteristics and Shear Fatigue Strength Using Universal Adhesives. *The journal of adhesive dentistry,* 19(3)**,** 267-275.

Van Der Veen M. H. & Ten Bosch J. J. 1995. Autofluorescence of bulk sound and in vitro demineralized human root dentin. *European journal of oral sciences,* 103(6)**,** 375-81.

Van Der Veen M. H. & Ten Bosch J. J. 1996. The Influence of Mineral Loss on the Auto-Fluorescent Behaviour of in vitro Demineralised Dentine. 30(1)**,** 93-99.

Van Dijken J. W. & Pallesen U. 2010. Fracture frequency and longevity of fractured resin composite, polyacid-modified resin composite, and resin-modified glass ionomer cement class IV restorations: an up to 14 years of follow-up. *Clinical oral investigations,* 14(2)**,** 217-22.

Van Ende A., Lise D. P., De Munck J., Vanhulst J., Wevers M. & Van Meerbeek B. J. D. M. 2017. Strain development in bulk-filled cavities of different depths characterized using a non-destructive acoustic emission approach. 33(4)**,** e165-e177.

Van Landuyt K. L., Snauwaert J., De Munck J., Peumans M., Yoshida Y., Poitevin A., Coutinho E., Suzuki K., Lambrechts P. & Van Meerbeek B. 2007. Systematic review of the chemical composition of contemporary dental adhesives. *Biomaterials,* 28(26)**,** 3757-85.

Vidal C. M., Tjaderhane L., Scaffa P. M., Tersariol I. L., Pashley D., Nader H. B., Nascimento F. D. & Carrilho M. R. 2014. Abundance of MMPs and cysteine cathepsins in caries-affected dentin. *Journal of dental research,* 93(3)**,** 269-74.

Visse R. & Nagase H. 2003. Matrix metalloproteinases and tissue inhibitors of metalloproteinases: structure, function, and biochemistry. *Circulation research,* 92(8)**,** 827-39.

Waggoner W. F. 2015. Restoring primary anterior teeth: updated for 2014. *Pediatric dentistry,* 37(2)**,** 163-70.

Wallman-Bjorklund C., Svanberg M. & Emilson C. G. 1987. Streptococcus mutans in plaque from conventional and from non-gamma-2 amalgam restorations. *Scandinavian journal of dental research,* 95(3)**,** 266-9.

Walters N. J., Xia W., Salih V., Ashley P. F. & Young A. M. 2016. Poly(propylene glycol) and urethane dimethacrylates improve conversion of dental composites and reveal complexity of cytocompatibility testing. *Dental materials : official publication of the Academy of Dental Materials,* 32(2)**,** 264-77.

Wang J. & Liu Z. 2000. Influence of amalgam on the growth of mutans streptococcus: an in vivo study. *The Chinese journal of dental research : the official journal of the Scientific Section of the Chinese Stomatological Association (CSA),* 3(2)**,** 33-7.

West N. X., Hughes J. A. & Addy M. 2001. The effect of pH on the erosion of dentine and enamel by dietary acids in vitro. *Journal of oral rehabilitation,* 28(9)**,** 860-4.

Wiegand A., Buchalla W. & Attin T. 2007. Review on fluoride-releasing restorative materials—Fluoride release and uptake characteristics, antibacterial activity and influence on caries formation. 23(3)**,** 343-362.

Wolff M. S. & Larson C. 2009. The cariogenic dental biofilm: good, bad or just something to control? *Brazilian oral research,* 23 Suppl 1**,** 31-8.

Wong S., Anthonappa R. P., Ekambaram M., Mcgrath C., King N. M. & Winters J. C. 2017. Quality of life changes in children following emergency dental extractions under general anaesthesia. *International journal of paediatric dentistry,* 27(2)**,** 80-86.

Xie X. J., Xing D., Wang L., Zhou H., Weir M. D., Bai Y. X. & Xu H. H. 2017. Novel rechargeable calcium phosphate nanoparticle-containing orthodontic cement. *International journal of oral science,* 9(1)**,** 24-32.

Xu H., Sun L., Weir M., Antonucci J. M., Takagi S., Chow L. C. & Peltz M. J. J. O. D. R. 2006. Nano DCPA-whisker composites with high strength and Ca and PO4 release. 85(8)**,** 722-727.

Xu H., Weir M., Sun L., Takagi S. & Chow L. J. J. O. D. R. 2007. Effects of calcium phosphate nanoparticles on Ca-PO4 composite. 86(4)**,** 378-383.

Xu H. H., Moreau J. L., Sun L. & Chow L. C. 2011. Nanocomposite containing amorphous calcium phosphate nanoparticles for caries inhibition. *Dental materials : official publication of the Academy of Dental Materials,* 27(8)**,** 762-9.

Xu H. H. K., Weir M. D. & Sun L. 2009. Calcium and phosphate ion releasing composite: Effect of pH on release and mechanical properties. 25(4)**,** 535-542.

Xu J., Stangel I., Butler I. S. & Gilson D. F. 1997. An FT-Raman spectroscopic investigation of dentin and collagen surfaces modified by 2-hydroxyethylmethacrylate. *Journal of dental research,* 76(1)**,** 596-601.

Xuan G. H. & Wang H. H. 2015. [The effect of acid etching on bond strength of different self-adhesive resin cements to dentin]. *Shanghai kou qiang yi xue = Shanghai journal of stomatology,* 24(3)**,** 302-6.

Yan F., Robert M. & Li Y. 2017. Statistical methods and common problems in medical or biomedical science research. *International journal of physiology, pathophysiology and pharmacology,* 9(5)**,** 157-163.

Yang B., Flaim G. & Dickens S. H. 2011. Remineralization of human natural caries and artificial caries-like lesions with an experimental whisker-reinforced ART composite. *Acta biomaterialia,* 7(5)**,** 2303-9.

Yap A., Low J. & Ong L. J. O. D. 2000. Effect of food-simulating liquids on surface characteristics of composite and polyacid-modified composite restoratives. 25(3)**,** 170-176.

Yap A. U., Chandra S. P., Chung S. M. & Lim C. T. 2002. Changes in flexural properties of composite restoratives after aging in water. *Operative dentistry,* 27(5)**,** 468-74.

Yasa B., Kucukyilmaz E., Yasa E. & Ertas E. T. 2015. Comparative study of radiopacity of resin-based and glass ionomer-based bulk-fill restoratives using digital radiography. *Journal of oral science,* 57(2)**,** 79-85.

Ye R., Xu H., Wan C., Peng S., Wang L., Xu H., Aguilar Z. P., Xiong Y., Zeng Z. & Wei H. 2013. Antibacterial activity and mechanism of action of epsilon-poly-L-lysine. *Biochemical and biophysical research communications,* 439(1)**,** 148-53.

Yildirim T., Ayar M. K., Akdag M. S. & Yesilyurt C. 2017. Radiopacity of bulk fill flowable resin composite materials. *Nigerian journal of clinical practice,* 20(2)**,** 200-204.

Yiu C. K., King N. M., Carrilho M. R., Sauro S., Rueggeberg F. A., Prati C., Carvalho R. M., Pashley D. H. & Tay F. R. 2006. Effect of resin hydrophilicity and temperature on water sorption of dental adhesive resins. *Biomaterials,* 27(9)**,** 1695-703.

Yoshida T. & Nagasawa T. 2003. epsilon-Poly-L-lysine: microbial production, biodegradation and application potential. *Applied microbiology and biotechnology,* 62(1)**,** 21-6.

Young A. M., Ng P. Y., Gbureck U., Nazhat S. N., Barralet J. E. & Hofmann M. P. 2008. Characterization of chlorhexidine-releasing, fast-setting, brushite bone cements. *Acta biomaterialia,* 4(4)**,** 1081-8.

Young A. M., Rafeeka S. A. & Howlett J. A. 2004. FTIR investigation of monomer polymerisation and polyacid neutralisation kinetics and mechanisms in various aesthetic dental restorative materials. *Biomaterials,* 25(5)**,** 823-33.

Yuan H., Li M., Guo B., Gao Y., Liu H. & Li J. J. J. O. a. D. 2015. Evaluation of Microtensile Bond Strength and Microleakage of a Self-adhering Flowable Composite. 17(6).

Zankuli M. A., Devlin H. & Silikas N. 2014. Water sorption and solubility of core build-up materials. *Dental materials : official publication of the Academy of Dental Materials,* 30(12)**,** e324-9.

Zhang K., Cheng L., Weir M. D., Bai Y. X. & Xu H. H. 2016. Effects of quaternary ammonium chain length on the antibacterial and remineralizing effects of a calcium phosphate nanocomposite. *International journal of oral science,* 8(1)**,** 45-53.

Zhang L., Weir M. D., Chow L. C., Antonucci J. M., Chen J. & Xu H. H. 2016. Novel rechargeable calcium phosphate dental nanocomposite. *Dental materials : official publication of the Academy of Dental Materials,* 32(2)**,** 285-93.

Zhu J. J., Tang A. T. H., Matinlinna J. P. & Hägg U. 2014. Acid etching of human enamel in clinical applications: A systematic review. 112(2)**,** 122-135.